

**Characterization of interaction sites between Kir6.0 and SUR  
subunits of ATP-sensitive potassium ( $K_{ATP}$ ) channels**

Thesis submitted for the degree of

Doctor of Philosophy

at the University of Leicester

by

Mohammed Aljohi (Msc)

University of Leicester

Department of Cardiovascular Science

December 2005

UMI Number: U203816

All rights reserved

INFORMATION TO ALL USERS

The quality of this reproduction is dependent upon the quality of the copy submitted.

In the unlikely event that the author did not send a complete manuscript and there are missing pages, these will be noted. Also, if material had to be removed, a note will indicate the deletion.



UMI U203816

Published by ProQuest LLC 2013. Copyright in the Dissertation held by the Author.  
Microform Edition © ProQuest LLC.

All rights reserved. This work is protected against  
unauthorized copying under Title 17, United States Code.



ProQuest LLC  
789 East Eisenhower Parkway  
P.O. Box 1346  
Ann Arbor, MI 48106-1346

### Abstract

This study investigated cytoplasmic inter-subunit interactions between the Kir6.2 and SUR2A subunits of the cardiac ATP-sensitive potassium channel. The channels are a heterooligomeric complex of pore-forming Kir6.2 subunits and sulphonylurea receptor (SUR2A) subunits. Interactions between the cytoplasmic loops, the nucleotide binding domains (NBF1 and NBF2) of SUR2A and the full length of Kir6.2 were determined. In co-immunoprecipitation experiments, fragments from the C-terminal of SUR2A containing residues 1294-1358 tagged with Maltose-binding protein (MBP) showed binding with the full length Kir6.2 subunit, while residues between 1358-1545 did not. This indicated involvement of a 65 amino acid domain in the proximal C-terminal of SUR2A in forming a direct interaction with Kir6.2. When HEK 293 cells stably expressing Kir6.2/SUR2A channels were transiently transfected with SUR2A fragments containing residues 1294-1359,  $K_{ATP}$  current was decreased. This current reduction was due to a decreased number of channel subunits in the cell membrane; this was demonstrated by using immunocytochemistry, which showed that anti- $K_{ATP}$  channel subunit-associated fluorescence was lower in the cell membrane and increased in the intracellular compartment in the presence of the binding region.

Use of SUR2A/MRP1 chimaeras of the putative binding domain showed that the last eleven amino acids of the binding region were important for binding activity but that they do not contain all the elements necessary for binding. Co-immunoprecipitation and assays of disruption of functional channels with the binding domain chimaeras suggested an important role for the residues between 1318 and 1337 in the Kir6.2 binding motif within the SUR2A C-terminal domain.

Chimaeras between Kir6.2/Kir2.1 were used to investigate the binding site for the SUR2A C-terminal binding motif. Fragment rSUR2A-CT-C containing residues 1295-1403 showed binding to all chimaeras containing the Kir6.2 C-terminal residues 315-390 but failed to bind when the C-terminal of Kir6.2 was replaced with Kir2.1 sequence. Specificity of the interaction of rSUR2A-CT-C with Kir6.2 315-390 was confirmed by the reduction of binding of the non-binding fragment from SUR2A (SUR2A-CT-D 1358-1545 aa) and an equivalent fragment from the non-interacting Multidrug resistance protein (MRP-CT-C 1280-1389 aa).

In summary, this study has localized a Kir6.2 binding motif to residues 1318-1337 of SUR2A and it's a putative binding site to the Kir6.2 C-terminal between residues 315-390.

### Acknowledgements

Although my name appears on the cover of this report, many people with incomparable talent contributed to this project. First of all, I would like to thank Dr. R. Norman for his support, guidance and patience, and for courageously undertaking the task of editing and organizing my text and figures. I would like to thank Dr. D. Lodwick for his generous support and for helping me with the molecular aspects of this project. I would like to thank all members of the Department of Cardiovascular Sciences for giving me the chance to be one of them, with special thanks to Mr. H. Petal, Miss J. Harris and Dr. H. Singh for all their help and assistance during my course.

I would also like to thank the members of the Cell Physiology and Pharmacology Department for their help and assistance during my studies. Thanks are due to Dr. C. Dart for her productive comments and suggestions concerning my first-year report. I would like to thank Dr. N. Davies for allowing me to use the patching instrument and Dr. D. Hudman for her help with the confocal microscopy. Last but not least, I thank Dr. R. Rainbow for his unending help in the patching and collaboration in this project.

I am grateful to the Ministry of Higher Education, represented by the Royal Embassy of Saudi Arabia Cultural Mission, for supporting me financially during my education. Finally, I would like to thank my parents, wife, brothers, sisters and friends, wherever they are, for their patience and for their moral and financial support. Finally, I would like to thank my uncle, MMB, for everything he has done for me. May God help us all to do the best for humanity.

### Abbreviations

ABC	ATP-Binding cassette transporter subfamily
ADP	Adenosine 5'-diphosphate
APT	Afterhyperpolarization
ATP	Adenosine 5'-triphosphate
BK	Large-conductance Ca-activated potassium channel
CFTR	Cystic fibrosis transmembrane conductance regulators
GFP	Green fluorescent protein
GLUT-2	Membrane-bound glucose transporter
HA	Human influenza virus hemagglutinin (YPYDVPDYA) polypeptide
HEK293	Human embryonic Kidney cells
HERG	Human ether-a-go-go-related channels
IK	Intermediate-conductance Ca-activated potassium channel
IPC	Ischemic preconditioning
KATP	ATP-sensitive potassium channels
Kb	Kilo base (DNA unit)
Kca	Ca <sup>2+</sup> -activated potassium channels
KCO	Potassium channel opener
KDa	Protein molecular weight unit (Kilo Dalton)
Kir	Inward rectifying potassium channels
Kv	Voltage-sensitive potassium channels
M1 and M2	Transmembrane segment of Kir
MDR	Multidrug resistance protein
MRP	Multidrug resistance associated protein
NBFs	Nucleotide-binding folds
P loop	The pore forming loop in Kir6.2 subunit
PCR	Polymerase chain reaction
PHHI	Persistent hyperinsulinemic hypoglycaemia of infancy
PIP2	Phosphatidylinositol-4,5-bisphosphate
PKA	Protein Kinase A
Rao	Kir6.2/Kir2.1 chimaers constructed by Dr. Sivaprasadarao
RKR	Endoplasmic reticulum retention sequence
ROMK (Kir1.0)	Inward rectifying potassium channels Kir1.1 subfamily
ROS	Reactive oxygen species
SK	Small-conductance Ca-activated potassium channel
SUR	Sulphonylurea receptor
Tin	Kir6.2/Kir2.1 chimaers constructed by Dr. Tinker
TMD	Transmembrane domain of SUR
WA and WB	ATP-binding WalkerA and WalkerB motifs

Table of contents

Title	Page
Abstract	I
Acknowledgements	II
Abbreviations	III
Table of contents	IV
List of tables	IX
List of figures	X
<b>Chapter One</b>	
Introduction	1
1.1- Ion channel and tool for investigating them	2
1.2- Potassium channels	5
1.2.1- 6TM/1P channels	7
1.2.1.1- Voltage-sensitive potassium channels	7
1.2.1.2- Calcium-activated potassium channels	8
1.2.1.3- Sodium activated potassium channels	9
1.2.1.4- Ether-a-go-go-related channels	10
1.2.2 - The 4TM and 8TM potassium channels	10
1.2.3- The 2TM/1P channels (Inward rectifier potassium channel)	11
1.3- Kir family	12
1.3.1- Kir1.0 subfamily	12
1.3.2- Kir2.0 subfamily	14
1.3.3- Kir3.0 subfamily	16
1.3.4- Kir4.0 and Kir5.0 subfamilies	17
1.3.5- Kir6.0 subfamily	17
1.3.6- Kir7.0 subfamily	17
1.3.7- KirD subfamily	18
1.4- Overview of the ATP-sensitive potassium channel	18
1.5- ATP-sensitive potassium channel function	20
1.5.1- Pancreatic $\beta$ -Cells	20
1.5.2- Cardiac cells	21
1.5.3- Vascular smooth muscle	22
1.5.4- Hepatocytes	22
1.5.5- In other tissues	23
1.6- The clinical relevance	24
1.6.1- The role of $K_{ATP}$ channels in Ischaemic preconditioning	24
1.6.2- The role of $K_{ATP}$ channels in Persistent Hyperinsulinemic-Hypoglycemia of Infancy	25
1.7- Hallmarks of the inwardly rectifying subunit of $K_{ATP}$ channels	26
1.7.1- Cloning of the Kir6.1 subunit	26
1.7.2- Cloning of the Kir6.2 subunit	27
1.7.3- Kir6.0 polypeptides	27
1.7.4- Endoplasmic reticulum retention sequence in Kir6.0 subunits	28
1.7.6- Binding of the C and N-termi of Kir6.0	28

1.7.7-	Heteromultimerization of Kir6.2 and Kir6.1	29
1.8-	Hallmarks of the sulphonylurea receptor subunit in $K_{ATP}$ channels	32
1.8.1-	Cloning of sulphonylurea receptor (SUR1)	32
1.8.2-	Cloning of the SUR2A subunit	32
1.8.3-	Cloning of the SUR2B subunit	33
1.8.4-	Sulphonylurea receptor polypeptide	33
1.8.5-	Endoplasmic reticulum retention site in SUR subunit	37
1.8.6-	Binding of the NBF1 and NBF2	37
1.9-	Stoichiometry of the $K_{ATP}$ channel	38
1.10-	Pharmacology of $K_{ATP}$ channels	39
1.10.1-	Potassium channel openers (KCO)	39
1.10.2-	Potassium channel inhibitors (Sulphonylureas)	41
1.11-	The regulation of $K_{ATP}$ channels by ATP, MgADP and MgATP	42
1.12-	The regulation of $K_{ATP}$ channels by pH and acidosis	46
1.13-	The affect of phosphatidylinositol 4,5 biphosphate upon $K_{ATP}$ channels	47
1.14-	Interactions between the $K_{ATP}$ channel subunits	48
1.15-	Aims and hypothesis	53
<b>Chapter Two</b>		
<b>Methods</b>		<b>55</b>
2.1-	Molecular biology methods	56
2.1.1-	Amplification of DNA by the polymerase chain reaction (PCR)	56
2.1.2-	Mutagenesis	56
2.1.3-	Purification of plasmid DNA	57
2.1.4-	Mini DNA purification (Wizard)	58
2.1.5-	Determination of yield of the DNA	59
2.1.6-	Determination of the purity of the DNA	59
2.1.7-	DNA gel extraction	59
2.1.8-	Restriction enzyme digests	60
2.1.9-	Reaction cleanup	60
2.1.10-	Removal of 5' phosphate groups for DNA	60
2.1.11-	DNA ligation	61
2.1.12-	Transformation of the DNA to host cells	61
2.2-	Biochemistry methods	62
2.2.1-	Protein expression	62
2.2.2-	7.5 % SDS polyacrylamide gel electrophoresis (SDS-PAGE)	62
2.2.3-	Western blotting	63
2.2.4-	Development of Western blots	63
2.2.5-	Maltose binding protein fusion polypeptide preparation	64
2.2.6-	Protein determination	65
2.2.7-	Co-immunoprecipitation of MBP-SUR2A fragments with Kir6.2	66
2.2.8-	GST-Tag fusion protein purification	67
2.2.9-	Determination of the concentration of protein tagged with GST (activity)	68
2.3-	Immunocytochemistry methods	

2.3.1-	Transfection of HEK 293 cells	69
2.3.2-	Fixation and permeabilization	70
2.3.3-	Staining and confocal microscopy	70
2.3.4-	Data acquisition and image processing	71
2.3.5-	Preparation of polyclonal antibodies	71
<b>Chapter Three</b>		
Preparation and modification of constructs for expression of polypeptide, chimaeras, mutant and epitope tagged K <sub>ATP</sub> channel subunits.		72
3.1-	Introduction	73
3.2-	Truncation of the SUR2A-CT-C fragment	75
3.3-	Construction of MRP1-CT-F/SUR2A (aa 1349-1359)	77
3.4-	Construction of SUR2A-CT-A-C fragment	79
3.5-	Construction of MRP1-CT-C	80
3.6-	Construction of SUR2A/MRP fragment chimaeras	81
3.7-	Construction of SUR2A fragment tagged with HA	86
3.8-	Construction of SUR2A fragments with a GST-tag	88
3.9-	Modification of Kir6.2/Kir2.1 chimaeras	90
<b>Chapter Four</b>		
Characterization of a Kir6.2 subunit binding site in NBF1 and NBF2 of the SUR2A subunit by biochemical analysis		93
4.1.1-	Introduction	94
4.1.2-	Expression and immunoprecipitation of Kir6.2 and Kir2.1	95
4.1.3-	Expression of MBP-rSUR2A-CT fragment	97
4.1.4-	Co-immunoprecipitation of MBP-rSUR2A-CT (NBF2) fragment with full-length Kir6.2 subunit	100
4.1.5-	Co-immunoprecipitation of MBP-rSUR2A-CT fragments with full-length Kir2.1 subunit	102
4.1.6-	Expression of truncated MBP-rSUR2A-CT-C and MBP-MRP1-CT-E fragment	102
4.1.7-	Co-Immunoprecipitation of the non-interacting MRP1 protein	105
4.1.8-	Co-immunoprecipitation of truncated MBP-rSUR2A-CT-C fragments, MBP-rSUR2A-CT-E,-F and -G	107
4.1.9-	Co-immunoprecipitation of MBP-MRP1-CT-F/rSUR2A (aa1349-1359)	108
4.1.10-	Co-immunoprecipitation of MBP-MRP1-C and MBP-rSUR2A-CT-A-C	108
4.2-	Investigate the binding site of NBF1 from SUR2A with full length of Kir6.2	111
4.2.1-	Expression of MBP-rSUR2A-NBF1 fragments	111
4.2.2-	Co-immunoprecipitation of the MBP-rSUR2A-NBF1 fragment with full length of Kir6.2	113
4.2.3-	Co-immunoprecipitation of the full length of Kir6.2 with the GST-rSUR2A-NBF1 and NBF2 fragments	113
4.3-	Summary	117

## **Chapter Five**

Immunocytochemical assay of  $K_{ATP}$  channel subunit targeting to the cell surface of cells expressing Kir6.2/SUR2A in the presence of interacting fragment 118

- 5.1- Subcellular targeting assay for the interacting fragment rSUR2A-CT-E, rSUR2A-CT-D and the empty vector 119
- 5.2- Subcellular targeting in the presence of the truncated rSUR2A-CT-C Fragment 121
- 5.3- Summary 123

## **Chapter Six**

Refinement of the Kir6.2 binding site in rSUR2A-CT-C using rSUR2A/MRP1-CT-C chimaeric constructs 124

- 6.1- Introduction 125
- 6.2- Expression of SUR2A/MRP1 chimaeras 125
- 6.3- Co-immunoprecipitation of SUR2A/MRP1 chimaeras with full length Kir6.2 126
- 6.4- Electrophysiology of Kir6.2/SUR2A channels in HEK 293 cells transiently expressing SUR2A/MRP1 chimaeras 130
- 6.5- Summary 133

## **Chapter Seven**

Investigation of the cognate binding site for the proximal C-terminal domain of SUR2A on the Kir6.2 subunit using Kir6.2/Kir2.1 subunit chimaeras 134

- 7.1- Introduction 135
- 7.2- Expression of the Kir6.2/Kir2.1 chimaeras 136
- 7.3- Characterization of the immunoprecipitation of Kir6.2/Kir2.1 chimaeras with the corresponding antibody 139
- 7.4- Co-immunoprecipitation of the interacting fragment MBP-rSUR2A-CT-C and the non-interacting fragment MPB-rSUR2A-CT-D with Kir6.2/Kir2.1 chimaeras 142
- 7.5- Co-immunoprecipitation of MBP-MRP1-C using the Kir6.2/Kir2.1 chimaeras 144

## **Chapter 8**

Discussion and Conclusion 146

- 8.1.1- Identification of the binding site in the C-terminal of SUR2A by biochemical assay 147
- 8.1.2- Effect of the binding fragment upon Kir6.2/SUR2A channel function 148
- 8.1.3- Effect of the binding fragment SUR2A-CT-E on the subcellular localization of Kir6.2/SUR2A channels using confocal microscopy 151
- 8.1.4- Truncation of the Kir6.2 binding site in NBF2 of SUR2A

(rSUR2A-CT-C)	151
8.1.5- Binding of SUR2A/MRP1 chimaeras binding with Kir6.2	154
8.1.6- Binding of NBF1 fragment with Kir6.2	158
8.2- Investigation of the cognate binding site for the proximal C-terminal domain of SUR2A on the Kir6.2 subunit using Kir6.2/Kir2.1 subunit chimaeras	158
8.3- Conclusion	163
8.4- Future work	165
9- Reference	168

List of tables

Table 2-1.	PCR Cycling Parameters for PfuUltra high-Fidelity DNA polymerase	56
Table 2-2.	The cycles number and temperature for the PCR	57
Table 3-1.	Oligonucleotide for SUR2A-CT-C truncation	77
Table 3-2.	Oligonucleotides for construction of MRP1-F+11of SUR2A	79
Table 3-3.	Oligonucleotides for construction of MRP1-C Rat	81
Table 3.4.	Oligonucleotide for construction of SUR2A/MRP fragment	85
Table 3-5.	Oligonucleotides used for making SUR2A-fragment with HA-tag	88
Table 3-6.	Oligonucleotide sequences for modification of Kir6.2/Kir2.1 chimaeras	91
Table 4-1.	Protein concentration of the MBP- fusion fragments	105

List of figures

Figure 1-1	Path clamp technique configuration	4
Figure 1-2	Membrane topology of potassium channels classes	6
Figure 1-3	Inward rectifying channels	13
Figure 1-4	ATP-sensitive potassium channels	19
Figure 1-5	Hallmarks of Kir6.2 subunit	30
Figure 1-6	Schematic representation of human SUR1 and SUR2 gene	34
Figure 1-7	Hallmarks of the sulphonylurea receptors subunit	36
Figure 1-8	Schematic representation of Kir6.2/Kir2.1 chimaeras from three studies	50
Figure 2-1.	Standard curve of Protein concentration using the Bradford assay	66
Figure 2-2.	Standard curve of GST activity	69
Figure 3-1	Schematic diagram of SUR2A fragments	74
Figure 3-2	Schematic diagram for the truncation of SUR2A-CT-C fragment	76
Figure 3-3	Construction of MRP1-F plus the last 11 amino acid residues from rSUR2A-CT-E (MRP1-CT-F/SUR2A aa 1349-1359)	78
Figure 3-4	Construction of MRP1/SUR2A chimaeras by overlap PCR	82
Figure 3-5	Construction and mapping of MRP1/SUR2A chimaeras	84
Figure 3-6	Construction of HA-SUR2A-fragments	87
Figure 3-7	Construction of GST-tagged SUR2A- fragments	89
Figure 3-8	Mutation of Kir6.2/Kir2.1 chimaeras to remove the FLAG epitope	92
Figure 4-1	In vitro translated [ <sup>35</sup> S]methionine-labelled Kir6.2 and Kir2.1	96
Figure 4.2	Immunoprecipitation of [ <sup>35</sup> S]methionine-labelled in vitro translated Kir6.2 and Kir2.1 polypeptides	98
Figure 4-3	Analysis of expressed and purified maltose binding protein-rSUR2A fusion fragments	99
Figure 4-4	Co-immunoprecipitation of MBP-rSUR2A-CT fragments with Kir6.2 subunit using anti-Kir6.2	101
Figure 4-5	Co-immunoprecipitation of MBP-rSUR2A-CT fragments with Kir2.1 subunit using anti-Kir2.1	103
Figure 4-6	Expression of the MBP-rSUR2A-CT-C truncations and the equivalent of the SUR2A-CT-E fragment from MRP1 (MRP1-CT-E)	104
Figure 4-7	Co-immunoprecipitation of MBP-rSUR2A-CT fragments with Kir6.2 subunit using anti-Kir6.2	106
Figure 4-8	Co-immunoprecipitation of MBP-rSUR2A-CT-A-C and MRP-C fragments with Kir6.2 subunit using anti-Kir6.2	110
Figure 4-9	Analyses of expressed and purified MBP-rSUR2A-NBF1 fusion fragments	112
Figure 4-10	Co-immunoprecipitation of MBP-rSUR2A-NBF1 fragments with Kir6.2 subunit using anti-Kir6.2 antiserum	114
Figure 4-11	GST-rSUR2A expression and co-precipitation with Kir6.2	116
Figure 5-1	The K <sub>ATP</sub> channel subunit distribution in HEK293 cells stably co-expressing Kir6.2/SUR2A and transiently transfected with rSUR2A fragments	120

Figure 5-2	The $K_{ATP}$ channel subunit distribution in HEK293 cells stably co-expressing Kir6.2/SUR2A and transfected with truncation fragment from rSUR2A-CT-C	122
Figure 6-1	Analysis of expressed and purified maltose binding protein tagged rSUR2A/MRP1 chimaeras	127
Figure 6-2	Co-immunoprecipitation of MBP-tagged polypeptide with Kir6.2 subunit using anti-Kir6.2	129
Figure 6-3	Effect of SUR2A/MRP1 chimaeras on SUR2A/Kir6.2 current	132
Figure 7-1	In vitro translated [ $^{35}$ S]methionine-labelled Kir6.2, Kir2.1 and Rao chimaeras	137
Figure 7-2	In vitro translated [ $^{35}$ S]methionine-labelled Kir6.2, Kir2.1 and Tin chimaeras	138
Figure 7-3	Immunoprecipitation of [ $^{35}$ S]methionine-labelled in vitro translated Kir6.2, Kir2.1 and Rao polypeptides	140
Figure 7-4	Immunoprecipitation of [ $^{35}$ S]methionine-labelled in vitro translated Tin chimaeras	141
Figure 7-5	Co-immunoprecipitation of MBP-SUR2A-CT-C and MBP-rSUR2A-CT-D fragments with WT-Kir subunits and Kir6.2/Kir2.1 chimaeras	143
Figure 7-6	Co-immunoprecipitation of MBP-MRP1-CT-C fragment with WT-Kir subunits and Kir6.2/Kir2.1 chimaeras	145
Figure 8-1	Current recording of $K_{ATP}$ channels in the presence of SUR2A-CT fragments	149
Figure 8-2	Three dimensional modeling of the Kir6.2 binding motif in the proximal C-terminal domain of rSUR2A using the crystal structure of MalK as template	153
Figure 8-3	Alignment of the SUR2A-CT-C fragment and the equivalent sequence from MRP1	155
Figure 8-4	Alignment of the rSUR2A-CT-E binding motif with SUR1 and MRP1 equivalents	159
Figure 8-5	Alignment of the full length Kir6.0 and Kir2.1 subunits	162

# **Chapter One**

## **Introduction**

### 1.1- Ion channels and tools for investigating them

The plasma membrane is composed of two layers of tightly packed lipid molecules, which acts as a barrier separating the cell contents from the outside, so that the ionic concentrations inside the cell can be maintained at levels appreciably different from those in the extracellular fluids. At the same time, these membranes allow a constant exchange of substances with the outside medium, including the uptake of oxygen and essential nutrients and the exclusion of unwanted and harmful materials. This structure is not readily permeable to polar molecules, such as sugars or amino acids, or to charged particles, such as sodium or potassium ions. Such substances can pass through the membrane only via special protein molecules embedded in it. Ion channels form one group of these proteins; they permit the rapid flow of ions across the membrane. Channels show selectivity to the ions to which they are permeable. The selectivity of channels and transporters within membranes prevents the random diffusion of substances and allows the cell to determine and control its internal environment while providing a number of different micro-environments, within the subcellular organelles. Ion channels are crucial components in the activity of living cells. They can control the movement of ion exchange across the membrane (Hall and Baker, 1977). To study the mechanism of channel activity and to understand how they work, many methods have been developed to distinguish these channels from other proteins and to assist with their classification.

Hermann (1905) found that the potential changes associated with the excited region of an axon would send small currents in a circuit down the axis cylinder. After that Cole (1939) studied the membrane properties by measuring the electrical impedance of cell suspensions or single cells. He found that cells have a high-conductance cytoplasm compared to the surroundings of the cells. In 1937, Hodgkin began to look for electrical spread of excitation beyond a region of nerve blocked locally by cold. He suggested that depolarization spreading passively from an excited region of membrane to a neighbouring unexcited region is the stimulus for propagation (Hodgkin, 1937). After that Cole and Curtis (1939) observed that the membrane conductance increase begins only after the membrane potential has raised many millivolts from the resting potential. They recognized

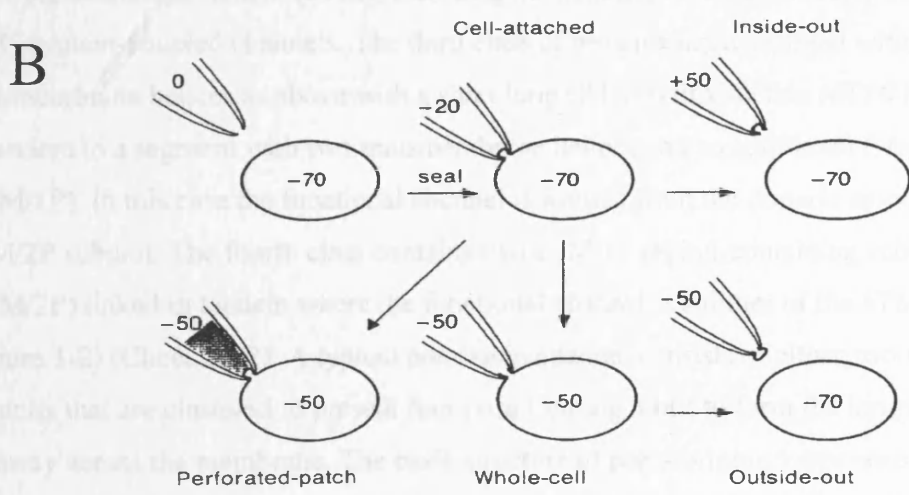
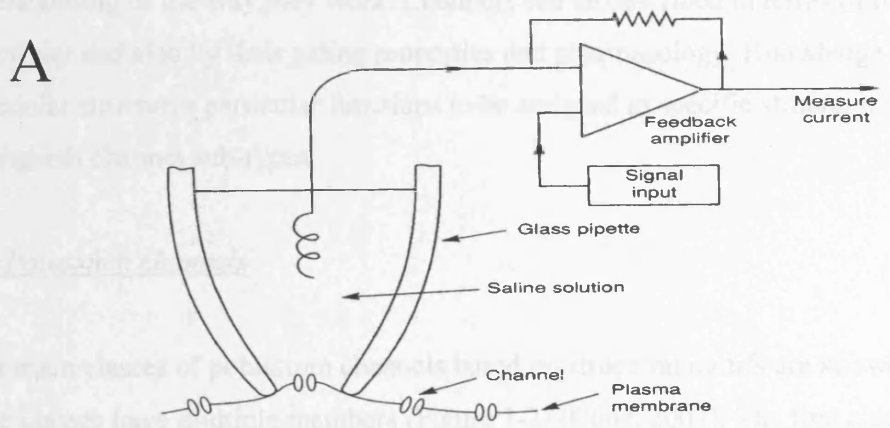
that the conductance is a measure of the ion permeability through the membrane. Later, Hodgkin and Huxley (1939) were able to measure the full action potential of an axon with an intracellular micropipette. This was a more specific technique for studying ion channels and called the voltage clamp (Hille, 2001).

Neher and Sakmann (1976) reported the first single-channel current records with an acetylcholine-activated channel. Hamill et al (1981) later showed that clean glass pipettes can fuse with clean cell membranes to form a seal of unexpectedly high resistance and mechanical stability. This allows the current flowing through an individual ion channel to be measured (Figure 1-1). This idea was proven and given a strong quantitative basis for some ion channels (Hille, 2001). The patch-clamp means measuring the current change across the cell membrane, where the movement of the ion across the membrane can be measured (Hille, 2001).

Another method of investigating ion channels has been the use of biochemical techniques. This was made possible from knowledge of the specific pharmacology of different ion channel types from electrophysiological measurement. By radiolabelling channel agonists or antagonists, molecular probes for specific ion channels were prepared that permitted ion channel proteins to be followed through purification protocols and subsequent analysis of molecular components (Catterall et al., 1982). Purified channel proteins were then reconstituted into artificial membrane bilayers for functional analysis to establish that polypeptides purified were indeed ion channel proteins. Electrophysiological recording of reconstituted channels in liposome preparations was not possible and so investigators used measurements of antagonist-sensitive radioactive ion fluxes to establish that functional ion channel proteins had been purified (Catterall et al., 1982).

Biochemical approaches provided a significant step forward in the understanding of overall channel structure but developments in molecular biology then allowed detailed primary structures to be determined and structure-function mapping to be carried out.

Knowing the structure and properties of channel proteins can give us a clue about their function. The structure of channels is very different from that of other proteins, and a knowledge of the structure of channels gives us an interesting understanding of the way they work. Channels are made of several subunits, and each subunit has a pore through which ions can pass. The pore is lined with amino acid side chains that can be charged or polar, and this determines the selectivity of the channel. For example, the potassium channel has a selectivity filter that is lined with carbonyl oxygen atoms, which attract and coordinate the potassium ions. This allows potassium ions to pass through the channel more easily than other ions. The structure of channels is also important for understanding how they are regulated. Some channels are gated, meaning that they can open or close in response to a signal. This signal can be a change in voltage, a chemical signal, or a mechanical signal. The structure of the channel determines how it is regulated, and this is important for understanding how channels contribute to the function of the cell.

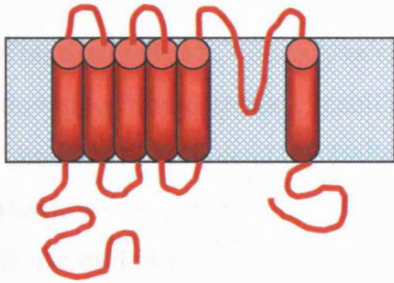
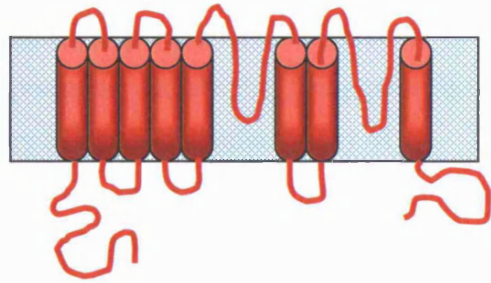
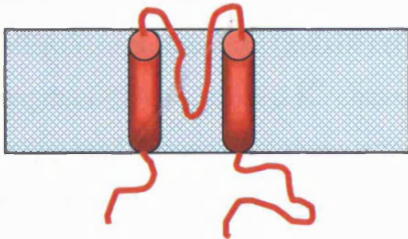
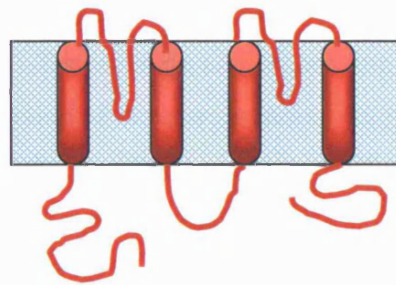


**Figure 1-1 Patch clamp technique and configuration.** A, The patch clamp technique allows the current flowing through an individual ion channel to be measured by isolating a small area of membrane. B, Different patch clamp configurations allow the of isolated patches to be controlled or the recording of whole cell currents (taken from Aidley and Stanfield, 1996).

Knowing the amino acid sequences of channel subunits can give strong clues about structures, and knowledge of the structures of channels gives us an increasing understanding of the way they work. Channels can be described in terms of their ionic selectivity and also by their gating properties and pharmacology. Knowledge of their molecular structures particular functions to be assigned to specific structural entities and to distinguish channel sub-types.

### 1.2- Potassium channels

Four main classes of potassium channels based on structural motifs are known and most of these classes have multiple members (Figure 1-2) (Choe, 2002). The first class contains six transmembrane helices and a P loop (6TM/1P), includes the voltage-sensitive potassium Kv channels and Ca<sup>2+</sup>-activated channels (K<sub>Ca</sub>). The second class contains proteins with two transmembrane helices (2TM), including the inward rectifiers, the K<sub>ATP</sub> channels and the G-protein-coupled channels. The third class of proteins has a segment with six transmembrane helices as above with a short loop (P loop) linking this (6TM/1P) segment in tandem to a segment with two transmembrane helices and an additional P loop (2TM/1P). In this case the functional channel is formed from the dimeric association of the 8TM/2P subunit. The fourth class contains two 2TM/1P region-containing subunits (4TM/2P) linked in tandem where the functional channel is a dimer of the 4TM/2P subunit (Figure 1-2) (Choe, 2002). A typical potassium channel consists of either two or four subunits that are clustered to present four pore forming motif to form the ion-permeation pathway across the membrane. The basic structure of pore-forming loops consists of two transmembrane helices and a P loop forming the core of the ion conduction pathway, and is the trademark of all K<sup>+</sup> channels. Both the N- and C-termini of all potassium channel proteins are located intercellularly, except Ca-activated K channels which have their N-termini extracellular (Choe, 2002).

**A****C****B****D**

**Figure 1-2 Membrane topology of potassium channels classes (Choe, 2002).** A, Six transmembrane helices and a P loop (6TM/1P). B, Two transmembrane helices and P loop (2TM/1P). C, Six transmembrane helices and a P loop linked to Two transmembrane helices and P loop (8TM/2P). D, Two transmembrane helices and P loop linked to another two transmembrane helices and P loop (4TM/2P).

### 1.2.1- 6TM/1P channels

#### 1.2.1.1- Voltage-sensitive potassium channels

Voltage-activated K<sup>+</sup> (Kv) channels play a crucial role in repolarizing the membrane following action potentials, stabilizing membrane potentials and shaping firing patterns of excitable cells (Hegde et al., 1999). Kv channels are a large and diverse family of potassium channels that are, as the name suggests, voltage dependent in their activation. The use of molecular biology techniques led to a rapid understanding of the structure of this class of potassium ion channels, and also led to the identification of differences between the sub-classes of potassium channel according to the amino acid sequence. A number of genes coding for voltage-sensitive K<sup>+</sup> channel  $\alpha$ -subunits have been cloned. These include genes from six sub-families, defined by six *Drosophila* K<sup>+</sup> channel genes: *Shaker* (Kv1.1-1.7), *Shab* (Kv2.1-2.2), *Shaw* (Kv3.1-3.4), *Shal* (Kv4.1-4.3), *ether-a-go-go* (HERG) and *slowpoke* (maxiK) (Hegde et al., 1999). The isolation and sequencing of full length cDNAs of cloned K<sup>+</sup> channels allowed prediction of the corresponding complete amino acid sequence of these proteins. It was found that the *Shaker* gene encoded a membrane protein that had structural similarities to the primary structures of Na<sup>+</sup> and Ca<sup>2+</sup> channel proteins, which later helped to confirm the general properties of Kv channels (Pongs et al., 1988). The study of *Shaker* K channel mutants provided the most thorough insight into the relationship between the structure and the function of K<sup>+</sup> channels (Pongs, 1992). Molecular analysis indicates that *Shaker* cDNAs are derived from a large transcription unit that contains at least 23 exons. Alternative splicing and alternative transcription start sites may lead to the synthesis of several different mRNAs encoding different K<sup>+</sup> channel subunits (Pongs et al., 1988).

The typical voltage-gated channel is an assembly of four similar transmembrane structural units surrounding a central pore. Each structural unit has six transmembrane crossings (S1-S6), with both N- and C-termini on the intracellular side of the membrane. The transmembrane segment S4 contains multiple positive charges at every third amino acid position, which allow the voltage across the membrane to be sensed by the protein (Pongs et al., 1988).

Upon membrane depolarisation potassium channels of the voltage-activated family open. In an action potential of a nerve fibre the sodium channels responsible for the upstroke of the action potential inactivate as the potassium channels are activating. Therefore sodium current is reduced and the outward movement of potassium has the effect of driving the membrane potential in a more negative direction due to the equilibrium potential for potassium having a negative value, typically -80 to -90 mV. Thus voltage-activated potassium channels underlie action potential repolarisation (Pongs et al., 1988).

#### 1.2.1.2- Calcium-activated potassium channels

$\text{Ca}^{2+}$ -activated potassium channels are present in many excitable cells, where they contribute to the integration of changes in intracellular  $\text{Ca}^{2+}$  ion concentration with membrane potential. Based on their biophysical and pharmacological properties, they have been classified into three categories (Vergara et al., 1998): large-conductance  $\text{Ca}^{2+}$ -activated (BK), intermediate-conductance channels (IK) and small-conductance (SK). In BK channels, unlike other voltage-dependent potassium channels, an additional four hydrophobic segments, S7-S10, have been identified in the cytoplasmic C-terminal domain (Meera et al., 1997; Wei et al., 1994). BK channels are characterized by a single-channel conductance of about 200-400 pS (in symmetrical potassium) (Sah and Faber, 2002) and are activated at low calcium concentration (1-10  $\mu\text{M}$ ). They are gated by both membrane depolarization and an increase in  $\text{Ca}^{2+}$  ion concentration (Piskorowski and Aldrich, 2002). BK channels play an important role in the repolarization of action potentials and in fast afterhyperpolarization. BK channels are composed of alpha and beta subunits in an  $\alpha_4 \beta_4$  stoichiometry (Bissonnette, 2002). Several pharmacological blockers of BK channels are known. These include tetraethylammonium (TEA) in the low micromolar range, charybdotoxin and iberiotoxin (Blatz and Magleby, 1986; Galvez et al., 1990).

SK channels were the second type of  $\text{Ca}^{2+}$ -activated potassium channel to be identified. They are characterized by their low single channel conductance in the range of 4 –14 pS (Vergara et al., 1998). SK channels are activated by increases in cytosolic calcium, with

half maximal activation in the 400-800 nM range, but are voltage-insensitive and are unaffected by low concentrations of the  $\text{Ca}^{2+}$  ion (Blatz and Magleby, 1986; Park, 1994). Subtypes of this type include SK1, SK2, and SK3 (Moczydlowski et al., 1988; Strong, 1990).

A third type of calcium-activated potassium channel (IK) has an intermediate single channel conductance (20-100 pS) (Ishii et al., 1997; Joiner et al., 1997). This type has been identified in cells of the haematopoietic system and in organs involved in salt and fluid transport, including the colon, lung, and salivary glands, also in the red blood cells and T lymphocytes (Begenisich et al., 2004; Ishii et al., 1997). IK is believed to contribute into the volume regulation of circulating blood cells such as lymphocytes and erythrocytes (Begenisich et al., 2004).

#### 1.2.1.3- Sodium activated potassium channels

This family of  $\text{K}^+$  channels was first identified in guinea pig cardiomyocytes (Kameyama et al., 1984). Subsequently, similar channels were reported in a variety of neurons (Bader et al., 1985; Dryer et al., 1989). The sodium fluxes during an action potential can lead to modifications of the intracellular sodium concentration near the cell membrane and this in turn may activate these potassium channels. The sodium-activated potassium channels may also contribute to the maintenance of membrane potential near the potassium equilibrium potential when cells are faced with intracellular sodium accumulation. In guinea-pig heart myocytes, the conductance of the  $\text{K}_{\text{Na}}$  channel decreases as the voltage is made more positive than +20 mV (Kameyama et al., 1984).

Moreover, the physiological roles of these channels appear to be distinct in different cell types. For example, in quail trigeminal ganglion neurons and in dorsal root ganglion neurons, it has been suggested that  $\text{K}_{\text{Na}}$  channels regulate the resting membrane potential (Haimann et al., 1992; Bischoff et al., 1998) and in other neurons,  $\text{K}_{\text{Na}}$  channels have been implicated in an apamin-insensitive, Na-dependent slow afterhyperpolarization (AHP) that follows a burst of action potentials (Dryer, 1994).

#### 1.2.1.4- Ether-a-go-go-related channels

The human ether-a-go-go related gene (HERG), encodes the pore-forming  $\alpha$ -subunit of the rapid delayed rectifier  $K^+$  channel (Subbiah et al., 2004), which is an important contributor to the repolarization phase of the cardiac action potential. HERG was discovered from a high-stringency screen of human hippocampus cDNA library (Warmke and Ganetzky, 1994) using a mouse ether-a go-go (eag) polymerase chain reaction fragment. HERG encodes a protein with the usual voltage-gated  $K^+$  channel topology with six-transmembrane spanning regions (Sanguinetti and Xu, 1999). The functional channel is composed of four similar subunits. The single-channel conductance of HERG is 12 pS between -50 and -110 mV. HERG is a member of the  $K_v$  family (Warmke and Ganetzky, 1994), in which gating is driven by changes in the membrane potential. During the plateau phase of the cardiac action potential, HERG passes little outward current, due to channel inactivation, but the channels play a critical role in normal cardiac repolarization, during which they rapidly recover from inactivation and pass a significantly larger outward current (Zhou et al., 1998; Hancox et al., 1998).

#### 1.2.2- The 4TM and 8TM potassium channels

These channels contain 4 or 8 TM segments possessing 2 pore-forming domains. Screening of the human genome sequence has revealed 12 members of the two P-loop channels (KCNK or TWIK family) (Goldstein et al., 2001). In 1995, the first example of a two P-domain channel subunit-TOK1 was found in the sequence database for the budding yeast *Saccharomyces cerevisiae*, which has 8TM with two P-loop domains (Ketchum et al., 1995). The 8TM channel of yeast may be one of its few  $K^+$  channels, perhaps serving a role in  $K^+$  transport. This channel conducts outward current. Opening is favoured by depolarization and by decreasing both  $K^+$  concentrations, and there is a voltage-dependent block by external  $Mg^{2+}$  ions (Cook, 1990). Later, KCNK0 was cloned from the neuromuscular tissues of the adult fruitfly *Drosophila melanogaster* on the basis of its capacity to rescue  $K^+$  transport-defective yeast cells. KCNK0 subunits were also found to have two P-Loop domains but just four predicted transmembrane segments (2P/4TM), and

provided the first example of  $K^+$ -selective leak conductance channel (Kim and Gnatenco, 2001). The 4TM/2P channels that have been cloned and expressed are with small rectification current. Some are sensitive to acid and others to intracellular second messenger signals or to mechanical stimuli (Kim and Gnatenco, 2001). There are five members of the 4TM/2P  $K^+$  channel subfamily. They are expressed in various tissues and behave as background  $K^+$  channels. TASK-1 and TASK-3 are involved in the regulation of membrane potential and neuronal firing in cerebellar granule neurons and motor neurons (Millar et al., 2000; Talley et al., 2000). TASK-2 is found mainly in the kidney and may be important for renal  $K^+$  transport (Reyes et al., 1998). TASK-4 is widely expressed in human tissues and is markedly activated at alkaline pH (Girard et al., 2001). TASK5 is expressed primarily in the adrenal gland and pancreas, and does not form a functional  $K^+$  current in the plasma membrane of COS-7 cells by itself (Kim and Gnatenco, 2001). In general, the 4TM/2P channels account for some of the K conductance that has been called “leak” in the past. They have been demonstrated to make some contribution in setting the resting potential, regulating cellular excitability, and giving K permeability to cells that need to transport  $K^+$  ions. They can also be closed by second-messenger systems (Millar et al., 2000; Talley et al., 2000), and some can be opened by volatile anaesthetics (Patel et al., 1999). Opening would hyperpolarize cells and lead to depressed brain activity under general anaesthesia (Cook, 1990).

### 1.2.3- The 2TM/1P channels (Inward rectifier potassium channels)

Inward rectifier potassium channels belong to a large subfamily of potassium channels whose main function is to contribute to the establishment of resting membrane potential. Inward rectification means that the inward movement of  $K^+$  ions is greater than that in the outward direction (Nichols and Lopatin, 1997). In the absence of rectification, the current flowing through a conductor is linearly proportional to the potential across it, when the conductance is constant and independent of voltage. A conductance is said to be rectified, if the conductance varies with potential difference, such that it conducts more readily in one direction than other (Aidley and Stanfield, 1996) (Figure 1-3,A). Inward rectifier potassium channels may be classified as ‘classical’, ‘strong’ or ‘weak’, depending on their

physiological function and tissue localization (Nichols and Lopatin, 1997). In biological membranes, strong rectification usually means that the ion channels carrying current are open at some membrane potentials and effectively shut at others (Hille, 2001). In cardiac cells, for example, the inward current carried below the reversal potential for potassium is relatively large, while the outward potassium current amplitude is relatively small at -50 mV and even smaller at 0 mV (Hille, 2001).

### 1.3- Kir family

The level of sequence identity among the Kir channel subfamilies, similar to that among the Kv channel subfamilies, is between 40 % and 60 % (Dounnik et al., 1995). Kir channel subunits have only two transmembrane domains within each subunit, but they retain the H5-loop that is responsible for K<sup>+</sup> selectivity in Kv channels. There are now at least seven Kir channel subfamilies known, with ~40 % similarity in their amino acid sequence and 60 % similarity between the members of each subfamily (Figure 1-3,B) (Nichols and Lopatin, 1997).

#### 1.3.1- Kir1.0 subfamily

Kir1.1 (ROMK1) is an ATP-regulated K<sup>+</sup> channel that is expressed predominantly in the kidney, but also expressed in the central nervous system, thalamus, hypothalamus and pituitary (Ho et al., 1993). Kir1.1 has weak inward rectifying properties (Wang et al., 1990). It contains a putative phosphate-binding loop in the C-terminal region, unlike the other members of Kir subfamilies (Ho et al., 1993). A direct interaction between phosphatidylinositol-4,5-bisphosphate (PIP<sub>2</sub>) and the channels is important for the constitutive opening of Kir1.1 channels (Liou et al., 1999). The activity of Kir1.1 is regulated by protein kinase A (PKA) (Liou et al., 1999). However, PKA phosphorylation

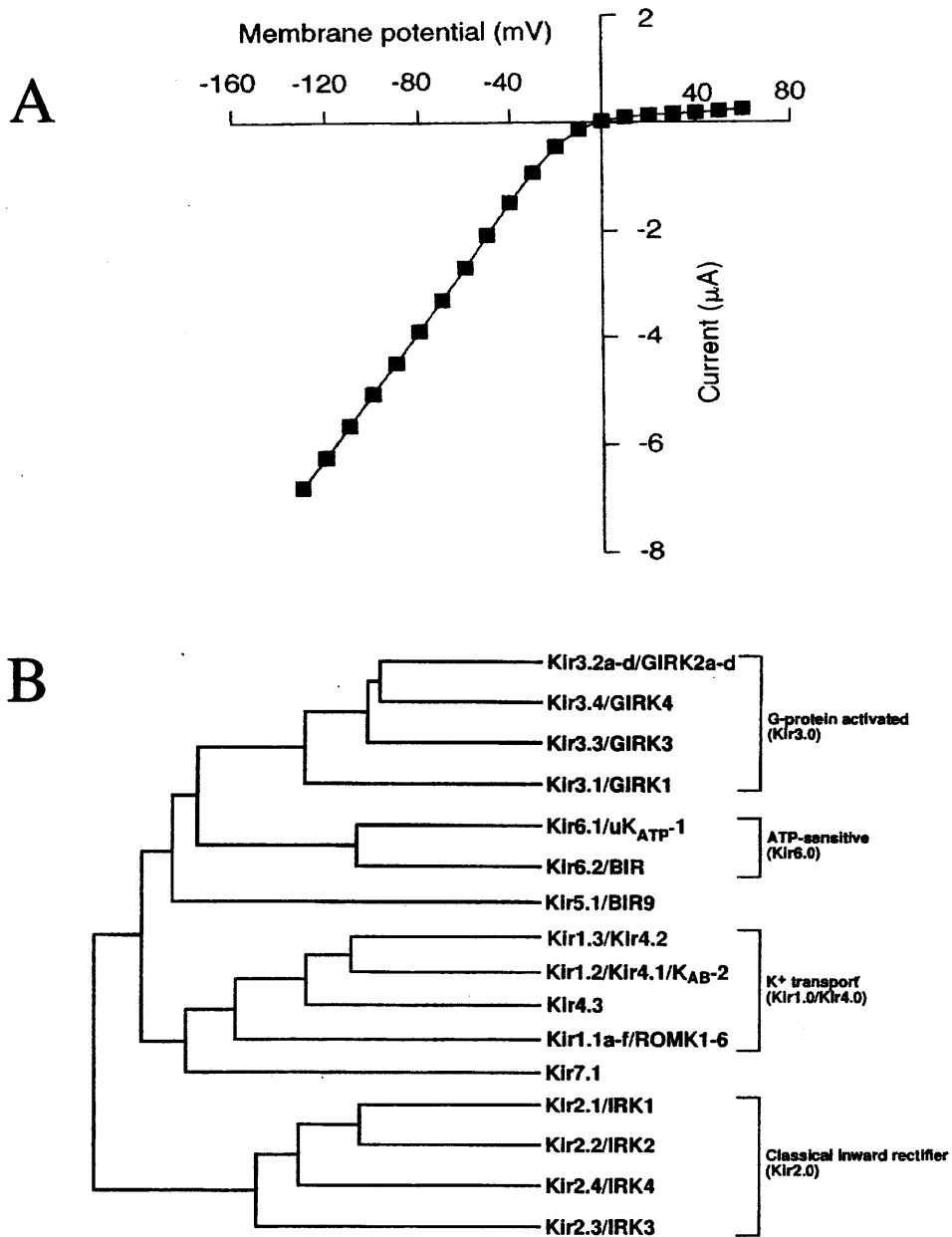


**Figure 1- 3 Inward rectifying channels.** A, The graph shows the current-voltage relation of a strongly inward rectifying Kir2.1 channel. B, The evolutionary tree of the inward rectifying K<sup>+</sup>- channel family with two membrane-spanning domain. Evolutionary relationships of Kir channel sequences (taken from Hille 2001).

does not activate the channel in the absence of PIP<sub>2</sub>, but rather PKA increases the sensitivity of the channels to activation by PIP<sub>2</sub>. The C-terminal domain of Kir1.1 binds PIP<sub>2</sub> and contains the PKA phosphorylation sites (Liou et al., 1999).

Kir1.1 channels are gated by intracellular pH, with acidification leading to channel closure (Schulte et al., 1998). Although a lysine residue (Lys 80) close to the first hydrophobic segment M1 has been identified as the pH sensor, little is known about how opening and closing of the channel is accomplished. The other members of this subfamily were identified during the molecular investigation for the channels responsible for renal K<sup>+</sup> secretion which resulted in cloning of ROMK (Kir1.1) and its splice variants ROMK2 and ROMK3 (Boim et al., 1995; Zhou et al., 1994). Splicing results in variable length of the respective N-termini, with ROMK2 shortened by 19 amino acids and ROMK3 exhibiting an extension of 7 residues with respect to ROMK1 (Schulte et al., 1998). The human Kir1.1 gene, located on chromosome 11 band q24, contains five exons which generate multiple variants with alternative splicing at the 5' end, resulting in at least five splice variants (Shuck et al., 1994).

### 1.3.2- Kir2.0 subfamily

There are four different members of the Kir2.0 subfamily and all are strong inward rectifiers. The predicted open reading frames encode 428, 434, 444 and 439 amino acids for gpKir2.1 (guinea pig), gpKir2.2, gpKir2.3 and gpKir2.4 respectively (Liu et al., 2001). Kir2.0 subfamily members are expressed in many cells types, including neurons, glial cells, skeletal muscle fibres, ventricular myocytes, vascular smooth muscle cells, endothelial cells, epithelial cells, macrophage and osteoclasts (Doupnik et al., 1995). Each member expresses a different single channel conductance. In patch clamp experiments with 140 mM K<sup>+</sup> in the pipette, the single channel conductance of MB-IRK2 (Kir2.2) was  $34.2 \pm 2.1$  picosiemens (pS), a value significantly larger than that of MB-IRK1 (Kir2.1) at  $22.2 \pm 3.0$  pS. Kir2.2 is expressed in forebrain, cerebellum, heart, kidney, and skeletal muscle (Liu et al., 2001). In the brain, the mRNA levels for Kir2.2 were much higher in cerebellum than in forebrain and vice versa in the case of Kir2.1. This showed that the Kir2.0 subfamily is

composed of multiple genes, which may play heterogeneous functional roles in various organs, including the central nervous system (Takahashi et al., 1994).

Unlike other members of the Kir2.0 subfamily, Kir2.3 couples with G proteins, a coupling that enables this channel to contribute to neurotransmission and cell-cell communications (Zhu et al., 1999). Also, Kir2.3 is known to be modulated by several intracellular and extracellular signal molecules such as polyamines, protons and protein kinase C (PKC) (Zhu et al., 1999). The amino acid sequence of Kir2.3 showed 61% and 64% resemblance to Kir2.1 and Kir2.2, respectively (Morishige et al., 1994). *Xenopus oocytes* injected with cRNA derived from the Kir2.3 clone expressed a potassium current which showed inward-rectifying channel characteristics similar to Kir2.1 and Kir2.2 currents but distinct from Kir1.1 or Kir3.1 currents. However, the single channel conductance of Kir2.3 was ~10 pS with 140 mM extracellular K<sup>+</sup>, which was distinct from that of Kir2.1 (20 pS). Kir2.3 mRNA is expressed specifically in the forebrain, which is clearly different to the distribution of mRNAs for Kir2.1 and Kir2.2 (Morishige et al., 1994). Expression of Kir2.1 and Kir2.2 has been demonstrated in the human atrium (Wible et al., 1995), while Kir2.3 has been found in the human ventricle (Morishige et al., 1994; Perier et al., 1994). The mean single-channel conductances measured in cardiomyocytes, in the presence of 150 mM external K<sup>+</sup>, 1 mM Ca<sup>2+</sup> and 1 mM Mg<sup>2+</sup>, were 23.8 pS for gpKir2.1, 34.0 pS for gpKir2.2 and 10.7 pS for Kir2.3 (Liu et al., 2001).

In the cardiovascular system, all four members of the Kir2.0 subfamily were found to be expressed in the cardiac ventricle and atrium, but Kir2.4 immunoreactivity was found exclusively in neuronal elements including perikarya of local parasympathetic ganglia (Liu et al., 2001). Kir2.4 shares 53-63 % similarity with other Kir2.0 subfamily members at the amino acid level. It is expressed predominantly in motoneurons of cranial nerve motor nuclei within the general somatic and visceral motor cell column. Heterologous expression of Kir2.4 in *Xenopus oocytes* and mammalian cells gives rise to low-conductance channels (15 pS) with a low Ba<sup>2+</sup> sensitivity, allowing dissection of Kir2.4 current from other Kir conductance (Topert et al., 1998).

### 1.3.3- Kir3.0 subfamily

The Kir3.0 subfamily is expressed as G-protein activated Kir channels in the heart, brain and endocrine tissues. Co-expressed G-protein coupled receptors activate Kir3.1 via G-protein  $\beta\gamma$  dimers. There is substantial evidence that the GIRK1/KGA (Kir3.1) carboxy-terminal tail is necessary for G  $\beta\gamma$  coupling, but not always sufficient. The G  $\beta\gamma$  subunits activate Kir3.1 by binding to the C-terminal (Reuveny et al., 1994). The human Kir3.1 gene has been mapped to chromosome 2 band q24.1 (Doupnik et al., 1995). The Kir3.1 (KGA) gene encodes a 501 amino acid polypeptide (Dascal et al., 1993) and the unique N- and C-terminal sequences within this structure are candidates involved in the control of gating by the  $\alpha$  and /or  $\beta\gamma$  subunits of G proteins (Dascal et al., 1993). Screening with the Kir3.1 cDNA probe resulted in the isolation of other members of this subfamily. The first predicted construct consists of a 414 amino acid polypeptide known as mbGIRK2 (Kir3.2); the second consists of 376 amino acids and is known as mbGIRK3 (Kir3.3) (Lesage et al., 1994). Kir3.2, like Kir3.1, displays a basal activity independent of G-protein coupled receptor activation. Kir3.2 and Kir3.3 are specifically expressed in the central nervous system, in contrast to Kir3.1 which is expressed in the heart as well as in the brain (Lesage et al., 1994). Kir3.3 may contribute further to Kir3.0 subfamily channel diversity by co-assembling with other members to form unique channels. For example, Kir3.2 exhibits receptor-evoked  $K^+$  currents like Kir3.1 when expressed in *Xenopus* oocytes with Kir3.3, but channel activity is not expressed by Kir3.3 by itself (Bradley et al., 1994).

The fourth member of this subfamily is called GIRK4 (Kir3.4), which encodes for 419 amino acids and shows high structural similarity to other subfamily members of G-protein-activated inwardly rectifying  $K^+$  channels (Spauschus et al., 1996). This member has been identified in the human hippocampus. Despite the structural similarity to a putative rat  $K_{ATP}$  channel (41 % similarity with Kir6.2 using <http://www.ebi.ac.uk/clustalw>), no ATP sensitivity or  $K_{ATP}$ -typical pharmacology was observed for Kir3.4 alone or Kir3.4 transfected in conjunction with other Kir3.0 channels in COS-7 (Spauschus et al., 1996).

#### 1.3.4- Kir4.0 and Kir5.0 subfamilies

Kir4 and Kir5 have been found in brain tissue (Bond et al., 1994; Takumi et al., 1995). Kir4.1 forms weakly rectifying K<sup>+</sup> channels when expressed alone (Bond et al., 1994). Similar to the Kir3.0 subfamily, Kir5.1 does not form channels by itself when expressed in *Xenopus* oocytes, but the two subunits, Kir4.1 and Kir5.1, can form a novel channel when expressed together (Takumi et al., 1995). They form dimers and tetramers producing channels with the properties of homomeric Kir4.1 channels. Kir5.1 may have a similar role to Kir3.3, permitting co-assembly with other Kir channel subunits (Doupnik et al., 1995).

#### 1.3.5- Kir6.0 subfamily

Based on the homology to Kir1.1 (Inagaki et al., 1995), a novel ubiquitously expressed gene was isolated, which was called uK<sub>ATP1</sub> (Kir6.1). Kir6.2, another isoform of the Kir6.0 subfamily, was cloned from pancreatic  $\beta$ -cells (Inagaki et al., 1995). Expression of active Kir6.0 channels required the co-expression of Kir6.2 or Kir6.1, with the high-affinity sulphonylurea receptor SUR (Nichols and Lopatin, 1997) (see section below).

#### 1.3.6- Kir7.0 subfamily

This subfamily is relatively newly discovered and is most homologous (38 %) to Kir1.3, but different in primary structure and function. Kir7.1 does not show any sensitivity to intracellular ATP. It has a very low single channel conductance (~50 fS) and low sensitivity to blockage by external Ba<sup>2+</sup>. The channel is expressed in a wide variety of tissues: brain, kidney, small intestine, prostate, testis, and other tissues (Krapivinsky et al., 1998). The Kir7.1 channel does not appear to be regulated and may be responsible for setting resting membrane potentials in a diverse array of tissues. Three amino acid residues are normally present in the pore regions of all other Kir, Leucine (L), Arginine (R), and Aspartic (E) or glutamic acid (D), but are replaced by serine (S), methionine (M), and glycine (G), respectively, in Kir7.1. These three amino acids may play a role in the determination of single channel conductance in this isoform (Krapivinsky et al, 1998).

### 1.3.7- KirD subfamily

The KirD subfamily is another newly identified family of inward rectifier channels with a double pore domain. It has been shown to have a structure equivalent to a Kir subunit in tandem with a six-transmembrane domain Kv subunit and expresses outwardly rectifying K<sup>+</sup> currents in *Xenopus* oocytes (Ketchum et al., 1994). It is notable that many Kv channels also show weak inward rectification under certain physiological conditions, which involves a weakly voltage-dependent block by internal Na<sup>+</sup> and Mg<sup>+</sup> ions (Nichols and Lopatin, 1997).

### 1.4- Overview of the ATP-sensitive potassium channel

The ATP-sensitive potassium channels (K<sub>ATP</sub>) are usually inactive in the normal condition and become activated by changes in intracellular nucleotide concentrations (Cook, 1990). K<sub>ATP</sub> channels exist as an octameric complex containing two distinct types of protein subunit (Shyng and Nichols, 1997). They compose four subunits from the inwardly rectifying K<sup>+</sup> channel family, Kir6.0, and four regulatory sulphonylurea receptor subunits (SUR) (Figure 1-4,B) (Babenko et al., 1998; Schwappach et al., 2000; Shyng and Nichols, 1997; Clement et al., 1997). There are two isoforms of the Kir6.0 subunit, Kir6.1 and Kir6.2, which are expressed in different tissues and subcellular compartments. Kir6.0 subunits have intracellular N- and C-termini and two transmembrane segments, M1 and M2, separated by a P-loop that forms the outer mouth of the pore (Figure 1-4,A) (Aguilar-Bryan and Bryan, 1999). There are three SUR isoforms that have been identified; SUR1 and SUR2 that produce SUR2A and SUR2B by splice variation. The SUR subunits are large proteins thought to contain three transmembrane domains, TMD0, TMD1 and TMD2, with 5 + 6 + 6 transmembrane alpha-helical segments, respectively (Aguilar-Bryan and Bryan, 1999). Nucleotide binding folds, which detect cytoplasmic nucleotide levels and reflect the metabolic status of the cell, are located on the intracellular loop between TMD1 and TMD2 and on the long intracellular C-terminus. Different subunit combinations are found in different tissues (Figure 1-4,C). For example, K<sub>ATP</sub> channels of pancreatic beta

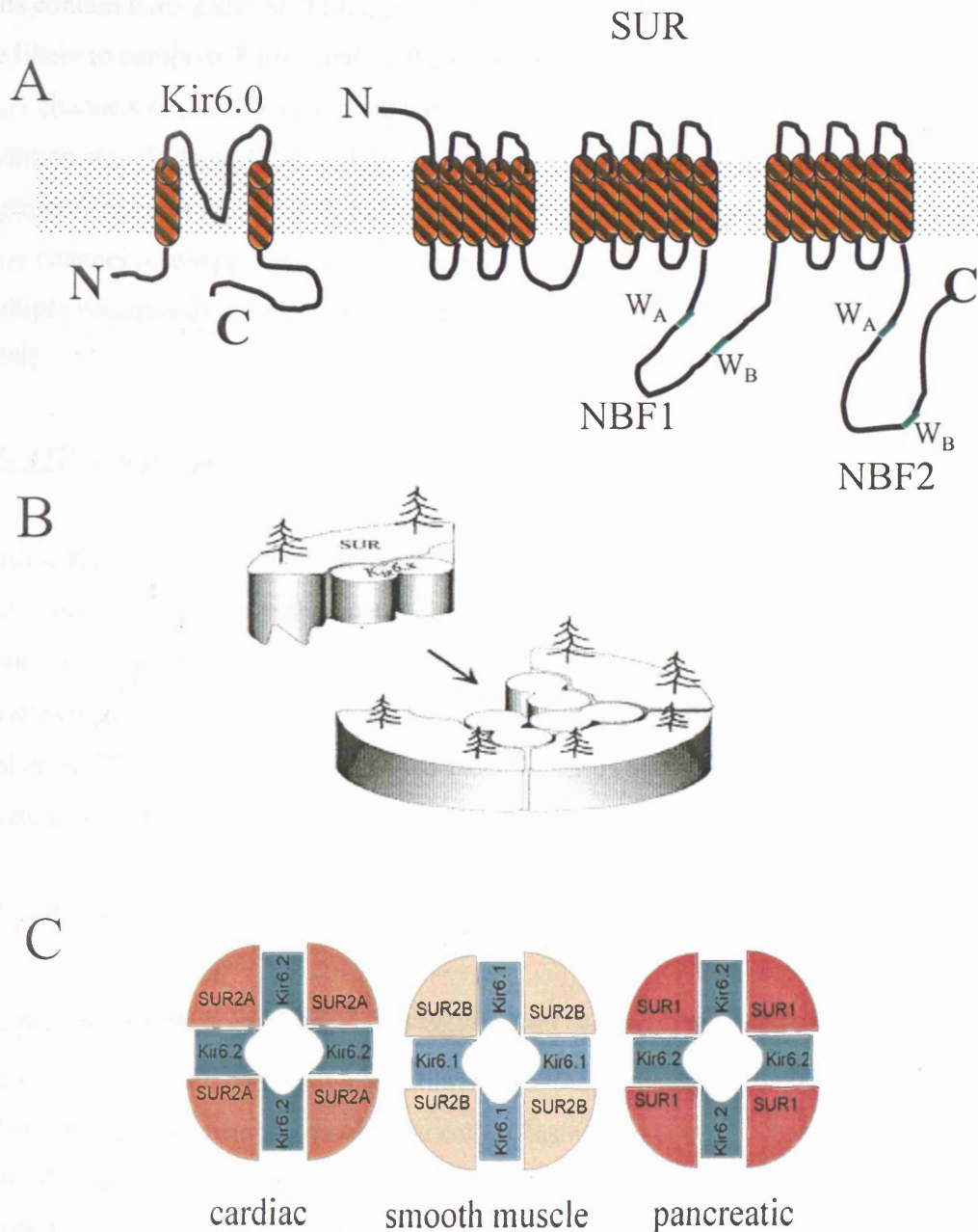


**Figure 1-4 ATP-sensitive Potassium channels.** A, Four Kir6.0 subunits form the pore region and sulphonylurea receptor subunits regulate the channel activity, which include NBF1 and 2 with W<sub>A</sub> and W<sub>B</sub> in both of them. B, Heteromultimers consist of four sulphonylurea receptor (SUR) and four Kir6.0 subunits. C, Expression of functional K<sub>ATP</sub> channels requires both subunit types to be present and in different cell types different isoforms are present (Babenko et al., 1998).

cells contain Kir6.2 and SUR1 subunits, while those in the sarcolemma of cardiac muscle are likely to comprise Kir6.2 and SUR2A (Yokoshiki et al., 1998). Expression of functional  $K_{ATP}$  channels requires both subunit types to be present, since endoplasmic reticulum (ER)-retention signals on each subunit are masked only when both subunits are expressed together (Zerangue et al., 1999; Schwappach et al., 2000). The molecular diversity of the  $K_{ATP}$  channel across species and tissue types is further expanded by the presence of multiple isoforms of the SUR (SUR1, SUR2A, SUR2B) (Figure 1-4,C) (Babenko et al., 1998).

### 1.5- ATP-sensitive potassium channel function

Cardiac  $K_{ATP}$  channels were first described in the heart in 1983 (Noma, 1983), then accumulating studies have shown that similar types of  $K^+$  channels are present in many tissues, including pancreatic  $\beta$ -cells, skeletal muscle cells, vascular and other smooth muscle cells, neuronal cells, endothelial cells, and renal epithelial cells (Figure 1-4, C) (Ashcroft, 1996; Ashcroft and Ashcroft, 1990; Edwards and Weston, 1993; Quast, 1996; Terzic et al., 1995).

#### 1.5.1- Pancreatic $\beta$ -cells

The presence of the  $K_{ATP}$  channel in  $\beta$ -cells is well defined. The opening of  $K_{ATP}$  channels in  $\beta$ -cells is regulated by the concentration of glucose in the blood, which modulates the cellular energy and metabolism of these cells, (Rasmussen et al., 1990; Cook and Taborsky, 1990; Prentki and Matschinsky, 1987). A number of studies have established that the metabolic and ionic events in  $\beta$ -cells are critical in stimulus-secretion coupling of insulin (Henquin and Meissner, 1984; Wollheim and Biden, 1986; Wolf et al. 1988).  $K_{ATP}$  channels play a pivotal role in this control by sensing the metabolic state of the cell (Cook et al., 1988; Ashcroft and Rorsman, 1989). When glucose increases in the blood it enters the  $\beta$ -cell through a specific membrane-bound glucose transporter GLUT-2 (Virsolvy-Vergine et al., 1996; Heron et al., 1998). It is then phosphorylated by the enzyme glucokinase and metabolised, resulting ultimately in the phosphorylation of ADP to ATP,

thereby increasing the ATP/ADP ratio. A rising ATP/ADP ratio causes the  $K_{ATP}$  channels to close, which results in depolarisation of the cell membrane and the opening of voltage dependent  $Ca^{2+}$  channels, thus increasing the  $Ca^{2+}$  influx through these channels. The consequent a rise in cytoplasmic  $Ca^{2+}$  eventually activates the release of insulin from the granules (Gembal et al. 1993). In diabetes,  $K_{ATP}$  channel activity can be regulated by drugs, the most common of which are the sulphonylureas (tolbutamide, glibenclamide, glipizide, and others), which cause closure of the channel, membrane depolarisation and insulin secretion. Diazoxide has the opposite effect, increasing the channel's mean open probability and inhibiting insulin secretion. Diazoxide is commonly used in states of unregulated insulin secretion, particularly insulinomas and some cases of hyperinsulin secretion (Glaser et al., 2000; Gembal et al., 1993).

#### 1.5.2- Cardiac cells

$K_{ATP}$  channels have been identified in heart tissue, and it is believed that the  $K_{ATP}$  channels of cardiomyocytes are usually closed (Deutsch et al. 1991). These channels open during hypoxia or ischaemia when the intracellular ATP levels decrease, and cause a marked shortening of the cardiac action potential (Nichols and Lederer, 1991). This limits  $Ca^{2+}$  influx and thereby decreases contractility (Allen and Orchard, 1987; Lederer et al., 1989). As a consequence, the force of contraction produced by these cells and their energy expenditure are greatly diminished. This is thought to represent a protective mechanism that adapts the local energy expenditure to local energy supply and protects the energy reserves of the cardiac muscle cells during periods of interrupted blood supply (Cole et al., 1991). During surgical cardioplegia, potassium channel openers (KCO) are used to prevent the high  $K^+$  concentration (16 mM) (used during cardioplegia) from producing the observed  $Ca^{2+}$  loading of cardiac myocytes, and substantial energy utilization (Lopez et al., 1996).

During ischaemia and upon reperfusion, cardiac arrhythmias are often observed (Manning and Hearse, 1984). This is thought to be due to the shortening of the action potential duration by activation of  $K_{ATP}$  channels during ischaemia, and the consequent reduction in refractory period (Yokoshiki et al., 1998).

### 1.5.3- Vascular smooth muscle

K<sub>ATP</sub> channels are present in vascular smooth muscle cells and play an important role in the vascular responses to a variety of pharmacological and endogenous vasodilators (Edward and Weston, 1993). To date, a variety of structurally distinct potassium channel openers (KCOs) have been developed, including enothiadiazines (e.g., diazoxide), cyanoguanidines (e.g., pinacidil, P1075), nicorandil, minoxidil, benzopyrans (e.g., cromakalim, levcromakalim, aprikalim, SR 47063), tertiary carbinols (e.g., ZD-6169), and dihydropyridine derivatives (e.g., ZM-244085) (Edward and Weston, 1993). Some of these compounds show diverse relaxation effects on different vascular tissues. For example, the benzopyran KCO, JTV-506, demonstrates some selectivity for coronary blood vessels over the aorta *in vitro* and increases coronary blood flow in the absence of substantial changes in blood pressure *in vivo* (Hirata and Aisaka, 1997). Other K<sub>ATP</sub> activators have been found to stimulate the formation of cAMP and increase the activity of protein kinase A, e.g. calcitonin gene-related peptide, vasoactive intestinal polypeptide, prostacyclin and adenosine (Brayden, 2002). Part of the mechanism of contraction in response to endogenous vasoconstrictors is due to inhibition of K<sub>ATP</sub> channels. Activation of K<sub>ATP</sub> channels using KCO to induce arterial dilation has provoked interest in these channels as potential targets for the pharmacologic control of vascular contractility in disease conditions, such as hypertension and vasospasm (Nelson and Quayle, 1995; Quayle et al., 1997)

### 1.5.4- Hepatocytes

Information on the occurrence and role of K<sup>+</sup> channels in hepatocytes is limited, but it has been thought that K<sub>ATP</sub> channels play an important role in regulating hepatocyte proliferation (Malhi et al., 2000; Roman et al., 2002) and possibly adenosine uptake (Dufloot et al., 2004). The expression of mRNAs encoding K<sub>ATP</sub> channels subunits, Kir6.1, SUR1, and SUR2 has been detected in human liver cells (Malhi et al., 2000). This finding was further confirmed functionally by electrophysiological recordings showing a minoxidil-activated current that was inhibited by glibenclamide (Malhi et al., 2000) and by

immunodetection of Kir6.1, Kir6.2, SUR2A and SUR2B in the FAO hepatoma cell line (Duflot et al., 2004).

To determine whether  $K_{ATP}$  channels control liver growth, primary rat hepatocytes and several human hepatoma cell lines have been investigated.  $K_{ATP}$  channel openers (minoxidil, cromakalim, and pinacidil) increased cellular DNA synthesis, whereas  $K_{ATP}$  channel blockers (quinidine and glibenclamide) attenuated DNA synthesis indicating a possible role for  $K_{ATP}$  in liver growth control. Activity of the  $Na^+$  dependent adenosine receptor (CNT2) in hepatocytes is also blocked by  $K_{ATP}$  antagonist and enhanced by KCO, suggesting a role for  $K_{ATP}$  in coupling intracellular energy status to the requirement for uptake of adenosine (Duflot et al., 2004).

#### 1.5.5- In other tissues

$K_{ATP}$  channels are also present in other tissues, including skeletal muscle, nonvascular smooth muscles, neurons, endocrine cells (e.g., adenohypophysis), renal cells, vascular endothelial cells, and follicular cells of the ovary (Edwards and Weston, 1993; Lawson, 1996; Quast, 1996; Terzic et al., 1995). In most endocrine cells, hormonal secretion (e.g., growth hormone, cholecystokinin, insulin) is stimulated by depolarization (excitation-secretion coupling) (Bernardi et al., 1993; Mangel et al., 1994). In the renal tubular system,  $K_{ATP}$  channels have been found in the proximal tubule, thick ascending limb of Henle's loop, and cortical collecting duct (Quast, 1996). These channels are active under physiological conditions, producing  $K^+$  efflux on either the basolateral side (in the proximal tubule) or the luminal side (in the ascending limb and collecting duct). In endothelial cells,  $K_{ATP}$  channels serve as a regulator of the resting potential during energy impairment and may modulate the release of endothelium-derived relaxing factor under such conditions (Janigro et al., 1993; Katnik and Adams, 1995; Katnik and Adams, 1997; Kuo and Chancellor, 1995).

## 1.6- The clinical relevance

### 1.6.1- The role of $K_{ATP}$ channels in Ischaemic preconditioning

The process of ischemic preconditioning (IPC) was first reported by Murry et al. in 1986. IPC refers to a phenomenon in which brief episodes of hypoxia provide protection against a subsequent more prolonged period of ischaemia (Murry et al., 1986; Ardehali, 2004). This protection includes a reduction in both infarct size and the incidence of cardiac arrhythmias. Several activation pathways have been proposed as playing a role in IPC, including protein kinase C, various G-protein coupled receptors, and the generation of reactive oxygen species (ROS) and nitric oxide (Sato et al., 1998; Sasaki et al., 2000; Zhang et al., 2001). The signalling pathways by which the sarcolemmal  $K_{ATP}$  channel is activated during IPC and how it produces cardioprotection is unclear; however, a number of studies have shed some light on this topic. Noma in (1983) suggested that opening of sarcolemmal  $K_{ATP}$  channels might mediate the cardioprotective effects of IPC. The opening of these channels leads to shortening of the action potential and hyperpolarizing of the cell membrane (Noma, 1983). Shortening of the action potential would inhibit  $Ca^{2+}$  entry into the cell via L-type channels and prevent  $Ca^{2+}$  overload. Furthermore, the slowing of depolarization would also reduce  $Ca^{2+}$  entry and slow or prevent the reversal of the  $Na^+/Ca^{2+}$  exchanger. These actions may increase cell viability via a reduction in  $Ca^{2+}$  overload during ischaemia and early reperfusion (Gross and Peart, 2003).

While the  $K_{ATP}$  channel in the sarcolemma is thought to play a role in cardiac protection, a mitochondrial  $K_{ATP}$  is also believed to be involved in this process (Ardehali, 2004). It is unclear how the opening of the  $K_{ATP}$  channel in the mitochondria would lead to cardioprotection; however, three hypotheses have emerged to explain the link between mito $K_{ATP}$  channel opening and cardioprotection: (1) a decrease in mitochondrial  $Ca^{2+}$  uptake, (2) swelling of the mitochondrial matrix and changes in ATP synthesis, and (3) changes in the levels of reactive oxygen species (ROS) (Ardehali, 2004).

Murata (2001) showed that opening of mito $K_{ATP}$  resulted in a reduction of  $Ca^{2+}$  accumulation in the mitochondrial matrix during simulated ischaemia reperfusion. It has

been known for some time that the opening of the mitochondrial matrix  $K_{ATP}$  channels causes swelling, and that this in turn activates the respiratory chain providing more ATP to support the recovering myocardium (Halestrap, 1989; Grover and Garlid, 2000). The reactive oxygen species generated during the preconditioning period are thought to be protective (Vanden Hoek et al., 1998). However, the ROS that are produced during reperfusion are detrimental and causes cell death (Zweier and Jacobus, 1987; Vanden Hoek et al., 2000). Until now, no clear pathway has been suggested to show how the  $K_{ATP}$  channel plays its role in the cardioprotection.

#### 1.6.2- The role of $K_{ATP}$ channels in Persistent Hyperinsulinemic-Hypoglycemia of Infancy

PHHI is an inherited genetic disorder of glucose metabolism that presents in newborns and infants, recognized by inappropriately high insulin levels regardless of the low level of glucose in the blood (Aynsley-Green et al., 1981; Sharma et al., 2000). About 50 known mutations in  $K_{ATP}$  channel genes have so far been identified in patients with PHHI (Kane et al., 1996; Permutt and Ghosh, 1996; Sharma et al., 2000). These mutations are present in both subunits of  $K_{ATP}$  channel (Kir6.2/SUR1), mostly in the SUR1 subunit, especially in the NBF2, and are thought to have different effects on the  $K_{ATP}$  function. The cause of PHHI is the failure of  $K_{ATP}$  channels to open in response to glucose deprivation. The failure of response might result from inability of the channel to respond to the stimulating effect of MgADP or decreased expression of the channel on the cell surface. As outline below (section 1.11), normal expression of the  $K_{ATP}$  channel requires co-assembly of SUR1 and Kir6.2 into an octameric complex. Mutation leading to C-terminal truncation of SUR1 may cause PHHI by preventing normal channel trafficking (Taschenberger et al., 2002). One of the mutations in SUR1 which affects normal assembly and trafficking on the channel is the mutation of leucine to proline at position 1544 (L1544P) (Taschenberger et al., 2002). Two other mutations have been reported to cause defective  $K_{ATP}$  channels:  $\Delta F1388$  and R1394H.  $\Delta F1388$  abolished expression from the cell surface (Cartier et al., 2001). The R1394H mutation has recently been reported to cause channel retention in the Golgi compartment when expressed in HEK293 cells (Partridge et al., 2001). The other form of PHHI results from a reduced response to MgADP stimulation. Examples of this kind of

mutation are F591L, T1139M, R1215Q and G1382S in the NBFs, which are expected to cause hyperinsulinism because the channel will be less responsive to an increase of intracellular [ADP]:[ATP] (Shyng et al., 1998). Together these results indicated that elements with the proximal C-terminal of the SUR subunit may be important for masking the ER retention site. The result also show the sensitivity of the channel to single point mutation in this region, which may lead to a failure of channel assembly or loss of the proper channel function (Partridge et al., 2001).

### 1.7- Hallmarks of the inwardly rectifying subunit of $K_{ATP}$ channels

#### 1.7.1- Cloning of the Kir6.1 subunit

Kir6.1 ( $uK_{ATP-1}$ ) was cloned by screening a rat pancreatic islet cDNA library with a  $^{32}P$ -labeled GIRK cDNA fragment as a probe, and this resulted in five positive  $\lambda$  clones. The sequence of 2389 base pairs contains a single open reading frame encoding a protein of 424 amino acids. The predicted amino acid sequence of Kir6.1, which represents a different Kir subfamily, shows 43, 46 and 43 % identity with ROMK1 (Kir1.1), IRK1 (Kir2.1) and GIRK1 (Kir3.1) respectively (Inagaki et al., 1995). Tissue expression of Kir6.1 was investigated by Northern blot analysis. This revealed that Kir6.1 is expressed in all the rat tissues that were examined with different expression levels. The mRNAs of Kir6.1 are expressed at high levels in the heart, ovary and adrenal gland, at moderate levels in skeletal muscle, lung, brain, stomach, colon, testis, thyroid and pancreatic islets, and at low levels in the kidney, liver, small intestine and pituitary (Inagaki et al., 1995). The absence of Kir6.1 mRNA in insulin-secreting cells suggests that another  $K_{ATP}$  channel subunit is expressed in these cells (Inagaki et al., 1995). Kir6.1 has been shown to reconstitute active  $K_{ATP}$  channels with SUR1, and SUR2B (Aguilar-Bryan et al., 1998) and with SUR2A under certain conditions i.e. in present of high concentration of dinucleotide (Kano et al., 2000).

### 1.7.2- Cloning of the Kir6.2 subunit

Kir6.2 (rBIR) was cloned in a hybridization probe of the rat genomic library using  $^{32}\text{P}$ -labelled full-length Kir6.1 cDNA as probe. Seventeen positive  $\lambda$  clones were sequenced with a distinct similarity to Kir6.1, and the longest clone revealed a single open reading frame encoding a 390 amino acid protein (Inagaki et al., 1995). Cloning and sequencing a cDNA library isolated from an insulin-secreting cell line showed a 96% identity with Kir6.2 (hBIR). The expression and localization of the Kir6.2 (BIR) subunit was investigated using Northern blot analysis. This revealed that the Kir6.2 gene is expressed in large amounts in pancreatic islets cells, and in smaller amounts in heart, skeletal muscle and brain. Similar analysis showed co-expression of SUR1 in large amounts in pancreatic islets cells but in smaller amounts in the brain, while it was absent from the heart (Inagaki et al., 1995). Kir6.2 has been shown to reconstitute  $\text{K}_{\text{ATP}}$  channels when co-expressed with SUR1, SUR2A and SUR2B (Aguilar-Bryan et al., 1998).

### 1.7.3- Kir6.0 polypeptides

The Kir6.0 subfamily has been predicted to have two transmembrane spanning domains (Clement et al., 1997), M1 and M2, flanking a pore loop with a Gly-Phe-Gly or Gly-Tyr-Gly sequence that has been identified in other potassium selective channels (Doupnik et al., 1995). The Kir6.0 channels are inwardly rectifying channels that allow potassium to pass weakly in the outward direction. Mutation of asparagine to aspartate at position 160 (N160D) of Kir6.2 leads to strong inwardly rectifying channels as a result of the induction of high sensitivity to blocking by intracellular spermine (Shyng and Nichols, 1997). By contrast, Kir2.1 (IRK1), a strong rectifier, can be changed to a weak rectifier by the mutation of the equivalent residue D172N (Tagliatela et al., 1995). The N160 in the Kir6.2 is located within the transmembrane M2 domain and suggests that this segment forms part of the  $\text{K}_{\text{ATP}}$  pore structure (Aguilar-Bryan et al., 1998). Expression of Kir6.0 alone *in vivo* did not produce functional  $\text{K}_{\text{ATP}}$  sensitive channels and expression requires the presence of a SUR subunit (Zerangue et al., 1999 Aguilar-Bryan et al., 1998).

#### 1.7.4- Endoplasmic reticulum retention sequence in Kir6.0 subunits

The cell surface expression of Kir6.0 subunits is regulated by a three amino acid sequence (RKR) in the C-terminal of the subunit, called the trafficking sequence, which is responsible for preventing the surface expression of Kir6.2 without co-assembly with a SUR subunit (Zerangue et al., 1999). The truncation of the C-terminal of Kir6.1 or Kir6.2 increases the surface expression of Kir6.1 or Kir6.2 without the need for co-expression of a SUR subunit (Tucker et al., 1997). Zerangue and colleagues (1999) investigated the trafficking mechanisms of  $K_{ATP}$  channel subunits. They found that removing 20 but not 18 amino acids from the end of Kir6.2 resulted in a channel that exhibited azide-induced currents and surface expression of Kir6.2 $\Delta$ 20 or Kir6.1 $\Delta$ 20. Comparing the sequences of Kir6.2 and Kir6.1 indicates that a cluster of three amino acid sequences (RKR) was conserved in the C-terminal of both subunits. This cluster was 20 amino acids away from the C-terminal end. Replacing the RKR sequence in Kir6.2 with alanine in each position (AAA), allowed the subunit to reach the surface. Transferring the RKR sequence to another inwardly rectifying  $K^+$  channel, Kir2.1, which is normally able to traffic to the cell surface without  $\beta$ -subunits, reduced the surface expression and currents of this isoform. Together these results indicate that when present the RKR sequence controls the surface expression of Kir subunits. The possible interaction of Kir6.2 with itself in the absence of SUR1 was also examined by Zerangue et al (1999). Injecting cells with equal amounts of mRNA for Kir6.2 $\Delta$ 36 and Kir6.2 reduced the surface expression of Kir6.2 $\Delta$ 36 current by over 90%. This indicates that in the absence of SUR1, wtKir6.2 formed mixed oligomer with Kir6.2 $\Delta$ 36, thereby reducing overall surface expression of  $K_{ATP}$  currents due to the presence of RKR sequence in the oligomer form.

#### 1.7.6- Interaction between the C- and N-termini of Kir6.0

A physical interaction between the two intracellular domains of Kir6.2 (N- and C-terminals) was defined within the N-terminal of the inwardly rectifying potassium channel (Kir6.2) (Tucker and Ashcroft, 1999). The binding of [ $^{35}$ S]methionine-labelled C-terminal domain to serial truncations of the N-terminal domain was investigated to identify binding

to the C-terminal. The truncated N-terminal of Kir6.2 still retained the ability to interact with the C-terminal when either residues 1-29 or residues 47-53 were deleted. This implied that the binding site for the C-terminal is within residues 30-46. This region showed a great sequence conservation between different Kir subfamilies and is predicted to contain two  $\beta$ -strand structures (Tucker and Ashcroft, 1999). The sequence homology and secondary structure conservation within the region suggests that this interaction is likely to be common to all members of the Kir channel family. Mutation of a highly conserved glycine residue (Gly-40) within the interaction domain of Kir6.2 to aspartate shows disruption in the current recording when expressed with SUR1 (Figure 1-5) (Tucker and Ashcroft, 1999). This interaction highlights the importance of this residue in this interaction and is found to be common to all members of the Kir channel family (Tucker and Ashcroft, 1999).

#### 1.7.7- Heteromultimerization of Kir6.2 and Kir6.1

Cui et al. (2001) were able to show that it is possible for different pore-forming subunits of  $K_{ATP}$  to co-assemble. Using mixtures of Kir6.1 and Kir6.2 expressed with SUR1 subunit were able to demonstrate a spectrum of five single-channel conductances, implying all possible combinations of Kir6.1 and Kir6.2 in homo- and heteromultimeric currents were present. A heteromultimeric construct (Kir6.1-Kir6.2) produced a single-channel conductance intermediate between those of Kir6.1 and Kir6.2 when expressed with SUR2B. They also showed co-immunoprecipitation of Kir6.2 with Kir6.1 and vice versa. Therefore, it is believed that Kir6.1 and Kir6.2 readily co-assemble to produce functional channels, and such phenomena may contribute to the diversity of nucleotide-regulated potassium currents seen in native tissues (Cui et al., 2001).

In another study, the variation in reported  $K_{ATP}$  channel conductances in different cardiac regions led to the suggestion that the composition of the hetero-octamer is more complex than what was thought (Pountney et al., 2001). For example, the unitary  $K_{ATP}$  channel conductance of atrial and purkinje cells is 58-60 pS, while in ventricular cells it was 77 pS (Pountney et al., 2001). Pountney and colleagues illustrated the possibility of

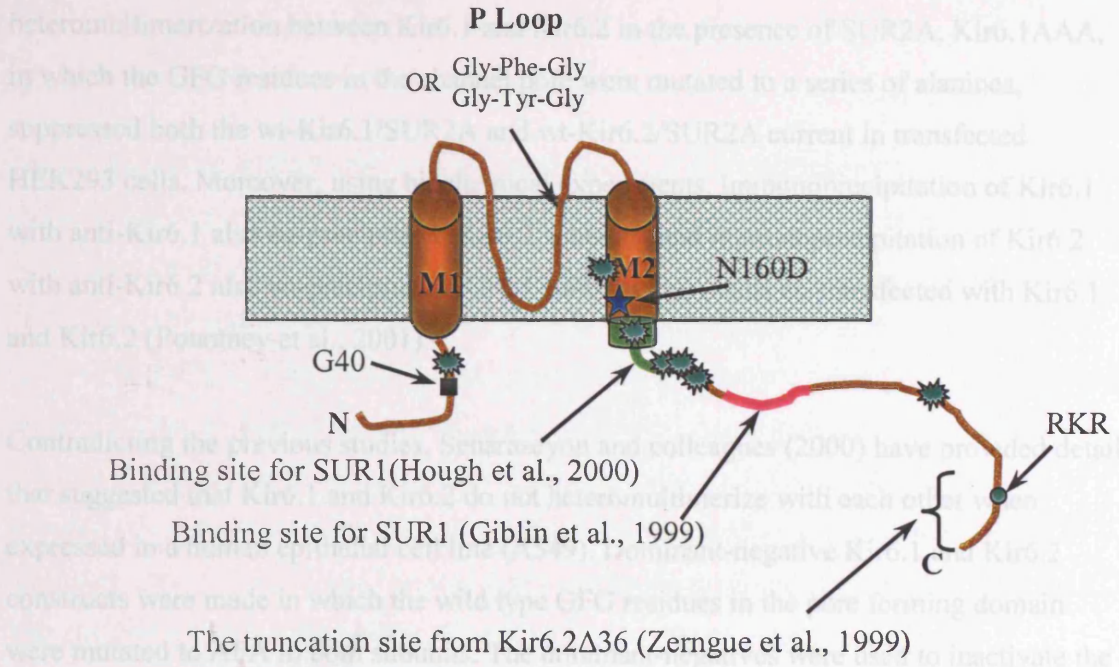


**Figure 1-5 Hallmarks of Kir6.2 subunit.** Diagram showing the C- and N- termini of Kir6.0 with some active region and showing the two transmembrane domain with the P loop between them. (●) RKR the endoplasmic retention sequence (Zerngue et al., 1999). (★) Mutation of asparagine to aspartate at position 160 leads to strong inward rectification (Shyng et al., 1997). (■) G40 involved in a physical interaction with C-terminal of Kir6.2 (Tucker et al., 1999). (⚡) ATP binding site R50, C166, T171, I176, E179, K185 (Tucker et al., 1998; 1997) and aa 334-337 (Drain et al., 1998).

heteromultimerization between Kir6.1 and Kir6.2 in the presence of SUR2A. Kir6.1AAA, in which the GFG residues in the channel pore were mutated to a series of alanines, suppressed both the wt-Kir6.1/SUR2A and wt-Kir6.2/SUR2A current in transfected HEK293 cells. Moreover, using biochemical experiments, immunoprecipitation of Kir6.1 with anti-Kir6.1 also co-precipitated Kir6.2 subunits, and immunoprecipitation of Kir6.2 with anti-Kir6.2 also co-precipitated Kir6.1 subunits from cells co-transfected with Kir6.1 and Kir6.2 (Pountney et al., 2001).

Contradicting the previous studies, Seharaseyon and colleagues (2000) have provided detail that suggested that Kir6.1 and Kir6.2 do not heteromultimerize with each other when expressed in a human epithelial cell line (A549). Dominant-negative Kir6.1 and Kir6.2 constructs were made in which the wild type GFG residues in the pore forming domain were mutated to AFA in both subunits. The dominant-negatives were used to inactivate the function of wild type subunits. Co-expressing A549 cells with Kir6.2/SUR2A and the dominant-negative Kir6.2AFA suppressed the pinacidil-activated surface  $K_{ATP}$  currents, but Kir6.1 AFA had no effect. The Kir6.1 AFA mutant was able to suppress the current from cells coexpressing Kir6.1/SUR2B, but not cells expressing Kir6.2/SUR2A. Therefore, it was concluded that Kir6.1 and Kir6.2 do not heteromultimerize with each other (Seharaseyon et al., 2000).

The use of different cells for the expression and the differences in the mutant construct may be behind the conflicting results; in conclusion the heteromultimerization of Kir6.0 subunits needs to be confirmed.

In another more recent study using similar methods, pore loop mutated rat Kir6.1 and Kir6.2 were both shown to suppress sarcolemmal  $K_{ATP}$  current in rat cardiomyocytes suggesting that both isoforms may co-assemble in the cardiac cell membrane (Van Bever et al., 2004).

## 1.8- Hallmarks of the sulphonylurea receptor subunit in $K_{ATP}$ channels

### 1.8.1 Cloning of the sulphonylurea receptors (SUR1)

The identification and cloning of SUR1 was initiated by the purification of the radioiodinated glyburide binding protein from hamster tissue which the N-terminal amino acid sequence (PLAFCGTENHSAAYRVDQVLNNGC) from the intact molecule was determined (Aguilar-Bryan et al., 1995). Two antibodies, against PLAFCGTE and HSAAYRVDQGV, were generated and were able to immunoprecipitate the photolabelled SUR. This amino acid sequence was used to generate a degenerate polymerase chain reaction (PCR) primer to screen for SUR1 sequence and a 1.1 Kb cDNA was cloned that encoded this protein segment. This cDNA fragment was used to screen phage libraries of rat insulinoma (RINm5F) and hamster insulin-secreting tumour cells (HIT T15). Northern blot analysis of mRNA from RINm5F and HIT T15 cells revealed transcripts of approximately 5000 nucleotides and open reading frames encoding 1582 residues with 98% identity were determined in each case. Cells transfected with hamster or rat SUR cDNA expressed a 140 KDa polypeptide that could be photolabelled with radioiodinated glyburide also co-migrated with native SUR1 from HIT cells (Aguilar-Bryan et al., 1995).

### 1.8.2- Cloning of the SUR2A subunit

SUR2A was isolated by screening a rat brain cDNA library with a  $^{32}\text{P}$ -labeled hamster SUR1 cDNA using low stringency hybridization conditions (Inagaki et al., 1996). This resulted in identification of a gene expressing a single open reading frame encoding a protein of 1545 amino acid residues, having 68% identity with SUR1 (Inagaki et al., 1996). The localization and the level of expression of SUR2A mRNA was investigated in rat tissues with the Northern blot technique. This showed a high level of expression in the heart, skeletal muscle and ovary; a moderate level in the brain, tongue and pancreatic islets; and a low level in the stomach, colon, thyroid and pituitary (Inagaki et al., 1996).

Co-expression of SUR2A and Kir6.2 in COS1 cells evoked  $\text{K}^+$  currents with a similar single channel conductance but with different kinetic and pharmacological properties, compared to the Kir6.2/SUR1,  $\beta$  cell  $K_{ATP}$  channel. Also the activity of Kir6.2/SUR2A

heterooligomer was less sensitive to ATP and glibenclamide inhibition. In addition, unlike Kir6.2/SUR1, diazoxide, a  $K_{ATP}$  opener, produced no  $K_{ATP}$  activation when Kir6.2 and SUR2A were co-transfected in COS1 cells (Inagaki et al., 1996).

#### 1.8.3- Cloning of the SUR2B subunit

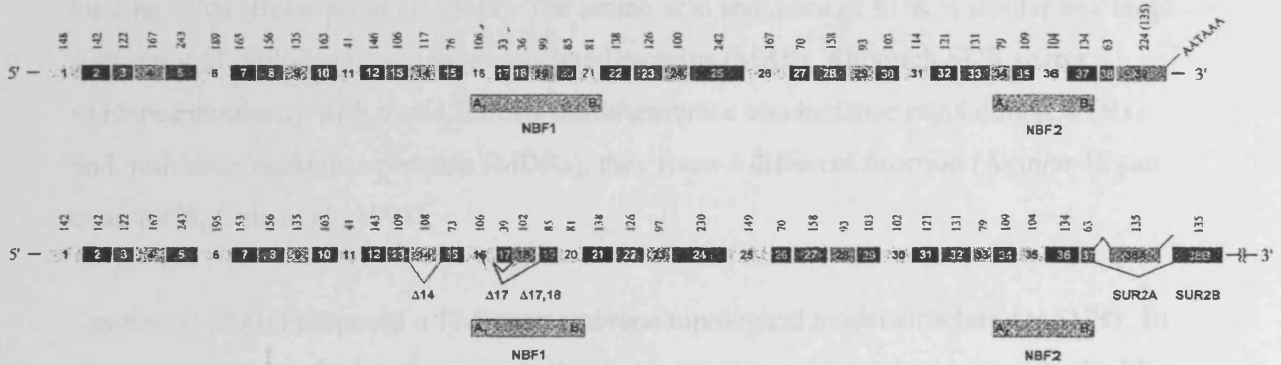
SUR2B was identified by screening a mouse heart cDNA library with a nucleotide fragment with 86 % sequence homology to SUR1 (Chutkow et al., 1996). Forty nine positive clones were obtained, and two of these clones, named MCS3 and MCS10, were sequenced. MCS10 contained a single open reading frame encoding a protein of 1546 amino acid residues. The amino acid sequence cloned showed 67% identity with rat SUR1 and 97% identity with that of rat SUR2A with variation only in the C-terminal 45 amino acid residues (Isomoto et al., 1996). The distributions of SUR2B and SUR2A in tissues were determined using an RT-PCR assay. This showed that SUR2A mRNA is expressed in the cerebellum, eye, atrium, ventricle, urinary bladder and skeletal muscle, whereas SUR2B is expressed in all the above and also in the forebrain, lung, liver, pancreas, kidney, spleen, stomach, small intestine, colon, uterus, ovary and fat tissue (Isomoto et al., 1996).

#### 1.8.4- Sulphonylurea receptor polypeptide

Mapping the intron-exon boundaries of the SUR1 and SUR2 genes shows a large similarity between them. The SUR1 gene has 39 exons spanning approximately 100 Kb of genomic DNA (Aguilar-Bryan et al., 1998). It encodes a protein of either 1581 or 1582 amino acids, depending on the alternative splice site at the 5' boundary of exon 17, which results in the inclusion of an additional serine residue (Babenko et al., 1998). The SUR2 gene has 38 exons spanning >100 Kb of DNA. The SUR2 gene specifies at least two main types of low-affinity sulphonylurea receptors, designated SUR2A and SUR2B, which result from differential usage of two 135 bp exons specifying the C-terminal 45 amino acids of the two proteins (Babenko et al., 1998) (Figure 1-6). In addition, splice variants SUR2 $\Delta$ 14,  $\Delta$ 17 and  $\Delta$ 17, 18 have been identified. It is not clear if the proteins produced from these

### SUR1 Gene (11p15.1)

- Average exon size is ~ 124 bp  
 - 39 Exons, 1581 amino acids.



### SUR2 Gene (12p11.12)

- Average exon size is ~ 122 bp  
 - 38 Exons, 1549 amino acids.

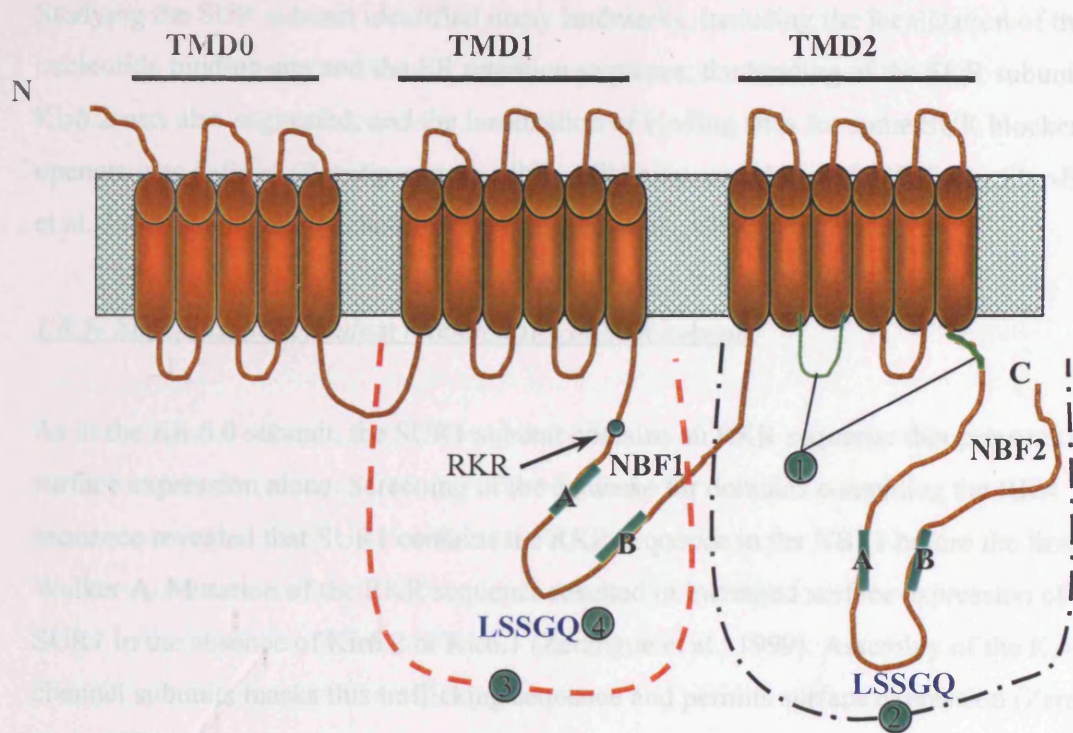
**Figure 1-6. Schematic representation of human SUR1 and SUR2 gene.** The SUR1 has 39 exons, whereas SUR2 gene has 38 exons. SUR2A and SUR2B differ in their last 45 amino acids ( taken from Aguilar-Bryan et al., 1998).

additional splice variants contribute to functional channels or are physiologically significant (Babenko et al., 1998).

SUR are members of a large family of proteins referred to as the ATP binding cassette (ABC) transporter superfamily with multiple transmembrane domains and two nucleotide-binding folds (Babenko et al., 1998). The amino acid sequence of SUR is similar to a large subfamily of multidrug resistance associated proteins (MRP). Although SUR shares sequence similarity with cystic fibrosis transmembrane conductance regulators (CFTRs) and multidrug resistance proteins (MDRs), they show a different function (Aguilar-Bryan et al. 1998; Cole et al., 1991).

Conti et al (2001) proposed a 17-transmembrane topological model structure for SUR1. In their study, two methods were used. In the first method, cysteine scanning was used with a biochemical surface-labelling assay to determine the location of external loops. In the second method, FLAG-epitope tags were introduced and evaluated for internal or external location using immunocytochemistry. This showed that the transmembrane segments of SUR1 are arranged in a 5 + 6 + 6 topology in the TM0, TM1 and TM2 domains respectively (Figure 1-7). It is likely that SUR2A and SUR2B have identical topologies to SUR1, given their high sequence homology, similar hydrophobicity profiles and similar function (Conti et al., 2001).

The SURs have two large cytosolic domains between TM11, TM12 and at the C-terminal that have been suggested to function as nucleotide-binding folds on the basis of consensus ATP-binding Walker A and Walker B motifs (Walker et al., 1982). The first nucleotide-binding fold 1 (NBF1) comes after the first 11 transmembrane domains (TM0 and TM1) and the second nucleotide-binding fold (NBF2) comes after the last 6 transmembrane domains (TMD2) (Tusnady et al., 1997). The NBFs of SUR have all of the hallmarks of the ABC family, including the Walker A (Gly-X-X-Gly-X-Gly-Lys-Ser/Thr- where X is any amino acid) and B (Y-Y-Y-Y-Asp- where Y is a hydrophobic amino acid) and a conserved Leu-Ser-Gly-Gly-Gln sequence (Aguilar-Bryan et al., 1998).



- RKR the endoplasmic retention sequence (Zerangue et al., 1999)
- ① Binding of KCO (P1075) in SUR1 (Uhde et al., 1999)
- ② Required for cromakalim stimulation in SUR2 (D'hahan et al., 1999)
- ③ Required for pyrimidine KCO, diazoxide stimulation (D'hahan et al., 1999)
- ④ Linker region (LSSGQ) (Ames and Lecar, 1992)

**Figure 1-7 Hallmarks of the sulphonylurea receptors subunit.** Diagram showing the 5+6+6 topological arrangement of the transmembrane segments of an SUR, TMD0, TMD1 and TMD2 domains. The first nucleotide-binding fold 1 (NBF1) comes after the first 11 transmembrane domains (TMD0 and TMD1) and the second nucleotide-binding fold (NBF2) comes after the last 6 transmembrane domains (TMD2) (Tusnady et al. 1997). Both of the NBFs contain a Walker A and B motif (Conti, 2001) and a linker (LSSGQ) region.

Studying the SUR subunit identified many landmarks, including the localization of the nucleotide binding site and the ER retention sequence; the binding of the SUR subunit with Kir6.2 was also suggested, and the localization of binding sites for some SUR blockers or openers was defined (Zerangue et al., 1999; Mikhailov and Ashcroft, 2000; Aguilar-Bryan et al. 1998; Shyng and Nichols, 1997; Babenko et al., 1998).

#### 1.8.5- Endoplasmic reticulum retention site in SUR subunit

As in the Kir 6.0 subunit, the SUR1 subunit contains an RKR sequence that prevents its surface expression alone. Screening of the database for domains containing the RKR sequence revealed that SUR1 contains the RKR sequence in the NBF1 before the first Walker A. Mutation of the RKR sequence resulted in increased surface expression of the SUR1 in the absence of Kir6.2 or Kir6.1 (Zerangue et al., 1999). Assembly of the  $K_{ATP}$  channel subunits masks this trafficking sequence and permits surface expression (Zerangue et al., 1999).

#### 1.8.6- Binding of the NBF1 and NBF2

In another similarity with the Kir6.0 subunit, intramolecular interaction within the SUR subunit has been suggested mediated by the NBFs (Mikhailov and Ashcroft, 2000). When SUR1 was divided into two halves at P-1042, such that each half contained one of the NBFs, individual expression resulted in no glibenclamide binding activity. However, significant glibenclamide binding activity was observed when the two halves were co-expressed. The GFP fusion protein NBF1G was distributed throughout the cell when expressed alone but co-expression of the C-terminal half of SUR1 with NBF1G showed plasma membrane localization of NBF1, demonstrating a strong interaction between the N- and C-terminal halves of SUR1 (Mikhailov and Ashcroft, 2000). NBF1 is the major cytosolic domain in the N-half of SUR1. It seemed that NBF1 interacts with the C-terminal half of SUR1 to facilitate formation of functional SUR1. Removal of the NBF2 from the C-half by truncation did not affect the binding of glibenclamide when expressed with the N-terminal half, which suggested that the NBF2 does not contribute to glibenclamide binding.

Also in this study, co-expression of Kir6.2 and GFP-C- or N-half of SUR1 showed no detectable membrane localization of either, which suggested that half of SUR1 was not sufficient to mask the ER sequence of Kir6.2 and to allow it to be trafficked to cell membrane Kir6.2 (Mikhailov and Ashcroft, 2000).

In a later study, Hough et al. (2002) were able to confirm this finding in two different ways. In the first method, using *in vivo* expression of NBFs, [<sup>35</sup>S]methionine NBF1 was tagged with FLAG and [<sup>35</sup>S]methionine NBF2 was tagged with His<sub>6</sub>. The anti-FLAG affinity resin bind was able to co-immunoprecipitate the NBF2-His<sub>6</sub> in the presence of NBF1-FLAG but not in its absence. In the second method, using the rabbit reticulocyte lysate *in vitro* translation system, the same result was obtained, where the anti-FLAG antibody was able to co-immunoprecipitate NBF2-His<sub>6</sub> in the presence of NBF1-FLAG but not in its absence. In the same study, the investigation of the binding of Kir6.2 with NBFs showed no binding of NBF1 and non-specific protein aggregation of the NBF2 to the resin in the immunoprecipitation experiment (Hough et al., 2002)

### 1.9- Stoichiometry of the K<sub>ATP</sub> channel

To investigate the stoichiometry of Kir6.2 and SUR1 within the K<sub>ATP</sub> hetero-oligomer, two fusion constructs were created: a wild type SUR1-Kir6.2 protein, in which the SUR1 C-terminal was linked to the N-terminal of the Kir6.2, and a fusion SUR1 with a mutant [N160D] Kir6.2, which generated a K<sub>ATP</sub> channel that rectified strongly in the presence of cytoplasmic spermine (Shyng and Nichols, 1997). Co-expression of these fusion poreains resulted in five different conductances that responded to intracellular spermine with different sensitivity. This suggested that five different species of tetrameric channels were randomly assembled, with channels containing 0, 1, 2, 3 or 4 wild type SUR1-Kir6.2 with 4, 3, 2, 1 or 0 mutant SUR1-Kir6.2 [N160D], respectively. This indicated that four of either fusion proteins were involved in forming the channel (Figure 1-4). Co-expression of monomeric Kir6.2 with the fusion protein suppressed the K<sub>ATP</sub> channel conductance, but co-expression of monomeric Kir6.2, monomeric SUR1 and the fusion SUR1-Kir6.2 was

able to rescue the  $K_{ATP}$  channel activity and permitted the requisite stoichiometry of the  $K_{ATP}$  channel (Shyng and Nichols, 1997).

Clement et al. (1997) tested whether a fusion protein of SUR1 and Kir6.2 with a 1:1 stoichiometry was sufficient to permit formation of active channels. The study showed that SUR1-Kir6.2 fusions generate functional ATP-sensitive potassium selective channels that are activated by metabolic poisoning (Clement et al., 1997; Shyng and Nichols, 1997). A triple fusion protein, SUR1-(Kir6.2)<sub>2</sub> with one SUR1 subunit and two Kir6.2 subunits, was also engineered. When the triple fusion SUR1-(Kir6.2)<sub>2</sub> was transfected to COSm6 cells, 90 % of the transfected cells showed no  $K_{ATP}$  channel activity. Co-transfection of the triple fusion construct with monomeric SUR1 rescued channel activity. In cross-link experiments, it has been shown that SUR1 and Kir6.2 are physically associated in COSm6 cells. A complex with an estimated molecular mass of ~950 KD, which is reasonably consistent with four SUR1 subunits (~ 170 KD) and four Kir6.2 subunits (~45 KD), was identified after cross-linking by SDS-PAGE (Clement et al., 1997).

Chromosome localization studies have shown that the SUR and Kir6.0 genes are paired in the human genome. SUR1 and Kir6.2 genes are localized on the short arm of chromosome 11 at 11P15.1 with ~4500 base pairs (bp) between them (Inagaki et al., 1995). The SUR2 and Kir6.1 genes are paired on chromosome 12, SUR2 at 12p1.12 and Kir6.1 at 12p11.23 (Chutkow et al., 1996), but the distance between them remains to be determined. Why these genes are clustered in pairs is not known (Babenko et al., 1998).

### 1.10- Pharmacology of $K_{ATP}$ channels

#### 1.10.1- Potassium channel openers (KCOs)

The  $K_{ATP}$  channels in different tissues are made up of different Kir and SUR subunits and it is the diversity of SUR subunits that underlines the tissue specific pharmacology of the  $K_{ATP}$  channels (Edwards and Weston, 1993). The binding sites of both KCO and antagonists are found in the SUR subunits (Schwanstecher et al., 1998). The most common potassium channel openers (KCOs) are diazoxide, pinacidil, cromakalim, minoxidil sulfate,

and nicorandil (Ashcroft and Gribble, 2000). The use of these drugs may lead to shortening of the cardiac action potential, relaxation of vascular smooth muscle, and inhibition of insulin secretion in  $\beta$ -cell or neurotransmitter release (Grover and Garlid, 2000; Aguilar-Bryan et al., 1995; Inagaki et al., 1996; Chutkow et al., 1996). The activation by KCOs is evident only in the presence of ATP, where binding of ATP to the NBFs of the SUR subunit is required (Tucker et al., 1997; Schwanstecher et al., 1998). The affinity of a KCO towards a  $K_{ATP}$  channel depends upon the type of SUR isoform present. The affinities of P1075, pinacidil, levcromakalim and diazoxide were lower for SUR1 than for SUR2B (Uhde et al., 1999). Chimaeras of the SUR2B isoform substituted with segments of the SUR1 isoform were used to investigate KCO sensitivity. Two parts of the cytosolic loop between TMD13 and 14 (The1059-Leu1087) and TMD 16 and 17, including the beginning of the C-terminal (Arg1218-Asn1320) of SUR1 were identified to be essential for the binding of [ $^3$ H]P1075 (Figure 1-7) (Uhde et al., 1999).

Another study by Babenko et al. (1999) showed that two different regions in SURs are necessary to determine the selective effects of KCOs. A panel of SUR2A/SUR1 segments was constructed to test their selectivity and to investigate the location of KCO binding in the SUR subunits. Segments of SUR2 from the glutamate-rich motif following NBF1, through to the intracellular segment preceding NBF2, confer sensitivity to the benzopyran and pyridine derivatives, whereas TMD6-11 and NBF1 of SUR1 respond to the pyrimidine KCO, diazoxide, and the TMD12-17 of SUR2 is required for cromakalim stimulation (Babenko et al., 1999; D'hahan et al., 1999).

Diazoxide is one of the KCO that showed differential affects to different isoforms (D'hahan et al., 1999). It is used clinically for the treatment of persistent hyperinsulinemic hypoglycaemia of infancy (PHHI). Diazoxide displays an apparently high selectivity for pancreatic  $\beta$ -cells and smooth muscle over cardiac  $K_{ATP}$  channels. When  $K_{ATP}$  current blocked with 100  $\mu$ M ATP, diazoxide (300  $\mu$ M) caused 5-fold increase in Kir6.2/SUR1 (pancreatic  $\beta$ -cells isoform) currents, but showed little effect on Kir6.2/SUR2A (cardiac  $K_{ATP}$  isoform). However, diazoxide can produce activation of cardiac  $K_{ATP}$  channels, with ADP serving as an essential cofactor (D'hahan et al., 1999). Activation of Kir6.2/SUR2A

by diazoxide in the presence of ADP may be recorded in excised inside-out patches (D'hahan et al., 1999). For Kir6.2/SUR2A channels, there is a sharp dependence of the effect of diazoxide on the concentration of ADP.

KCOs have also been known for their ability to protect mitochondria from anoxic injury (Ozcan et al., 2001). The cardiac mitochondria are sensitive to injury caused by oxidative stress which eventually to myocardial dysfunction. Reactive oxygen species (ROS) mediated oxidant injury damages proteins, lipids, and nucleic acids and eventually routes myocytes through apoptotic pathways of cell death. The surge of ROS production observed at reoxygenation could be the results of disrupted mitochondrial electron transport (Ozcan et al., 2002) by reduced ADP-stimulated oxygen consumption, which blunts ATP production. This change the ATP/ADP ratio at the same time affects the  $K_{ATP}$  function. Therefore, modulators of mitochondrial ROS production are actively being considered for enhanced mitochondrial protection against anoxic injury. Interest has focussed on the use of KCOs such as diazoxide and nicorandil, which preferentially target mitochondrial functions and have been recognized for their strong cardioprotective properties (Garlid et al., 1997; Ozcan et al., 2001).

#### 1.10.2- Potassium channel inhibitors (Sulphonylureas)

The sulphonylurea druges,  $K_{ATP}$  channel inhibitors, are known to stimulate insulin secretion from  $\beta$ -cell of the islets of langerhans by inhibiting the opening of  $K_{ATP}$  channels. Some sulphonylureas have also been shown to be selective inhibitors of  $K_{ATP}$  channels in cardiac myocytes and skeletal muscle (Edwards and Weston, 1993).

Sulphonylureas stimulate insulin secretion from pancreatic  $\beta$ -cells and are widely used in the treatment of type 2 diabetes. The Kir6.1/SUR1 channels, or pancreatic channels, are inhibited by tolbutamide with high affinity ( $K_i \cong 5 \mu\text{mol/l}$ ), whereas Kir6.2/SUR2A channels, cardiac channels, are blocked only with low affinity ( $K_i \cong 2 \text{ mmol/l}$ ) (Gribble et al., 1998). But the case is different with glibenclamide, which blocks both Kir6.2/SUR1 and Kir6.2/SUR2A with two different mechanisms. The inhibition of Kir6.2/SUR2A was

found to be reversible, but with Kir6.2/SUR1 it was not (Gribble et al., 1998). The protein region in the SUR1 subunit that is involved in high-affinity tolbutamide blocking was discovered by Ashfield et al. (1999). A series of chimaeras between SUR1 and SUR2A was constructed, coexpressed with Kir6.2 in *Xenopus* oocytes, and  $K_{ATP}$  currents measured using inside-out membrane patches. Results showed that the SUR2A chimaera in which transmembrane domains 14-16 (amino acid residues 1035-1277) were replaced with those of SUR1 expressed channels with high-affinity tolbutamide inhibition, whereas channels with the SUR1 chimaera containing transmembrane domains 13-16 of SUR2A, showed abolished high-affinity tolbutamide inhibition. It was also found that by mutating Ser<sup>1237</sup> to tyrosine within this region of SUR1, both high-affinity tolbutamide inhibition and [<sup>3</sup>H]-glibenclamide binding were abolished. In another chimaera study, both the N- and C-terminal domains of SUR1 were shown to be essential for glibenclamide binding (Mikhailov and Ashcroft, 2000). Manning Fox et al (2002) found that the sulphonylurea HMR1098 is a selective inhibitor of Kir6.2/SUR2A in the lower micromolar range, compared to Kir6.2/SUR1, for which 400 to 800 fold increases in the concentration was needed to show inhibition (Manning Fox et al., 2002).

The pharmacological tools described above are important resources for  $K_{ATP}$  channel characterisation. The differences in  $K_{ATP}$  channels response to the KCOs or inhibitors make them potential discriminators for drug treatment, where treating one isoform will not affect the other.

### 1.11- The regulation of $K_{ATP}$ channels by ATP, MgADP and MgATP

As their name implies, ATP plays an important role in the inhibition of  $K_{ATP}$  channels. The Kir6.2 subunit is proposed to be the primary binding site for ATP producing inhibition, while the SUR subunits mediate the stimulatory effects of MgADP (Tucker et al., 1998). The truncated form of Kir6.2 (Kir6.2 $\Delta$ 26), which travels to the cell membrane independently of SUR subunit and expresses channel activity, shows ATP sensitivity but is not stimulated by MgADP. The truncation Kir6.2 $\Delta$ 26 was used to investigate the binding site of ATP on Kir6.2 (Tucker et al., 1998). The N-terminal, C-terminal and the M2 domain

of Kir6.2 $\Delta$ 26 were screened for the predicted binding site. Single point mutations were made to identify the amino acids responsible for the effect on ATP affinity. When the lysine 185 was mutated to glutamine (K185Q) ATP showed a significantly reduced ability to inhibit channel activity (Tucker et al., 1997). This was not the only amino acid found to contribute to the ATP inhibition effect on the Kir6.2 subunit. Five other amino acids have been defined using single point mutation (R50G, E179Q, C166S, I167M and T171A) (Tucker et al., 1998). Three of these mutations (R50G, E179Q, and K185Q) had altered ATP sensitivity without a significant change in channel kinetic properties. In contrast, the C166S, I167M and T171A mutations, which are close to the M2 domain, demonstrated a decrease in the long closed state and a four-fold increase in the channel open probability (Tucker et al., 1998). This suggested that in these cases changes in the single channel kinetics may reduce the ATP sensitivity. In conclusion, all six mutants showed reduced ATP sensitivity compared to wild type Kir6.2. The mutations may alter the ATP sensitivity of Kir6.2 $\Delta$ C26 by either impairing the ability of the channel to close, interfering with the transduction mechanism by which ATP binding induces pore closure, or decreasing the affinity of the ATP-binding site (Tucker et al., 1998).

Another study introduced a new region within the proximal C-terminal of Kir6.2 (amino acids 334-337) responsible for ATP sensitivity (Drain et al., 1998). When this region was replaced with the equivalent sequence from Kir1.1, Kir2.1 and Kir4.1, a large decrease in the ATP sensitivity was demonstrated. On the other hand, replacing the N-terminal of Kir6.2 with the equivalents from Kir1.1 did not affect the ATP sensitivity (Drain et al., 1998).

Non-hydrolysable analogues of ATP showed inhibition to the Kir6.2 $\Delta$ C36 current, which suggests that ATP hydrolysis is not required for channel inhibition (Tucker et al., 1998). Further, the ability of ADP to inhibit channel activity, with a  $K_i=260 \pm 22 \mu\text{M}$ , compared with  $115 \pm 6 \mu\text{M}$  for ATP, suggests that the  $\beta$ -phosphate is essential for channel inhibition (Tucker et al., 1998).

In contrast to the Kir6.2 subunit which has no known motif for ATP binding, the SUR subunit contains Walker A and Walker B motifs, which are known to form nucleotide-binding pockets for MgATP and MgADP (Aguilar-Bryan et al., 1995; Inagaki et al., 1996). ADP potentiated Kir6.2/SUR1 current in the presence of intracellular  $Mg^{2+}$ , while ADP in the absence of  $Mg^{2+}$  or at high  $Mg^{2+}$  concentration was inhibitory. MgADP acts on  $K_{ATP}$  channels by binding to the NBF's of SUR (Gribble et al., 1997). These motifs are known to catalyse ATP hydrolysis in a range of ABC cassette proteins. An aspartate in the  $W_B$  motif coordinates the  $Mg^{2+}$  ion of MgATP and is required for nucleotide binding, while a lysine in the  $W_A$  motif interacts with the  $\gamma$  and  $\beta$  phosphate group of ATP and is essential for ATP hydrolysis (Azzarie et al., 1989; Carson et al., 1995; Ko and Pedersen, 1995; Saraste et al., 1990; Tian et al., 1990).

In addition to the Walker A and B motifs, there are amino acid sequences between them called 'Linker regions' (LSSGQ) thought to be involved in transducing conformational changes resulting from ATP hydrolysis (Ames and Lecar, 1992). In SUR1 and SUR2B, mutating the serine residue to arginine in the linker region of NBF1 had no effect on ATP or ADP binding, but weakened the ability of MgADP to enhance channel activity (Matsuo et al., 2002). It has been suggested that the linker region may be involved in the cross-talk between NBF1 and NBF2. MgATP or MgADP binding to NBF1 is required for activation of SUR2B and SUR1. Mutation of the NBF2 linker blocks this effect and impairs nucleotide activation because the linker of NBF2 serves as a sensor of whether the nucleotide is bound at NBF1. This cannot be the case for SUR2A, because MgADP binding to NBF2 is sufficient to activate the  $K_{ATP}$  channel (Matsuo et al., 2002).

Mutation of the highly conserved glutamine and histidine residues in NBF2 of SUR1 reduced  $K_{ATP}$  channel activation by MgADP (Walter et al., 1992). The two NBFs of SUR1 show strong cooperativity in nucleotide binding and  $K_{ATP}$  channel activation requires both NBFs of SUR1 to be functional (Gribble et al., 1997; Nichols et al., 1996).

An important function of the SUR subunit is to confer sensitivity to cellular ADP concentration (Shyng and Nichols, 1997) through binding to NBF2 (Ueda et al., 1999). The

importance of NBF2 was shown by mutation in the Walker A and B motifs in NBF2, K1385M and D1506N, abolished the stabilizing effect of MgADP binding on nucleotide binding to NBF1. 8-azido-ATP was known to bind only to NBF1, since affinity labelling of SUR1 with this reagent was blocked only when Walker motifs in NBF1 were mutated (Ueda et al., 1999). The reduction in affinity of 8-azido-ATP binding in the NBF1 following application of MgADP to NBF2 mutants of SUR1 suggested that the binding of MgADP to NBF2 stabilised the binding of 8-azido-ATP at NBF1 of SUR1. It is thought that MgADP induces a conformational change at NBF2 that transduces another conformation change in NBF1 to stabilis ATP binding at NBF1 (Ueda et al., 1999). The degree of MgADP activation of  $K_{ATP}$  channels is greater than that of MgATP activation, which occurs over the same concentration range (0.1-1 mM) (Ueda et al., 1999). The intracellular concentration of MgADP is the primary factor in the determination of the active state of SUR1, although ATP is also required for the action of SUR1. An aspartate in the Walker B motif coordinates the  $Mg^{2+}$  ion of MgATP and is required for nucleotide binding, while a lysine in the Walker A motif interacts with the  $\gamma$  and  $\beta$  phosphate group of ATP and is essential for ATP hydrolysis (Azzarie et al., 1989; Carson et al., 1995; Ko and Pedersen, 1995; Saraste et al., 1990; Tian et al., 1990). Both of the Walker A mutant channel currents (Kir6.2/K719A-SUR1 and Kir6.2/K1384M-SUR1) were inhibited rather than activated by MgADP, indicating that the effect of MgADP is mediated by the interaction of the nucleotide diphosphate with the NBFs of SUR1 and that the Walker A lysine residues play a critical role in the interaction (Dabrowski et al., 2002).

In modelling experiments of whole cardiomyocytes currents Michailova et al. (2005) showed that only one molecule of ATP is sufficient to close the channel via the Kir6 subunit, while interaction of one or two MgADP molecules with only one of the four SUR2A subunits is sufficient to increase the channel activation (Nichols et al., 1996; Gribble et al., 1997; Ueda et al., 1997; Ashcroft and Gribble, 1998). Other nucleotides, like GTP and ADP, stimulate  $K_{ATP}$  channels in the presence of  $Mg^{2+}$  by acting on the NBFs of SUR (Trapp et al., 1997).

The interaction of sulphonylureas with SUR1 abolishes the stimulatory effect of MgADP on  $K_{ATP}$  channels (Tucker et al., 1997). However, the sensitivity of the  $K_{ATP}$  channel to sulphonylureas is increased in the presence of MgADP compared to its absence (Zunkler et al., 1988; Gribble et al., 1997) even though MgADP can no longer activate the channel. Mutation of the Walker A motif in either NBF of SUR2B eliminated ATP activation of KCO binding, while mutating the highly conserved Walker A lysine (K711R or K1352R) in either NBF of SUR2B did not alter the affinity for P1075 binding, but decreased the  $B_{max}$  (maximal number of KCO binding sites) caused by elimination of the ATP activation of KCO binding (Schwanstecher et al., 1998). This suggests that SUR subunits are the KCO receptors of  $K_{ATP}$  channels and that the binding of KCO requires ATP. It is thought that ATP binding and presumably hydrolysis at both NBFs induces a conformational change in SUR that greatly increases its affinity for KCOs (Schwanstecher et al., 1998).

#### 1.12- The regulation of $K_{ATP}$ channels by pH and acidosis

ATP levels are the major factor in controlling  $K_{ATP}$  channel activity, but other intracellular factors, such as pH, have also been shown to affect  $K_{ATP}$  channel activity (Fan et al 1994; Xu et al., 2001; Piao et al., 2001). Several Kir channels, Kir1.1 Kir1.2, Kir2.3, Kir2.4, Kir4.1, Kir4.2 and the heteromeric Kir4.1-Kir5.1 show pH-sensitivity; they are all inhibited by intracellular and/or extracellular protons, although the sensitivity varies among individual members (Piao et al., 2001). On the other hand, the  $K_{ATP}$  channel may be stimulated by an increase in intracellular protons (Wu et al. 2002). The maximum activation of the  $K_{ATP}$  channel (Kir6.1/SUR1) in responding to pH-stimulation was in the pH range 5.9-6.2. Further decrease in pH caused rapid current inhibition, which appeared to be related to channel rundown, because channel activity showed little or no recovery with washout at pH 7.4 (Wu et al., 2002; Davies et al., 1992; Koyano et al., 1993). It has been shown that several amino acids in the Kir subunit are responsible for the pH sensitivity. In the N-terminal, the lysine residue (Lys-80 in Kir1.1, Lys-67 in Kir4.1) plays an important role in the pH-sensitivity (Fakler et al., 1996; Xu et al., 2000). Kir1.1 and Kir4.1 channels are inhibited by acidic pH (Fakler et al., 1996; Yang et al., 1999) and a lysine residue (Lys-80 in Kir1.1, Lys-67 in Kir4.1) has been shown by mutagenesis to play an important role in

the pH sensitivity of these channels. The equivalent residue in Kir6.2 is a threonine (Thr-71), suggesting that this motif is not important in conferring pH sensitivity in  $K_{ATP}$  channels. Instead of the lysine residue, Kir6.2 has a threonine (Thr-71) in this position. In the C-terminal, His-175 and His-216 (Piao et al., 2001; Baukrowitz et al., 1999) are shown to be involved in the pH sensitivity of the Kir6.2 channels. Moreover, mutation in the M2 region of Cys-166 changes the rectification and the pH sensitivity of the Kir6.2 channel. Therefore, the pH sensitivity of Kir6.2 requires two separate protein domains in the C-terminus, and the M2 region, but the N-terminal region involved in some other Kir channels does not contribute to pH sensitivity in Kir6.2 (Piao et al., 2001).

### 1.13- The effect of phosphatidylinositol 4,5 bisphosphate upon $K_{ATP}$ channels

Phosphatidylinositol 4,5-bisphosphate ( $PIP_2$ ) plays an important role in regulating the gating of many ion transporters and channels, such as the  $Na^+/Ca^{2+}$  exchanger (Hilgemann and Ball, 1996), the inositol-1,4,5-triphosphate ( $IP_3$ ) receptor  $Ca^{2+}$  channel (Lupu et al., 1998), mammalian rod cyclic nucleotide-gated channels (Womack et al., 2000) and several inwardly rectifying  $K^+$  channels (Hilgemann and Ball, 1996; Huang et al., 1998; Sui et al., 1998). In 1996, Hilgemann & Ball showed that  $PIP_2$  and MgATP, upregulated the activities of  $K_{ATP}$  channels and  $Na^+-Ca^{2+}$  exchangers in the large patch membranes excised from cardiac myocytes. They concluded that MgATP affected the replenishment of  $PIP_2$  by lipid kinases rather than protein phosphorylation. This was confirmed by the treatment of the patch membrane with phospholipase C (PLC), or antibody against  $PIP_2$ , which promoted the rundown of the  $K_{ATP}$  channel and  $Na^+-Ca^{2+}$  exchanger. Thereafter, addition of MgATP and  $PIP_2$  restored these activities. Moreover, treatment with PI-specific PLC and abolished the effect of MgATP by depleting PI, a precursor for  $PIP_2$  production (Hilgemann and Ball, 1996). These findings, together with the observation that very high concentrations of wortmannin, an inhibitor of  $PIP_2$  production, prevents  $K_{ATP}$  channel reactivation by MgATP (Xie et al., 1999), have led to the interpretation that reactivation by MgATP is due to  $PIP_2$  resynthesis (Hilgemann and Ball, 1996).

The amount of PIP<sub>2</sub> in the plasma membrane can be changed by the enzymes involved in phosphoinositide metabolism, such as phosphoinositide kinases and phosphatase, and the enzymes that use PIP<sub>2</sub> as a substrate, e.g. phospholipase C, phosphatidylinositol 3 kinase. Phospholipase C (PLC) hydrolyzes PIP<sub>2</sub> into diacylglycerol (DAG) and inositol-1,4,5-triphosphate (IP<sub>3</sub>), thus causing the depletion of PIP<sub>2</sub> (Cho et al., 2005). Therefore, the stimulation of Gq-coupling receptors inhibited the recombinant K<sub>ATP</sub> channel that was previously activated by metabolic inhibition or by KCOs. Under such conditions, the ATP-sensitivity was significantly increased (Baukrowitz et al., 1998; Xie et al., 1999). Furthermore, associated changes in PIP<sub>2</sub> level and the ATP-sensitivity of K<sub>ATP</sub> were observed during the metabolic inhibition in COS cells (Loussouarn et al., 2001). Conversely, overexpression of PI-4-phosphate 5-kinase decreased ATP-sensitivity by means of the elevation of the PIP<sub>2</sub> level (Shyng et al., 2000).

Although the stimulatory effects of PIP<sub>2</sub> were first attributed to cytoskeletal interaction (Furukawa et al., 1996), the primary mechanism of PIP<sub>2</sub> action seems to be an electrostatic effect between negatively charged anionic heads of PIP<sub>2</sub> and positively charged amino acid residues of Kir6.2. This idea is based on the following observations: anionic phospholipids other than PIP<sub>2</sub>, such as PIP, phosphatidylinositol-3,4,5 phosphates (PIP<sub>3</sub>), and phosphatidylserine possess similar stimulatory effects on K<sub>ATP</sub> channels (Fan and Makielski, 1999): positively charged molecules such as poly-lysine and l-palmitoylcarnitine show opposite effects on K<sub>ATP</sub> channels (Shyng and Nichols, 1998; Baukrowitz et al., 1998; Haruna et al., 2000). Systematic site-directed mutagenesis replacing positively charged amino acids with alanine revealed that the PIP<sub>2</sub> interaction sites on Kir6.2 were the proximal region of C-terminal (R176~K222) and the distal region of C-terminal (R301~R314). Amino acid sequences in these regions are highly conserved in Kir families (Fan and Makielski, 1999).

#### 1.14- Interactions between the K<sub>ATP</sub> subunits

From the above sections, it can be seen that there must be complex allosteric information transfer between different structures within the K<sub>ATP</sub> channel oligomer and, therefore, that

important molecular contacts must exist between the heterologous subunit.  $K_{ATP}$  channels need to assemble perfectly to be able to form functional channels. This assembly will happen when the subunits interact together to form a heteromultimeric complex with the right stoichiometry. Such assembly of correctly targeted functional channels requires binding the two heterologomer subunits to mask ER sequences in both subunits. This has been studied by different groups. For example, a chimaera between the Kir6.2 and Kir2.1 subunits has been used to localize a binding site in Kir6.2 that binds SUR subunit (Hough et al., 2000; Giblin et al., 1999). Similarly, a chimaera between the SUR and the MRP1 subunits has been used to define structures in SUR necessary for binding to Kir6.2 (Schwappach et al., 2000). A number of studies have been carried out based on this method using a variety of chimaeric Kir6.2/Kir2.1 constructs to contribute to the identification of binding sites in each subunit (Hough et al., 2000; Giblin et al., 1999).

Chimaeras of Kir6.2/Kir2.1 based on the N-terminal of Kir6.2 were constructed to study the trafficking of the Kir6.2 subunit (Hough et al., 2000). These chimaeras Rao 1, Rao 2, Rao 3, and Rao 4 (Figure 1-8) lacked the ER retention signal (RKR) (Zerangue et al., 1999). The Kir6.2/Kir2.1 chimaeras and the sulphonylurea receptor (SUR1) were each epitope-tagged on either the N- or C-terminal. Tagging SUR1 on the C-terminal prevented formation of functional channels when expressed with full-length of Kir6.2 (Hough et al., 2000). On the other hand, tagging Kir6.2 at the C-terminal showed no effect on the expression of functional channels. None of the constructed Kir6.2/Kir2.1 chimaeras was able to produce channel currents when expressed with or without SUR1 (Hough et al., 2000). When expressed alone, the Kir2.1 subunit was targeted to the plasma membrane and expressed functional channels (Hough et al., 2000; Giblin et al., 1999). Rao1-3 were also targeted to the plasma membrane when expressed alone, but Rao 4, which contained the N-terminal of Kir6.2 (residues 1 to 179) and the C-terminal of Kir2.1 (residues 192 to 428), showed no staining in the plasma membrane in the absence of SUR1 and surface expression was not rescued by co-expression with SUR1. This result was interpreted to indicate that the M2 segment of Kir6.2 and the 13 amino acids in the proximal C-terminal domain might play a role in trafficking to the cell surface (Hough et al., 2000). This

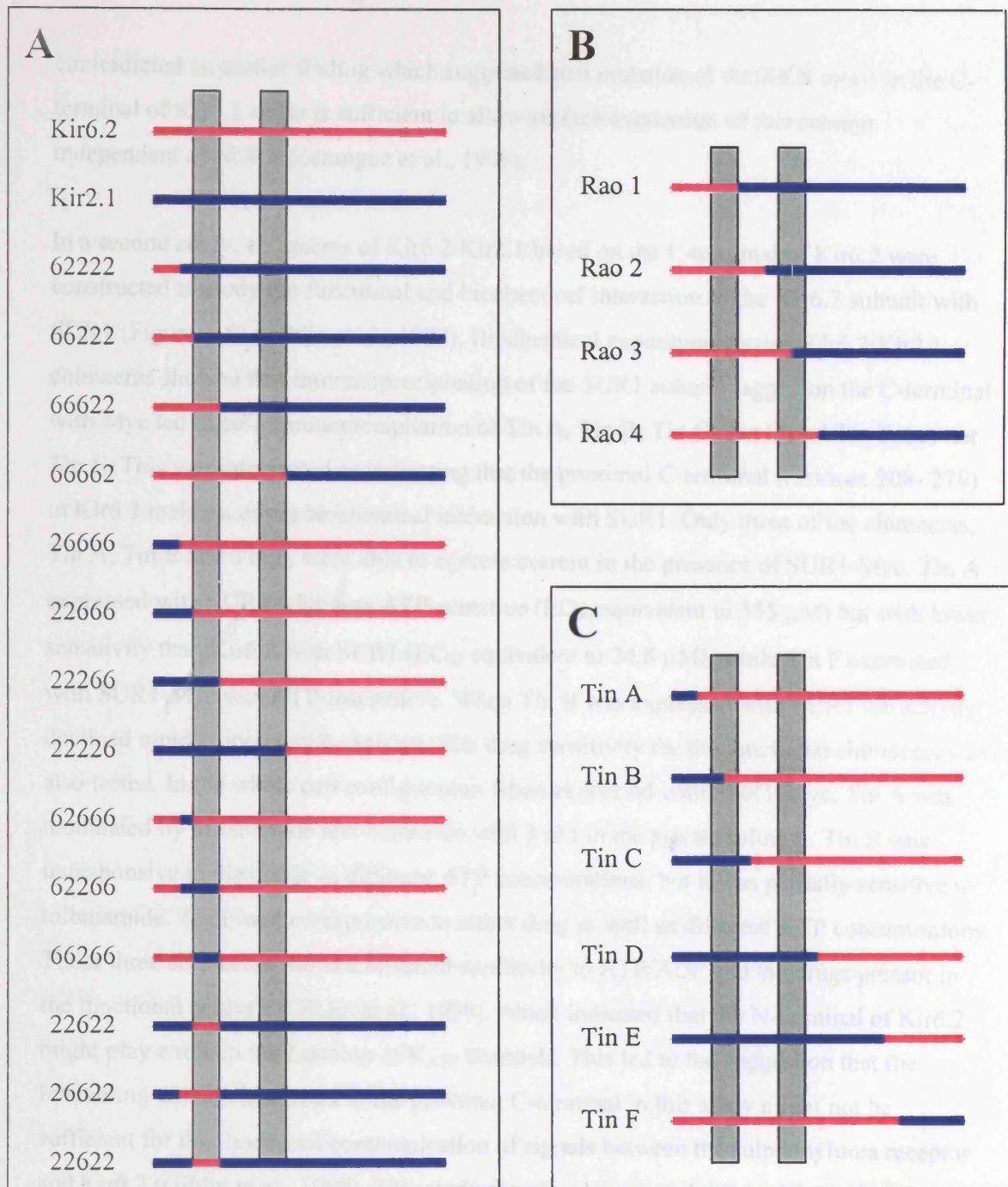


**Figure 1-8 Schematic representation of Kir6.2/Kir2.1 chimaeras from three studies.** A, chimaeras constructed by exchanging five blocks between the two homologous Kir6.2 and Kir2.1 subunits (Schwappach et al., 2000). B, Chimaeras constructed based on the N-terminal of Kir6.2, to study the trafficking of the Kir6.2 subunit (Hough et al., 2000). C, chimaeras constructed based on the C-terminal of Kir6.2, to study the functional and biochemical interaction of the Kir6.2 subunit with SUR1 (Giblin et al, 1999).

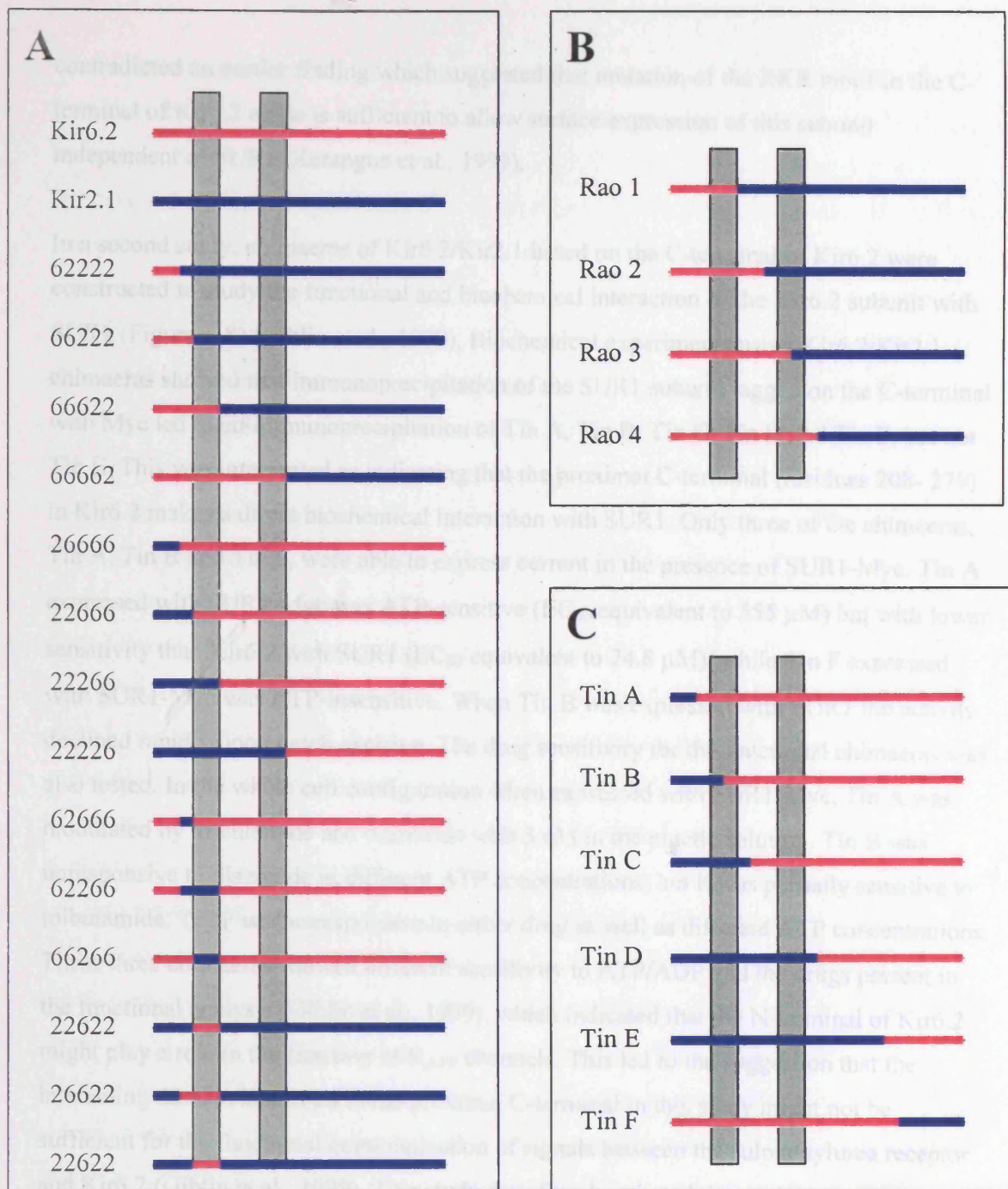


**Figure 1-8 Schematic representation of Kir6.2/Kir2.1 chimaeras from three studies.** A, chimaeras constructed by exchanging five blocks between the two homologous Kir6.2 and Kir2.1 subunits (Schwappach et al., 2000). B, Chimaeras constructed based on the N-terminal of Kir6.2, to study the trafficking of the Kir6.2 subunit (Hough et al., 2000). C, chimaeras constructed based on the C-terminal of Kir6.2, to study the functional and biochemical interaction of the Kir6.2 subunit with SUR1 (Giblin et al, 1999).

contradicted an earlier finding which suggested that mutation of the RKR motif in the C-terminal of Kir6.2 alone is sufficient to allow surface expression of this subunit independent of SUR1 (Zerangue et al., 1999).

In a second study, chimaeras of Kir6.2/Kir2.1 based on the C-terminal of Kir6.2 were constructed to study the functional and biochemical interaction of the Kir6.2 subunit with SUR1 (Figure 1-8) (Giblin et al., 1999). Biochemical experiments using Kir6.2/Kir2.1 chimaeras showed that immunoprecipitation of the SUR1 subunit tagged on the C-terminal with Myc led to co-immunoprecipitation of Tin A, Tin B, Tin C, Tin D and Tin F, but not Tin E. This was interpreted as indicating that the proximal C-terminal (residues 208- 279) in Kir6.2 makes a direct biochemical interaction with SUR1. Only three of the chimaeras, Tin A, Tin B and Tin F, were able to express current in the presence of SUR1-Myc. Tin A expressed with SUR1-Myc was ATP-sensitive ( $EC_{50}$  equivalent to 555  $\mu$ M) but with lower sensitivity than Kir6.2 with SUR1 ( $EC_{50}$  equivalent to 24.8  $\mu$ M), while Tin F expressed with SUR1-Myc was ATP-insensitive. When Tin B was expressed with SUR1 the activity declined rapidly upon patch excision. The drug sensitivity for the functional chimaeras was also tested. In the whole cell configuration when expressed with SUR1-Myc, Tin A was modulated by tolbutamide and diazoxide with 3 nM in the pipette solution. Tin B was unresponsive to diazoxide at different ATP concentrations, but it was partially sensitive to tolbutamide. Tin F was unresponsive to either drug as well as different ATP concentrations. These three chimaeras showed different sensitivity to ATP/ADP and the drugs present in the functional analysis (Giblin et al., 1999), which indicated that the N-terminal of Kir6.2 might play a role in the function of  $K_{ATP}$  channels. This led to the suggestion that the interacting domain identified in the proximal C-terminal in this study might not be sufficient for the functional communication of signals between the sulphonylurea receptor and Kir6.2 (Giblin et al., 1999). This study therefore, supported the model previously suggested, whereby both the distal C-terminal and N-terminal of Kir6.2 are involved in determining  $K_{ATP}$  function (Tucker et al., 1998; Babenko et al., 1999).

Schwappach et al. (2000) took a different approach to the construction of their chimaeras, in which they exchanged five blocks between the two homologous Kir6.2 and

Kir2.1 subunits (Figure 1-8). Swapping of the distal N-terminus, membrane-proximal N-terminus, transmembrane segment M1, pore loop (H5) plus transmembrane segment M2, and cytosolic C-terminus resulted in chimaeras that were designated by five digits specifying the origin of each of the five swapped regions (Schwappach et al., 2000). They used two different assays to identify whether Kir6.2 assembled with the SUR subunit. The first assay was based on trafficking enhancement of the assembled complex; assembly of the two subunits and formation of the  $K_{ATP}$  channel enhanced the expression of both subunits in the cell surface. The second assay was based on trafficking trap of the assembled complex, where adding an extra ER retention sequence at the end of one of the subunits prevented the other subunit being expressed in the cell surface. This study confirmed that the C-terminal half of the Kir6.2 protein contains the essential determinant of homotypic subunit assembly for Kir6.2 and Kir2.1 (Giblin et al., 1999; Tinker et al., 1996). Also, using the enhancement assay, several chimaeras containing the M1 domain of Kir6.2 showed an interaction with both SUR2A and SUR1 subunits. The first transmembrane segment (M1) and the N-terminus of the Kir6.2 subunit are important for specifying assembly with SUR1 and SUR2A. Furthermore, an inverse of this chimaera, called 66266, showed an interaction with SUR2A and SUR1. Therefore, the M1 segment of Kir6.2 cannot be the only domain that interacts with SUR1. Neither the N-terminal of Kir6.2 by itself, chimaera 66222, or the C-terminal of the Kir6.2, chimaera 22266, showed any interaction with the SUR subunit in these experiments. This indicated that interaction of both termini of Kir6.2 is required to make a complete interaction with the SUR subunits (Schwappach et al., 2000). Using the trapping assay, chimaera 22622 with an additional ER retention sequence reduced SUR1 surface expression; therefore, the M1 segment of Kir6.2 appeared to be sufficient to confer interaction with SUR1 in both the trafficking enhancement and trafficking trap assays. Changing the threonine-methionine-serine (TMS) sequence at the beginning of M1 to the corresponding cysteine-leucine-alanine (CLA) sequence in Kir2.1 or 22622 chimaer disrupted the binding of the construct with the SUR subunit. Similarly, removing the last two amino acids from the M1 segment (phenylalanine-alanine) of the 22622 chimaer also reduced the binding with SUR1 and SUR2A. This localized the binding site on the M1 domain to five amino acids near the beginning and the end of M1.

To investigate the binding site of the M1 domain from Kir6.2 with the SUR1 subunit, chimaeras were constructed between SUR1 and MRP1 (a homologous ABC protein that does not assemble with Kir6.2). Replacing one or both of the NBF1 and NBF2 domains stimulated the expression of Kir6.2 or 66266 to the cell membrane, which suggests that NBFs are not required for assembly with the cytoplasmic domains of Kir6.2. Changing any of the transmembrane domains of SUR1 to the equivalent region from MRP1 showed little or no cell membrane expression of Kir6.2 or 66266 chimaera, which suggested that all these transmembrane domains of the SUR subunit are important in the assembly of functional and properly trafficking channels (Schwappach et al., 2000).

### 1.15- Aims and hypothesis

$K_{ATP}$  channels couple cellular metabolic status to electrical activity and play an important role in protecting cells against hypoxic insult (see section 1.6.1). Responses to cellular nucleotides are mediated by allosteric information transfer between subunits (see section 1.11).

The hypothesis addressed in this thesis is that NBF1 and NBF2 of  $K_{ATP}$  channel SUR subunits make direct contact with cytoplasmic N- and/or C-terminal domains in the pore-forming Kir6.0 subunits of  $K_{ATP}$  channels. These interactions may be important for allosteric information transfer between SUR and Kir6.0 polypeptides.

“Beauty is said to lie in the eye of the beholder; this seems equally true for the subunits of  $K_{ATP}$  channels. Some researchers consider the Kir subunits to be of importance, whereas others find the sulphonylurea receptors more interesting and important” (Aguilar-Bryan, 1998). His group saw that both subunits are important in forming an active  $K_{ATP}$  channel, and that full understanding of these channels would come with equal consideration of both subunits (Aguilar-Bryan, 1998). This project took both subunits into consideration by investigating the interaction of the C-terminal of SUR2A with the full length of Kir6.2 and investigating the corresponding SUR binding site on Kir6.2.

The aims of this project were to provide a detailed molecular characterization of the inter-subunit interaction between the cytoplasmic domains of Kir6.2 and SUR2A subunits of the cardiac  $K_{ATP}$  channel. This was investigated by:

- Synthesizing fragments of SUR2A subunit with a maltose binding protein (MBP) epitope-tag to permit subunit fragments to be tracked.
- Using co-immunoprecipitation of MBP-SUR2A fragments with full-length Kir6.2 subunit protein in experiments to identify interaction sites.
- Using confocal microscopy to determine the localization of the  $K_{ATP}$  channel subunit in HEK293 cells.
- Looking for the effect of the SUR2A-CT-fragment on Kir6.2/SUR2A current fragments in the HEK293 cells stably expressing Kir6.2/SUR2A current, using electrophysiological assays.
- Construction of chimaeric subunit fragments of SUR2A and multidrug resistance protein 1 (MRP1) subunits to permit the mapping of the Kir6.2 binding site in SUR2A.
- Having determined an interaction domain in the proximal C-terminal of the SUR2A subunit a further aim was to use Kir6.2/Kir2.1 chimaeras to identify the cognate site of binding of the SUR2A subunit on the Kir6.2 subunit.

## **Chapter Two**

### **Methods**

## 2.1- Molecular biology methods

### 2.1.1- Amplification of DNA by the polymerase chain reaction (PCR)

Amplification of DNA using polymerase chain reaction (PCR) is one of the most common techniques used in molecular genetics. The PCR mixture for a typical run was 40.6  $\mu$ l of ddH<sub>2</sub>O, 5  $\mu$ l (10X *PfuUltra* HF reaction buffer (stratagene, Cat# 600380)), 0.4  $\mu$ l (25 mM dNTPs), 1  $\mu$ l (100 ng/ $\mu$ l) DNA template, 1  $\mu$ l (100 ng/ $\mu$ l) from primer 1 and 2, and 1  $\mu$ l *PfuUltra* High-Fidelity (HF) DNA polymerase (2.5 U/ $\mu$ l (Stratagene, Cat# 600380)), in a 50  $\mu$ l total volume reaction. The general PCR cycling parameters for the *PfuUltra* HF DNA polymerase were as shown in table 2-1, although minor adjustments were made with a few reactions.

**Table 2-1 PCR Cycling Parameters for PfuUltra high-Fidelity DNA polymerase.**

Segment	Number of cycles	Temperature	Duration
1	1	95 °C	3 minutes
2	20	95 °C	30 seconds
		60 °C	1 minute
		72 °C	2 minutes
3	1	72 °C	5 minutes

### 2.1.2- Mutagenesis

Quikchange® site-directed mutagenesis kits (Stratagene, Cat# 20018) were used to delete, change or add single or multiple amino acids. Two oligonucleotides (primers) containing the desired mutation were made by MWG- Biotech. A PCR reaction was set up by adding 5  $\mu$ l of 10 X reaction buffer, 50 ng of dsDNA template (the plasmid vector containing the required gene), 125 ng of oligonucleotide primers # 1 and # 2, 1  $\mu$ l of 10 mM dNTP mix and ddH<sub>2</sub>O to make the final volume to 50  $\mu$ l. Then, 1  $\mu$ l of *Pfu*-Turbo DNA polymerase was added before the reaction was run in a PCR machine following the recommended cycling parameters from the manufacturer (Table 2-2). The parental DNA template was

digested by adding 1  $\mu$ l of *Dpn* I restriction enzyme to digest methylated DNA for 1 hour at 37°C. DNA treated with *Dpn* I was transferred to 50  $\mu$ l DH5 $\alpha$  supercompetent cells in a 15 ml polypropylene tube.

**Table 2-2** The cycles number and temperature for the PCR.

Cycles	Temperature	Time
1	95°C	30 seconds
2-18	95°C	30 seconds
	55°C	1 minute
	68°C	1 minute/Kb of plasmid length

### 2.1.3- Purification of plasmid DNA

Plasmid DNA purification was performed using the QIAfilter Midi Kit (QIAGEN, Cat# 12643). A confirmed plasmid with the desired insert was used to transform into 50  $\mu$ l DH5 $\alpha$  competent cells (Invitrogen, Cat# 18265-017) (see section 2.1.12). The cells were plated on an LB agar plate and incubated overnight at 37°C. A colony was picked to inoculate 5 ml LB medium (10 g NaCl, 10 g tryptone, 5 g yeast extract, in one liter of dH<sub>2</sub>O) with 5  $\mu$ l of 100  $\mu$ g/ml of the required antibiotic. The LB medium was incubated overnight at 37°C with 220 rpm shaking. A large scale 50 ml LB medium was inoculated with 1 ml of the overnight culture and incubated for 12-16 h with shaking at 220 rpm. The bacterial cells were harvested by centrifugation at 11000 g for 30 min at room temperature. The pellet was resuspended in 6 ml of buffer P1 (50 mM Tris-HCl (pH8.0), 10 mM EDTA, 100  $\mu$ g/ml RNase A) and 6 ml of Buffer P2 (200 mM NaOH, 1 % SDS (w/v)) was added to the mixture before gently inverting 4-6 times and incubated at room temperature for 5 min. Chilled neutralization buffer P3 (3 M potassium acetate (pH 5.5)) was added to the lysed cells and mixed immediately by inverting the tube 4-6 times. The lysate was poured into a QIAfilter cartridge (QIAGEN) and left for 10 min at room temperature. The lysate was filtered through the QIAfilter cartridge and transferred to a Hispeed Midi column that was previously equilibrated with 4 ml of QBT buffer (750 mM NaCl, 50 mM MOPS (pH 7.0),

15 % isopropanol (v/v), 0.15 % Triton X-100 (v/v)). The filter lysate was allowed to pass through the resin by gravity flow. The column was washed with 20 ml of QC buffer (1.0 M NaCl, 50 mM MOPS (pH 7.0), 15 % isopropanol (v/v)). DNA was eluted from the Hispeed column with 5 ml QF buffer (1.25 M NaCl, 50 mM Tris-HCl (pH 8.5), 15 % isopropanol (v/v)) and precipitated by adding 3.5 ml 100 % isopropanol, with mixing and incubation at room temperature for 5 min. The precipitated DNA was transferred to a 20 ml syringe attached to QIAprecipitator Midi Module and the mixture was filtered through the QIAprecipitator. The DNA was eluted with 1 ml of TE buffer (10 mM Tris-HCl (pH 8.0), 1 mM EDTA). The DNA was re-precipitated by mixing 500 µl of the eluted DNA with 1 ml 100 % ethanol and 75 µl 3 M Na acetate (pH 5.2) and incubation for 30 min at -20°C. The mixture was centrifuged at 11600 g at 4°C and the pellet dried and resuspended in 50 µl TE buffer.

#### 2.1.4- Mini DNA purification (Wizard)

In order to analyze large numbers of transformants, plasmid DNA was isolated from overnight cultures of *E. coli* (DH5α) that were grown from single colonies. This method yielded DNA of sufficient quantity and purity to perform restriction analyses and double stranded dideoxytermination sequencing. Using the Wizard Plus SV Minipreps DNA Purification System (Promega, USA, Cat# A1470) protocol, a large number of samples could be analyzed in one experiment. This was done by culturing a plasmid-containing *E. coli* in 5 ml LB-medium containing the required antibiotic overnight with 220 rpm shaking at 37 °C. Bacteria were pelleted at 5000 g for 10 min and resuspended in 250 µl Cell Resuspension Solution. An equal amount of Cell lysis Solution was added to each sample with gentle mixing and then incubated for 5 min. The mixture was neutralized by the addition of 350 µl of Neutralization Solution, with inversion of the sample to mix. The precipitate was pelleted at 11600 g for 10 min. The supernatants were transferred to spin columns and centrifuged at 11600 g for 1 min to bind the DNA. The DNA was washed with 750 µl washing buffer. DNA was eluted with 100 µl of Nuclease-Free water by centrifugation for 1 min at 11600g. The DNA yield was determined by spectrophotometric analysis as described in section 2.1.5.

### 2.1.5- Determination of yield of the DNA

The DNA concentration was determined by taking the absorption at 260 nm with a UV spectrophotometer. The absorption was multiplied by the coefficient factor (1.0  $A_{260}$  unit dsDNA= 50 $\mu$ g/ml) and dilution factor to give the concentration in  $\mu$ g/ml. In addition, another method was used for low amounts of DNA. Gel-purified DNA fragments and PCR products were quantified by running against a mass ladder (HYPERLADDER I, Bioline, London, UK, Cat# BIO-33025) of known amount of DNA in 0.8 % agarose gels.

### 2.1.6- Determination of the purity of the DNA

DNA samples were electrophoresed on 0.8 % agarose gels. Electrophoresis agarose (0.4 g) was heated in 50 ml of TAE (40 mM Tris-acetate, 1 mM EDTA) until dissolved, cooled slightly, then 2  $\mu$ l of ethidium bromide (10 mg/ml) was added prior to pouring onto a perspex gel slab. The DNA samples were mixed with DNA loading buffer (65 % sucrose (w/v), 10 mM Tris-HCl (pH 7.5), 10 mM EDTA, 0.001 % bromophenol blue (w/v)) and loaded into wells cast in the solidified gel slab. The gel was run in 250 ml TAE buffer supplemented with 7 $\mu$ l of ethidium bromide (10 mg/ml) at 90 V for 2 to 3 h. The size of the DNA was determined by comparing with a 1 Kb DNA ladder (Invitrogen, Cat# 15615-016), which was loaded in an adjacent lane.

### 2.1.7- DNA gel extraction

MinElut Gel Extraction Kits (Qiagen, Germany, Cat#28604) were used to extract and purify DNA from standard agarose gel in TAE buffer. The DNA fragment was excised from the agarose gel and weighed. To dissolve the agarose gel, three volumes of buffer QG to one volume gel weight in grams was added and incubated at 50 °C for 10 min or until the gel slice completely dissolved. After the gel slice dissolved, one gel volume of isopropanol was added to the sample and the tube was mixed several times. The sample was applied to a MinElute column and centrifuged for 1 min to bind the DNA to the

column. The column was washed with 750 µl of PE buffer and centrifuged for 1 min. DNA was eluted with 10 µl of EB buffer (10 mM Tris-HCl, pH 8.5).

#### 2.1.8- Restriction enzyme digests.

Restriction enzymes were used according to the manufacturers' instructions. In general, plasmid DNA was cut with the desired restriction enzyme by incubation of 5 µg of the DNA in 20 µl reaction volume with the required buffer for 2 h and at the recommended temperature. Where multiple digests were to be performed, the buffer conditions were selected to be compatible with both enzymes. When this was not possible, after completion of the first digest, the buffer conditions were adjusted accordingly and the second digest performed. After restriction digests, the reaction was cleaned up using a MinElute Reaction Cleanup Kit.

#### 2.1.9- Reaction cleanup

MinElute Reaction Cleanup Kits (Qiagen, Germany, Cat#28204) were used to purify DNA fragments from enzymes, primers, nucleotides and salt. The enzymatic reaction was mixed with 300 µl of ERC buffer; the enzymatic reaction should be less than 100 µl and the colour of the mixture should be yellow. The sample was applied to MinElute column and centrifuged at 11600 g for 1 min to bind the DNA to the column. The column was washed with 750 µl of PE buffer and centrifuged at 11600 g for 1 min. DNA was eluted with 10 µl of EB buffer (10 mM Tris-HCl, pH 8.5).

#### 2.1.10- Removal of 5' phosphate groups for DNA

Shrimp alkaline phosphatase (Fermentas) was used to remove 5'-phosphate groups from DNA. The reaction was performed in a total volume of 50 µl. Following restriction endonuclease digestion, dephosphorylation of the vector was carried out using 0.5 U phosphatase per reaction for 30 min at 37°C. This enzyme was completely inactivated by heating at 70°C for 20 min.

### 2.1.11- DNA ligation

Plasmids were digested with restriction endonucleases. Following restriction endonuclease digestion, the vector DNA was treated with shrimp alkaline phosphatase prior to being used in this reaction. Also, the insert was digested with restriction endonucleases to produce cohesive ends compatible to the vector ends. Subsequent to restriction endonuclease digestion, the insert DNA was purified using the reaction cleanup Kit (section 2.1.9) and prepared for the ligation reaction. This protocol was used to join DNA fragments with a plasmid vector to produce circular recombinant molecules. The reaction was set up by adding 4  $\mu$ l of 5X ligase reaction buffer (Invitrogen, Cat# 15224-017), 30 fmol of insert DNA, 90 fmol of vector DNA, 1  $\mu$ l of T4 DNA Ligase (1 U/ $\mu$ l) (Invitrogen, Cat# 15224-017) and ddH<sub>2</sub>O to makeup the total volume to 20  $\mu$ l. The mixture was incubated for 1 hour at room temperature.

### 2.1.12- Transformation of the DNA to host cells

Ligation reactions (2  $\mu$ l) or supercoiled plasmid DNA (1 ng) were used to transform DH5  $\alpha$  *E. coli*. DNA was incubated with the competent cells (DH5 $\alpha$  Invitrogen, Cat# 18265-017) for 30 min on ice in a 15 ml polypropylene tube. The tube was heated for 45 seconds at 42°C and then placed on ice for 2 min. The competent cells were incubated with 0.9 ml of SOC medium (2 % peptone, 0.5 % yeast extract, 0.05 % NaCl, 1 ml of 250 mM KCl (pH 7.0), which was autoclaved and then 0.5 ml 2 M MgCl<sub>2</sub> and 2 ml of 1 M glucose added to make a final volume of 100 ml) for 1h at 37°C with shaking at 225 rpm. The cells were plated overnight in LB agar plates supplemented with the appropriate antibiotic for the plasmid vector. Colonies were picked for further culture then used either for protein expression or plasmid production.

## 2.2- Biochemistry methods

### 2.2.1- Protein expression

The TNT Quick Coupled Transcription/Translation System (Promega; Cat# L1170 for T7 promoter, or Cat# L2080 for SP6 promoter) was used to express Kir6.2, [<sup>35</sup>S]Kir6.2, Kir2.1, and [<sup>35</sup>S]Kir2.1 *in vitro*. Kir6.2 and [<sup>35</sup>S]Kir6.2 were expressed by taking 4 µg of purified Kir6.2 plasmid per reaction with 40 µl of TNT Quick master Mix, 1 µl of Canine Pancreatic Microsomal Membrane (Promega; Cat# Y4041), 1 µl of 1 mM methionine or 2 µl of [<sup>35</sup>S]methionine (1,000 Ci/mmol) (Amersham Pharmacia Biotech; Cat# SJ1015), respectively, or both, and Nuclease-free water to make the final volume to 50 µl. The mixture was incubated for 90 min at 30°C. The expressed protein was analyzed by SDS-PAGE on 7.5 % mini gels.

### 2.2.2- 7.5 % SDS polyacrylamide gel electrophoresis (SDS-PAGE)

Polyacrylamide gel electrophoresis was performed using a Mini-PROTEAN II Electrophoresis cell (BIO-RAD). The separation gel (7.25 ml 0.75 M Tris-HCl (pH 8.8); 3.5 ml acrylamide/bisacrylamide, 1 ml 1.5 % SDS, 2.67 ml deionized water, 60 µl ammonium persulfate, 20 µl TEMED (N,N,N',N'-Tetramethylethylenediamine)) was poured into the gel sandwich leaving 0.5 cm below the teeth of the inserted comb. A poured gel was overlaid with water and left for 30 min to polymerize. The water was removed and the stacking gel (5 ml 0.75 M Tris-HCl (pH 6.8), 1.33 ml acrylamide/bisacrylamide, 0.7 ml 1.5 % sodium dodecyl sulphate (SDS), 2.67 ml deionized water, 40 µl ammonium persulfate, 15 µl TEMED) was added and left to polymerize for 30 min. Samples were denatured in an equal volume of denaturing buffer (220 mM sucrose, 2 % SDS, 18 mg/ml dithiothreitol (DTT), 62 mM Tris-HCl (pH 6.8), 0.001 % bromophenol blue stain) for 30 min at room temperature. Normally, the supernatant was heated for 5 min at 95°C, and then loaded onto the gel with protein molecular markers in an adjacent lane. Sample containing Kir6.2 were denatured at room temperature to prevent aggregation of the polypeptide. Gels were electrophoresed for 90 min at 120 V using a power pack 300 (Bio-Rad).

### 2.2.3- Western blotting

Samples were loaded and electrophoresed on a 7.5% SDS gel. The gel was soaked in blotting buffer (200 mM glycine, 25 mM Tris-HCl, 10 % methanol (pH 8.3)) for 10 min before being sandwiched between one sheet of scotch bright and one sheet of 3 MM filter paper, with a Hybond-P membrane (Amersham Biosciences, Cat# RNP303F) on top of the gel in the direction of blotting electrophoresis. Hybond-P membrane was pre-washed in 100% methanol for 10 seconds then put in ddH<sub>2</sub>O before use. The electrophoretic transfer was run for 2 h at 150 mA at 4°C. After transfer, the membrane was removed and the molecular marker lane was cut and stained with amino black stain (0.1 % amino black stain, 45 % methanol, 10 % acetic acid) for 2 min, then de-stained with 1 % acetic acid for 2 min. Sample lanes were placed in blocking solution (10 mM Tris-HCl (pH 7.5), 0.9 % NaCl, 0.05 % Tween-20, 5 % dry milk powder) for 1 h at room temperature. The membrane was incubated overnight with the appropriate dilution of primary antibody in blocking solution. Following washes with TBS-T (50 mM Tris-HCl (pH 7.5), 150 mM NaCl, 0.05 % Tween-20) three times for 10 min and with TBS (50 mM Tris-HCl (pH 7.5), 150 mM NaCl) twice for 10 min, the membrane was incubated with HRP-conjugated secondary antibody (see below) for 2 h at room temperature. Before developing the signal, the membrane was washed with TBS-T three times and then two times with TBS for 10 min.

### 2.2.4- Development of Western blots

The ECL Western blotting detection system (Amersham Biosciences, CAT# RPN2106) was used to visualise bound antibody. The secondary antibody used in this method was anti-mouse IgG labeled horseradish peroxidase (HRP) 1/7,000 dilution (Amersham Biosciences, CAT# NA931). Equal volumes of ECL detection solution 1 and detection solution 2 were mixed to provide a final volume of 0.125 ml/cm<sup>2</sup> membrane. After removal of the secondary antibody and wash, the excess washing buffer was drained and the mixed detection reagent applied to the membrane, protein side up. The membrane was incubated

for 1 min at room temperature. The excess detection solution was drained and the membrane was placed on to a fresh piece of saran wrap, protein facing side down, and wrapped for autoradiography on autoradiography film (Hyperfilm ECL, Amersham Biosciences, CAT#RPN2114K). Films were exposed routinely for 2, 5 and 15 min.

### 2.2.5- Maltose binding protein fusion polypeptide preparation

Fragments of SUR2A were cloned in the pMAL-c2x vector (New England Biolabs, UK, Cat# 800-76). Confirmed SUR2A fragment sequences were transformed into competent DH5 $\alpha$ . *E. coli* cells. A colony was picked to inoculate 5 ml LB medium containing the required antibiotic and incubated overnight at 37°C. The cells were grown overnight so that the absorption at 600 nm was > 1.0. A large scale preparation of each fragment was made by inoculation of 250 ml of LB with 1 ml of the overgrown culture. The cells were grown for 3 h at 37°C with 220 rpm shaking until the absorption at 600 nm was approximately 0.5 to 0.6. MBP-fragment expression was induced with 0.3 mM isopropyl  $\beta$ -D-thiogalactoside (IPTG) in water (1.5 ml of 50 mM IPTG) and incubated for a further 2 h at 37°C with 220 rpm shaking. Cells were pelleted by centrifugation for 30 min at 2800 g and lysed by freezing at -20°C overnight. The pellets were thawed in a water bath at room temperature and resuspended in 2 ml column buffer (20mM Tris-HCl (pH 7.4), 200 mM NaCl, 1 mM EDTA, 10 mM  $\beta$ -mercaptoethanol). The resuspended cells were sonicated for 20 seconds and centrifuged at 6900 g for 20 min. The supernatant was incubated overnight at 4°C with 1 ml of a 1:1 slurry of Amylose resin (New England Biolabs, Cat# E8021S) that has been pre-generated with 3 column volumes of water, 3 column volumes of 0.1 % SDS, 1 column volume of water, then 3 column volumes of column buffer, with occasional mixing. The Amylose resin was recovered by centrifugation at 100 g for 5 min at 4°C. The resin was then washed three times with 6 ml column buffer. The MBP-SUR2A fragments were eluted with 1 ml column buffer containing 20 mM maltose for 5 min at 4°C and the eluate recovered by centrifugation as above. The resin was re-eluted with another 1 ml of column buffer containing 20 mM maltose.

### 2.2.6- Protein determination

The Bradford assay was used to determine the concentration of the SUR2A fragments (Bradford, 1976). A stock solution (100 ml of 95 % ethanol, 200 ml of 88 % phosphoric acid, and 350 mg of Serva Blue G) was used to make the Bradford working solution (425 ml distilled water, 15 ml of 95 % ethanol, 30 ml of 88 % phosphoric acid, and 30 ml of stock solution). An equal volume was added to the samples and the standard protein samples (dilution of 1 mg/ml of Bovine Serum Albumin (BSA) in elution buffer (20 mM Tris-HCl (pH 7.4), 200 mM NaCl, 1 mM EDTA, 10 mM  $\beta$ -mercaptoethanol) containing 20 mM maltose. BSA solution was used to produce a standard curve of protein concentration. The working standards were prepared containing the following amounts of BSA: 1  $\mu$ g, 2.5  $\mu$ g, 5  $\mu$ g, 10  $\mu$ g, 12.5  $\mu$ g, 15 $\mu$ g, 17.5  $\mu$ g, and 20  $\mu$ g made up in a volume of 100  $\mu$ l with distilled water (Fig2-1). Protein samples 10  $\mu$ l, 20  $\mu$ l, and 30  $\mu$ l were diluted with distilled water to a final volume of 100  $\mu$ l, then 1 ml of working solution was add to each tube and incubated at room temperature for 5 min. The concentration of the protein samples was determined by measuring the absorption at 595 nm wavelength using a spectrophotometer.

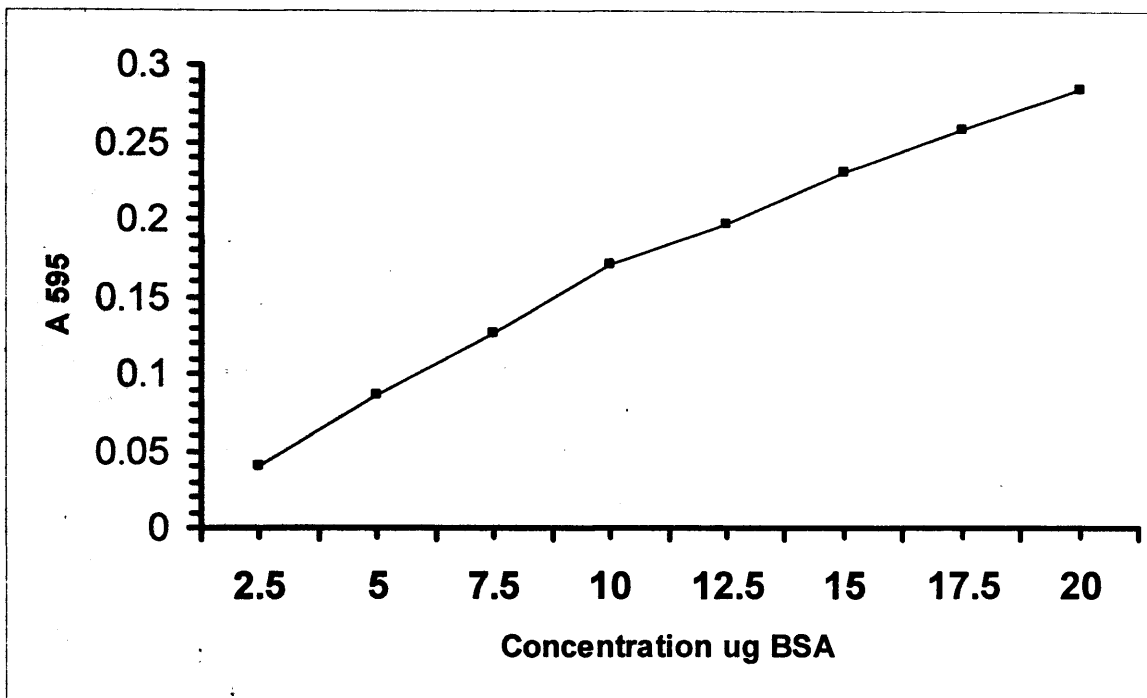


**Figure 2-1. Standard curve of Protein concentration using the Bradford assay.** The concentration of BSA is given on the abscissa and Absorbance at 595 nm ordinate.

#### 2.2.7- Co-immunoprecipitation of MBP-SUR2A fragments with Kir6.2

Interaction between Kir6.2 and MBP-SUR2A fragments was carried out in a Pyrex tube. The proteins (1  $\mu$ l TNT expressed Kir6.2, 3  $\mu$ l TNT expressed [ $^{35}$ S]Kir6.2 and 20  $\mu$ l MBP-SUR2A fragments containing 180 ng protein) were mixed and sonicated 8 times for 15 seconds at 37°C with 15 second reset. The mixture was incubated at 37°C for 1 h, then at room temperature overnight. For each MBP-SUR2A fragment, two tubes were set up; one containing a mixture of Kir6.2, [ $^{35}$ S] Kir6.2 and SUR2A fragment, the other containing only the SUR2A fragment as a control. The mixtures were transferred into 0.5 ml microfuge tubes and incubated with 23  $\mu$ l of 1.5% Triton-X100 in 20 mM Tris-HCl (pH 7.4) for 30 min at 4°C. The samples were centrifuged at 11600 g for 15 min at room temperature, to remove insoluble material, and the supernatants were added to the following mixture, (5  $\mu$ l of 20 mM Tris-HCl (pH 7.4), 40  $\mu$ l 25 % bovine serum albumin in

20 mM Tris-HCl (pH 7.4), 20  $\mu$ l 2.5 M KCl in 20 mM Tris-HCl (pH 7.4), 4  $\mu$ l of anti-Kir6.2 antiserum (86130) and 50  $\mu$ l 100 mg/ml protein A-Sepharose(5 mg) in PBS (pH 7.4)) and incubated overnight at 4°C with rolling. Samples were centrifuged at 620 g for 1 min at 4°C and supernatants were removed and discarded. Resin pellets were washed three times with 0.5 ml IP buffer (20 mM Tris-HCl, (pH 7.4), 500 mM KCl, 0.1 % Nonidet P40) and bound proteins eluted by addition of 15  $\mu$ l SDS- denaturing buffer (220 mM sucrose; 2 % SDS; 18 mg/ml dithiothreitol (DTT); 62 mM Tris-HCl (pH 6.8); 0.001 % bromophenol blue stain). Eluted proteins were electrophoresed in a 7 % SDS-PAGE.

#### 2.2.8: GST-Tag fusion protein purification

Fragments of SUR2A were generated in pET-41a (+) plasmid (Novagen, USA Cat# N41534,). The confirmed SUR2A fragment sequences, GST-SUR2A-CT1 (aa 1358-1545), GST-SUR2A-E (aa 1358-1545), and GST-SUR2A-NBF1 1/4 (aa 683-873) were transformed into competent NovaBlue (DE3) cells (Novagen, USA, Cat# 69284-4). A 5 ml culture of BL21 containing 5  $\mu$ l of kanamycin sulphate (Gibco, Cat# 11815-024)(50 mg/ml) was inoculated and incubated overnight at 30°C. The cells were overgrown so that the absorption at 600 nm was > 1.0. A large scale preparation of each fragment was made by inoculation of 50 ml of LB with 1 ml of the overgrown culture. The cells were grown for 6 h at 30°C with 220 rpm shaking until the absorption at 600 nm was approximately 0.5 to 0.6. GST- fragment expression was induced with 0.3 mM isopropyl  $\beta$ -D-thiogalactoside (IPTG) in water (1.5 ml of 50 mM IPTG) and incubated overnight at 30°C with 220 rpm shaking. Cells were pelleted by centrifugation for 30 min at 2800 g and lysed by freezing at -20°C overnight. The GST-fusion protein was purified using the GST-Bind Kits (Novagen, USA, Cat# 70534-3). The pellets were thawed in a water bath at room temperature, and re-suspended in 2 ml GST Binding/Washing buffer (4.3 mM Na<sub>2</sub>HPO<sub>4</sub>, 14.7 mM KH<sub>2</sub>PO<sub>4</sub>, 137 mM NaCl, 2.7 mM KCl, (pH 7.3)). The re-suspended cells were sonicated for 20 seconds and centrifuged at 6900 g for 20 min at 4°C. The supernatant was incubated overnight at 4°C with 200  $\mu$ l of a 1:1 slurry of GST-binding resin. The resin was washed by resuspending the resin in 10 volumes of GST- binding/washing buffer, then centrifugation for 1 min at 620 g, and was repeated three times. The GST- fusion protein was eluted with

100  $\mu$ l Elution buffer (50 mM Tris-HCl, pH 8.0, 100 mM reduced glutathione) by incubating the reaction for 10 min at room temperature with gentle agitation. The eluted protein was recovered by centrifugation as above.

### 2.2.9- Determination of the concentration of protein tagged with GST (activity)

The GST-tag assay kit is designed to perform quantitative colorimetric assays of glutathione S-transferase by using direct enzymatic assay (Novagen, Cat# 70532-3).

Stock chemicals were prepared and stored in  $-20$  °C.

Assay Buffer (43 mM  $\text{Na}_2\text{HPO}_4$ , 14.7 mM  $\text{KH}_2\text{PO}_4$ , 137 mM NaCl, 2.7 mM KCl (pH 7.3))

- a- 100 mM reduced glutathione by dissolving 1 g of glutathione in 32.5 mL of  $\text{dH}_2\text{O}$
- b- 100 mM CDNB by dissolving 20.6 mg of 1-chloro-2,4-dinitrobenzene (CDNB) substrate 1 ml of 100% ethanol

The concentration of the standard and the sample were determined by transfer 1ml of substrate solution (100  $\mu$ l of 10X Assay Buffer, 10  $\mu$ l of 100 mM CNDB, 10  $\mu$ l of 100 mM reduced glutathione, and 880  $\mu$ l  $\text{dH}_2\text{O}$ ) to a clean 1ml quartz cuvette and the absorbance reading at 340 nm adjusted to zero. A standard curve was prepared by making a serial dilution of the supplied GST-Tag Standard (0.5 mg/ml) in the same buffer in which the samples were suspended to give the following concentrations 0.0625, 0.125, 0.250, 0.5, 1 and 1.5 mg/ml. Test samples were measured by adding 2  $\mu$ l of purified GST-fragment to the cuvette and mixed by covering the cuvette with parafilm and inverting several times. Absorbance reading was recorded every 30 sec over a period of 5 min, and the calculation was performed to determine the  $\Delta A_{340}/\text{min}$  for each standard and sample reaction. The change in absorbance  $\Delta A_{340}/\text{min}$  was calculated using the following formula where  $t_{\text{final}}$  and  $t_{\text{initial}}$  are the last and the first time point, respectively with the 1min absorbance as the initial.

$$(\Delta A_{340})/\text{min} = A_{340} (t_{\text{final}}) - (t_{\text{initial}}) / (\text{Assay duration in min})$$

by plotting  $\Delta A_{340}/\text{min}$  versus  $\mu\text{g}$  GST, a standard curve was generated that was used to determine the mass of active GST present in the sample.

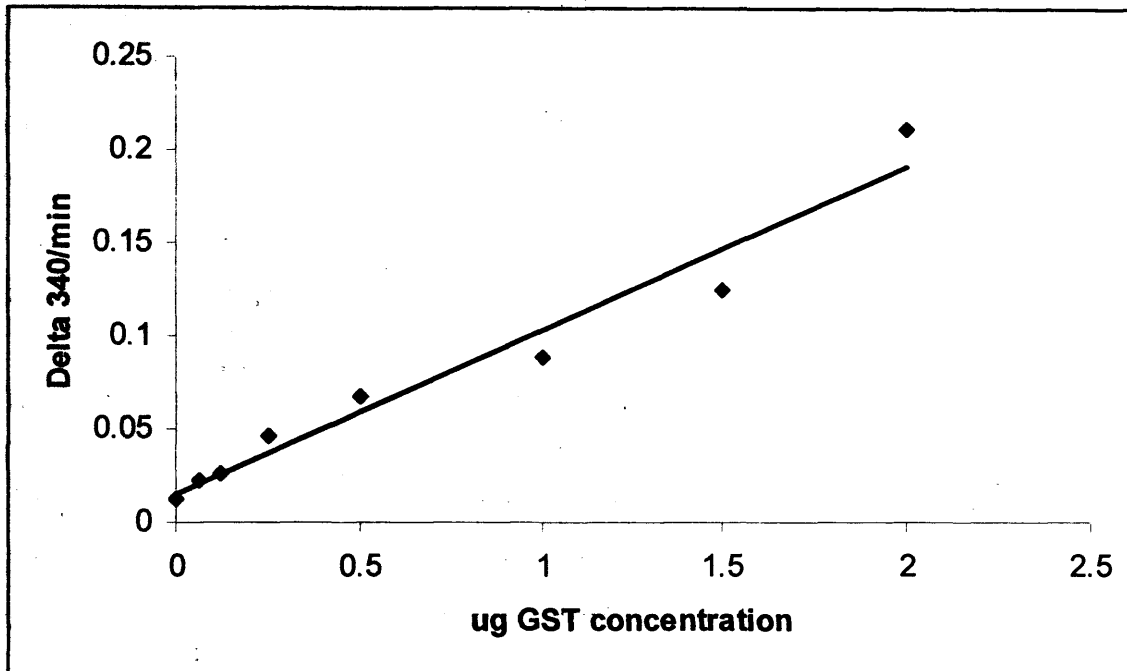


**Figure 2-2. Standard curve of GST activity.** The mass of active GST present in the sample is given on the abscissa and the change in  $A_{340}$  /min on the ordinate.

### 2.3- Immunocytochemistry methods

#### 2.3.1- Transfection of HEK 293 cells

A characterised HEK 293 cell line stably expressing Kir6.2/SUR2A (provided by Dr. A. Tinker; University College, London) was grown in a 75 cm flask with complete medium (88 % EMEM, 10 % FCS, 1 % Glutamine). On the day of transfection, the cells were 80-90 % confluent. The cells were washed with PBS (2.7 mM KCl, 1.5 mM  $\text{KH}_2\text{PO}_4$ , 137 mM NaCl,  $\text{Na}_2\text{HPO}_4$ , adjusted to pH 7.4), then detached with 3 ml of trypsin (0.1 % trypsin, 0.02 % EDTA) and incubated at 37°C for 5 min. Complete medium was added to deactivate the trypsin and cells were harvested by centrifugation at 400 g for 5 min. Cells were resuspended in 1 ml of complete medium and plated in a 6 well plate for transfection. A dilution was made to the transfection reagent stock by adding 3  $\mu\text{l}$  of Lipofectamine 2000 to 90  $\mu\text{l}$  of MEM-ES (Gibco, Cat# 21090-022) without bovine serum albumin and L-glutamine. The mixture was incubated for 5 min at room temperature. One microgram of cDNA was then added to the reagent mixture and incubated for 20 min at room

temperature. The lipid-DNA complex was added drop-wise to the required well containing 2 ml of the complete medium (without antibiotic) with gentle agitation. Cells were then incubated at 37°C under 5 % CO<sub>2</sub> 95% O<sub>2</sub> for 48 hours after transfection. Cells were harvested as above for fixation and staining.

### 2.3.2- Fixation and permeablization

The cell suspension was added to a 2.5 cm coverslip coated with polylysine and incubated for 20 min at 4°C to allow the cells to settle. Fixative solution (2 ml, 2 % paraformaldehyde in PBS (pH 7.4)) was added to the cells and incubated for 10 min at room temperature. Fixative solution was aspirated from the cells and 2 ml of 0.1 M glycine buffer adjusted pH of 7.4 was added and incubated for 10 min at room temperature. The glycine was removed and permeablization solution (2 ml, 0.1 % Triton-X 100 in PBS (pH 7.4)) was added for 10 min. The coverslip was washed gently three times with PBS (pH 7.4) for 5 min without dislodging the cells.

### 2.3.3- Staining and confocal microscopy

The coverslip was blocked with antibody dilution buffer ((SSC; 150 mM NaCl, 15 mM Na<sub>3</sub> citrate (pH 7.4)), 2 % goat serum, 1 % bovine serum albumin, 0.05 % Triton-X 100) for 30 min at room temperature. The primary antiserum, anti-Kir6.2 or anti-SUR2A, (1/1000 dilution see below) was added and incubated for 1 h. The secondary antibody, goat-anti rabbit IgG labeled with Alexa Fluor 568 (Molecular- Probes, Cat# A-11011) (1/2000 dilution) was added and incubated for 1h in the dark. The coverslip was washed after each antibody incubation with washing buffer (SSC (pH 7.4), 0.05 % Triton-X 100). The cells were analyzed using an Ultra view confocal scanner using 488nm and 568 nm lasers with Perkin Elmer software.

#### 2.3.4- Data acquisition and image processing

Confocal image processing was performed using the Ultra-view software (v4.0) (Perkin Elmer, Beaconsfield, UK). As a device to represent distribution of fluorescent intensity in rSUR2A-CT transfected cells, data was presented as intensity across a line created from individual cell images drawn horizontally through the confocal plane at the center of the cell. Peak fluorescent intensities for EGFP-F and anti-K<sub>ATP</sub> channel antibody binding were normalized. Plasma membrane-associated fluorescence signal associated with anti-K<sub>ATP</sub> channel antibody binding at the plasma membrane was expressed as a ratio of the plasma membrane EGFP-F fluorescent signal.

#### 2.3.5- Preparation of polyclonal antibodies

Antisera were raised to peptides corresponding to the C-terminal domain of the rat Kir6.2 (D86039), SUR2A (D83598) and Kir2.1 proteins has been raised by others in the laboratory (Singh et al 2003; Stonehouse et al. 1999). Briefly, the peptides were synthesized in accordance with standard methodology (Atherton and Sheppard, 1985) and were composed of the following amino acid residues: Kir6.2: (C)KAKPKFSISPDSLS (residues 377-390, Research Genetics Inc. Huntsville, USA); SUR2A: PNLLQHKNGLFSTLVMTNK(C) (residues 1527-1545, Pepceuticals Ltd., Leicester, UK); Kir2.1(C)HNQASVPLEPRPL (residues 409-421). N- or C-terminal cysteine residues were added to the peptides to facilitate conjugation to ovalbumin (Kir2.1) or Keyhole Limpet Haemocyanin carrier proteins (Larochelle et al., 1985) and were not part of the channel protein sequences. The peptide-ovalbumin conjugates were inoculated into New Zealand White rabbits. Antibody titer was estimated by ELISA using microtiter plates coated with 1 µg/ml peptide.

## **Chapter Three**

# **Preparation and modification of constructs for expression of polypeptide, chimaeras, mutant and epitope tagged K<sub>ATP</sub> channel subunits**

### 3.1- Introduction

Use of molecular biology techniques has considerably expanded the possibility for ion channel research. These techniques have enabled the researcher to find the complete amino acid sequence of most of the channel proteins and has helped to draw an outline of their three dimensional structures. Molecular biology also enables channel subunits to be labelled with specific epitope tags, to facilitate their detection, and the construction of subunit chimaeras, mutants and fragments of selected parts of the subunit protein to permit focused studies of sub-domains within the channel subunit polypeptides.

The main aim of this project was to provide a detailed molecular characterization of the inter-subunit interactions between the cytoplasmic domains of Kir6.2 and SUR2A subunits. In addition to the masking of ER retention signals to permit release from the endoplasmic reticulum and target to the cell surface, other interactions between cytoplasmic domains of Kir6.2 and SUR2A polypeptides are also likely to contribute to assembly and allosteric interactions within the channel. The possibility of an interaction of the NBF1 and NBF2 domains with the full length of Kir6.2 subunit of the  $K_{ATP}$  channel complex has not been reported in the literature. In order to investigate the possibility of an interaction between the two subunits of the cardiac  $K_{ATP}$  channel, fragments of the SUR2A subunit were constructed with an epitope tag on the N-terminal of the fragment for use in co-immunoprecipitation experiment with Kir6.2. The same fragments were also made untagged for study of subunit localization within cells and for electrophysiological experiments. Some of the fragments were provided by Dr. M Routledge. These included N-terminally MBP tagged fragments created on the NBF2 of SUR2A called as follows: MBP-rSUR2A-CT-A (amino acid 1294-1545), MBP-rSUR2A-CT-B (aa 1254-1403), MBP-rSUR2A-CT-C (aa 1294-1403), and MBP-rSUR2A-CT-D (aa 1358-1545) (Figure 3-1) (Rainbow et al, 2004). Two other N-terminally MBP tagged fragments from the NBF1 of SUR2A, MBP-rSUR2A-NBF1-1 (aa 683-873), and MBP-rSUR2A-NBF1-2 (aa 832-975) (Figure 3-1), were also provided. These fragments were used to investigate the binding of the NBF-contrarily cytoplasmic domains of SUR2A to full length Kir6.2 subunits. Additional MBP-tagged SUR2A fragments were constructed in the current study to further localize the Kir6.2 binding site to a small region in SUR2A.

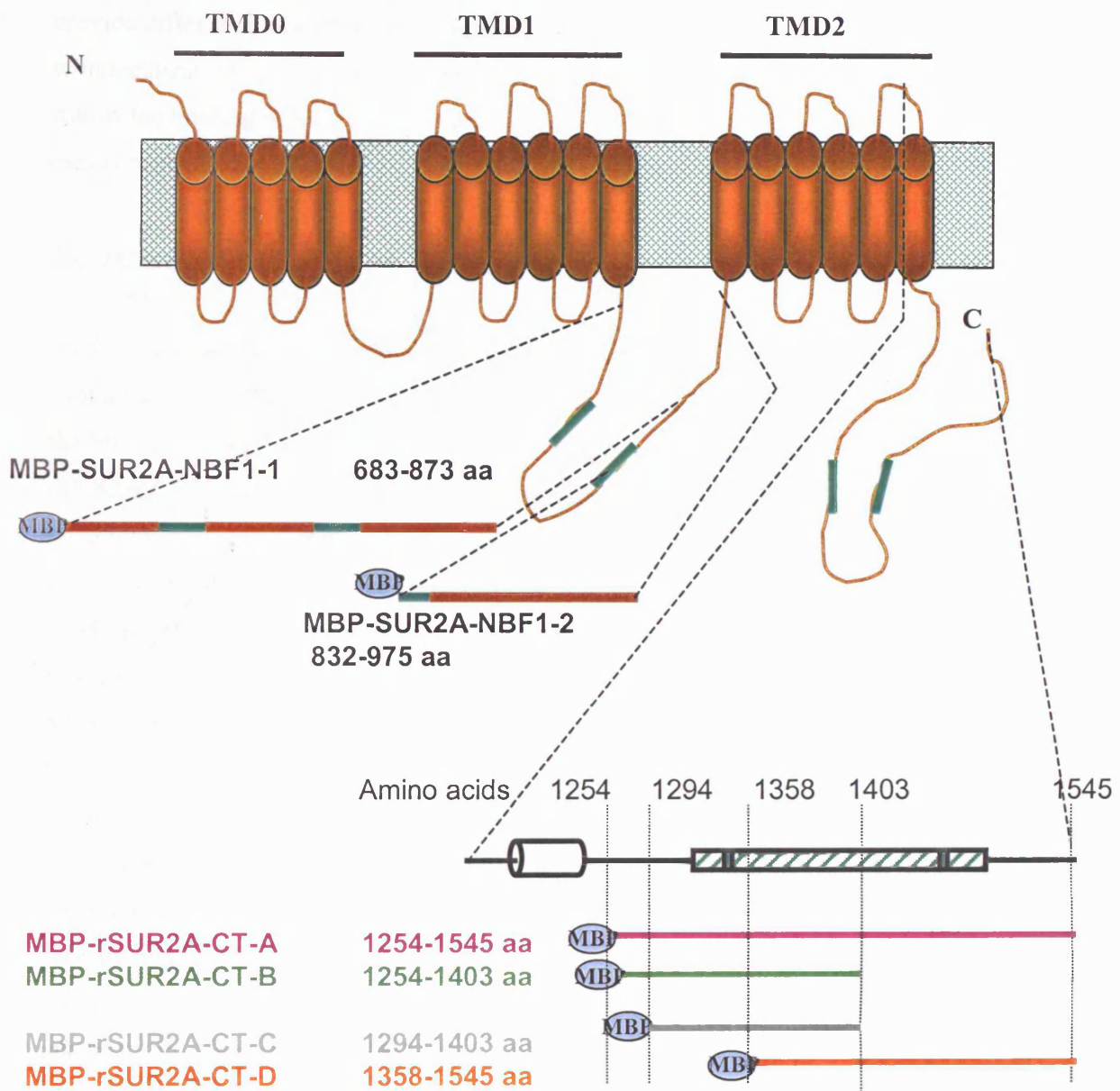


**Figure 3-1 Schematic diagram of SUR2A fragments.** The top of the figure shows the full structure of the SUR2A subunit. The N-terminal MBP tagged fragments of NBF1 and the C-terminal are shown underneath (amino acids numbered). These fragment constructs were created by Dr. M Routledge.

Furthermore, other tagging systems (HA, GST) were used to confirm the findings and to provide different tools for the investigation. HA-SUR2A fragments were developed to help with localization experiments and GST-SUR2A-fragments were created as a second way to follow the binding of SUR2A-fragments with the Kir6.2 subunit in co-precipitation experiments.

### 3.2- Truncation of the SUR2A-CT-C fragment

To drive a series of truncation polypeptides from the rSUR2A-CT-C fragment, a stop codon was inserted at different points within the cDNA sequence of rSUR2A-CT-C. Using the Stratagene QuikChange™ site-directed mutagenesis kit, a mutation was made in rSUR2A-CT-C fragment present in the pIRES2-EGFP-F and pMAL-c2x plasmids. Those mutations produced C-terminally truncated fragments of rSUR2A-CT-C of 65, 54, and 43 amino acids, which were called rSUR2A-CT-E (aa 1294-1403), rSUR2A-CT-F (aa 1294-1348) and rSUR2A-CT-G (aa 1294-1337), respectively (Figure 3-2). The stop code was inserted by using oligonucleotides designed with mutant nucleotides, which would insert a STOP code at the desired point. The mutagenic regions of the oligonucleotide were within the centre of the sequence. This was done to reduce the rejection of the mismatched bases during the synthesis of the mutated cDNA, as there would be larger regions of matched bases on either side of the mutagenic region. The oligonucleotides were made by MWG. For example, the generation of rSUR2A-CT-E (aa 1294- 1358), two oligonucleotides, forward and backward, were made for each reaction (Table 3-1). The mutant bases in the forward oligonucleotide are written in bold letters which forms the stop code is shown underlined for each construct (Table 3-1). A basic outline method of the mutagenesis kit is provided within the methods (section 2.1.2). Once the PCR reaction had completed, the template DNA was digested with the restriction enzyme *Dpn* I. *Dpn* I endonuclease selectively digests methylated and hemimethylated DNA, therefore, digests the parent strand so that only non-methylated mutated cDNA remained. The construct was then transformed into DH5α competent cells as outlined in the methods (section 2.1.12). Colonies were analysed for successful mutants by purifying the cDNA using the Miniprep,

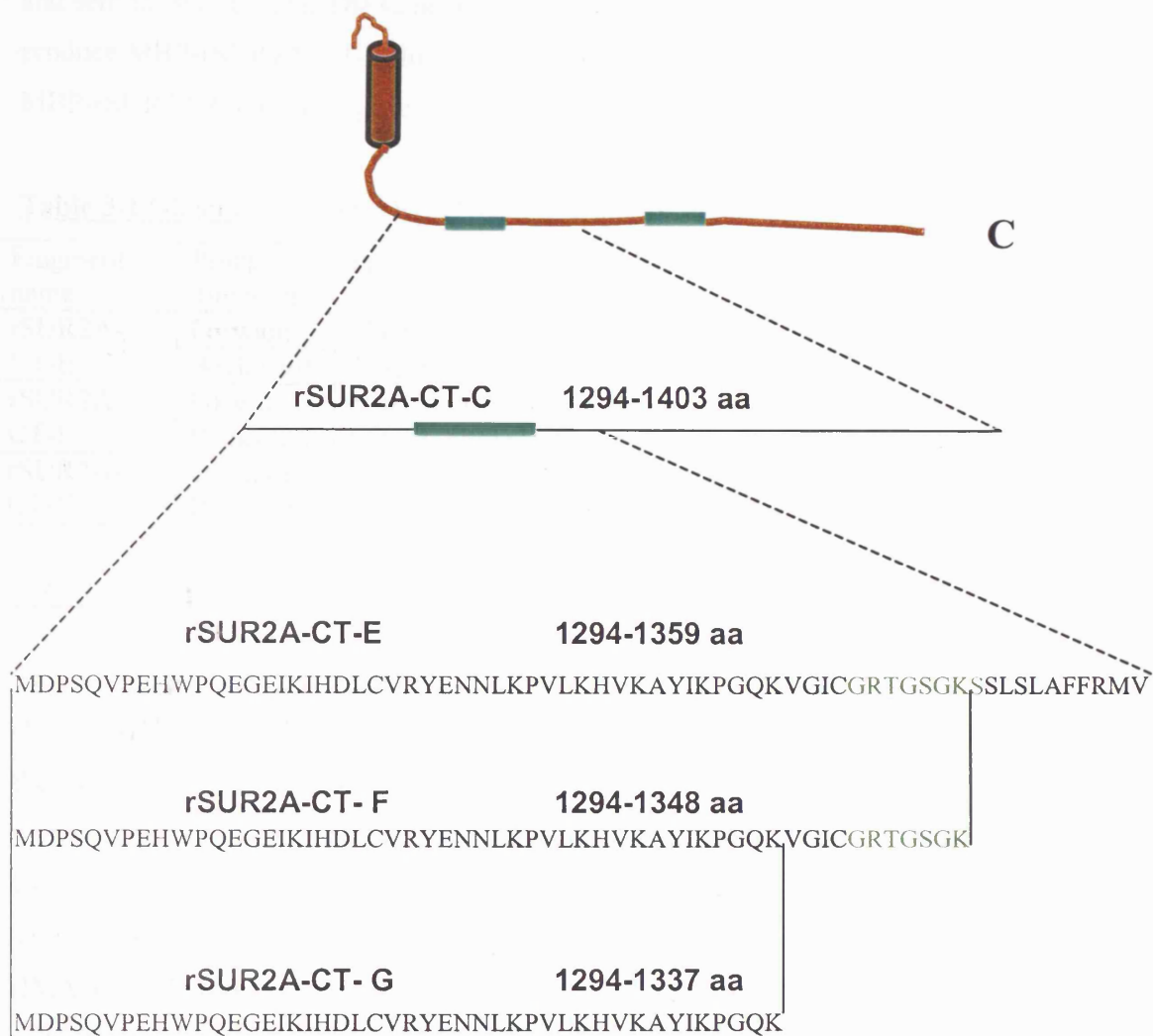


**Figure 3-2 Schematic diagram for the truncation of SUR2A-CT-C fragment.** The top of this figure represents a drawing of the C-terminal of SUR2A (SUR2A-CT-C). SUR2A-CT-C was truncated to produce the fragments rSUR2A-CT-E, rSUR2A-CT-F, and rSUR2A-CT-G. The amino acid sequences of the new truncated fragments are presented in this diagram. Walker A and B motifs are indicated in green.

and sent for sequencing. The same protocol was followed with pMAL-c2x vector to produce MBP-rSUR2A-CT-E. In addition, other constructs MBP-rSUR2A-CT-F, and MBP-rSUR2A-CT-G were generated in the same fashion.

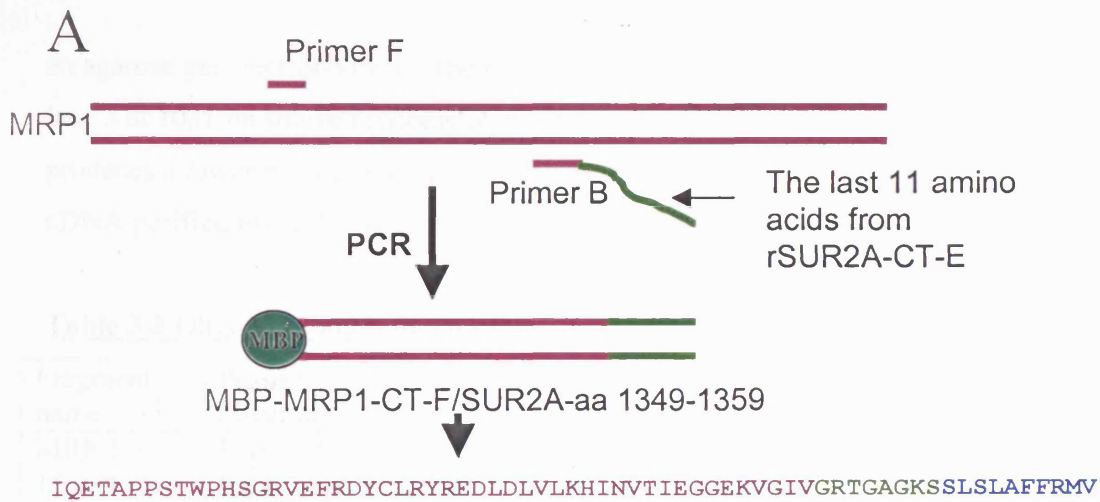
**Table 3-1** Oligonucleotide for SUR2A-CT-C truncation

Fragment name	Primer direction	Primer sequence
rSUR2A-CT-E	Forward	5' GCTTTCTTCAGAAGTGTCTAGATATTTGATGGAAAG 3'
	Backward	5' ATCTTCCATCAAATATCTAGACCATTCTGAAGAAA 3'
rSUR2A-CT-F	Forward	5' ACCGGTAGTGGGAAG TAG TCTCTATCTCTGGC 3'
	Backward	5' GCCAGAGATAGAGACTACTCCCACTACCGGT 3'
rSUR2A-CT-G	Forward	5' CCTGGGCAGAAGTAGGGCATCTGTGG 3'
	Backward	5' CCACAGATGCCCTACTTCTGCCCAGG 3'

### 3.3- Construction of MRP1-CT-F/SUR2A (aa 1349-1359)

To investigate possible interaction with Kir6.2 through the last 11 amino acids of the rSUR2A-CT-E fragment, these residues were moved into a chimaeric construct based on the equivalent sequence (MRP1-CT-E) of the non-interacting ABC cassette protein, multidrug resistance protein 1 (MRP1). Residues 1349-1359 of SUR2A were added to the C-terminal of the MBP-MRP1-CT-F fragment using a PCR strategy (Figure 3-3).

The reaction was made by using the cDNA from mouse MRP1 in pCMV-SPORT6 vector (IMAGE, 53231099) as template. The priming oligonucleotides were designed to include a restriction enzyme sequence, *Bgl*III in the forward oligonucleotide written in italic (Table 3-2), followed by a methionine then the hybrid sequence of the MRP1. The backward oligonucleotide consisted of restriction enzyme sites for *Pst*I after the stop codon, the sequence of the last 11 aa of SUR2A-CT-E followed by a hybrid sequence from the MRP1 sequence. After the PCR reaction had completed, the cDNA product was digested with the restriction enzymes *Bgl*III and *Pst*I and the plasmid double digested with *Bam*HI and *Pst*I, then treated with Shrimp alkaline phosphatase (SAP). The PCR product was inserted into the pMAL-c2x vector. Colonies were then picked and streaked out, then indicated clones selected and grown in overnight cultures in carbenicillin containing medium for selection. Colonies were analysed for successful recombination by DNA purification using Miniprep (see section 2.1.4), followed by restriction digest with *Bgl*III and *Hind*III and running on



**B**

**rSUR2A-CT-E amino acid sequence**

MDPSQVPEHWPQEGEIKIHDLVCVRYENNLKPVLKHVKAYIKPGQKVGICGRTGSGKSSLSLAFFRMV  
 IQETAPPSTWPHSGRVEFRDYCLRYREDLDLVLKHINVTIEGGEKVGIVGRTGAGKSSLTGLFRIN

**MRP1-CT-E amino acid sequence Walker A**

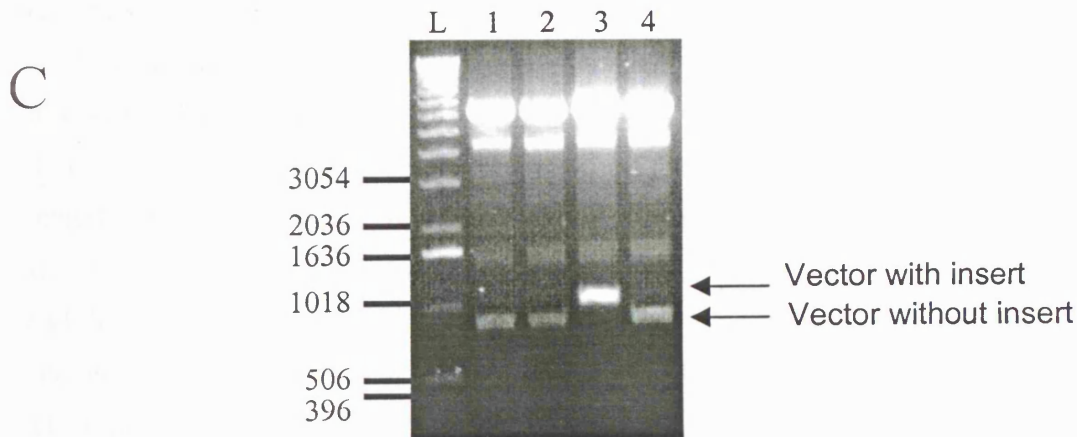


**Figure 3-3 Construction of MRP1-F plus the last 11 amino acid residues from rSUR2A-CT-E (MRP1-CT-F/SUR2A aa 1349-1359).** A, PCR reaction strategy applied to make the above fragment. The purple colour represents the MRP1 segment and the blue represents the SUR2A segment. B, shows the amino acid alignment for the rSUR2A-CT-E fragment with the equivalent sequence from MRP1 (MRP1-CT-E). C, Gel photograph showing a digest of pMAL-c2x recombinant constructs with *Hind*III and *Bgl*II. Lane 1,2,4 shows the vector without insert but lane 3 shows an insertion of the fragment (indicated by a slower migrating band). The result were confirmed by nucleotide sequencing.

an agarose gel electrophoresis. The result is shown in (Figure 3-3). The higher band size in lane 3 at 1031 bp showed successful insertion of the construct, whereas the vector by itself produces a lower band at 830 bp. This construct was grown in a larger culture and the cDNA purified using the Midiprep (see section 2.1.3) then sent for sequencing.

**Table 3-2** Oligonucleotides for construction of MRP1-F+11 of SUR2A

Fragment name	Primer direction	Primer sequence used (5' to 3')
MRP-F + 11aa from SUR2A	Forward	5' CAATGGAGATCT <b>ATG</b> CAAGAGACAGCTCCAC 3'
	Backward	5' TAACCGCTGCAGCTAGACCATTCTGAAGAAAGCCAG AGATAGAGAGGATTTCCCAGCTCCCGTACG 3'

#### 3.4- Construction of SUR2A-CT-A-C fragment

A PCR reaction was carried out in order to generate a SUR2A-CT fragment that did not overlap with rSUR2A-CT-C using the rat cDNA of SUR2A present in pCMV6c vector (provided by Prof. S. Seino). This construct was formed to include the C-terminal end of SUR2A, amino acids 1403 to 1545 as a non-interacting control fragment. The forward oligonucleotide (*GATCCGAATCAGCATGGGATCCTGAATGCA AGTGCA*) was designed to include a restriction enzyme sequence, for *EcoRI* (written in italics and underlined) followed by a methionine (also underlined), followed by the beginning sequence of the SUR2A-CT-A-C fragment. The backward oligonucleotide (*ATCGGCTCGAGCTACTTGTGGTCAT CACCA*) consisted of a restriction enzyme site sequence for *XhoI* (written in italic and underlined), followed by a stop codon (in bold) and a hybrid base sequence from the end of SUR2A fragment. After the PCR reaction had completed, (reaction details in section 2.1.1), the DNA product was double digested with the restriction enzymes *EcoRI* and *XhoI*. The plasmids, pMAL-c2x and pIRES2-EGFP-F, were double digested with *EcoRI* and *SalI*, treated with SAP and cleaned with the Cleanup Kit (see section 2.1.9). The concentration of the purified PCR product and the plasmids, after being treated with the restriction enzyme, was determined using a molecular weight marker (mass ladder). Each cut plasmid and the prepared SUR2A-CT-A-C fragment sequence amount were measured and a ligation reaction was performed to insert the

fragment sequence into both vectors (see section 2.1.11). Colonies were then picked and streaked out. Selected colonies were then grown in overnight cultures in Kanamycin/ Ampicillin containing medium for selection. The selected colonies were analysed for successful recombination by digesting the DNA product from Miniprep (Wizard) purification with appropriate restriction enzyme. A successful recombinant with pIRES2-EGFP-F produced a band of  $\approx 1796$  bp when digested with *Bgl*II whereas the vector alone produced a band of  $\approx 1374$  bp range when analysed on a 0.8% agarose gel; examples are shown in (Figure 3-5). For the pMAL-c2x vector a successful recombinant produced a band of 1266 bp when digest with *Hind*III and *Bgl*II, whereas the vector alone produced a lower band size of 840 bp. Successful insertion was confirmed by the presence of a higher DNA band size than the vector without insert, were grown in a larger culture for Midiprep and the sequence of the higher quality cDNA confirmed by dideoxy nucleotide sequencing.

### 3.5- Construction of MRP1-CT-C

The full length cDNA of the mouse MRP1 clone in pCMV-SPORT6 vector was used as template (IMAGE 5323109) in producing the construct MRP1-CT-C. The cDNA sequence of the corresponding rSUR2A-CT-C from MRP1 (aa 1280-1389), which was called MRP1-CT-C, was inserted into the pMAL-c2x vector to create a construct with a MBP tag at the N-terminal. At the same time, the cDNA was inserted into the pIRES2-EGFP-F vector to produce the construct alone without any tag. The construct was made following the steps described above (section 3.4). The descriptions of the priming oligonucleotides that were used in the reaction can be found in Table 3.3.

Modification of the MRP1-CT-C construct was carried out to convert the construct from a mouse clone to a rat clone, there being a single amino acid difference between the two species Ile in mouse to Val in rat (I1356V). The modification was done using the PCR reaction. The recombinant construct was sequenced to confirm the modification.

**Table3-3 Oligonucleotides for Construction of MRP1-C Rat**

Fragment name	Primer name	Primer sequence
MRP1-CT-C	MRP-C6A (Forward)	GATCC <u>GAAATTCAGCAT</u> GATCCAGGAAACAGCTCCAC
	MRP-C6B (Backward)	ATCGG <u>CTCGAGCT</u> ACAAGTTCATGCGGAGGGA
Mouse to Rat	MRP-M>R	AATGAGTCTGCAGAAGGGGAGATCATCATTGATGGG ATCAACATCGCCAAGATCGG

3.6- Construction of SUR2A/MRP fragment chimaeras

Four chimaeras were constructed from SUR2A and MRP1 to represent the amino acid sequence of rSUR2A-CT-C (aa 1294-1403)(Figure 3-4). The first chimaera, called MRP1(25)SUR2A (aa 1280-1304/1318-1403), consisted of 25 amino acids of MRP1 corresponding to the first 25 amino acid sequence of the rSUR2A-CT-C followed by the remaining residues of rSUR2A-CT-C. The second chimaera, called SUR2A(25)MRP1 (aa 1294-1317/1305-1389), was the reverse chimaera and consisted of the first 25 amino acids of rSUR2A-CT-C followed by the corresponding amino acid sequence of MRP1 from the rSUR2A-CT-C. The third chimaera called, MRP1(45)SUR2A (aa 1280-1324/1338-1403) consisted of 45 amino acid of MRP which corresponding to the first 45 amino acids of rSUR2A-CT-C followed by the remaining of the rSUR2A-CT-C. The fourth chimaera, called SUR2A(45)MRP1 (aa 1294-1337/1325-1389), had the first 45 amino acids of rSUR2A-CT-C followed by the corresponding amino acid sequence from MRP1 to the rSUR2A-CT-C.

The full length cDNA of SUR2A in pCMV6c vector and the C-terminal of MRP1 in pCMV-SPORT6 vector were used as templates (provided by Dr. D. Lodwick) in the production of the constructs. The cDNA sequence of the chimaeras were inserted into the pMAL-c2x vector to create chimaeras with an MBP-tag at the N-terminal. At the same time the chimaeras were inserted into the pIRES2-EGFP-F vector to produce the chimaeras alone without any tag. For each chimaera, four oligonucleotides were designed to produce the required sequence from SUR2A with a hybrid sequence of the MRP1 at the start

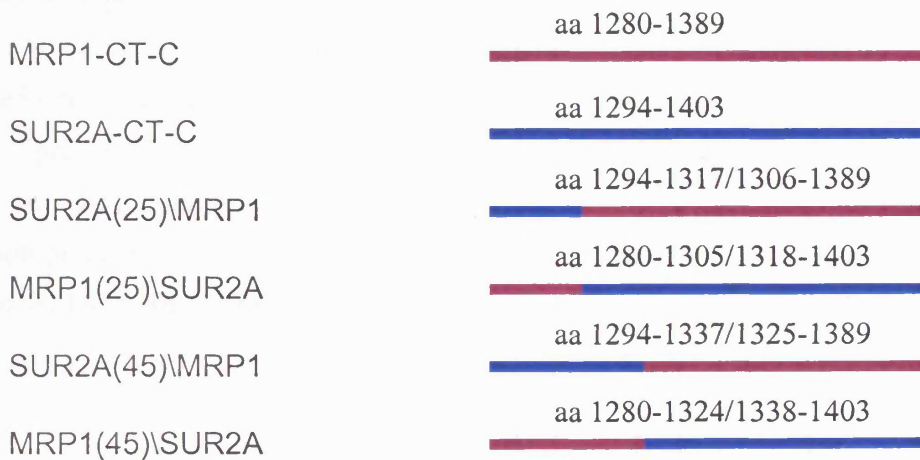
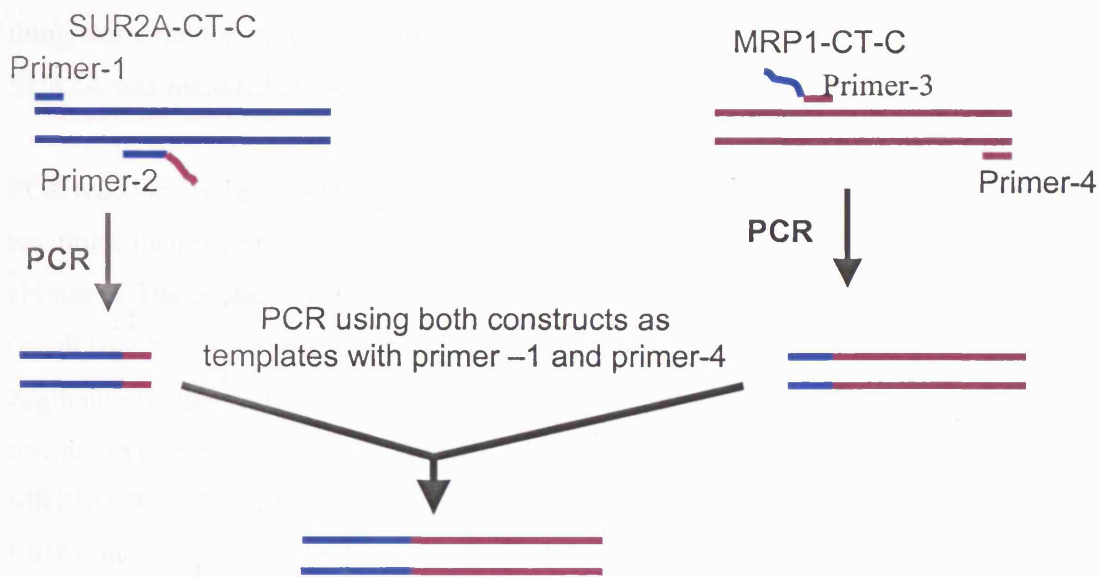


**Figure 3-4. Construction of MRP1/SUR2A chimaeras by overlap PCR.** The top panel shows the strategy used to make the MRP1/SUR2A chimeras. Overlapping MRP1 and SUR2A PCR products were generated by using chimaeric primers and then combined in a second reaction. The bottom diagram shows the final structure of the MRP1/SUR2A chimaeras, where purple represents MRP1 and the blue represents SUR2A.

or the end, depending which part of the chimaera was the first (Figure 3-4). The same thing was done for chimaeras based on MRP1 sequence where a hybrid sequence from the SUR2A was included at one of the ends.

PCR reactions were carried out to produce each segment of the chimaera in separate reactions, then the products of those reactions were used as templates to construct the final chimaera. The forward primer was designed to include a restriction enzyme sequence (*EcoRI* written in italic and underlined Table 3-4) followed by a methionine and then the beginning sequence of the SUR2A- fragment. The backward primer consisted of a restriction enzyme site *XhoI* followed by a stop codon followed by the hybrid sequence of MRP1 or SUR2A. In the chimaeras starting with MRP1, the forward primer was from MRP1 and the backward primer was from SUR2A. After the PCR reaction had completed, the product DNA was digested with restriction enzymes *EcoRI* and *XhoI*. Both plasmids were double digested with *EcoRI* and *SalI* and then treated with SAP. The PCR product was inserted into the pIRES2-EGFP-F and pMAL-c2x vector. Colonies were then picked and streaked out, then grown in overnight cultures in Kanamycin/Ampicillin containing medium for selection. Expanded colonies were analysed for successful recombination by Miniprep, restriction digest and electrophoresis on an agarose gel; examples are shown in (Figure 3-5). Successful insertion, identified by the presence of a new restriction site as appropriate, was grown in a larger culture for Midiprep DNA purification and the higher quality DNA was sent for sequencing.

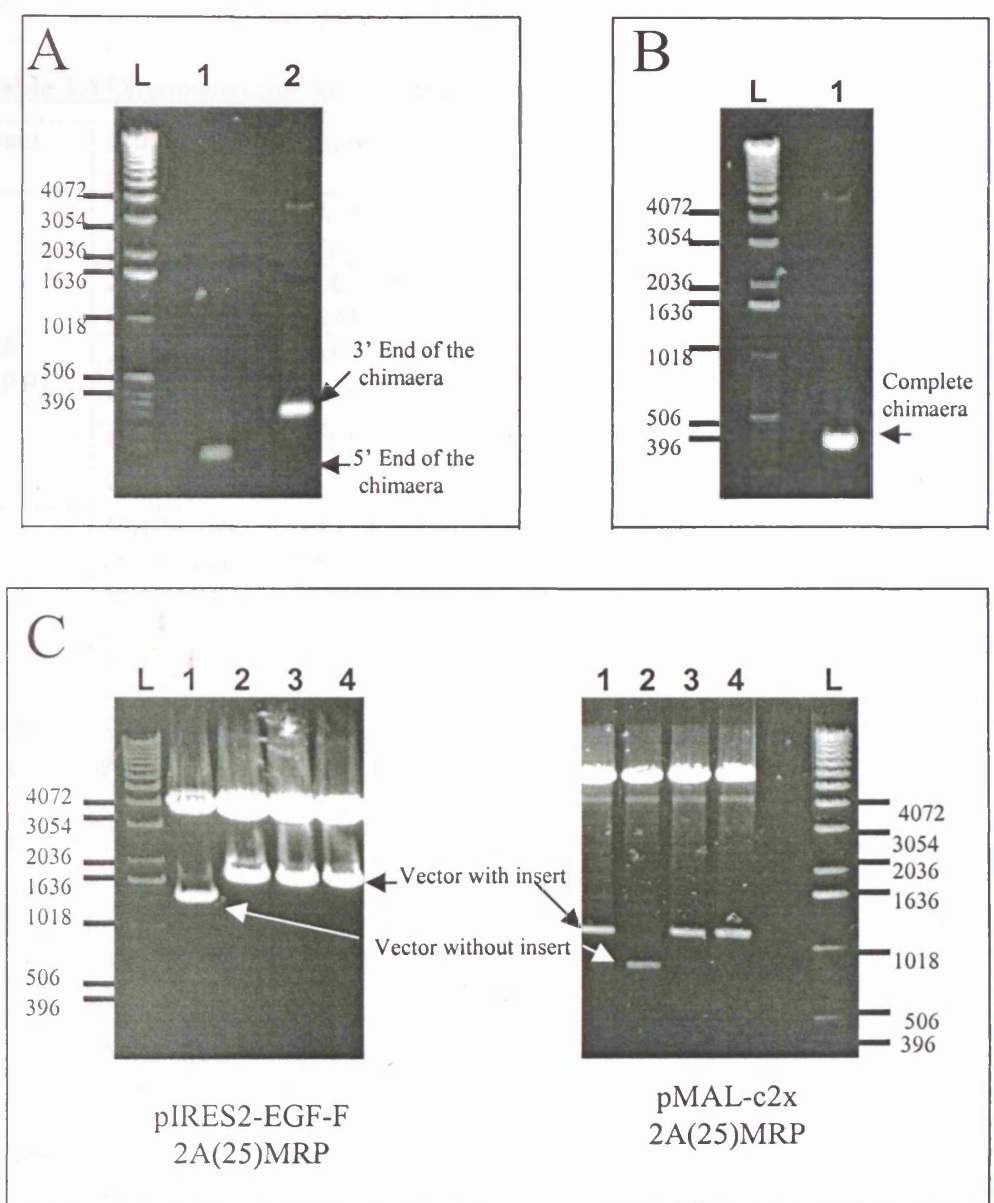


**Figure 3-5 Construction and mapping of MRP1/SUR2A chimaeras.** In this figure the constructing and mapping of the SUR2A(25)MRP1 chimaera is used as an example. A, Gel photograph showing the PCR product for the first part of SUR2A, which encodes the first 25 amino acid from the chimera (lane 1) and the second MRP1 part of the PCR chimaera product. B, Gel photograph showing the PCR product of the final product of the chimaera. C, The left-hand gel shows *Bgl*III digests of the recombinant fragment in pIRES2-EGFP-F. Lane 1 shows the vector without insert, and lanes 2, 3 and 4 show insertion of the fragment. The right-hand gel shows a double digest of pMAL-c2x recombinants with *Hind*III and *Bgl*III; lane 2 shows the vector without insert and lanes 1, 3 and 4 show insertion of the fragment.

**Table 3.4** Oligonucleotide for Construction of SUR2A/MRP fragment

Fragment name	Primer name	Primer sequence	
SUR2A (25)MRP1	2A25A (Forward)	GATCCGAATTCAGCATGGATCCTTC TCAAGTCCC	To produce the SUR2A part of the chimaera, the first 25 amino acid.
	2A25B (Backward)	ACCAAGTCCAAGTCTTCTCGATATC TGACGCATAGATCGTG	
	2A25C (Forward)	CACGATCTATGCGTCAGATATCGAG AAGACTTGGACTTGGT	To produce the MRP1 part of the chimaera. 2A25A and MRP-C6B were used to produce the full construct.
	MRP-C6B (Backward)	ATCGGCTCGAGCTACAAGTTCATGC GGAGGGA	
MRP1(25) SUR2A	MRP-C6A (Forward)	GATCCGAATTCAGCATGATCCAGGA AACAGCTCCAC	To produce the MRP1 part of the chimaera, the first 25 amino acid.
	MRP25B (Backward)	ACGGGCTTCAGGTTATTTTCATACC TCAGGCAGTAATCCC	
	MRP25C (Forward)	GGGATTACTGCCTGAGGTATGAAA ATAACCTGAAGCCCGT	To produce the SUR2A part of the chimaera. MRP-C6A and MRP25D were used to produce the full construct.
	MRP25D (Backward)	ATCGGCTCGAGCTACAAGTTAAATC TGATAGAG	
SUR2A (45)MRP1	2A25A (Forward)	GATCCGAATTCAGCATGGATCCTTC TCAAGTCCC	To produce the SUR2A part of the chimaera, the first 45 amino acid.
	2A45A (Backward)	GTACGACCTACAATACCCACCTTCT GCCAGGCTTGATG	
	2A45B (Forward)	CATCAAGCCTGGGCAGAAGGTGGG TATTGTAGGTCGTAC	To produce the MRP1 part of the chimaera. 2A25A and MRP-C6B were used to produce the full construct.
	MRP-C6B (Backward)	ATCGGCTCGAGCTACAAGTTCATGC GGAGGGA	
MRP1(45) SUR2A	MRP-C6A (Forward)	GATCCGAATTCAGCATGATCCAGGA AACAGCTCCAC	To produce the MRP1 part of the chimaera, the first 45 amino acid.
	MRP45A (Backward)	GCGACCACAGATGCCACCTTTTCT CCACCCTCAATG	
	MRP45B (Forward)	CATTGAGGGTGGAGAAAAGGTGGG CATCTGTGGTCGC	To produce the SUR2A part of the chimaera. MRP-C6A and MRP25D were used to produce the full construct.
	MRP25D (Backward)	ATCGGCTCGAGCTACAAGTTAAATC TGATAGAG	

### 3.7- Construction of SUR2A fragment tagged with HA

Using the cDNA of rat SUR2A present in pCMV-6c vector (provided by Prof. S. Seino), PCR reactions were carried out in order to tag the SUR2A-fragments with HA-tag at the N-terminal, HA-rSUR2A-CT-A (aa 1254-1545), HA-rSUR2A-CT-D (aa 1358-1545), and HA-rSUR2A-NBF1-1 (aa 683-873).

The oligonucleotides were designed to include a restriction enzyme sequence, (*XhoI*, written in italic and underlined Table 3-5), followed by a methionine, then the HA-tag coding sequence (underlined in the table) followed by the beginning sequence of the SUR2A- fragment in the forward oligonucleotide. The backward oligonucleotide consisted in sequence of a restriction enzyme site for *BglIII*, a stop codon and a hybrid base sequence from the desired sequence of the SUR2A fragment. After the PCR reaction had completed, (detailed protocol in section 2.1.1), the DNA product was double digested with the restriction enzymes *XhoI* and *BglIII*. The plasmid was double digested with *XhoI* and *BamHI* and then treated with SAP and purified using a Cleanup Kit (see section 2.1.9). Also the PCR product, after treatment with the restriction enzyme, was purified and the amount of the DNA was determined using a molecular weight marker (mass ladder). Then a ligation reaction (section 2.1.11) was performed to insert the fragment sequence into the pIRES2-EGFP-F vector. Colonies were then picked and streaked out, then grown in overnight cultures in Kanamycin containing medium for selection. The colonies were analysed for successful recombination by digest of the DNA product from a Miniprep (Wizard) with restriction enzyme *BglIII* and electrophoresis on an agarose gel; examples are shown in (Figure 3-6). Successful insertion, identified by the presence of a higher DNA band size than the vector without insert, were grown in a larger culture for Midiprep and the higher quality DNA sent for sequencing.

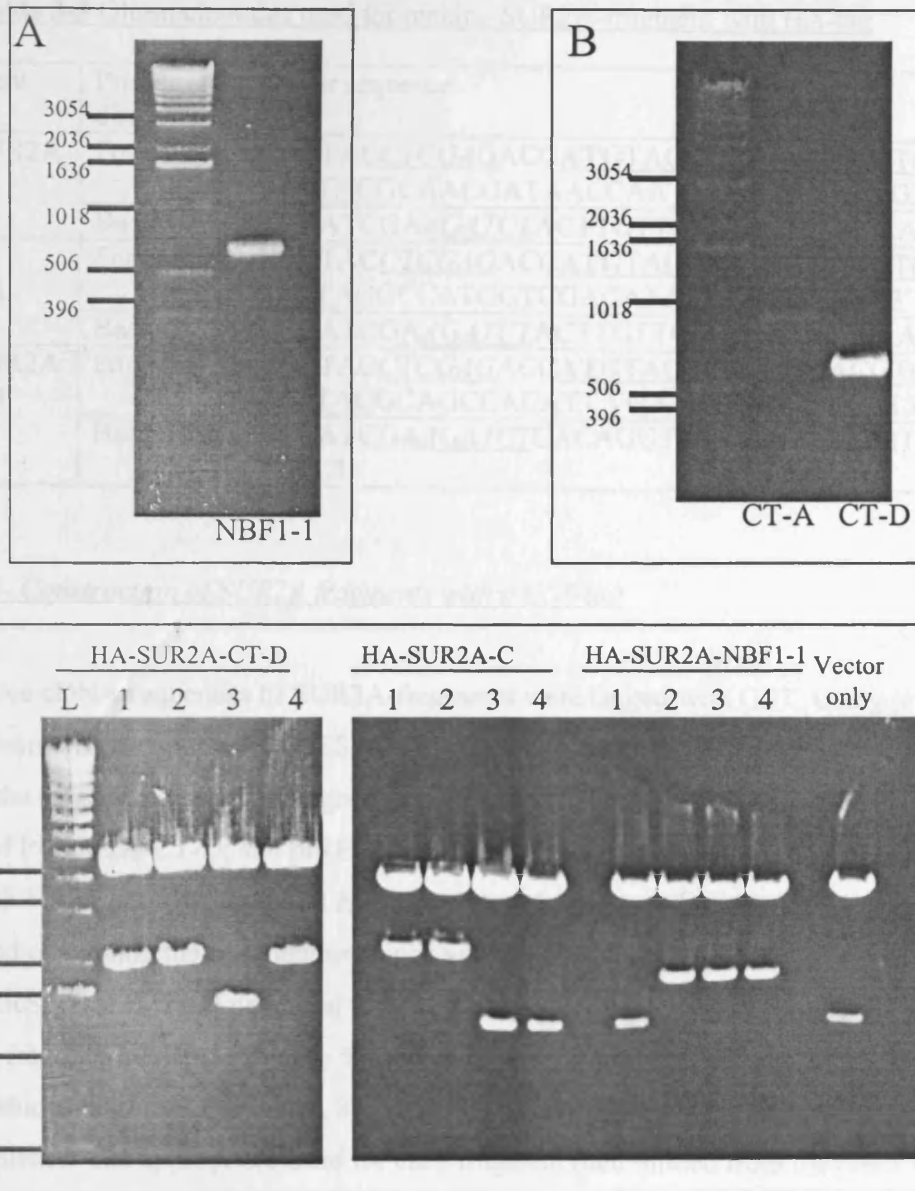


**Figure 3-6 Construction of HA-SUR2A-fragments.** A, Gel photograph of the PCR product of the rSUR2A-NBF1-1 fragment. B, Gel photograph showing the PCR product of rSUR2A-CT-A and rSUR2A-CT-D constructs. C, Gel photograph showing the restriction enzyme digest of the constructs with *Bgl*II. For HA-SUR2A-CT-D lanes 1, 2, and 4 show insertion of the fragment. HA-SUR2A-CT-C, lanes 1 and 2, and SUR2A-NBF1-1, lanes 2, 3, and 4, show successful insertion when compared to the digest of the vector by itself in the last lane. This was confirmed by further restriction digests with different endonucleases and by sequencing.

**Table 3-5** Oligonucleotides used for making SUR2A-fragment with HA-tag

Fragment name	Primer direction	Primer sequence
HA-SUR2A-CT-A	Forward	5' <u>CCTACCTCGAGACCATGTACCCATACGACGTCCCT</u> <u>GATTACGCAACGATAACCAATTACCTGAATTG3'</u>
	Backward	5' <u>CCATCGAAGATCTACTTGTGGTCATCACCAA3'</u>
HA-SUR2A-CT-D	Forward	5' <u>CCTACCTCGAGACCATGTACCCATACGACGTCCCT</u> <u>GATTACGCCATGGTCGACATATTTGATGGAA3'</u>
	Backward	5' <u>CCATCGAAGATCTACTTGTGGTCATCACCAA3'</u>
HA-SUR2A-NBF1-1	Forward	5' <u>CCTACCTCGAGACCATGTACCCATACGACGTCCCT</u> <u>GATTACGCAGCCACATTATCCAATATTGACAT3'</u>
	Backward	5' <u>CCATCGAAGATCTCACAGGTACTGTAGTTTGTGAG</u> <u>TCAC3'</u>

### 3.8- Construction of SUR2A fragments with a GST-tag

Three cDNA sequences of SUR2A-fragments were tagged with GST. Using previously constructed fragments in pIRES2-EGFP vector, the cDNA of the fragment was transferred to the pET41a vector. The fragments used were pIRES2-EGFP-SUR2A-NBF1-1, pIRES2-EGFP-SUR2A-CT-D, and pIRES2-EGFP-SUR2A-CT-A. The digestion of the pIRES2-EGFP-NBF1-1 with *Bgl*III and *Hind*III produced three bands of 5025, 594, and 269 bp, the band containing the fragment sequence was the 594 bp band. Where the digestion of the pIERS2-EGFP-CT-D produced three bands of 5025, 585, and 269 bp, the band containing the fragment sequence was the 585 bp band. The digestion of the pIRES2-EGFP-CT-A also produced three bands of 5025, 897, and 269 bp; the band at 897 bp contained the fragment sequence. The appropriate band for each fragment (determined from the predicted size of cleavage products) was extracted using the gel extraction kit (see section 2.1.7) (Figure 3-7). The pET41a vector, which encodes the GST-tag at the N-terminal of the fragment, was digested with *Bam*HI and *Hind*III restriction enzymes. The pET41a plasmid and the cDNA for the fragments were purified and their concentrations were determined. The resulting fragments were ligated into the pET41a vector to produce constructs of the fragment with a GST-tag in the N-terminal. The constructed clones were confirmed by enzyme restriction mapping using two restriction enzymes at alternate ends of the fragment cDNA sequence, *Xho*I and *Bgl*III (Figure 3-7).

**SPECIAL NOTE**

**THE FOLLOWING**  
**IMAGE IS OF POOR**  
**QUALITY DUE TO THE**  
**ORIGINAL DOCUMENT.**

**THE BEST AVAILABLE**

**IMAGE HAS BEEN**

**ACHIEVED.**

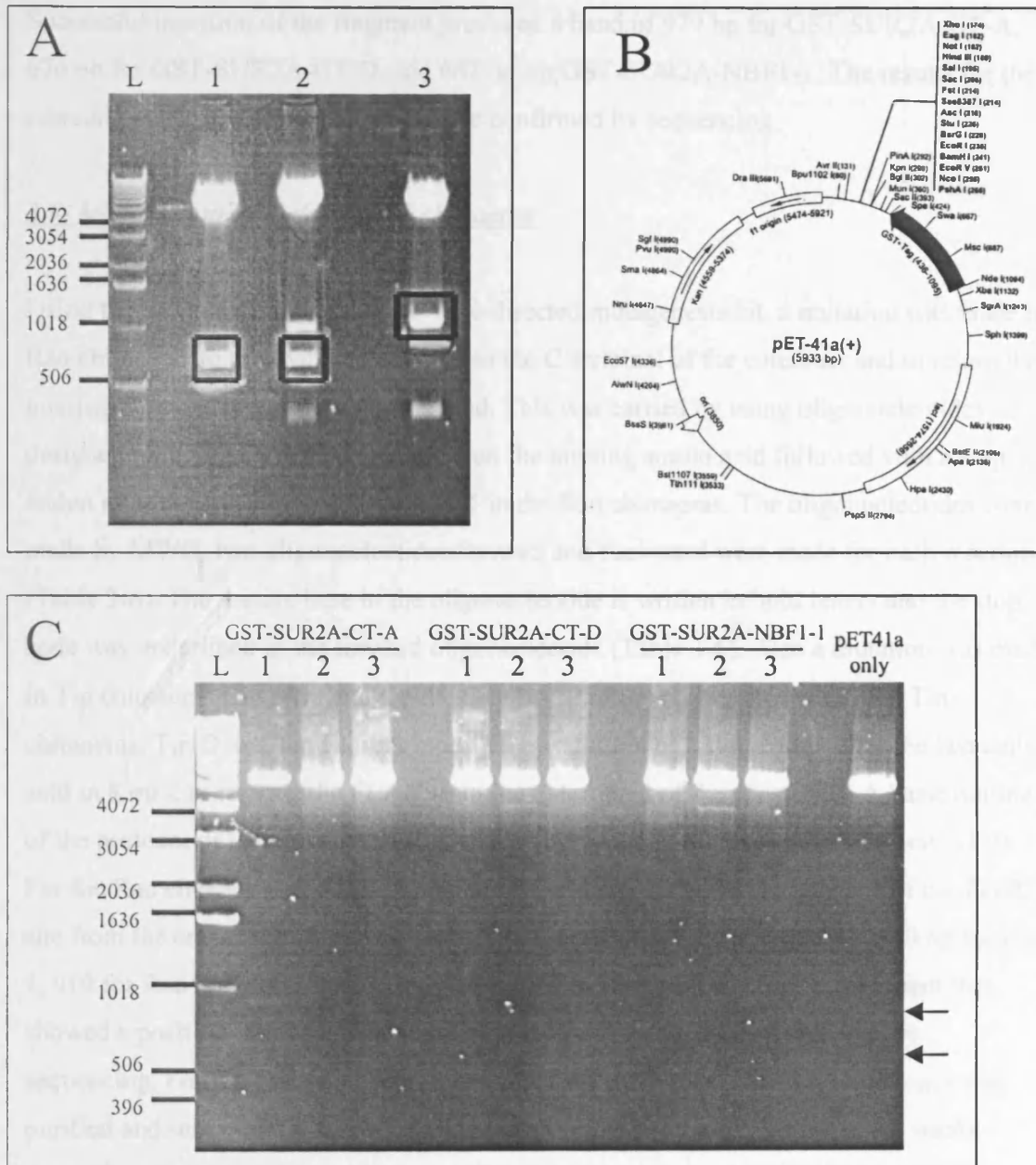


**Figure 3-7 Construction of GST-tagged SUR2A- fragments.** A, gel photograph for *BglIII/HindIII* digests of pIRES2-EGFP-SUR2A-NBF1-1 (lane 1), pIRES2-EGFP-SUR2A-CT-D (lane 2) and pIRES2-EGFP-SUR2A-CT-A (lane 3). B, shows the GST expression vector (image taken from Novagen catalogue). C, gel photograph of recombinant SUR2A fragment in GST vector, 5  $\mu$ l cDNA from three bacterial colonies of each construct were digested for more than 2 hours using the enzymes *BglIII* and *XhoI*. Those containing a band of 979 bp for GST-SUR2A-CT-A (lane 1), 676 bp for GST-SUR2A-CT-D (lane 2) and 667 bp for GST-SUR2A-NBF1-1 (lane 2), appeared to have the correct insert when compared to the vector digest on the right of the gel. This was confirmed by sequencing.

Successful insertion of the fragment produced a band of 979 bp for GST-SUR2A-CT-A, 676 pb for GST-SUR2A-CT-D, and 667 bp for GST-SUR2A-NBF1-1. The results for the correctly constructed recombinants were confirmed by sequencing.

### 3.9- Modification of Kir6.2/Kir2.1 chimaeras

Using the Stratagene QuikChange™ site-directed mutagenesis kit, a mutation was made in Rao chimaeras to remove the FLAG from the C-terminal of the construct and to return the missing amino acid at the C-terminal end. This was carried by using oligonucleotides designed with mutant nucleotides to insert the missing amino acid followed with a stop codon after the last amino acid of Kir2.1 in the Rao chimaeras. The oligonucleotides were made by MWG, two oligonucleotides forward and backward were made for each reaction (Table 3-6). The mutant base in the oligonucleotide is written in bold letters and the stop code was underlined in the forward oligonucleotide (Table 3-6). Also a mutation was made in Tin chimaeras that have a tag in the C-terminal of the construct. Two of the Tin chimaeras, Tin D and Tin E, were modified by addition of a stop codon after the last amino acid in Kir6.2 to remove the FLAG from the C-terminal of the constructs. A basic outline of the protocol of the mutagenesis kit is provided in the Methods section (section 2.1.2). For the Rao chimaeras a successful mutation was determined by the absence of the *EcoRI* site from the end of the chimaera, where the unmutated produce a band of 1080 bp for Rao 1, 910 for Rao 2, 830 for Rao 3, and 711 for Rao 4 (Figure 3-8). The recombinant that showed a positive result with the restriction enzyme mapping was confirmed by sequencing. For the Tin chimaeras, Tin E and Tin D, the cDNA from four colonies was purified and sent directly for sequencing to determine successful mutation. No useful restriction sites were available for analysis.

**Table 3-6** Oligonucleotide sequences for modification of Kir6.2/Kir2.1 chimaeras

Fragment name	Primer direction	Primer sequence
Rao	Forward	5'TAAGGCGAGAATCGGAGATCT <u>TAAT</u> CCCCGCGCATCCGTTG
	Backward	5'CAACGGATGCGCGGGATTAGATCTCCGATTCTCGCCTTA
Tin	Forward	5'CCAGATTCCTTGTCCT <u>AGT</u> ACAAGGACGACGA
	Backward	5'TCGTCGTCCTTGTAGGACAAGGAATCTGG



## **Chapter Four**

### **Characterization of a Kir6.2 subunit binding site in NBF1 and NBF2 of the SUR2A subunit by biochemical analysis**

#### 4.1.1- Introduction

The cytoplasmic nucleotide-binding domains 1 (NBF1) and 2 (NBF2) in the sulphonylurea receptor subunits confer nucleotide diphosphate sensitivity to the  $K_{ATP}$  channel hetero-oligomer in a co-operative manner (Yokoshiki, 1998) and direct functional coupling of these domains with the pore-forming Kir6.0 subunits. While strong NBF1-NBF1 and NBF1-NBF2 interactions have been demonstrated (Mikhailov, 2000), there is no evidence in the literature for direct NBF-Kir6.0 interactions (Schwappach, 2000; Mikhailov, 2000). Previous studies in our laboratory using yeast two-hybrid methods failed to identify specific inter-subunit interactions between SUR2A and Kir6.2 subunits. To address this possibility in a different manner in this study, it was proposed to investigate, more directly, possible cytoplasmic interactions between domains of the SUR2A subunit and full length Kir6.2 subunit in co-immunoprecipitation experiments. The first step after the construction of the SUR2A fragments was to investigate whether binding site of those fragments with full-length of Kir6.2 occurred. On demonstration of a binding interaction, it was further proposed to investigate the importance of the interaction using subunit fragments to attempt to disrupt channel structure. It was hypothesised that interaction of subunit fragments might disrupt channel structure leading to abnormal assembly and sub-cellular targeting, increased turnover or modified functional properties. These possibilities were investigated in this study by assays of channel sub-cellular targeting and, in parallel, by assays of channel function conducted by Dr. Richard Rainbow (Cell Physiology and Pharmacology, University of Leicester).

To investigate the interaction of the SUR2A-CT fragment with the full length Kir6.2 another polypeptide was needed as a negative control. The Kir2.1 polypeptide was chosen as an homologous inward rectifying potassium channel with no known sensitivity to cytoplasmic nucleotides or sulphonylurea drugs. This was checked by Dr. Rainbow, in parallel with this study, which showed that currents expressed by Kir2.1 co-expressed with SUR2A were insensitive to added nucleotides or the sulphonylurea antagonist, glibenclamide (Rainbow et al. 2004a).

MBP- tagged fragments were used to assist the research for binding interaction. At the beginning of this study, a set of the MBP-rSUR2A-NBFs fragments (Figure 3-1) constructed by Dr. M. Routledge, was used. Later, other fragments were made with both MBP-tags and with GST-tags to assist the investigation in co-immunoprecipitation experiment of the fragments with the Kir6.2 subunit. Co-immunoprecipitation experiments were performed between the MBP-rSUR2A-NBFs fragments and full length of Kir6.2 to scan for a possible interaction. Before starting the investigation, the co-immunoprecipitation protocol went through series of optimization steps. These experiments addressed issues such as the buffer composition, the protein A-Sepharose resin concentration, formation of immunoprecipitation matrix by pre-binding anti-Kir6.2 antibodies to protein A-Sepharose, the concentration of MBP-rSUR2A fragments used, and pre-blocking of non-specific binding sites on protein A-Sepharose resin. A series of experiments was carried out to optimize the interaction mixture.

#### 4.1.2- Expression and immunoprecipitation of Kir6.2 and Kir2.1

cDNA encoding Kir6.2 and Kir2.1 were expressed in the TNT rabbit reticulocyte lysate Quick coupled transcription/translation system, SP6 and T7, respectively, to produce proteins labelled with [<sup>35</sup>S]methionine. The expression of the proteins required canine pancreatic microsomal membranes in order to obtain a higher yield of Kir polypeptides. Satisfactory expression of both polypeptides was achieved, and the molecular weights of the polypeptides in 7.5% polyacrylamide gels were shown to be Kir6.2, 38kDa and Kir2.1, 48Da (Figure 4-1,A). The polypeptides were expressed for 1.5 h; increasing the expression time led to a decrease in the level of Kir polypeptides expression suggesting that the Kir6.2 or Kir2.1 polypeptides were not stable for a long time in the presence of the reticulocyte lysate system. Adding protease inhibitor before starting the reaction prevented the expression of Kir subunits. Therefore, protease inhibitor was added after Kir6.2 and Kir2.1 expression was completed to stop further proteolysis (Figure 4-1,B).

The expression of the Kir6.2 and Kir2.1 polypeptides was verified by immunoprecipitation of [<sup>35</sup>S]methionine labelled Kir6.2 and Kir2.1 proteins with the corresponding anti-Kir6.2 and anti-Kir2.1 antisera. Immunoprecipitation of target polypeptides by anti-Kir6.2

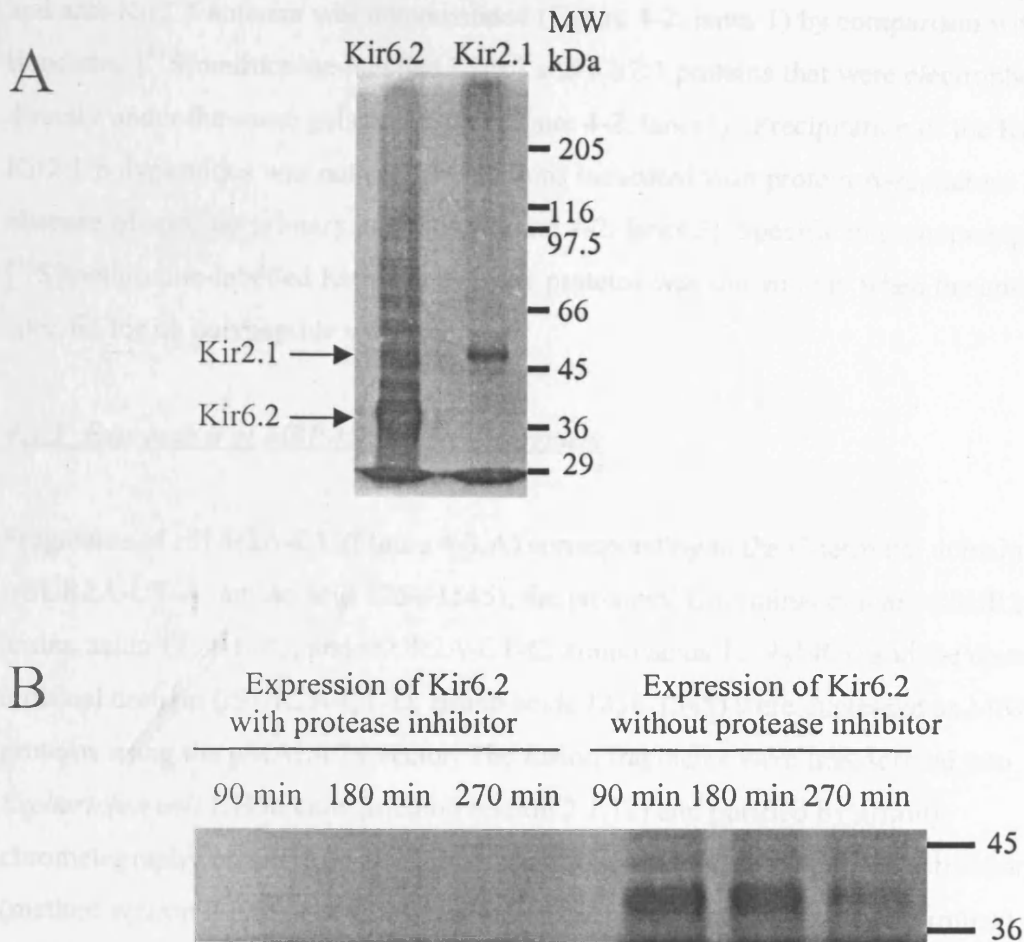


**Figure 4-1** *In vitro* translated [<sup>35</sup>S]methionine labelled Kir6.2 and Kir2.1. **A**, Autoradiograph showing electrophoretically separated [<sup>35</sup>S]methionine-labelled *in vitro* translated Kir6.2 and Kir2.1 polypeptides on a denaturing 7.5% polyacrylamide mini-gel. The Kir6.2 was expressed using SP6 and Kir2.1 was expressed using the T7 TNT<sup>®</sup> Quick-coupled transcription/translation kit (Promega) from cloned cDNAs. The [<sup>35</sup>S]methionine labelled Kir6.2 and Kir2.1 polypeptides migrated with apparent molecular weights of 38 and 48 kDa, respectively. **B**, Autoradiograph showing expression of Kir6.2 at different time points of 90, 180, and 270 minutes in the presence or absence of protease inhibitors at the beginning of the reaction. Representative experiment (n =2).

and anti-Kir2.1 antisera was demonstrated (Figure 4-2, lanes 1) by comparison with *in vitro* translated [<sup>35</sup>S]methionine-labelled Kir6.2 and Kir2.1 proteins that were electrophoresed directly under the same gel conditions (Figure 4-2, lanes3). Precipitation of the Kir6.2 and Kir2.1 polypeptides was not seen in reactions incubated with protein A-sepharose in the absence of specific primary antibody (Figure 4-2, lanes 2). Specific immunoprecipitation of [<sup>35</sup>S]methionine-labelled Kir6.2 and Kir2.1 proteins was shown only when the antisera specific for its polypeptide was used.

#### 4.1.3- Expression of MBP-rSUR2A-CT fragment

Fragments of rSUR2A-CT (Figure 4-3,A) corresponding to the C-terminal domain (rSUR2A-CT-A, amino acid 1254-1545), the proximal C-terminal domain (rSUR2A-CTB, amino acids 1254-1403, and rSUR2A-CT-C, amino acids 1294-1403) and the distal C-terminal domain (rSUR2A-CT-D, amino acids 1358-1545) were expressed as MBP fusion proteins using the pMAL-c2x vector. The fusion fragments were transformed into *Escherichia coli* DH5 $\alpha$  cells (method section 2.1.12) and purified by affinity chromatography on amylose-Sepharose according to the manufacturer's instructions (method section 2.2.5). The concentration of the fusion fragments was determined by the Bradford assay (method section 2.2.6) using 1  $\mu$ l and 10  $\mu$ l of the eluted fragment; 10  $\mu$ l aliquots was used where expression of protein was low. The concentration of the rSUR2A-CT-A was 20  $\mu$ g/ml, rSUR2A-CT-B was 250  $\mu$ g/ml, rSUR2A-CT-C was 740  $\mu$ g/ml, rSUR2A-CT-D was 60  $\mu$ g/ml, and the MBP-tag alone was 3500  $\mu$ g/ml. Western Blotting was performed to transfer the protein to Hybond-P membrane for detection with the ECL technique using mouse anti-MBP IgG as primary antibody and anti-mouse IgG-HRP as secondary antibody. The membrane was exposed to the ECL-film for 2 min and developed (Figure 4-3,B). The autoradiograph confirm expression of each MBP-rSUR2A-CT fragment and their detection by anti-MBP antiserum in immunoblots.

## **SPECIAL NOTE**

**THE FOLLOWING**  
**IMAGE IS OF POOR**  
**QUALITY DUE TO THE**  
**ORIGINAL DOCUMENT.**

**THE BEST AVAILABLE**  
**IMAGE HAS BEEN**  
**ACHIEVED.**

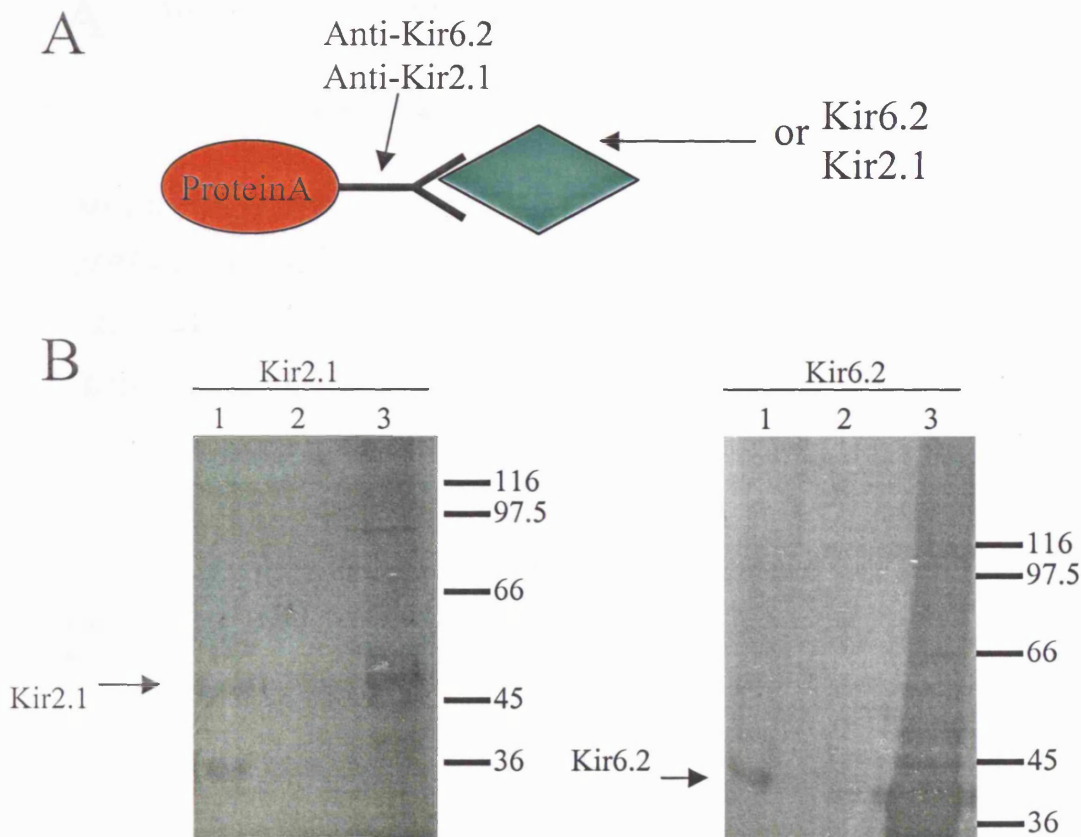


**Figure 4.2 Immunoprecipitation of [<sup>35</sup>S]methionine-labelled *in vitro* translated Kir6.2 and Kir2.1 polypeptides.** A, Schematic diagram for the immunoprecipitation complex using protein A and antibody from antisera. B, Immunoprecipitated fractions were electrophoresed on a 7.5 % polyacrylamide mini-gel. The immunoprecipitation of *in vitro* translated [<sup>35</sup>S]methionine-labelled Kir6.2 and Kir2.1 subunits resulted in bands corresponding to polypeptides of 38 and 48 kDa, respectively (lanes 1) which were used to confirm specific immunoprecipitation of target polypeptides by the cognate antisera. Lanes 2, contained immunoprecipitation fractions with no primary antibody; lanes 3, contained a direct load of 5  $\mu$ l [<sup>35</sup>S]-methionine labelled Kir polypeptide. Representative experiment (n = 2).

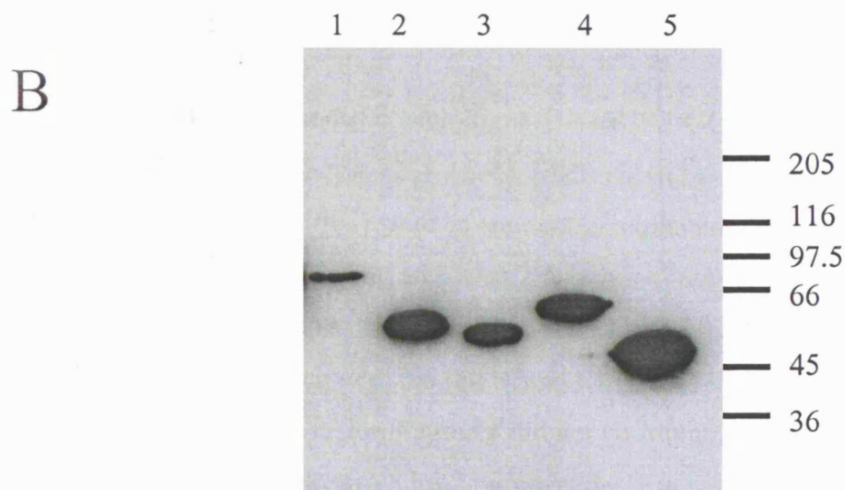
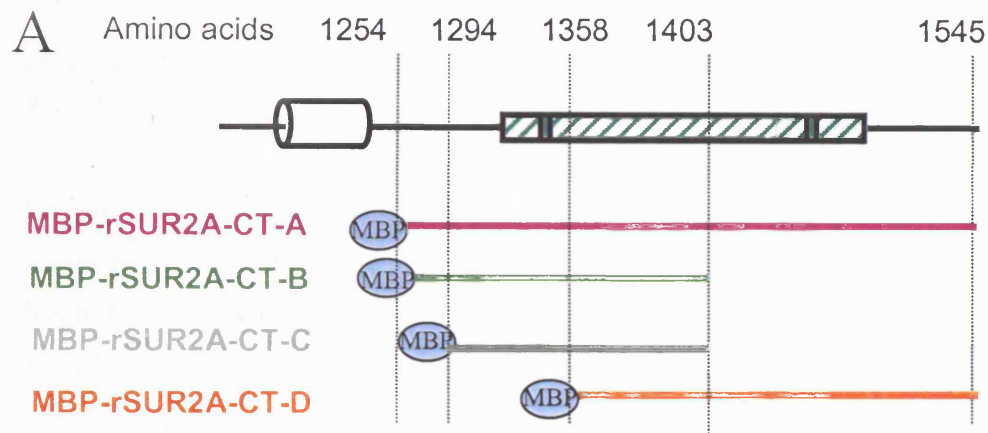


**Figure 4-3 Analysis of expressed and purified maltose binding protein-rSUR2A fusion fragments.** A, Schematic diagram of MBP-rSUR2A C-terminal fragments. B, shows the purified MBP-rSUR2A-CT fragments analysed by Western blot stained with mouse anti-MBP IgG as primary antibody and anti-mouse IgG-HRP as secondary antibody. Lane 1, 1  $\mu$ l (0.006  $\mu$ g/ml) of eluted MBP-rSUR2A-CT-A; lane 2, MBP-rSUR2A-CT-B; lane 3, MBP-rSUR2A-CT-C; lane 4, MBP-rSUR2A-CT-D; lane 5, MBP alone.

#### 4.1.4- Co-immunoprecipitation of MBP-rSUR2A-CT (NBF2) fragment with full-length Kir6.2 subunit

Co-immunoprecipitation experiments were conducted to investigate direct physical association between fragments of the C-terminal domain of the SUR2A subunit and full-length Kir6.2 subunits. In initial experiments, co-immunoprecipitation of full-length Kir6.2 and SUR2A subunits from mixtures of [<sup>35</sup>S]methionine-labelled *in vitro*-translated subunits using anti-Kir6.2 subunit antiserum was established (not shown). This co-immunoprecipitation technique was used to scan for interaction with a panel of C-terminal fragments of SUR2A, expressed as MBP-rSUR2A-CT, and full-length Kir6.2 subunit (Figure 4-4,A).

Three of the Walker A motif containing, MBP-rSUR2A-CT fusion proteins, MBP-rSUR2A-CT-A (amino acids 1254-1545), MBP-rSUR2A-CT- B (1254-1403), and MBP-rSUR2A- CT-C (1294-1403) were co-immunoprecipitated with the full length *in vitro* translated Kir6.2 subunit using anti-Kir6.2 C-terminal antiserum (Figure 4-4, B lane 1). Under the same conditions, the fourth fragment, MBP-rSUR2A-CT-D (1358- 1545), did not co-immunoprecipitate with the full length Kir6.2 polypeptide. In addition, as a control reaction MBP lacking a fusion fragment did not co-immunoprecipitate under the same conditions with the full length Kir6.2 polypeptide. For each fragment, a control reaction in the absence of the Kir6.2 subunit was performed and analysed in an adjacent lane (Lane 2). A direct load of the rSUR2A-CT fragment in a third lane was loaded onto the 7.5 % SDS gel to assess the relative migration of the fragment. The co-immunoprecipitation reactions were centrifuged for 5 min at 11600 g, at room temperature before loaded to the SDS-gel. Western blotting was performed to transfer the protein to Hybond-P membrane. The membrane was incubated with mouse anti-MBP-IgG (1:4000 dilution), then with anti-mouse IgG-HRP, as secondary antibody (1:5000 dilution). The membrane was treated with ECL for HRP detection and then exposed to the ECL-film for 2 min and developed (Figure 4-4,B). The results were reproducible and the number of repeats in each case is shown in figure 4-4,C.

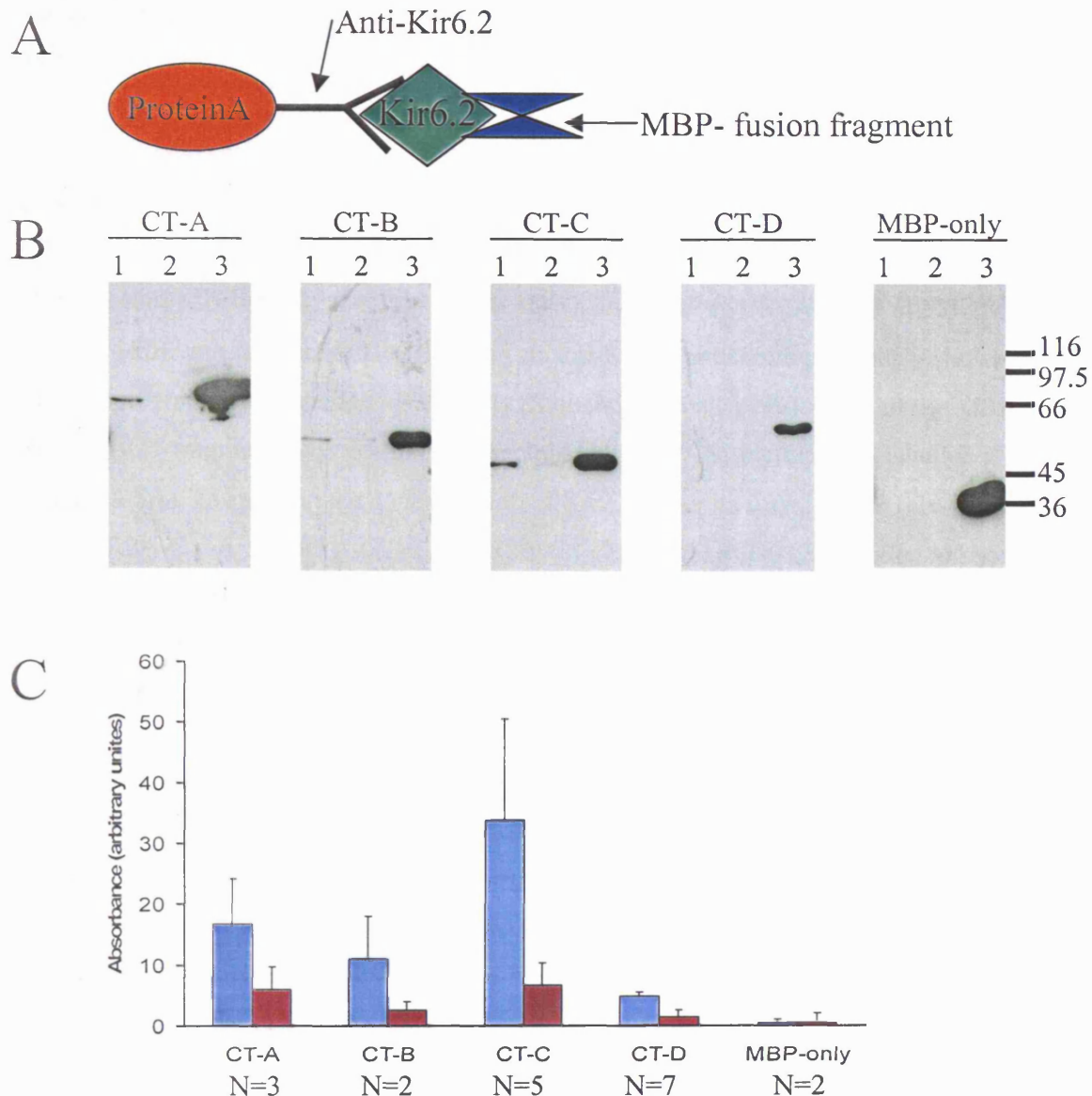


**Figure 4-4 Co-immunoprecipitation of MBP-rSUR2A-CT fragments with Kir6.2 subunit using anti-Kir6.2.** A, Schematic diagram for the co-immunoprecipitation complex formed. B, shows ECL-film exposure of a Western blot stained with mouse anti-MBP IgG as primary antibody and anti-mouse IgG-HRP as secondary antibody. Lane 1, co-immunoprecipitation of MBP-rSUR2A-CT fusion protein with Kir6.2 using anti-Kir6.2 antiserum, lane 2, control reaction in the absence of Kir6.2, lane 3, direct load of the rSUR2A fragments (0.006  $\mu$ g/ml). The fragments included in this figure from left to right are rSUR2A-CT-A, rSUR2A-CT-B, rSUR2A-CT-C, rSUR2A-CT-D; and MBP alone. C, Histogram representing mean  $\pm$  SEM of the amount of co-immunoprecipitation of each rSUR2A-CT fragment in the absence (dark red) or presence (blue) of Kir6.2 determined by densitometry of the ECL exposure of Western blots expressed for 2 min.

#### 4.1.5- Co-immunoprecipitation of MBP-rSUR2A-CT fragments with full-length Kir2.1 subunit

As a control for the non-specific interaction of the fragments with the Kir subunit, similar experiments were conducted to investigate the co-immunoprecipitation of MBP-rSUR2A-CT fragments (MBP-rSUR2A-CT-A (amino acids 1254 – 1545), MBP-rSUR2A-CT-C (1294- 1403) MBP-rSUR2A-CT-D (1358- 1545), and MBP-rSUR2A-CT-E (1294-1358) (Figure 4-6)) with full-length Kir2.1, using an anti-Kir2.1 antiserum previously shown to immunoprecipitate this subunit specifically (Stonehouse et al. 1999). None of the MBP-rSUR2A-CT fragments was co-immunoprecipitated with [<sup>35</sup>S]-methionine- labelled Kir2.1 (Figure 4-5A). Even when the concentration of Kir2.1 subunits was doubled (not shown) the rSUR2A-CT-A, rSUR2A-CT-C, rSUR2A-CT-D, and rSUR2A-CT-E failed to show a co-immunoprecipitation with full length Kir2.1 polypeptide.

#### 4.1.6- Expression of truncated MBP-rSUR2A-CT-C and MBP-MRP1-CT-E fragment

Fragments of rSUR2A-CT corresponding to the proximal C-terminal domain rSUR2A-CT-E, (amino acids 1294-1358) and two truncated fragment rSUR2A-CT-F (aa 1294-1348), and rSUR2A-CT-G (aa 1294-1337) were expressed as MBP fusion proteins (Figure 4-6,A). Also an equivalent fragment to the rSUR2A-CT-E from MRP1 (MRP1-CT-E aa 1278-1343 aa) and the equivalent region to rSUR2A-CT-F from MRP1 (MRP1-CT-F/rSUR2A aa 1349-1359) plus the last eleven amino acids from rSUR2A-CT-E were expressed as MBP fusion proteins using the pMAL-c2x protein fusion system in *Escherichia coli* DH5a cells and purified by affinity chromatography on amylose-Sepharose according to the manufacturer's instructions. The concentration of the fusion fragments was determined by the Bradford assay (method section 2.2.6) for 10 µl and 20 µl of the eluted fragment then the concentration of the fragment in 1 µl from eluted protein was calculated (Table 4-1). After electrophoresis on 7.5% SDS-PAGE Western blotting was performed to transfer the protein to Hybond-P membrane. The membrane was incubated with mouse anti-MBP-IgG (1:4000 dilution), then with anti-mouse IgG-HRP as secondary antibody (1:5000 dilution).

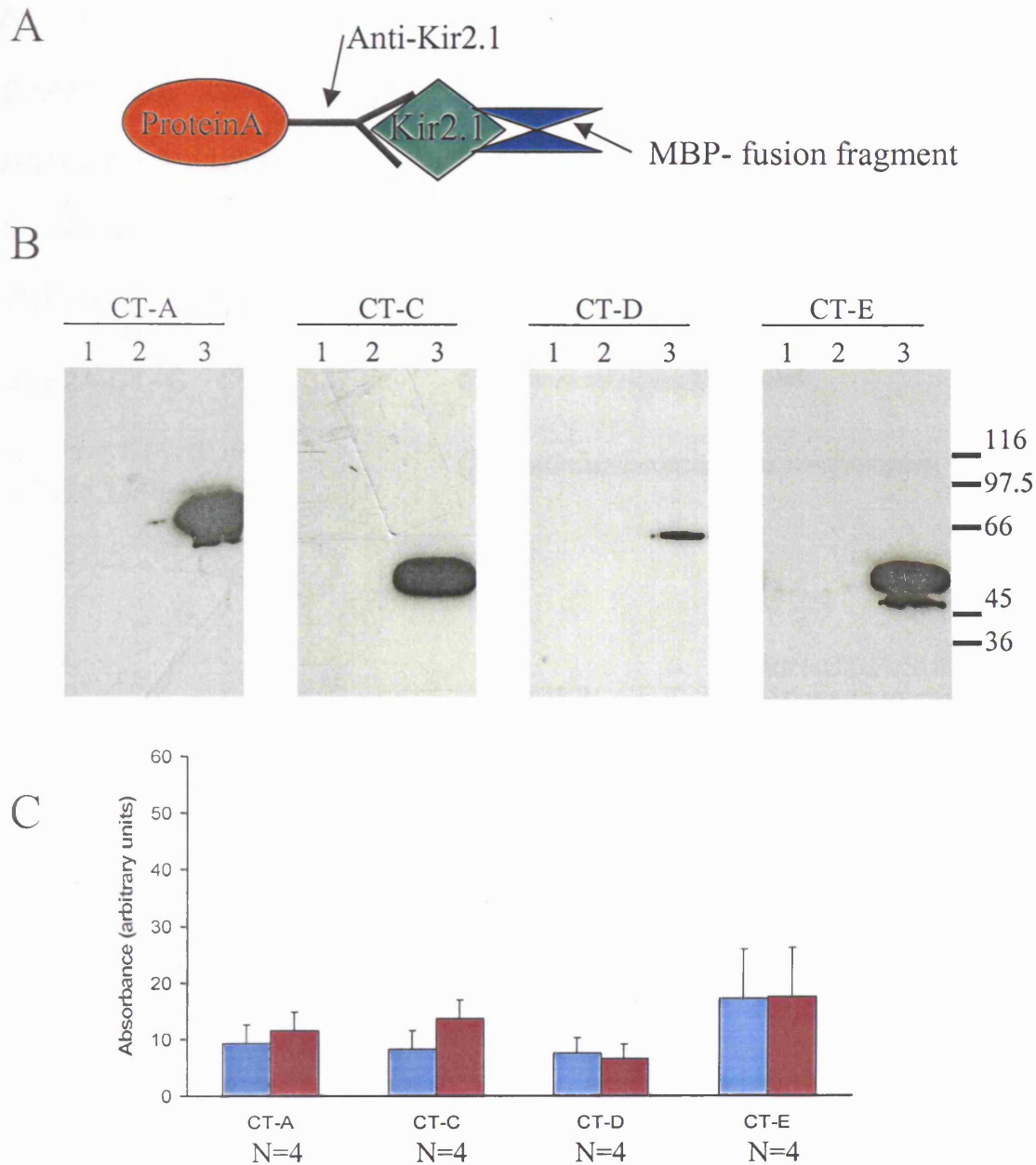
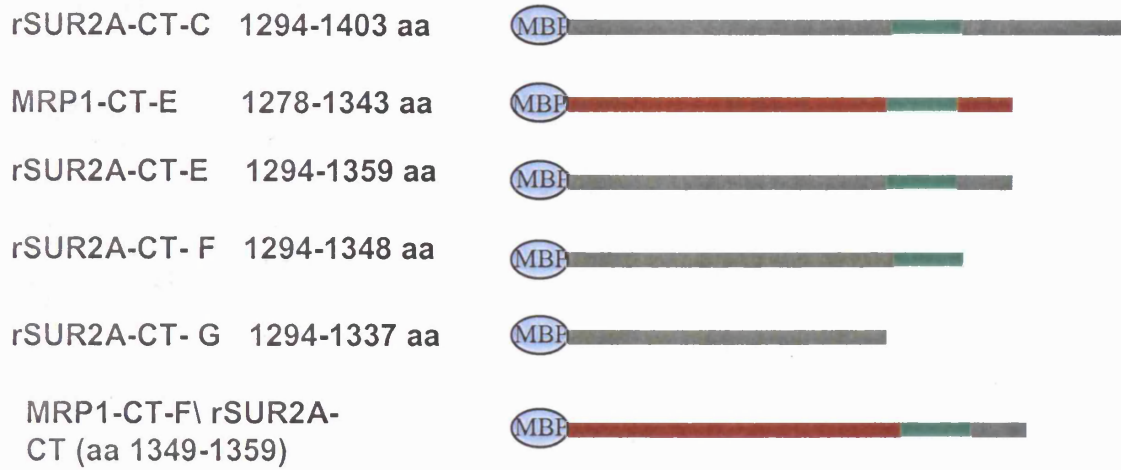


**Figure 4-5 Co-immunoprecipitation of MBP-rSUR2A-CT fragments with Kir2.1 subunit using anti-Kir2.1.** A, Schematic diagram for the co-immunoprecipitation complex forming. B, shows ECL-film exposure of a Western blot stained with mouse anti-MBP IgG as primary antibody and anti-mouse IgG-HRP as secondary antibody. Lane 1, co-immunoprecipitation of MBP-rSUR2A-CT fusion protein with Kir2.1 using anti-Kir2.1 antiserum, lane 2, control reaction in the absence of Kir2.1, lane 3, direct load of the rSUR2A fragments (0.006  $\mu\text{g/ml}$ ). The fragments included in this figure from left to right are rSUR2A-CT-A, rSUR2A-CT-C, rSUR2A-CT-D, and rSUR2A-CT-E. C, Histogram representing mean  $\pm$  SEM of the amount of co-immunoprecipitation of each rSUR2A-CT fragment in the absence (dark red) or presence (blue) of Kir2.1 determined by densitometry of the ECL exposure of Western blots expressed for 2 min.

A



B

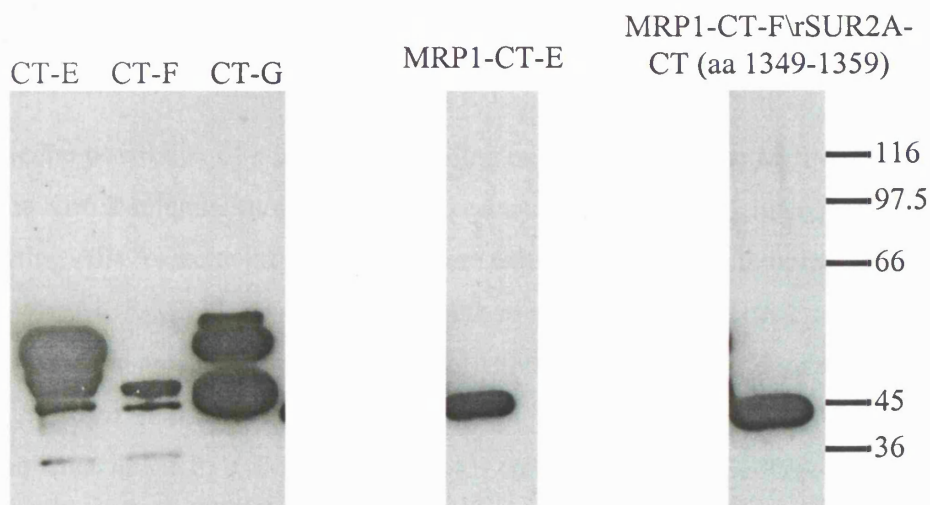


**Figure 4-6 Expression of the MBP-rSUR2A-CT-C truncations and the equivalent of the SUR2A-CT-E fragment from MRP1(MRP1-CT-E).** A, Schematic diagram showing sub-fragments prepared based on the interacting fragment rSUR2A-CT-C. B, purified MBP-rSUR2A-CT fragments analysed by SDS/PAGE (7.5 %gel) and western blot with anti-MBP antibody. Lane 1, (0.006  $\mu$ g/ml) of eluted MBP-rSUR2A-CT-E; lane 2, MBP-rSUR2A-CT-F; lane 3, MBP-rSUR2A-CT-G; lane 4, MBP-MRP1-CT-E; lane 5, MRP1-CT-F/rSUR2A-CT (aa 1349-1359).

The membrane was treated with ECL for HRP detection, then exposed to the ECL-film for 2 min and developed (Figure 4-6,B).

**Table 4-1** Protein concentration of the MBP- fusion fragments

The fragment name	The concentration mg/ml	Comment in the expression
rSUR2A-CT-E	10	Low expression
rSUR2A-CT-F	7	Low expression
rSUR2A-CT-G	50	Within the working concentration
MRP1-CT-E	170	Within the working concentration
MRP1-CT-F/rSUR2A-CT-E (aa 1349-1359)	20	Low expression

4.1.7- Co-Immunoprecipitation of the non-interacting MRP1 protein

To investigate the possibility of non-specific binding or adsorption of the MBP-rSUR2A-CT-C with the Kir6.2 subunits further control experiments using equivalent sequence from a non-interacting ABC cassette protein MRP1 were carried out. Co-immunoprecipitation experiments with MBP-MRP1-CT-E and full length *in vitro* translated Kir6.2 subunit using anti-Kir6.2 C-terminal antiserum were conducted. Although there is considerable sequence conservation between SUR2A and multi-drug resistant protein 1 (MRP1) (Figure 3-3), the equivalent sequence in MRP1-CT-E (aa 1278-1343) corresponding to rSUR2A-CT-E (aa 1294-1358) did not show co-immunoprecipitation with Kir6.2 when equivalent amount of fragment peptide were added to the immunoprecipitation reaction. This observation further confirmed a specific interaction between the Kir6.2 and rSUR2A-CT-C fragment (Figure 4-7,B). In addition, no non-specific adsorption to protein-A sepharose was seen in a control reaction performed in the absence of the Kir6.2 subunit analysed in an adjacent lane on the gel (Figure 4-7).

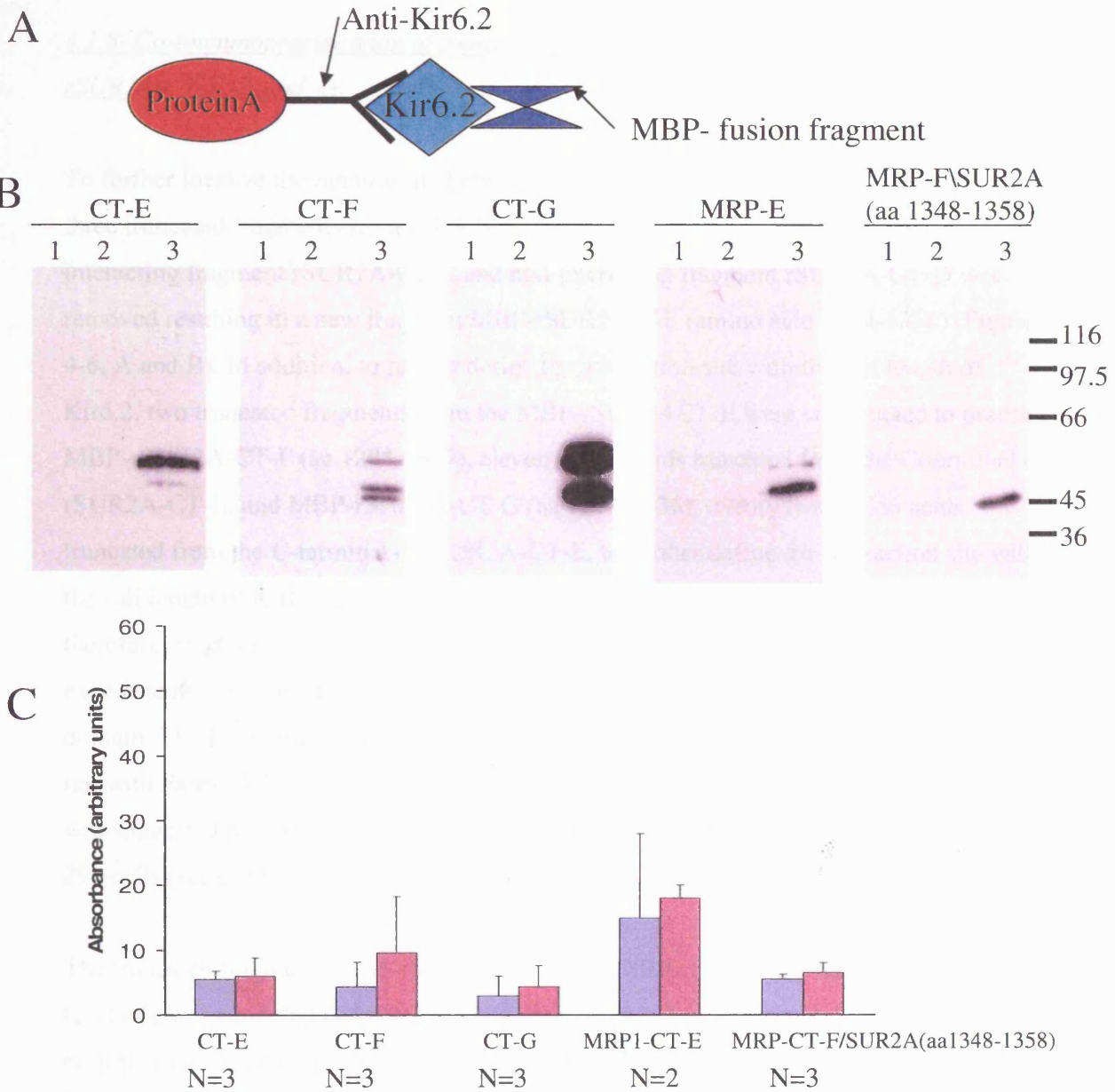


**Figure 4-7 Co-immunoprecipitation of MBP-rSUR2A-CT fragments with Kir6.2 subunit using anti-Kir6.2.** A, Schematic diagram for the co-immunoprecipitation complex formed. B, shows ECL-film exposure of a Western blot stained with mouse anti-MBP IgG as primary antibody and anti-mouse IgG-HRP as secondary antibody. Lane 1, co-immunoprecipitation of MBP-rSUR2A-CT fusion protein with Kir6.2 using anti-Kir6.2 antiserum, lane 2, control reaction in the absence of Kir6.2, lane 3, direct load of the rSUR2A fragments (0.006  $\mu$ g/ml). The fragments included in this figure from left to right are rSUR2A-CT-E, rSUR2A-CT-F, rSUR2A-CT-G, MRP1-E, and MRP1-F/rSUR2A-CT (aa 1348-1358). C, Histogram representing mean + SEM of the amount of co-immunoprecipitation of each rrSUR2A-CT fragment in the absence (dark red) or presence (blue) of Kir6.2 determined by densitometry of the ECL exposure of Western blots expressed for 2 min.

#### 4.1.8- Co-immunoprecipitation of truncated MBP-rSUR2A-CT-C fragments, MBP-rSUR2A-CT-E, -F and -G

To further localize the binding site between the C-terminal domain of SUR2A and Kir6.2, three truncated fragments from rSUR2A-CT-C were made. The overlap between the interacting fragment rSUR2A-CT-C and non-interacting fragment rSUR2A-CT-D was removed resulting in a new fragment MBP-rSUR2-CT-E (amino acid 1294-1358) (Figure 4-6, A and B). In addition, to further define the interaction site with the full length of Kir6.2, two truncated fragments from the MBP-rSUR2ACT-E were constructed to produce, MBP-rSUR2A-CT-F (aa 1294-1347), eleven amino acids truncated from the C-terminal of rSUR2A-CT-E, and MBP-rSUR2A-CT-G (aa 1294-1336), twenty two amino acids truncated from the C-terminal of rSUR2A-CT-E, to further define the interaction site with the full length of Kir6.2. The fragment MBP-rSUR2A-CT-E was poorly expressed, therefore, since only low fragment concentration could be used, co-immunoprecipitation experiments using this fragment failed to confirm localization of the interaction into this domain. The fragment expression was detectable by Western blot using ECL technique but not with Fairbank I staining of the protein. Interaction between rSUR2A-CT-E and Kir6.2 was suggested by disruption of surface expression of Kir6.2 and SUR2A channels in HEK 293 cells (see chapter five).

The truncated fragments MBP-rSUR2A-CT-F and MBP-rSUR2A-G showed a reasonable level of expression that permitted amount equivalent to earlier experiment to be added to co-immunoprecipitation experiment. Both truncated fragments MBP-rSUR2A-CT-F and MBP-rSUR2A-CT-G failed to demonstrate any binding with the full length *in vitro* translated Kir6.2 subunit on co-immunoprecipitation experiment with anti-Kir6.2 C-terminal antiserum (Figure 4-7,B). For each fragment, a control reaction in the absence of the Kir6.2 subunit was performed in an adjacent lane demonstrating no non-specific precipitation by protein A sepharose gel. It was noted that all of the truncated fragments rSUR2A-CT-E, rSUR2A-CT-F, and rSUR2A-CT-G showed several bands in the ECL-development of immunoblots (Figure 4-7,B) that were under the expected molecular size, which may indicate relative instability of these peptide fragments.

#### 4.1.9- Co-immunoprecipitation of MBP-MRP1-CT-F/rSUR2A (aa1349-1359)

Removing the last eleven amino acids from the C-terminal of MBP-rSUR2A-CT-E (MBP-rSUR2A-CT-F) was enough to disrupt the interaction of rSUR2A-CT fragment with Kir6.2 (Figure 5-2). This indicated that those eleven amino acids were important in the binding interaction or in the stabilizing the binding site configuration within the fragment. Since the minimum size of an active interacting fragment of the SUR2A C-terminal domain was contained in the rSUR2A-CT-E fragment (section 4.1.8), experiment to further localize the binding site were failed in fragment of this size. For this reason, the equivalent sequence to rSUR2A-CT-F from MRP1 (aa 1278-1333) plus the last 11 amino acids of the rSUR2A-CT-E (Figure 4-6) was constructed to investigate whether the binding site was restricted to the last 11 amino acids of rSUR2A-CT-E. No evidence of interaction of the new fragment MRP1-CT-F/rSUR2A(aa 1349-1359) with full length of Kir6.2 was found (Figure 4-7).

#### 4.1.10- Co-immunoprecipitation of MBP-MRP1-C and MBP-rSUR2A-CT-A-C

The truncated fragments from rSUR2A-CT-C showed no binding with the Kir6.2 and the equivalent fragments from MRP1 present the same observation. From this it was inferred that the fragments had lost their binding activity or had become unstable. Therefore, the main focus of the investigation was refocused on the larger rSUR2A-CT-C fragment for which interaction was reproducible in co-immunoprecipitation experiments. From the absence of interaction of the rSUR2A-CT-D fragment it has been inferred that the portion of sequence overlapping with rSUR2A-CT-C was not involved in the interaction with Kir6.2. However, in some experiment a weak co-immunoprecipitation signal with rSUR2A-CT-D was observed (not shown) suggesting that this overlapping sequence might be involved in stabilizing the binding domain with the rSUR2A-CT-C fragment. It was hypothesised, that a construct rSUR2A-CT-A-C would produce a clear or true negative control for an interacting fragment. In addition the equivalent sequence to the rSUR2A-CT-C fragment was prepared from MRP1 (MRP1-CT-C) as a direct control for rSUR2A-CT-C binding. Both control constructs were expressed as MBP fusion proteins using the pMAL-c2x protein fusion system in *Escherichia coli* DH5 $\alpha$  cells and purified by affinity

chromatography on amylose-Sepharose according to the manufacturer's instructions (section 2.2.5). The concentration of the fusion fragments was determined by the Bradford assay (method section 2.2.6) in 1  $\mu$ l and 10  $\mu$ l of the eluted fragment.

Under condition in which MBP-rSUR2A-CT-C (aa 1294-1403) was co-immunoprecipitated with full length of Kir6.2, no evidence for co-immunoprecipitation of the MBP-rSUR2A-CT-A-C (aa 1404-1545) or MBP-MRP1-CT-C (aa 1278-1387) fragments was observed with these peptides when added at equivalent concentration (Figure 4-8,B). This observation confirmed a specific interaction between the Kir6.2 and rSUR2A-CT-C fragment as well as an absence of interaction with the C-terminal of rSUR2A, rSUR2A-CT-A-C with Kir6.2 (Figure 4-8,B).

## SPECIAL NOTE

THE FOLLOWING  
IMAGE IS OF POOR  
QUALITY DUE TO THE  
ORIGINAL DOCUMENT.

THE BEST AVAILABLE  
IMAGE HAS BEEN  
ACHIEVED.

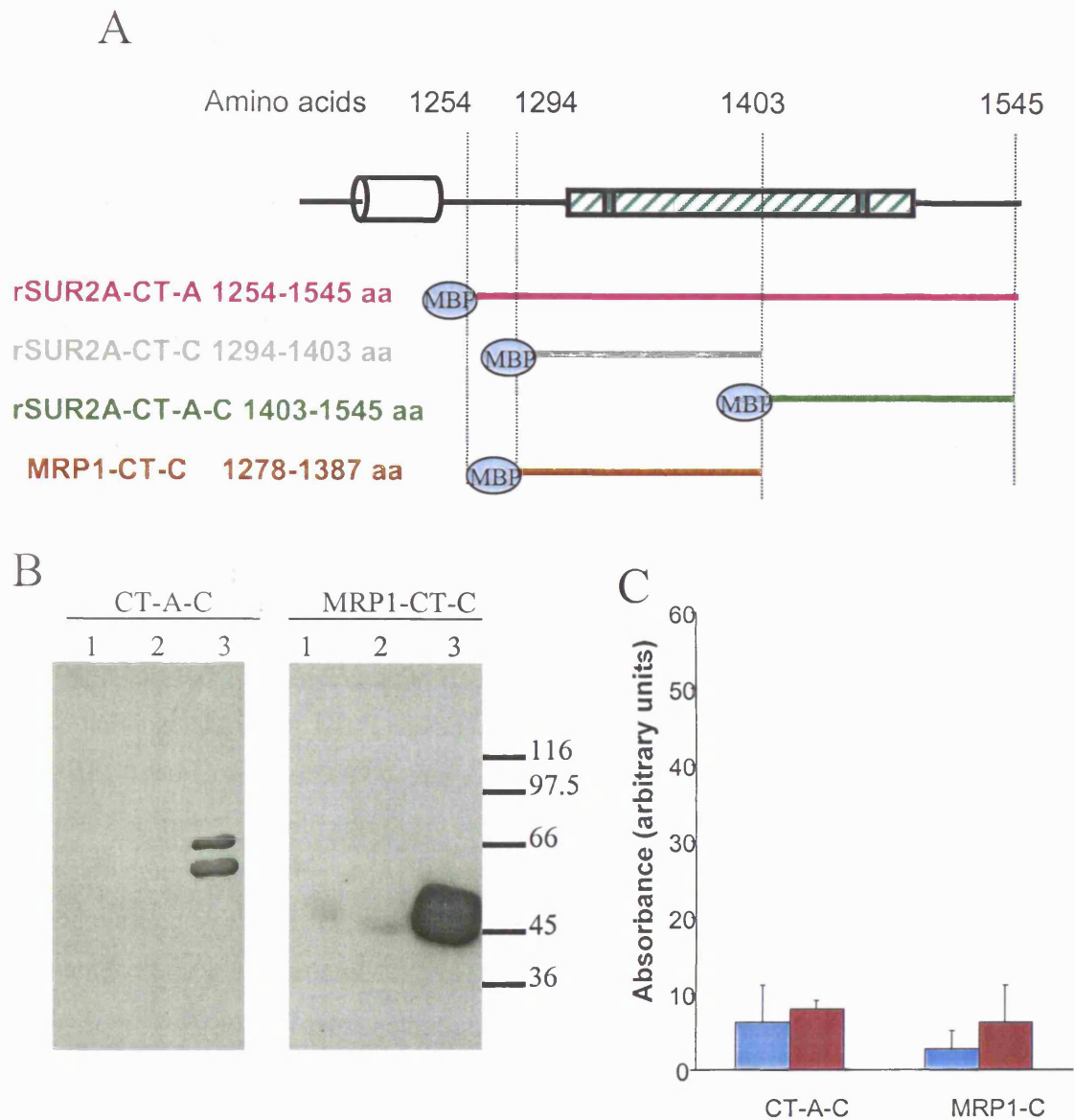


**Figure 4-8 Co-immunoprecipitation of MBP-rSUR2A-CT-A-C and MRP1-CT-C fragments with Kir6.2 subunit using anti-Kir6.2.** **A** Schematic diagram of MBP-rSUR2A-A-C and MRP1-CT-C without and with tagged fragments. **B**, shows ECL-film exposure of a Western blot stained with mouse anti-MBP IgG as primary antibody and anti-mouse IgG-HRP as secondary antibody. Lane 1, co-immunoprecipitation of MBP-fusion protein with Kir6.2 using anti-Kir6.2 antiserum, lane 2, control reaction in the absence of Kir6.2, lane 3, direct load of the fragments. The fragments included in this figure from left to right are rSUR2A-CT-C and rMRP1-CT-C. **C**, Histogram representing mean + SEM of the amount of co-immunoprecipitation of each rSUR2A-CT fragment in the absence (dark red) or presence (blue) of Kir6.2 determined by densitometry of the ECL exposure of Western blots expressed for 2 min.

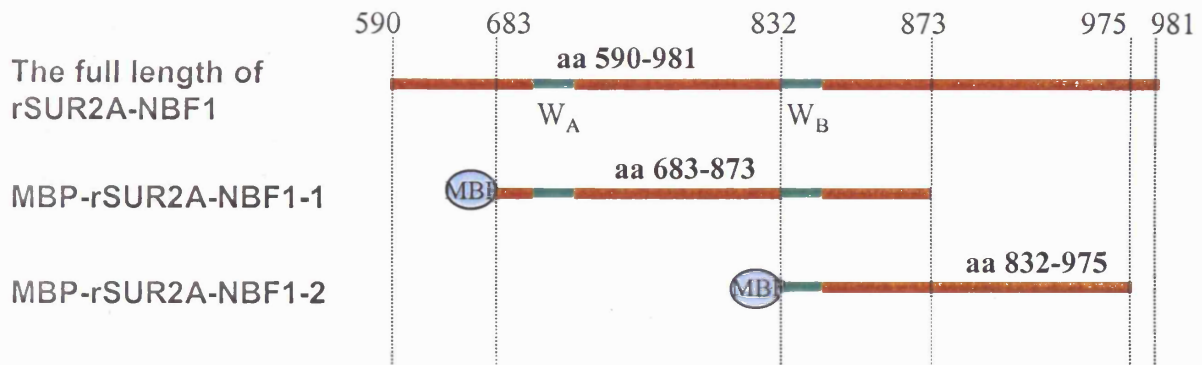
#### 4.2- Investigate the binding site of NBF1 from SUR2A with full length of Kir6.2

As for rSUR2A-CT (NBF2), fragments from the NBF1 were made as shown in chapter 3 (Figure 3-1). Following the same strategy and methods used for rSUR2A-CT fragments the direct binding of the NBF1 to Kir6.2 was investigated. Co-immunoprecipitation experiments of MBP-rSUR2A-NBF1 fragments were carried out to determine the possibility of a Kir6.2 interaction site in the NBF1 of SUR2A. Two fragments from the first nucleotide binding fold (NBF1) were made by Dr. M. Routledge (rSUR2A-NBF1-1, amino acid 683-873, and rSUR2A-NBF1-2; amino acid 832-975, (Figure 4-9) and were tagged with maltose binding protein in the N-terminal of the fragment.

##### 4.2.1- Expression of MBP-rSUR2A-NBF1 fragments

Fragments of rSUR2A (Figure 4-9,A) corresponding to the nucleotide binding fold 1 containing most of the NBF1 including the Walker A and Walker B motifs (rSUR2A-NBF1-1, amino acid 683-873), and the C-terminal half of nucleotide binding fold 1 starting from the walker B motif (rSUR2A-NBF1-2, amino acids 832-975) were expressed as MBP fusion proteins using the pMAL-c2x protein fusion system in *Escherichia coli* DH5 $\alpha$  cells and purified by affinity chromatography on amylose-Sepharose according to the manufacturer's instructions. The concentration of the fusion fragments was determined by the Bradford assay. The concentration of the MBP-rSUR2A-NBF1-1 in 1ul of eluted protein was 375  $\mu$ g/ml and was 125  $\mu$ g/ml for MBP-rSUR2A-NBF1-2. Fusion protein preparations were analysed by SDS/PAGE (7.5 % gels) and transferred to membrane using the Western blot technique. ECL detection of MBP revealed several stained bands when purified MBP-rSUR2A-NBF1 was analysed suggesting either expression of some truncated fragments or instability of the MBP-fusion protein (Figure 4-9). Although, less pronounced, some evidence of smaller polypeptides than the predicted MBP-fusion were also seen for rSUR2A-NBF1-2.

A



B

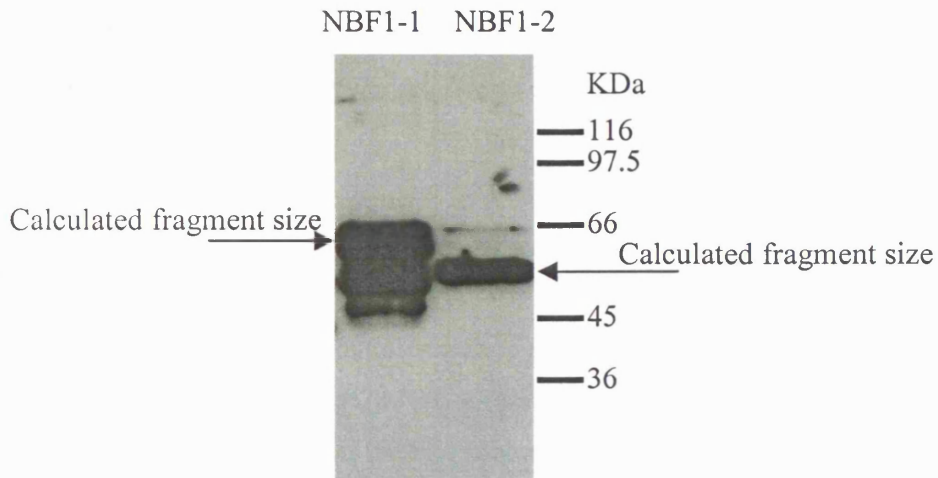


**Figure 4-9 Analyses of expressed and purified MBP-rSUR2A-NBF1 fusion fragments.** A, Schematic diagram of rSUR2A NBF1 fragments the green line represent  $W_A$  and  $W_B$ . B, Purified MBP-rSUR2A-NBF1 fragments analysed by SDS/PAGE (7.5 %gel) and Western blot with anti-MBP. Lane 1, (0.006  $\mu\text{g/ml}$ ) of eluted MBP-rSUR2A-NBF1-1, lane 2, MBP-rSUR2A-NBF1-2.

#### 4.2.2- Co-immunoprecipitation of the MBP-rSUR2A-NBF1 fragment with full length of Kir6.2

Co-immunoprecipitation experiments were conducted to investigate direct physical association between fragments of the NBF1 domain of the SUR2A subunit and full-length Kir6.2 subunits using the same co-immunoprecipitation technique that was used to screen for interaction between rSUR2A-CT (NBF2) with full-length Kir6.2 subunit. When an equivalent concentration of rSUR2A-NBF1 fragment was used to that used in experiments with rSUR2A-CT fragments there was no binding with either fragment. When the concentration of the MBP-fragment was increased three fold (180 ng/μl), both MBP-rSUR2A-NBF1 fusion protein were co-immunoprecipitated with full-length Kir6.2 using anti-Kir6.2 C-terminal antiserum (Figure 4-10). The results were reproduced 3 times with the same condition.

#### 4.2.3- Co-immunoprecipitation of the full length of Kir6.2 with the GST-rSUR2A-NBF1 and NBF2 fragments

Co-immunoprecipitation experiments were conducted to investigate possible direct physical association between fragments from the NBF1 and NBF2 of the SUR2A subunit and full-length Kir6.2 subunits. In this series of experiments, selected fragments that showed binding with Kir6.2, rSUR2A-CT-A (amino acids 1254 – 1545 aa) and rSUR2A-NBF1-1 (aa 683-873), and the non-binding fragment rSUR2A-CT-D (aa 1358- 1545) were tested with different tagging tool. In these experiments, rSUR2A-CT fragments were tagged with GST and interaction with Kir6.2 tested by GST-resin pull down of in vitro translated [<sup>35</sup>S]methionine-labelled Kir6.2. Fragments were expressed as GST fusion proteins using the pET41a protein fusion system in NovaBlue (DE3) cells and purified by affinity chromatography using the GST-Bind Kits according to the manufacturer's instructions (method section 2.2.8). The GST-tag assay kit (section 2.2.9) was used to determine the concentration of the expressed fragment on 1 μl of the eluted polypeptide.

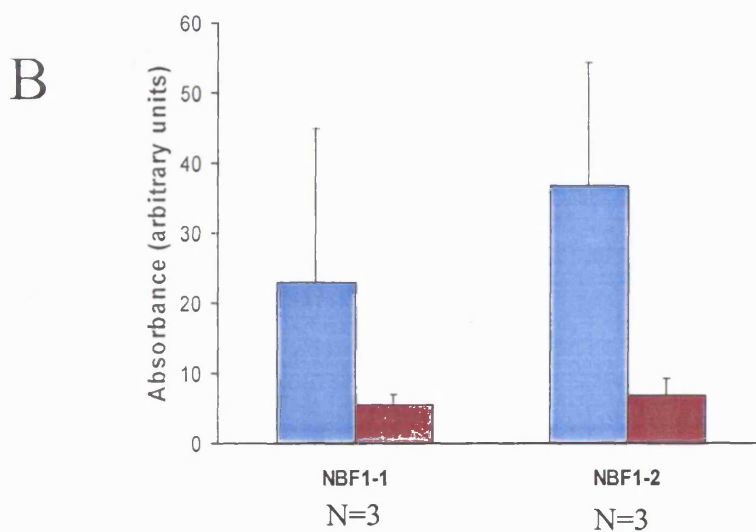
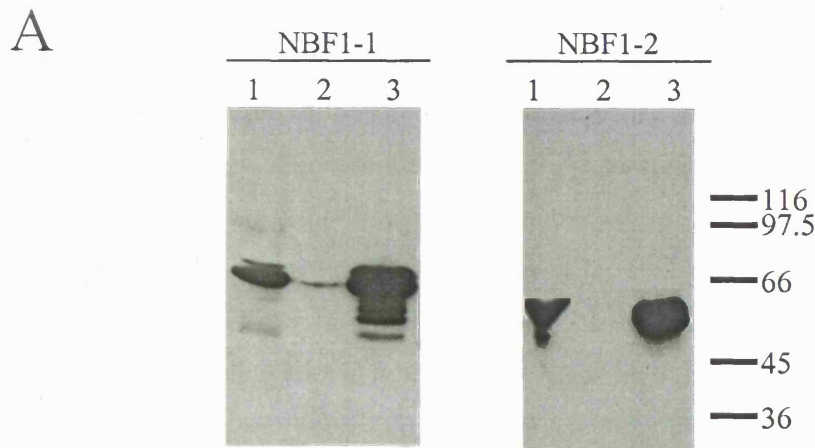


**Figure 4-10 Co-immunoprecipitation of MBP-rSUR2A-NBF1 fragment with Kir6.2 subunit using anti-Kir6.2 antiserum.** A, Shows ECL-film exposure of a Western blot stained with mouse anti-MBP IgG as primary antibody and anti-mouse IgG-HRP as secondary antibody. Lane 1, co-immunoprecipitation of MBP-rSUR2A-NBF1 fusion protein with Kir6.2 using anti-Kir6.2 antiserum. lane 2, control reaction in the absence of Kir6.2, lane 3, direct load of the rSUR2A fragments (0.006  $\mu\text{g/ml}$ ). The fragments included in this figure from left to right are rSUR2A-NBF1-1 and rSUR2A-NBF1-2. B, Histogram representing mean  $\pm$  SEM of the amount of co-immunoprecipitation of each rSUR2A-NBF1 fragment in the absence (dark red) or presence (blue) of Kir6.2 determined by densitometry of the ECL exposure of Western blots expressed for 2 min.

The concentration of the fusion fragments was determined by the GST-tag assay kit (see method section 2.2.9) in 1  $\mu$ l of the eluted fragment. An equal amount of the GST-tag (0.5  $\mu$ g/ml) polypeptide was incubated with the GST-resin to purify the GST-tag polypeptide. Then the co-precipitation of the [<sup>35</sup>S]methionine-labelled Kir6.2 was carried. The co-precipitation the [<sup>35</sup>S]methionine-labelled Kir6.2 determine the binding. The eluted mixture, GST-fragment and [<sup>35</sup>S]methionine-labelled Kir6.2, was analysed in an SDS-gel. Control reaction was performed in the absence of the GST-fusion fragment. The gel was dried and exposed to X-ray film for 3 days. The film showed non-specific pull down of [<sup>35</sup>S]methionine-labelled Kir6.2 from every reaction including the control reaction, where GST-fragment was absent (result not shown) even under the stringent resin washing condition applied (20 mM Tris-HCl, 0.1% NP-40, 500 mM KCl). In addition, after storage GST-tag polypeptide for seven days at 4°C, and when analysed by SDS-PAGE, the expressed GST-tagged fragments were characterised by two bands for each fragment. The lower molecular sized polypeptide was consistent with the size of free GST and the larger polypeptide with GST-tagged SUR2A peptide (Figure 4-11).

**SPECIAL NOTE**

**THE FOLLOWING**  
**IMAGE IS OF POOR**  
**QUALITY DUE TO THE**  
**ORIGINAL DOCUMENT.**

**THE BEST AVAILABLE**  
**IMAGE HAS BEEN**  
**ACHIEVED.**

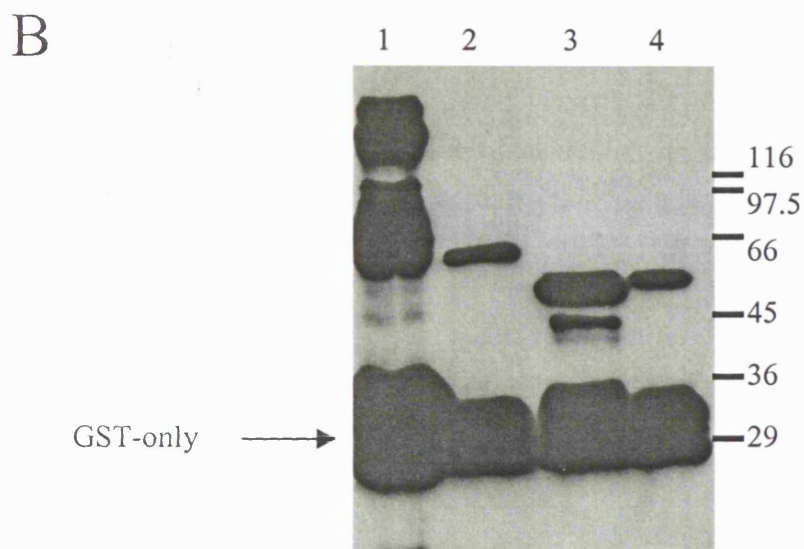
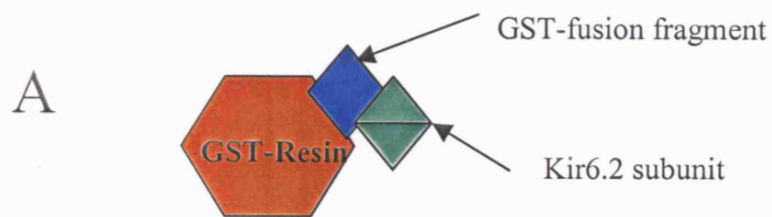


**Figure 4-11 The GST-rSUR2A expression and co-precipitation with Kir6.2.** A, Schematic diagram showing the complex formed co-precipitation of [<sup>35</sup>S]methionine-labeled-Kir6.2 using GST-fusion and GST-resin. B, shows 10 % SDS-PAGE analysis of the expression of the GST-fragments, lane 1, GST-only (showing many band resulting from overload the track); lane 2, GST-rSUR2A-CT-A fragment; lane 3, GST-rSUR2A-NBF1-1 and lane 4, GST-rSUR2A-CT-D. Representative experiment (n=2).

### 4.3- Summary

The binding site in the C-terminal of SUR2A was determined between amino acid residues 1294-1403, rSUR2A-CT-C. However, the rSUR2A-CT-D (aa 1358-1454) fragment failed to show binding with the full length of Kir6.2, which suggests that the binding site on SUR2A-CT is within the rSUR2A-CT-E fragment (aa 1294-1358). To confirm this finding, the equivalent of this sequence from MRP1 (MRP1-CT-E, aa 1280-1344) failed to demonstrate any binding with the full length of Kir6.2. Moreover, the rSUR2A-CT-fragments failed to demonstrate binding with the full length of Kir2.1. This chapter has shown the degree of difficulty of the biochemical methods used in the investigation. The limitation of the tagging method was one of the factors, where the GST-tag failed to remain stable for a sufficiently long time through the experimental procedure. Although some questions raised about the stability of tagged polypeptides, the finding in this chapter was confirmed by cell physiology experiments (chapter 6), which investigated the disruption of the Kir6.2/SUR2A subunit in the presence of a binding fragment.

## **Chapter Five**

### **Immunocytochemical assay of $K_{ATP}$ channel subunit targeting to the cell surface of cells expressing Kir6.2/SUR2A in the present of interacting fragment**

5.1- Subcellular targeting assay for the interacting fragment rSUR2A-CT-E, rSUR2A-CT-D and the empty vector

To investigate whether the presence of rSUR2A-CT fragments containing residues 1294-1358 could affect channel hetro-oligomer assembly or cause disruption of channels on the cell surface or lowered surface expression, HEK-293 cells stably expressing Kir6.2/SUR2A and transiently transfected with the rSUR2A-CT-E fragment were subjected to immunocytochemistry using anti-Kir6.2 and anti-SUR2A antisera to look for possible changes in the subcellular localization of this subunit. A membrane-localized form of EGFP was co-expressed with the rSUR2A-CT fragments from pIRES2-EGFP-F vectors. The membrane-localized expression of EGFP-F was used to identify transfected cells after permeabilization and immunocytochemistry. Optical sections of cells were taken systematically in the horizontal axis across the centre of all cells to determine the localization of the plasma-membrane-associated EGFP fluorescence (green) and anti-K<sub>ATP</sub> channel subunit fluorescence (red). Optical sections are presented as pixel profiles (Figure 5-1 B,D and F). In cells transfected with empty pIRES2-EGFP-F vector or rSUR2A-CT-D, most of the Kir6.2 polypeptide-associated immunofluorescence co-localized with plasma-membrane-associated EGFP-F fluorescence (Figure 5-1,C-F). In comparison, plasma-membrane-located anti-Kir6.2-associated fluorescence was significantly lower in most of the cells transiently expressing fragment rSUR2A-CT-E, with most of the anti-Kir6.2-associated fluorescence shifted to an intracellular compartment close to the plasma membrane (Figure 5-1,A-B).

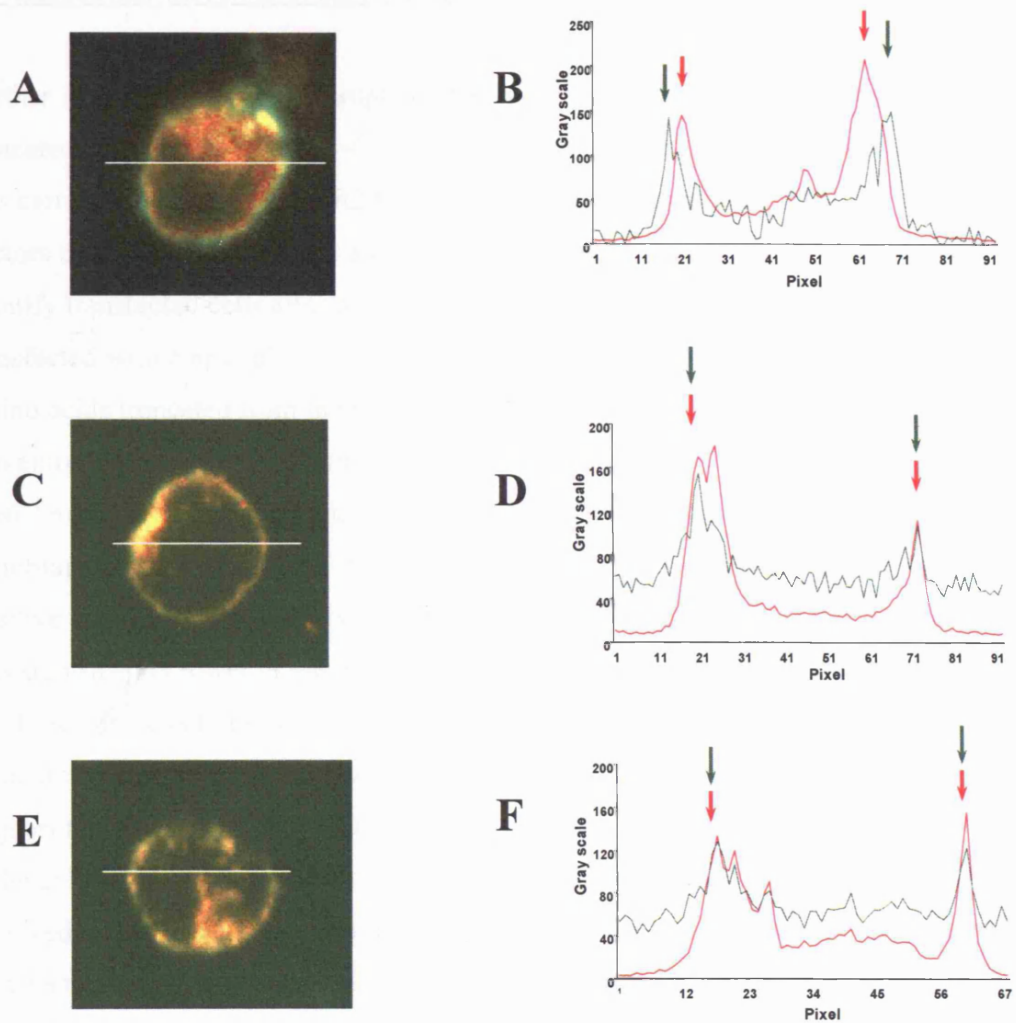


**Figure 5-1 The  $K_{ATP}$  channel subunit distribution in HEK293 cells stably co-expressing Kir6.2/SUR2A and transiently transfected with rSUR2A fragments.** A, C and E representative images of EGFP-F (green) and anti-Kir6.2 subunit antibody-associated immunofluorescence (red) in Kir6.2/SUR2A expressing cells transiently transfected with rSUR2A-CT-E (A), rSUR2A-CT-D (C), and empty pIRES2-EGFP-F vector (E). The horizontal line through the cells in A, C and E describe the optical section shown in B, D and F, respectively. The optical sections represent the pixel profiles of fluorescent intensity of EGFP-F (green) and anti Kir6.2 subunit-associated fluorescence (red), which shows a shift of the anti Kir6.2 subunit-associated fluorescence in cell transfected with rSUR2A-CT-E (A and B) but no effect in cells transfected with rSUR2A-CT-D (C and D) or with empty vector (E and F).

### 5.2- Subcellular targeting in the presence of the truncated rSUR2A-CT-C fragment

Further investigation of the disruption of Kir6.2/SUR2A channel localization with a truncated fragment of rSUR2A-CT-C in a HEK293 cells stably expressing Kir6.2/SUR2A was carried out. As above, SUR2A fragments were expressed from pIRES2-EGFP-F vectors containing the gene for a membrane-localized form of EGFP, which was used to identify transfected cells after permeabilization and immunocytochemistry. In cells transfected with empty pIRES-EGFP-F vector, rSUR2A-CT-D, rSUR2A-CT-F (eleven amino acids truncated from the C-terminal of rSUR2A-CT-E) or rSUR2A-CT-G (twenty two amino acids truncated from the C-terminal of rSUR2A-CT-E), the majority of the Kir6.2 and SUR2A polypeptide-associated immunofluorescence co-localized with plasma membrane-associated EGFP-F fluorescence (Figure 5-2). In the same experiments, as a positive control, plasma membrane located anti-Kir6.2 and SUR2A-associated fluorescence was significantly lower in the majority of cells transiently expressing fragment rSUR2A-CT-E than in cells transfected with empty vector, with a raised level of fluorescence located in a compartment beneath the plasma membrane (Figure 5-1,A-B). These results suggest that after truncation of the last 11 amino acids from the C-terminal of rSUR2A-CT-E the ability to disrupt surface expression of Kir6.2/SUR2A channel appeared to be removed and the channel distribution in the presence of the fragment resembled that in cell transfected with empty vector. This lead to an early assumption that the last 11 amino acids in rSUR2A-CT-E was either an important region in the direct binding interaction with Kir6.2 or that it contributed to the stabilization of other interacting structures and, therefore, for the channel disruption.

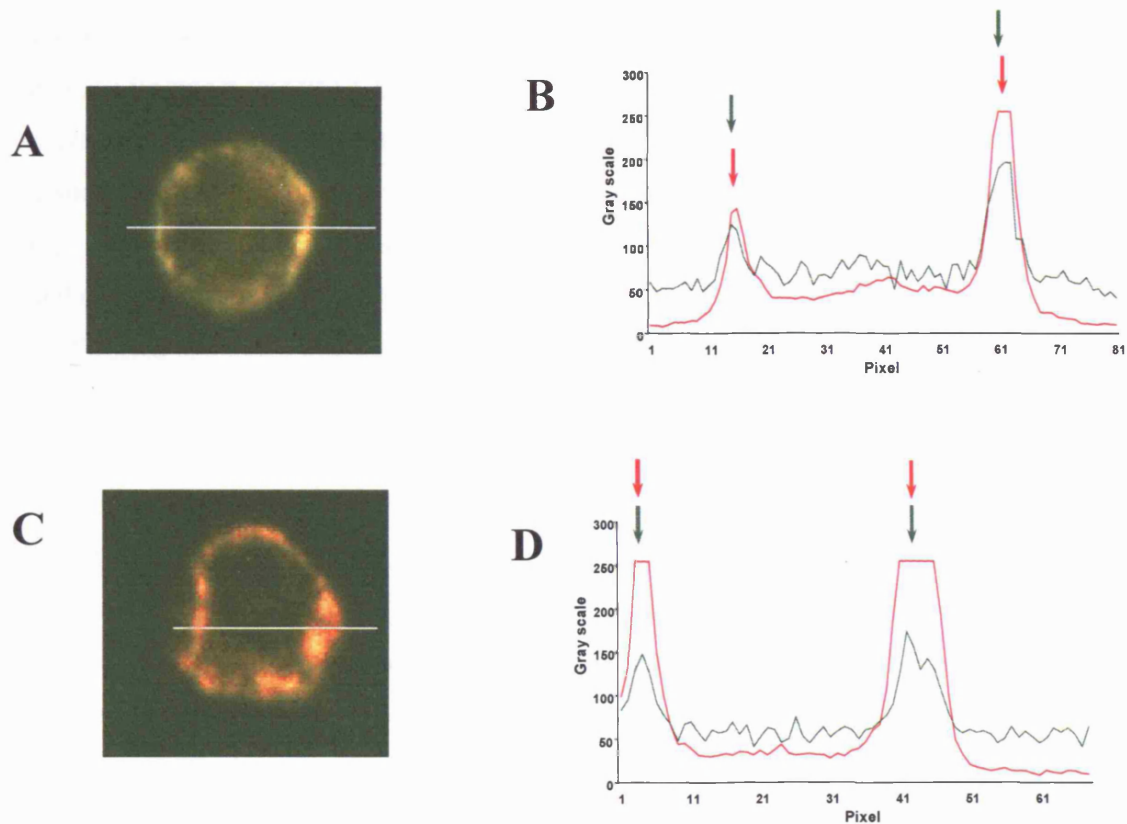


**Figure 5-2 The  $K_{ATP}$  channel subunit distribution in HEK293 cells stably co-expressing Kir6.2/SUR2A and transiently transfected with truncation fragment from rSUR2A-CT-C.** A and B representative images of EGFP-F (green) and anti-Kir6.2 subunit antibody-associated immunofluorescence (red) in Kir6.2/SUR2A expressing cells transiently transfected with rSUR2A-CT-F (A) and rSUR2A-CT-G (C). The horizontal line through the cells in A and C describe the optical section shown in B and D, respectively. The optical section represent the pixel profiles of fluorescent intensity of EGFP-F (green) and anti Kir6.2 subunit-associated fluorescence (red), which shows no change in plasma membrane localization of Kir6.2 in cells transfected with rSUR2A-CT-F or with rSUR2A-CT-G (B and D).

### 5.3- Summary

The immunocytochemistry method was used to confirm the findings from chapter four. The binding fragment (rSUR2A-CT-E) showed disruption on the surface expression of  $K_{ATP}$  channel in cells stably expressing Kir6.2/SUR2A. The altered location of fluorescence associated with Kir6.2 compared to that of the membrane localized fluorescence EGFP-F represented the removal of the channel from the cell surface, induct of channel disruption and turnover at the cell surface or reduced plasma membrane targeting of newly synthesised channels. The non-binding fragment rSUR2A-CT-D showed no affect on the channel surface density. The truncation of the binding fragment (rSUR2A-CT-E), by removing eleven (rSUR2A-CT-F) or twenty two amino acids (SUR2A-CT-G) from the C-terminal of the fragment resulted in a loss of  $K_{ATP}$  channel disruption. This finding corroborated the biochemical result, which suggested that the C-terminal of rSUR2A-CT-E fragment is needed for the fragment interaction, but this region cannot form the binding site with Kir6.2 by itself. Therefore, it is been suggested that this region has important in the binding but cannot form the full element of binding with the full length of Kir6.2 *in vitro*. Different methods were applied to investigate the disruption of the channel assembly.

To improve this method of investigation, an attempt was made to tag the fragments with a HA-tag in C-terminal to be followed by anti-HA antibody. This would have allowed the localization of the fragments with the  $K_{ATP}$  channel subunit to be followed using anti-HA antibody conjugated with fluorescence. This method failed to confirm the finding, since no binding of anti-HA could be detected; also a Western blot for cells transfected with HA-SUR2A fragments failed to show expression of the tagged fragments. As positive control to test the sensitivity of the anti-HA, HA-Kir2.1 was expressed and showed polypeptide expression with one of three anti-HA antisera that was used. Tagging the SUR2A fragments and expressing them in mammalian cell was also unsuccessful. It is possible that tagging made the polypeptide unstable and increases their breakdown.

## **Chapter Six**

### **Refinement of the Kir6.2 binding site in rSUR2A-CT-C using rSUR2A/MRP1-CT-C chimaeric constructs**

## 6.1- Introduction

In this chapter a different approach to investigate the Kir6.2 binding site on the C-terminal of the SUR2A subunit were taken. Instead of making a smaller polypeptide from the rSUR2A-CT-C fragment, fragment chimaeras between the SUR2A and MRP1 representing rSUR2A-CT-C domain were designed to investigate the interaction in more detail. As described in chapter 3, a set of chimaeras was made by removing 25 or 45 amino acids from the N-terminal of rSUR2A-CT-C replacing them with the equivalent residues from MRP1-CT-C. Complementary MRP1-CT-C based chimaeras were made by replacing the N-terminal 25 or 45 amino acids of MRP1-CT-C with equivalent residues from rSUR2A-CT-C. This approach was taken to overcome the instability of the small fragments created from rSUR2A-CT-C, also to support the polypeptide structure.

In this sub-study, MBP-tagged chimaeras were investigated in co-immunoprecipitation experiments with full-length Kir6.2 to further localize the binding site of Kir6.2 in the C-terminal of SUR2A. In addition, the same chimaeras were expressed in pIRES2-EGFP-F vector without tag to be used in electrophysiology experiments, with the help of Dr R. Rainbow (Cell Physiology Department, Leicester), to measure the effect of the chimaeric fragments on Kir6.2\SUR2A assembly when expressed in HEK 293 cells stably expressing Kir6.2 and SUR2A.

## 6.2- Expression of SUR2A/MRP1 chimaeras

Four chimaeras were constructed from SUR2A and MRP1 to represent the amino acid sequence of rSUR2A-CT-C (aa 1294-1403)(Figure 6-1), MRP1(25)SUR2A (aa 1280-1304/1318-1403), SUR2A(25)MRP1 (aa 1294-1317/1305-1389), MRP1(45)SUR2A (aa 1280-1324/1338-1403), and SUR2A(45)MRP1 (aa 1294-1337/1325-1389). These constructs were expressed as MBP fusion proteins using the pMAL-c2x vector. The fusion fragments were transformed into *Escherichia coli* DH5 $\alpha$  cells (method section 2.1.12) and purified by affinity chromatography on amylose-Sepharose according to the manufacturer's instructions (method section 2.2.5). The concentration of the fusion fragments was

determined by the Bradford assay (method section 2.2.6) using 1  $\mu$ l of the eluted fragment. The concentration of MRP1(25)SUR2A, SUR2A(25)MRP1, MRP1(45)SUR2A, and SUR2A(45)MRP1, was 375, 3200, 600, and 1400  $\mu$ g/ml, respectively. The concentration of the expressed chimaeras was diluted to 0.060  $\mu$ g/ml and 1  $\mu$ l was loaded to 7.5% SDS-PAGE. Western Blotting was performed to transfer the protein to Hybond-P membrane for detection with the ECL technique using mouse anti-MBP IgG as primary antibody and anti-mouse IgG-HRP as secondary antibody. The membrane was exposed to the ECL-film for 2 min and developed (Figure 6-1,B). The autodiagram confirmed expression of each MBP-chimaera and their detection by anti-MBP antiserum in immunoblots. It is noticeably, that each construct, except MRP(45)SUR2A, run as an MBP-stained doublet on SDS-PAGE. The reasons for this were not determined.

### 6.3- Co-immunoprecipitation of SUR2A/MRP1 chimaeras with full length Kir6.2

Co-immunoprecipitation experiments were conducted to investigate the direct physical association between SUR2A/MRP1 chimaeras corresponding to rSUR2A-CT-C and full-length Kir6.2 subunits. Four chimaeras were used in this investigation MBP-MRP1(25)SUR2A, MBP-SUR2A(25)MRP1, MBP-MRP1(45)SUR2A, and MBP-SUR2A(45)MRP1. In addition, MBP-rSUR2A-CT-C was included a positive control fragment, and MBP-MRP1-CT-C was included as a negative control fragment (chapter 4). For each fragment, a control reaction in the absence of the Kir6.2 subunit was performed and analysed in an adjacent lane (Lane 2). A direct load of the chimaeras in a third lane was loaded onto the 7.5 % SDS gel to assess the relative migration of any precipitated fragment. Experiments with SUR2A/MRP1 chimaeras were complicated by non-specific binding of chimaeric fragment to the immunomatrix in the absence of Kir6.2 in some experiment. The co-immunoprecipitation result was obtained from three 'successful' experiments out of seven attempted. Experiments were declared successful when the positive control showed binding to Kir6.2 and unsuccessful when the positive control either showed no binding to Kir6.2 or showed non-specific absorption with the reaction mixture in the absence of Kir6.2. The co-immunoprecipitation experiments showed that the two chimaeras containing residues 1318-1337 of SUR2A, MRP1(25)SUR2A, SUR2A(45)MRP1,

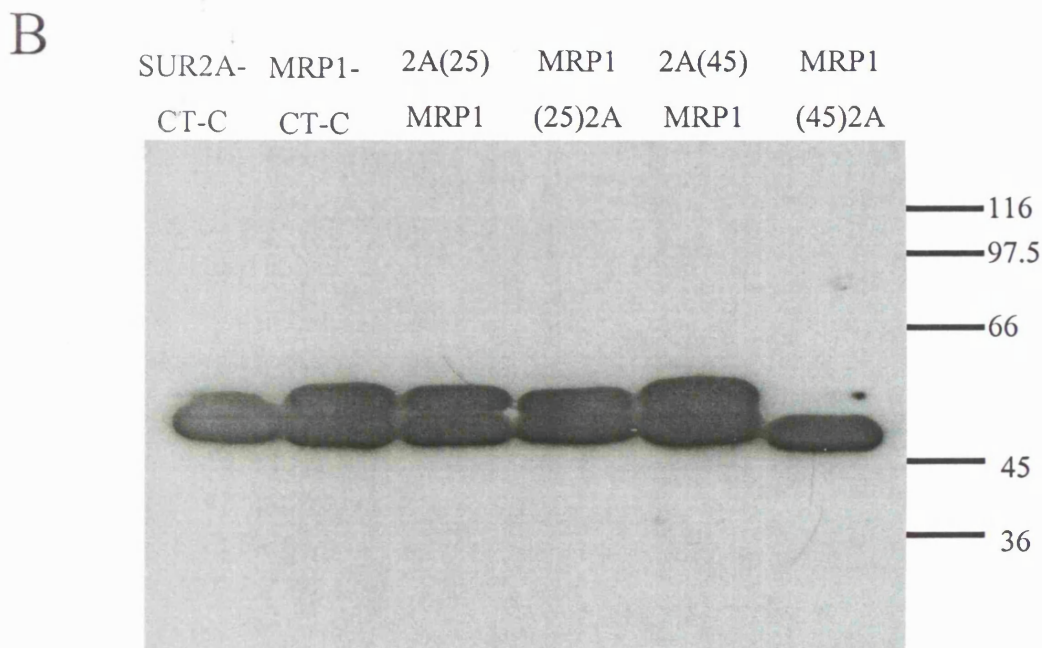
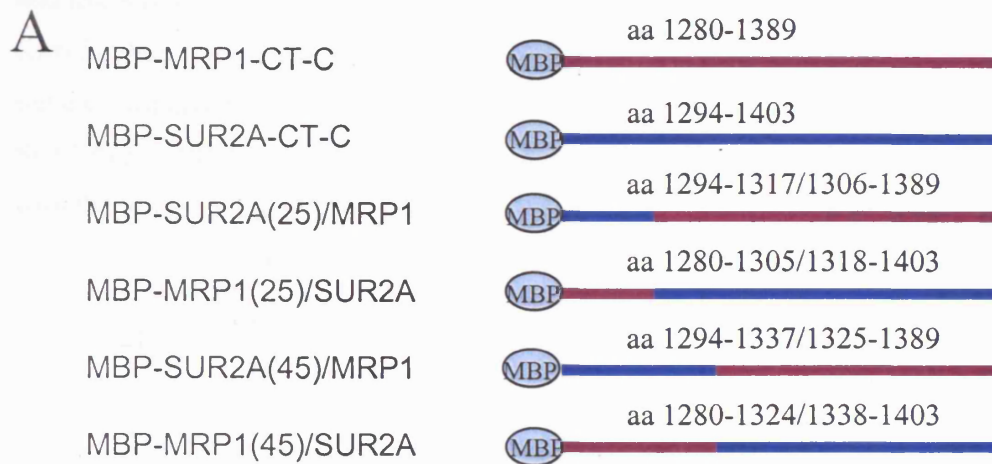


**Figure 6.1 Analysis of expressed and purified maltose binding protein tagged rSUR2A/MRP1 chimaeras.** A, Schematic diagram of rSUR2A/MRP1 chimaeras tagged with MBP in the N-terminal. B, Shows the purified rSUR2A/MRP1 chimaeras (0.006  $\mu\text{g/ml}$ ) analysed by SDS-PAGE (7.5 %gel). Lane 1, MBP-rSUR2A-CT-C; lane 2, MBP-MRP1-CT-C; lane 3, MBP-SUR2A(25)MRP1 chimaera; lane 4, MBP-MRP1(25)SUR2A chimaera; lane 5, MBP-SUR2A(45)MRP1 chimaera, and lane 6, MBP-MRP1(45)SUR2A chimaera.

and rSUR2A-CT-C were co-immunoprecipitated with the full length *in vitro* translated Kir6.2 subunit using anti-Kir6.2 C-terminal antiserum (Figure 6-2, A lane 1). Under the same conditions, the other two chimaeras containing residues 1305-1324 of MRP1, SUR2A(25)MRP1, MRP1(45)SUR2A, and MRP1-CT-C did not co-immunoprecipitate with the full length Kir6.2 polypeptide.

**SPECIAL NOTE**

**THE FOLLOWING**  
**IMAGE IS OF POOR**  
**QUALITY DUE TO THE**  
**ORIGINAL DOCUMENT.**

**THE BEST AVAILABLE**  
**IMAGE HAS BEEN**  
**ACHIEVED.**

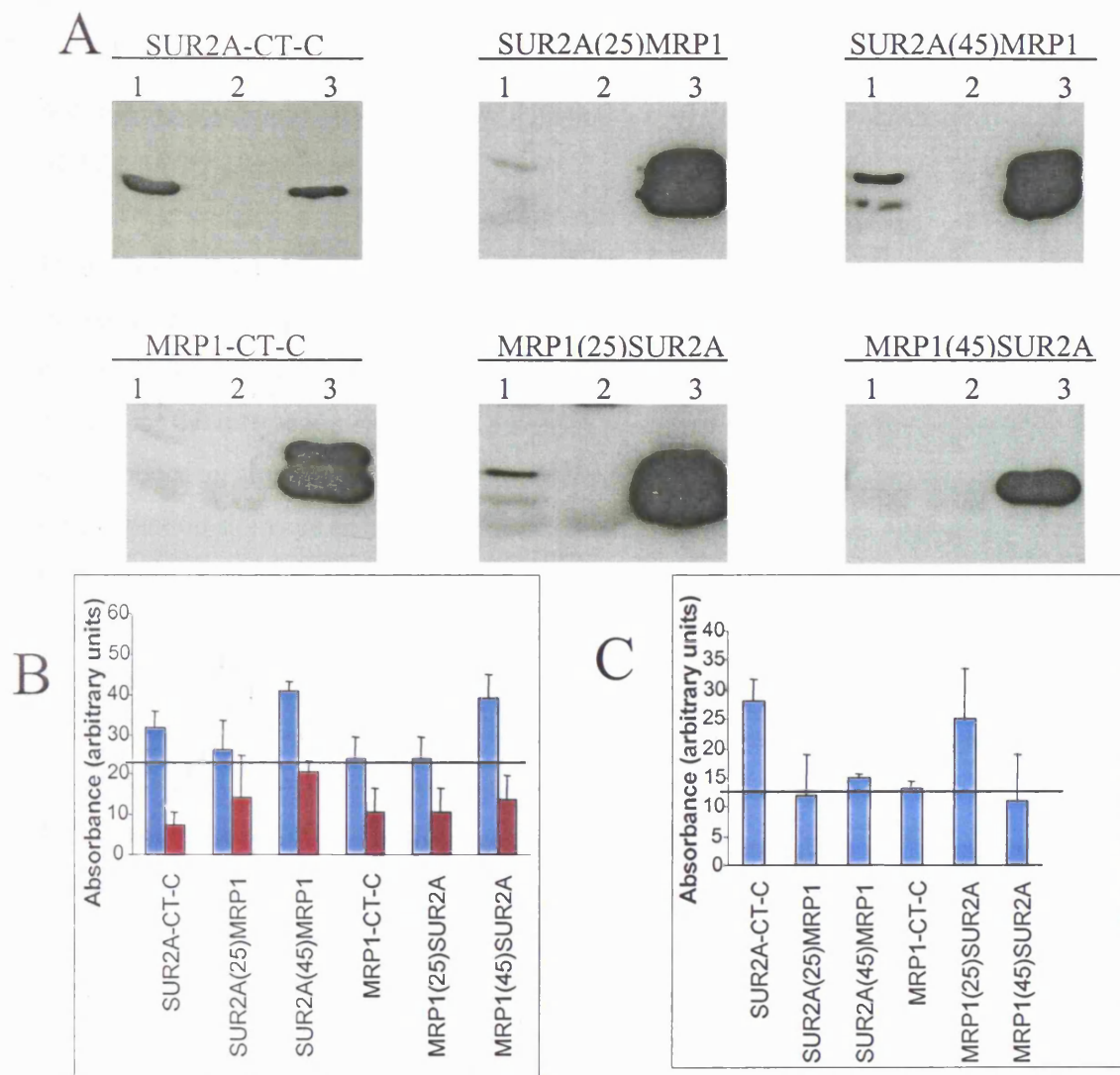


**Figure 6-2 Co-immunoprecipitation of MBP-tagged polypeptide with Kir6.2 subunit using anti-Kir6.2.** A, ECL-film exposure of a Western blot stained with mouse anti-MBP IgG as primary antibody and anti-mouse IgG-HRP as secondary antibody. Lane 1, co-immunoprecipitation of MBP-fusion protein with Kir6.2 using anti-Kir6.2 antiserum, lane 2, control reaction in the absence of Kir6.2, lane 3, direct load of the polypeptide. The MBP-fusion protein included in this figure are MBP-rSUR2A-CT-C, MBP-SUR2A(25)MRP1 chimaera, MBP-SUR2A(45)MRP1 chimaera, MBP-MRP1-CT-C, MBP-MRP1(25)SUR2A chimaera, and MBP-MRP1(45)SUR2A chimaera. B, Histogram representing mean  $\pm$  SEM (n=3) of the amount of co-immunoprecipitation of each tagged polypeptide in the absence (purple) or presence (blue) of Kir6.2 determined by densitometry of the ECL exposure of Western blots for 2 min. C, Histogram representing the mean  $\pm$  SEM for specific co-immunoprecipitate of each tagged polypeptide detected by the same ECL exposure from (B). Signal for the non-specific adsorption to resin was subtracted from the total co-immunoprecipitation for each experiment and the mean taken (n=3), and the line drawn above the MRP1-CT-C adsorption.

#### 6.4- Electrophysiology of Kir6.2/SUR2A channels in HEK 293 cells transiently expressing SUR2A/MRP1 chimaeras

In that study, it was hypothesised that regions of interaction with Kir6.2 contained within the sequence of the SUR2A C-terminal, when expressed as polypeptide fragments, would disrupt the Kir6.2/SUR2A channel complex by competing with the full length SUR2A protein for the interaction site. It was proposed that disruption of channel structure might then produce an alteration in current properties. When SUR2A-CT fragments containing the interaction site were transiently expressed in HEK 293 cells stably expressing Kir6.2/SUR2A channels a significant reduction in channel current density at the cell surface was observed, suggesting either functional disruption of surface channels or modification of channel turnover (Rainbow et al., 2004). This was investigated further in this study using confocal microscopy to investigate the sub-cellular localisation of Kir6.2/SUR2A channels (chapter 5). In the presence of interacting fragments, the distribution of Kir6.2/SUR2A channels was found to be altered, with much reduced surface labelling and significant clustering of channel polypeptides in a vesicular compartment close to the plasma membrane. Thus, the reduction in current density in the presence of interacting fragments was shown to be due to channel redistribution rather than functional disruption of surface channels. To provide a second complementary assay to investigate the interaction of the SUR2A/MRP1-CT-C chimaeras with Kir6.2, the electrophysiological assay was employed. In this case, it was hypothesised that chimaeras containing regions of SUR2A-CT-C involved in the interaction with Kir6.2 would disrupt surface targeting of Kir6.2/SUR2A channels, while those containing equivalent sequences in non-interacting MRP1 would not.

A HEK 293 cell line stably expressing Kir6.2 and SUR2A was used to investigate the effects of the SUR2A/MRP1-CT-C chimaeras on the surface targeting of functional Kir6.2/SUR2A channels. The Kir6.2/SUR2A cells line was kindly provided by Dr Andrew Tinker (UCL) for this series of experiments. Disruption of Kir6.2/SUR2A channel

assembly by rSUR2A-CT-C was established in a parallel study conducted by Dr. R. Rainbow (Cell physiology and pharmacology, Leicester) (see Discussion Figure 8-1).

At 2 days after transfection, cells transiently expressing the rSUR2A/MRP1 chimaeras were identified by their green fluorescence at 488 nm under mercury lamp illumination. The bath and perfusion solution contained, in mM, 135 NaCl, 6 KCl, 0.33 NaH<sub>2</sub>PO<sub>4</sub>, 5 Na pyruvate, 10 glucose, 10 HEPES, 1 MgCl<sub>2</sub> and 2 CaCl<sub>2</sub> as required, pH 7.4. Solution was perfused and maintained at 30 ± 2 °C. (Note – solution has to be at around 30 °C as pinacidil will not work unless it's warm enough!) The pipette solution contained 140 mM KCl, 1.2 mM MgCl<sub>2</sub>, 2.6 mM CaCl<sub>2</sub> and 5 mM Hepes (pH7.4). Electrodes were pulled from thick walled borosilicate glass and firepolished to a resistance of between 4-6 MΩ. Currents were recorded in the whole cell recording configuration voltage clamped to 0 mV, a potential at which a large outward current was observed when cells were perfused with pinacidil.

On perfusion with 100 μM pinacidil, cells stably transfected with Kir6.2/SUR2A alone or additionally transiently transfected with MRP1-CT-C showed a substantial increase in outward current, which was blocked by 10 μM glibenclamide, indicative of K<sub>ATP</sub> channel current (not shown). Similarly, glibenclamide-sensitive, pinacidil-stimulated currents were observed for cells transiently transfected with SUR2A(25)MRP1 and MRP(45)SUR2A (Fig. 6-3). By contrast, cells stably expressing Kir6.2/SUR2A and transiently transfected with either SUR2A(45)MRP1 or MRP1(25)SUR2A showed significantly reduced current (both P < 0.001- ANOVA with Bonferoni multiple comparison) to about 0.1 % the level of that seen in the presence of SUR2A(25)MRP1 and MRP(45)SUR2A (Fig. 6-3). Together, these results indicate that expression of the two chimaeras containing SUR2A residues 1318-1337 resulted in reduction in surface targeting of Kir6.2/SUR2A channels, while those with the equivalent sequence from MRP1 did not, further localising the Kir6.2 interaction site to this domain.

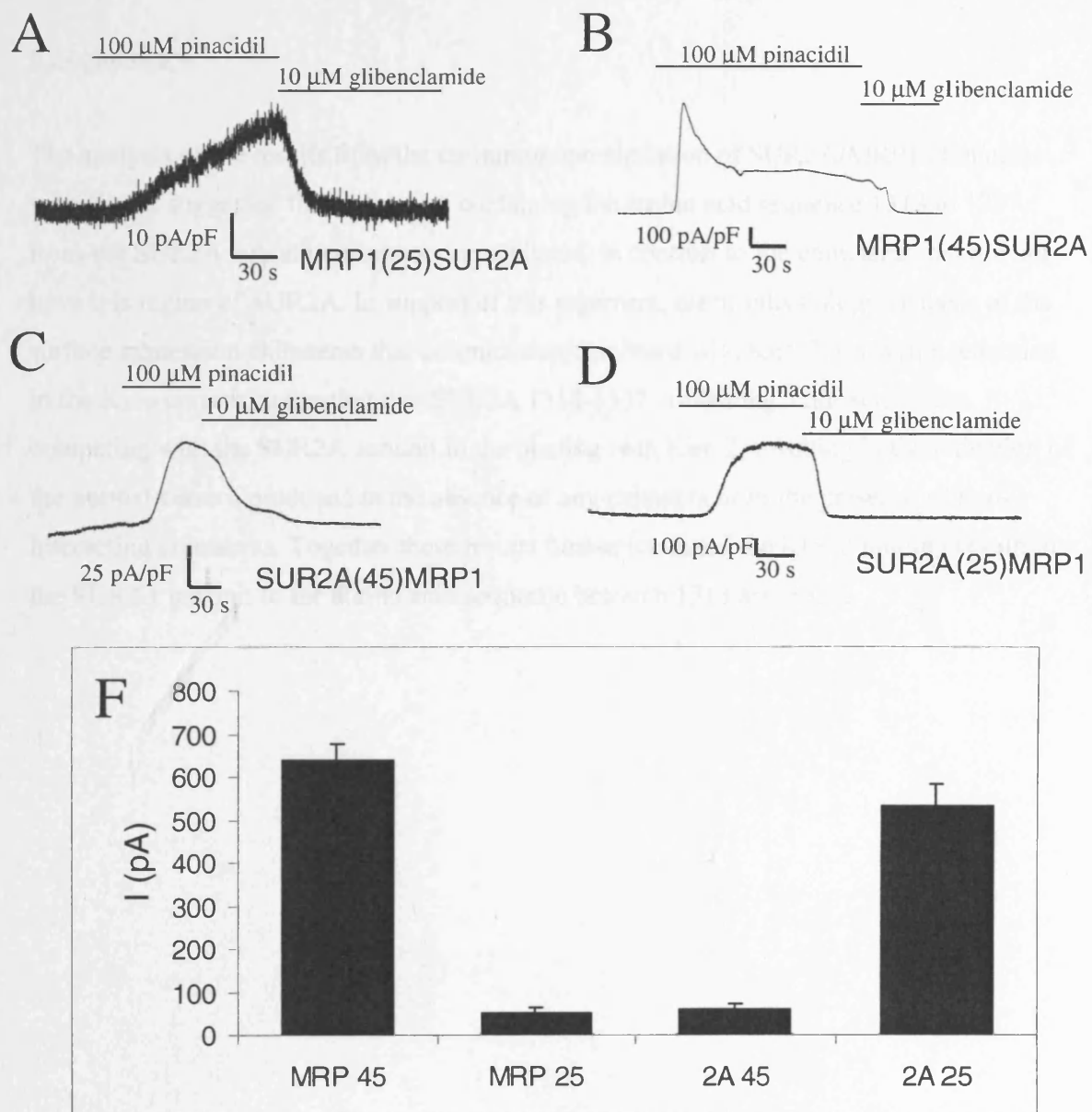


**Figure 6-3 Effect of SUR2A/MRP1 chimaeras on SUR2A/Kir6.2 Current.** A,B,C and D recordings of whole-cell current from HEK 293 stably expressing SUR2A and Kir6.2 and transiently expressing MRP1(25)SUR2A, MRP1(45)SUR2A, SUR2A(25)MRP1, SUR2A(45)MRP1, respectively. Currents were activated by perfusion with 100  $\mu$ M pinacidil at a holding potential of 0 mV eliciting an outward current in the potassium gradients used. F, histogram showing mean current  $\pm$  S.E.M., normalised to cell capacitance, from four cells for each protein fragment transfection. ( $P < 0.001$  (all data columns are compared to all other), ANOVA with bonferoni posthoc test.)

### 6.5- Summary

The analysis of the results from the co-immunoprecipitation of SUR2A/MRP1 chimaeras with Kir6.2 suggested that chimaeras containing the amino acid sequence 1318 to 1337 from the SUR2A subunit co-immunoprecipitated, in contrast to the chimaeras that did not have this region of SUR2A. In support of this argument, electrophysiology analysis of the surface expression chimaeras that co-immunoprecipitated with Kir6.2, showed a reduction in the  $K_{ATP}$  current suggesting that SUR2A 1318-1337 containing, chimaeras were competing with the SUR2A subunit in the binding with Kir6.2, resulting in the reduction of the normal current produced in the absence of any chimaera or in the presence of non-interacting chimaeras. Together these results further localized the Kir6.2 binding region in the SUR2A subunit to the amino acid sequence between 1318 and 1337.

## **Chapter Seven**

**Investigation of the cognate binding site for the proximal C-terminal domain of SUR2A on the Kir6.2 subunit using Kir6.2/Kir2.1 subunit chimaeras**

## 7.1- Introduction

After the binding site on the proximal C-terminal of SUR2A was determined, a further aim of this project was to define the corresponding binding site within the Kir6.2 using chimaeras between Kir6.2 subunit and non-interacting Kir2.1 subunit. The SUR2A-CT fragment used in this part of the investigation was MBP-SUR2A-CT-C. This fragment comprised a region of 109 amino acids containing the Kir6.2 interacting domain in a polypeptide that had permitted co-immunoprecipitation experiments most reproducibly in previous experiments, possibly by contributing some secondary structural constraints to the interaction domain. The non-interacting fragments MBP-rSUR2A-CT-D (aa 1359-1545) and MBP-MRP1-CT-C, which presented an equivalent amino acid sequence to rSUR2A-CT-C, were used as negative controls for Kir6.2 interaction.

Two sets of Kir6.2/Kir2.1 chimaeras were modified from published resources. The first set with the N-terminal corresponds to Kir6.2 and C-terminal to Kir2.1 (provided by Dr. Sivaprasadrao, Leeds) was used previously to study the trafficking of Kir6.2 in the absence or presence of SUR2A (Hough et al, 2000). The second set with the N-terminal corresponding to Kir6.2 and the C-terminal to Kir6.2 (provided by Dr. Tinker, University College, London), was previously used to study the function and the biochemical interaction between  $K_{ATP}$  subunits (Giblin et al, 1999). In this study, the two sets of chimaeras were used to investigate the physical interaction of Kir6.2 with SUR2A subunit fragments.

To study the biochemical interaction of the  $K_{ATP}$  channel, the Kir6.2/Kir2.1 chimaeras were expressed *in vitro*. Before use, chimaeric constructs were modified where necessary to remove C-terminal epitope tags that had been added in the original studies using these constructs (Hough et al 2000, Giblin et al 1999; see section 3.9 and Figure 3-8). Immunoprecipitation of the chimaeras was performed using either anti-Kir6.2 or anti-Kir2.1 antisera corresponding to the appropriate C-terminal in each of the chimaera to effect specific immunoprecipitation. Immunoprecipitation of the chimaeras was used as the

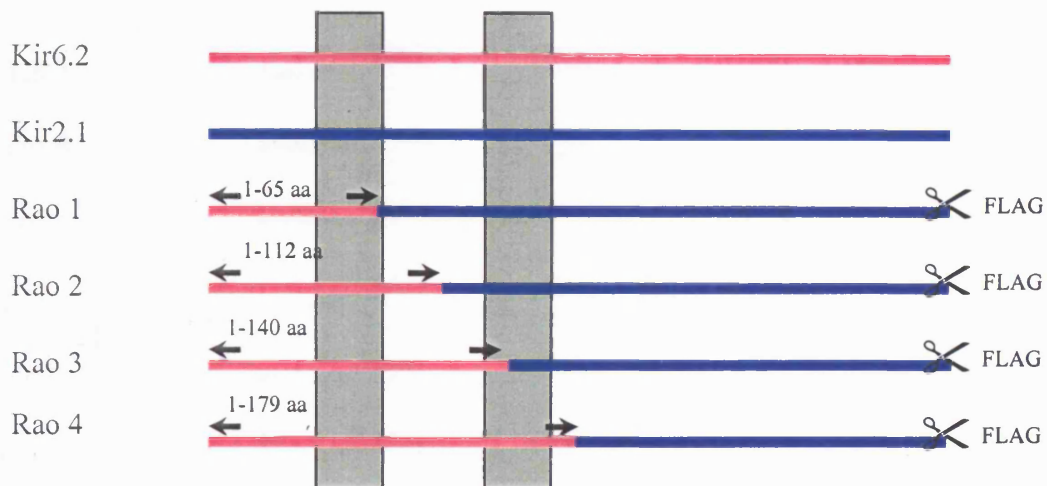
basis for co-immunoprecipitation of MBP-tagged SUR2A-CT fragments to determine the binding site of this fragment in the Kir6.2 subunit.

### 7.2- Expression of the Kir6.2/Kir2.1 chimaeras

The first step towards the co-immunoprecipitation of the fragment was to express the chimaeras. Kir6.2/Kir2.1 chimaera cDNA's were expressed in the (T7) TNT rabbit reticulocyte lysate Quick coupled transcription/translation system to produce polypeptide labelled with [<sup>35</sup>S]methionine. The expression of the proteins required canine pancreatic microsomal membranes in order to obtain a high yield of Kir6.2/Kir2.1 chimaeras. Satisfactory expression of all of the polypeptides was achieved, and the molecular weights of the polypeptides in 7.5% polyacrylamide gels were determined. The molecular weight for Kir2.1, Rao 1, Rao 2, Rao 3, and Rao 4 was approximately 48 kDa compared to band of 48, 38 kDa for Kir2.1 and Kir6.2 polypeptides, respectively; the large size do the large Kir2.1 C-terminal sequence (see Figure 7-1, B). Tin A, Tin B, Tin C, and Tin D had approximate molecular weights of 38 kDa; Tin E was 46 kDa; and Tin F was 48 kDa as shown in (Figure 7-2, B).

The level of expression of Rao chimaeras, Kir2.1 and Tin E was lower compared to other Tin chimaeras or Kir6.2. The amounts of these polypeptides used in co-immunoprecipitation experiments was double what was add for the other polypeptide construct (Tin A, Tin B, Tin C, Tin D, Tin F and Kir6.2) to ensure more equivalent amounts of subunit in each experiment.

A



B

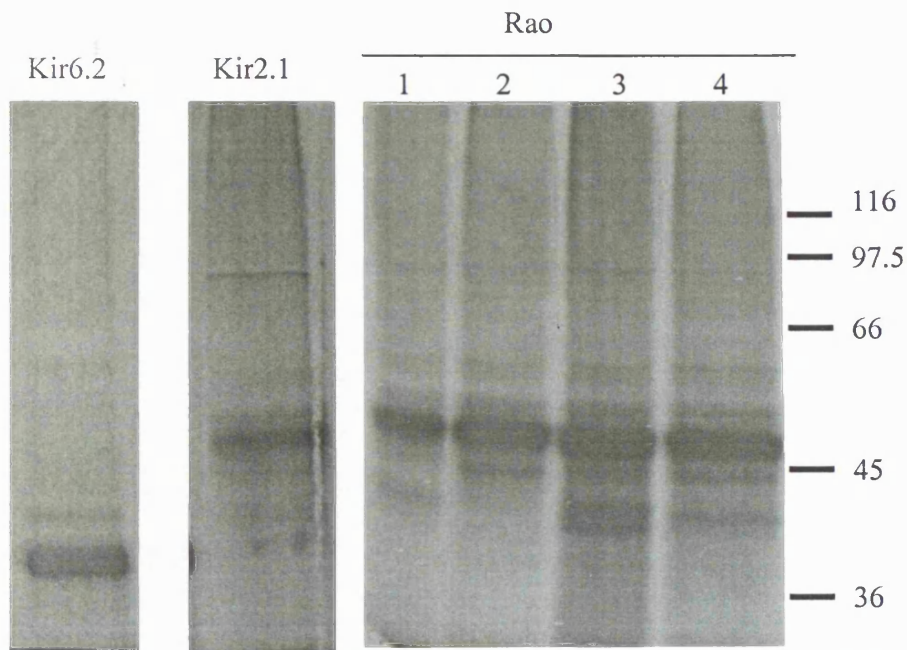


**Figure 7-1** *In vitro* translated [<sup>35</sup>S]methionine-labelled Kir6.2, Kir2.1 and Rao chimaeras. A, Schematic diagram for Rao chimaeras showing the removal of the FLAG-tag from the C-terminal and showing the full length of Kir6.2 and Kir2.1. The amino acid sequence for Kir6.2 present in each chimaeras is also shown. B, Autoradiograph showing electrophoretically separated [<sup>35</sup>S]methionine-labelled *in vitro* translated polypeptides on a denaturing 7.5% polyacrylamide mini-gel. The Kir6.2 was expressed using SP6 TNT<sup>®</sup>; Kir2.1 and Rao chimaeras were expressed using the T7 TNT<sup>®</sup> Quick-coupled transcription/translation kit (Promega) from cloned cDNAs. The [<sup>35</sup>S]methionine-labelled Kir6.2 polypeptide migrated with an apparent molecular weight of 38kDa but Kir2.1 and the Rao chimaeric polypeptides migrated with apparent molecular weights of 48 kDa. Representative experiment (n =2).

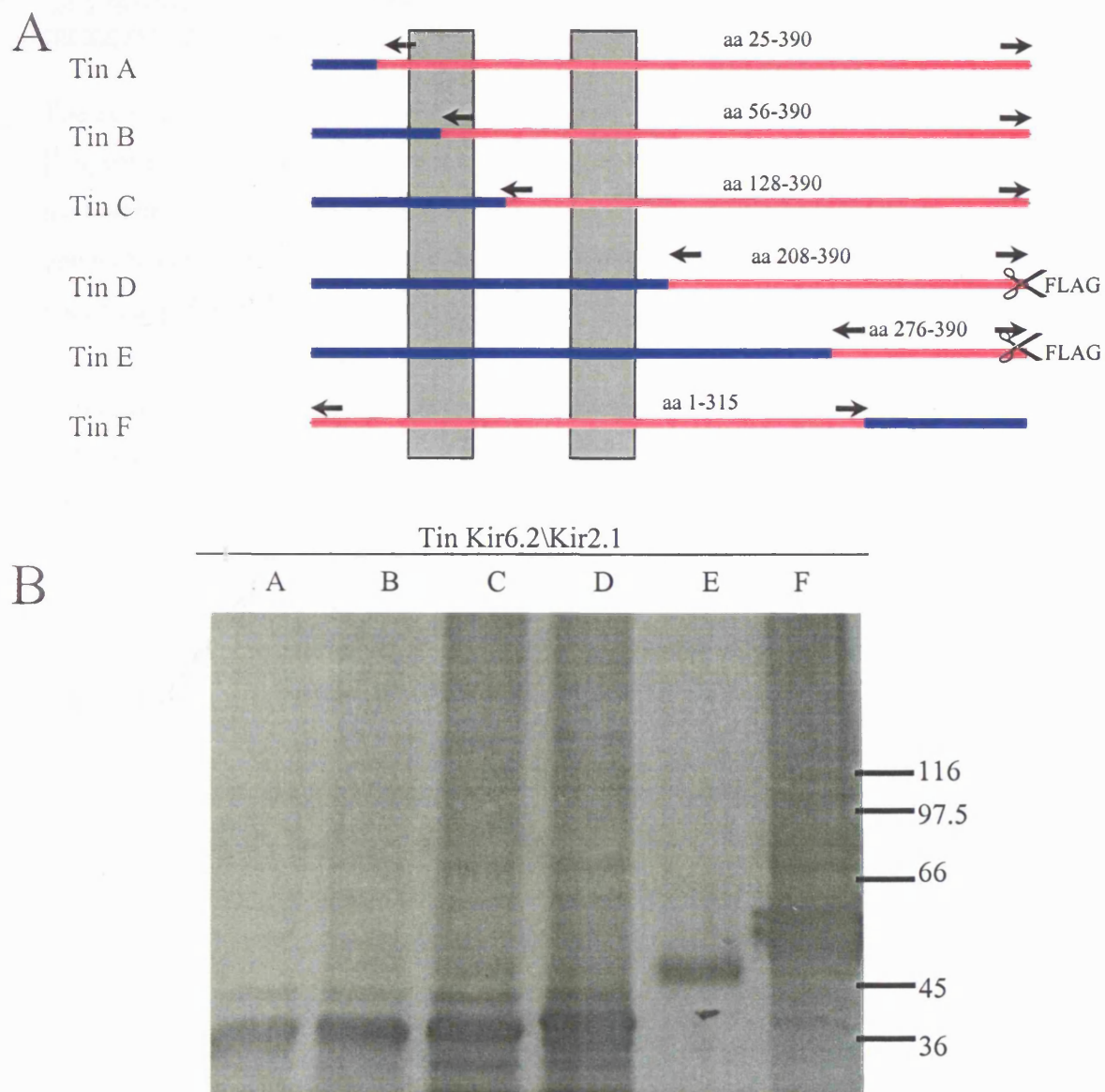


**Figure 7-2 *In vitro* translated [<sup>35</sup>S]methionine labelled Tin chimaeras.**

A, Schematic diagram for Tin chimaeras showing the removal of the FLAG-tag from the C-terminal of TinD and TinE. The amino acid sequence for the Kir6.2 present in each chimaeras is shown for each construct. B, Autoradiograph showing electrophoretically separated [<sup>35</sup>S]methionine-labelled *in vitro* translated polypeptides on a denaturing 7.5% polyacrylamide mini-gel. The Tin chimaeras were expressed using T7 TNT<sup>®</sup> Quick-coupled transcription/translation kit (Promega) from cloned cDNAs. The [<sup>35</sup>S]methionine labelled polypeptides migrated with different molecular weights TinA, TinB, TinC, and TinD with approximate molecular weight of 38KDa, TinE of 46KDa and TinF of 48KDa. Representative experiment (n =2).

### 7.3-Characterization of the immunoprecipitation of Kir6.2/Kir2.1 chimaeras with the corresponding antibody

The expression of the Kir6.2/Kir2.1 chimaeras was verified by immunoprecipitation of the [<sup>35</sup>S]methionine-labelled Kir6.2/Kir2.1 polypeptides with the corresponding antiserum to the C-terminal of each chimaera. For each chimaera, two different reactions were set up, one with anti-Kir6.2 antiserum and another with anti-Kir2.1 antiserum to determine the specificity of immunoprecipitation of each chimaera.

Immunoprecipitation of chimaeras containing a C-terminal tag was unachievable. It was not possible to immunoprecipitate Rao 1, Rao 2, Rao 3, Rao 4, Tin D, and Tin E with either antisera (results not shown). The inability of the antisera to immunoprecipitate Kir6.2/Kir2.1 chimaeras tagged on the C-terminal suggested that the presence of C-terminal FLAG was probably blocking the epitope from the antibody, thereby preventing the immunoprecipitation of the chimaeras. In these cases a modification was made to remove the tag to reveal the WT-C-terminal.

After the modification of these chimaeras, immunoprecipitations of [<sup>35</sup>S]methionine-labelled polypeptides were performed using the antisera-Kir6.2 and antisera-Kir2.1. Specific immunoprecipitation of [<sup>35</sup>S]methionine-labelled Kir6.2 and Kir2.1 proteins were shown only when the antisera specific for the appropriate C-terminal domain present. Immunoprecipitation of Rao1, Rao 2, Rao 3, Rao 4, Kir2.1 and Tin F was achieved using anti-Kir2.1 and immunoprecipitation of Tin A, Tin B, Tin C, Tin D, Tin E and Kir6.2 with anti-Kir6.2 as expected. No immunoprecipitation was seen with the opposite antibody, indicating the specificity of the immunoprecipitation in each case (Figures 7-3 and 7-4).

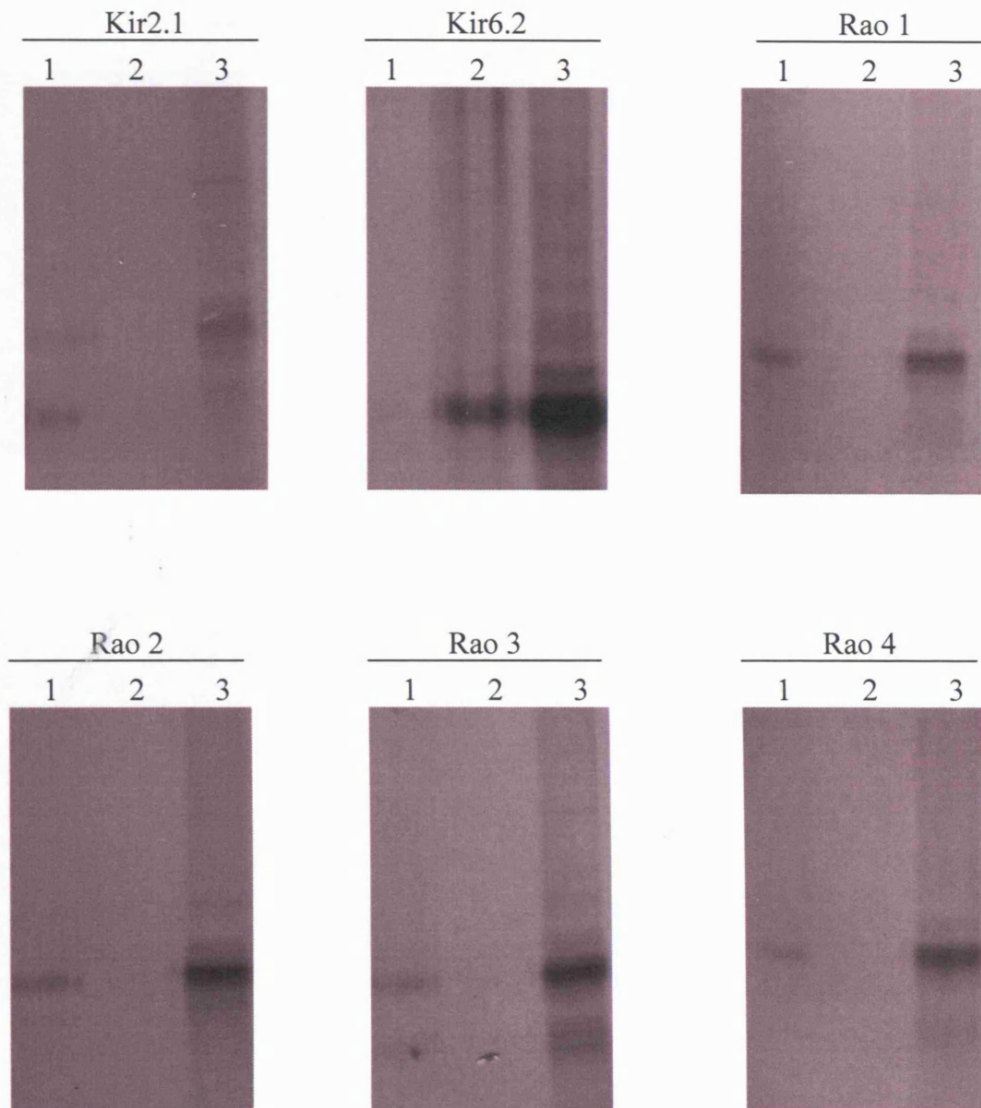


**Figure7-3 Immunoprecipitation of [<sup>35</sup>S]methionine-labelled *in vitro* translated Kir6.2, Kir2.1 and Rao polypeptides.** Immunoprecipitated fractions were electrophoresed on a 7.5 % polyacrylamide mini-gel. The immunoprecipitation of *in vitro* translated [<sup>35</sup>S]methionine-labelled polypeptides was with (lane 1) anti-Kir2.1, (lane 2) anti-Kir6.2. Lane 3, a direct load of 5  $\mu$ l [<sup>35</sup>S]methionine-labelled Kir polypeptide. The immunoprecipitation of [<sup>35</sup>S]methionine-labelled polypeptide shows Rao 1, Rao 2, Rao 3, Rao 4 and Kir2.1 immunoprecipitated with anti-Kir2.1, whereas Kir6.2 was immunoprecipitated with anti-Kir6.2. Representative experiment (n = 2).

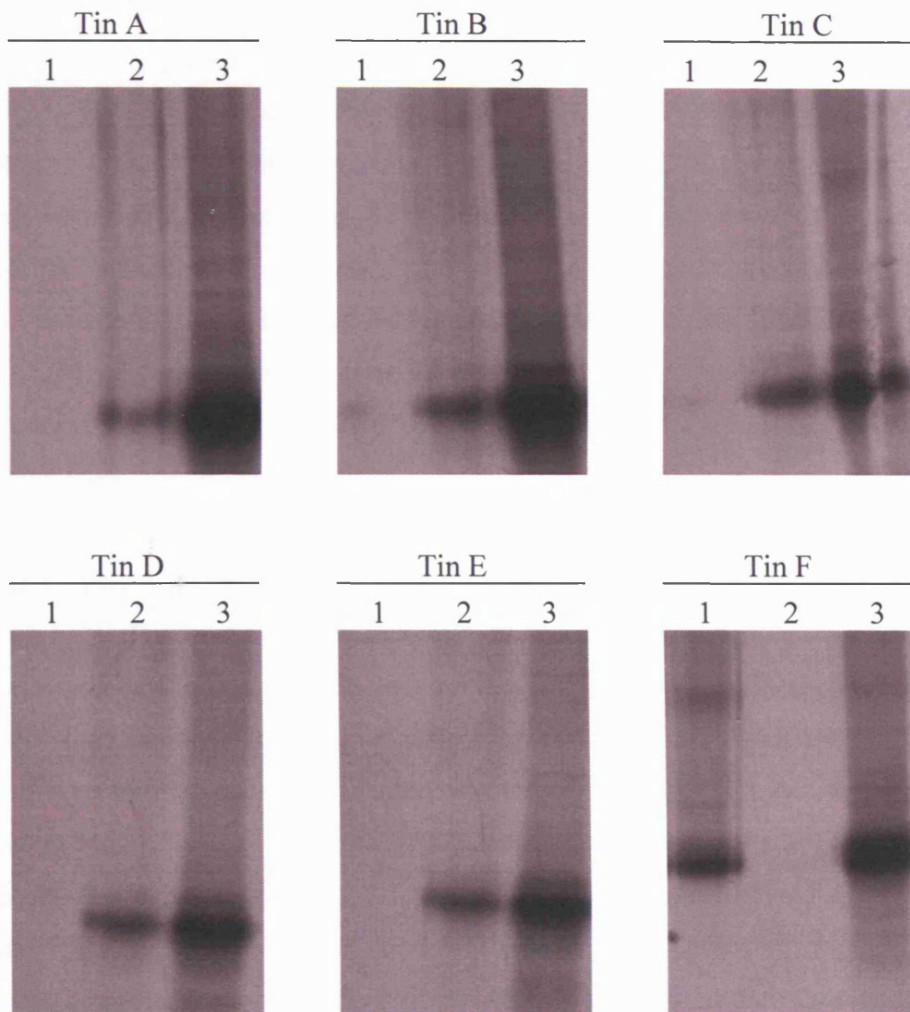


**Figure7-4 Immunoprecipitation of [<sup>35</sup>S]methionine-labelled *in vitro* translated Tin chimaeras.** The immunoprecipitation of *in vitro* translated [<sup>35</sup>S]methionine-labelled polypeptides was (lane 1) with anti-Kir2.1, (lane 2) anti-Kir6.2 Lanes 2, and (lane 3) a direct load of 5 μl [<sup>35</sup>S]-methionine labelled Kir polypeptides. The immunoprecipitation of [<sup>35</sup>S]-methionine labelled polypeptide shows TinA, TinB, TinC, TinD and TinE immunoprecipitated with anti-Kir6.2, whereas TinF was immunoprecipitated with anti-Kir2.1. Representative experiment (n = 2).

#### 7.4- Co-immunoprecipitation of the interacting fragment MBP-rSUR2A-CT-C and the non-interacting fragment MBP-rSUR2A-CT-D with Kir6.2/Kir2.1 chimaeras

Co-immunoprecipitation experiments were conducted to investigate the binding site of the rSUR2A-CT-C fragment on Kir6.2 using the Kir6.2/Kir2.1 chimaeras. As has been shown in chapter 4, the co-immunoprecipitation of rSUR2A-CT-C fragment with full-length Kir6.2 from mixtures containing [<sup>35</sup>S]methionine-labelled *in vitro*-translated subunits using anti-Kir6.2 subunit antiserum was established. This co-immunoprecipitation technique was used to screen for interaction between interacting fragment, rSUR2A-CT-C, and the panel of Kir6.2/Kir2.1 chimaeras to define the binding site of this fragment in the Kir6.2 subunit. The interacting fragment rSUR2A-CT-C was co-immunoprecipitated with five of the chimaeras containing the C-terminal of Kir6.2, Tin A (aa 25-390), Tin B (aa 56-390), Tin C (aa 128-390), Tin D (aa 208-390), Tin E (aa 276-390), and the full length of the Kir6.2 (aa 1-390) (Figure 7-5). Under the same conditions, the other chimaeras, Rao 1 (aa 1-65), Rao 2 (aa 1-112), Rao 3 (aa 1-140), Rao 4 (aa 1-179), Tin F (aa 1-315), and the full length of Kir2.1 were not able to co-immunoprecipitate the rSUR2A-CT-C fragment. A similar result was obtained when the amount of the expressed protein from Rao chimaeras and Kir2.1 were double in these reactions. In addition, control reactions were included, where the fragment MBP-rSUR2A-CT-C was incubated with anti-Kir6.2 or anti-Kir2.1 antisera in the absence of Kir6.2/Kir2.1 chimaeras to investigate the non-specific binding of the fragment to the precipitating immunomatrix and the fragment did not show any binding. As a negative control the non-interacting fragment SUR2A-CT-D, which showed reduced binding with the full length of Kir6.2 (section 4.1.4), was tested with the chimaeras. All of the chimaeras showed no significant binding with MBP-rSUR2A-CT-D (aa 1358-1545), although there was a small amount of co-immunoprecipitation of the fragment with some chimaeras; the chimaeras containing the C-terminal of Kir6.2, Tin A (aa 25-390), Tin B (aa 56-390), Tin C (aa 128-390), Tin D (aa 208-390), Tin E (aa 276-390), and the full length of the Kir6.2 (aa 1-390), but the binding was reduced compared to that of the SUR2A-CT-C fragment (Figure 7-5).

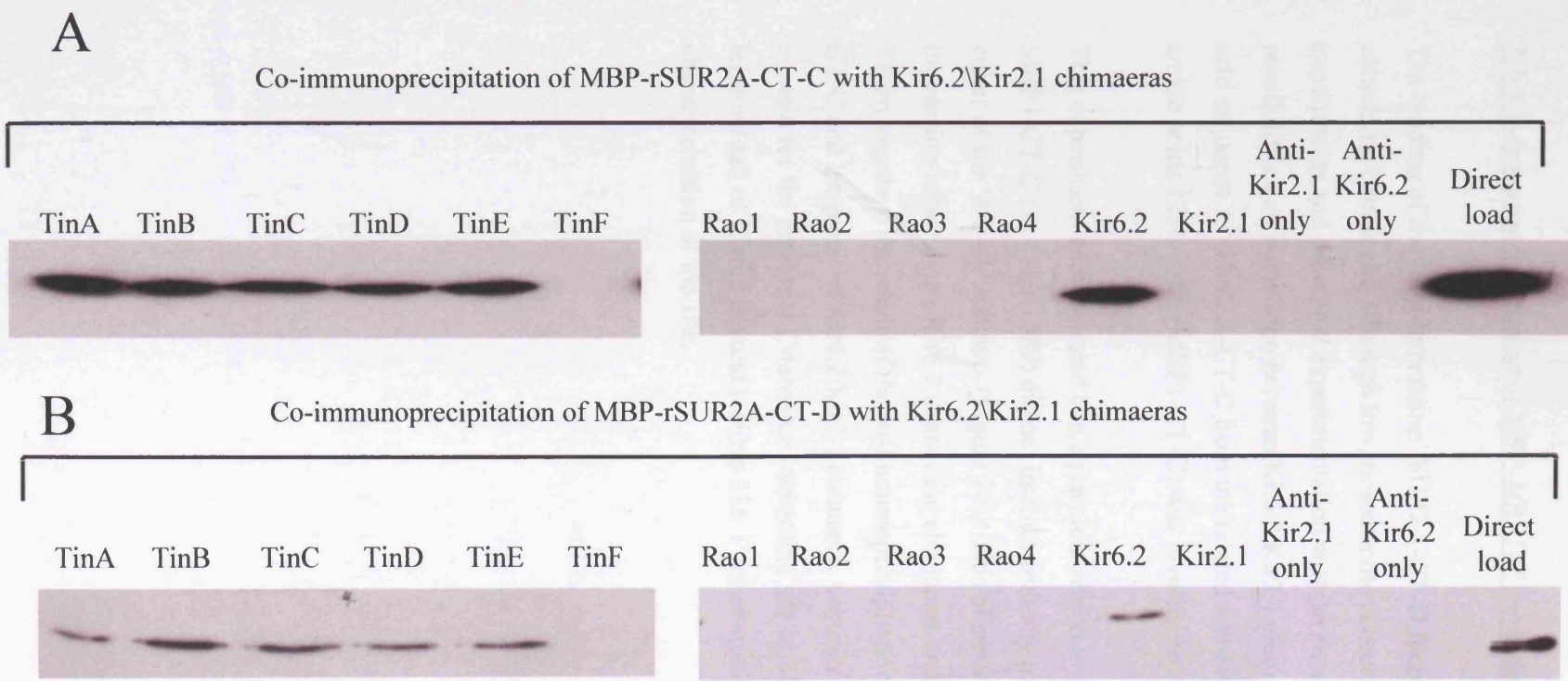


**Figure 7-5 Co-immunoprecipitation of MBP-SUR2A-CT-C and MBP-rSUR2A-CT-D fragments with WT-Kir subunits and Kir6.2/Kir2.1 chimaeras.** A, ECL-film exposure of a Western blot stained with mouse anti-MBP IgG as primary antibody and anti-mouse IgG-HRP as secondary antibody. The co-immunoprecipitation of MBP-rSUR2A-CT-C with TinA, TinB, TinC, TinD, TinE and Kir6.2 and the co-immunoprecipitation of the fragment was compared with the direct load of (0.006  $\mu\text{g/ml}$ ) MBP-rSUR2A-CT-C polypeptide. B, Shows the absence or much lower co-immunoprecipitation of MBP-rSUR2A-CT-D with any of the Kir6.2/Kir2.1 chimaeras or the full length of Kir6.2 or Kir2.1, which was compare with the direct load of the fragment in 7.5% SDS-PAGE.

### 7.5- Co-immunoprecipitation of MBP-MRP1-C using the Kir6.2/Kir2.1 chimaeras

The binding of the 'non-interacting' SUR2A-CT-D fragment with Kir6.2 C-terminal containing chimaeras, although low, raised some concern over the negative control in these experiments and prompted experimentation with an alternative. For this reason, the possibility of an interaction between Kir6.2/Kir2.1 chimaeras with an equivalent amino acid sequence to rSUR2A-CT-C from the related non-interacting polypeptide MRP1, amino acids 1280-1389 (MRP1-CT-C) was investigated.

This experiment demonstrated that equivalent region to r SUR2A-CT-C (aa 1294-1403) in MRP1-CT-C (aa 1280-1389) did not interact with any of the Kir6.2/Kir2.1 chimaeras or either of the WT-Kir subunits (Figure 7-6). This observation confirmed the specific interaction between the Kir6.2 containing chimaeras and the SUR2A-CT-C fragment. Taken together, the result of the co-immunoprecipitation experiment with MBP-rSUR2A-CT-C and the panel of Kir6.2/Kir2.1 chimaeric subunits demonstrated that the binding domain for the proximal C-terminal interacting site in SUR2A is located within the C-terminal tail of Kir6.2 beyond residue 315. Further studies are required to refine the characterisation of the site.

Co-immunoprecipitation of MBP-MRP1-CT-C with Kir6.2/Kir2.1 chimaeras

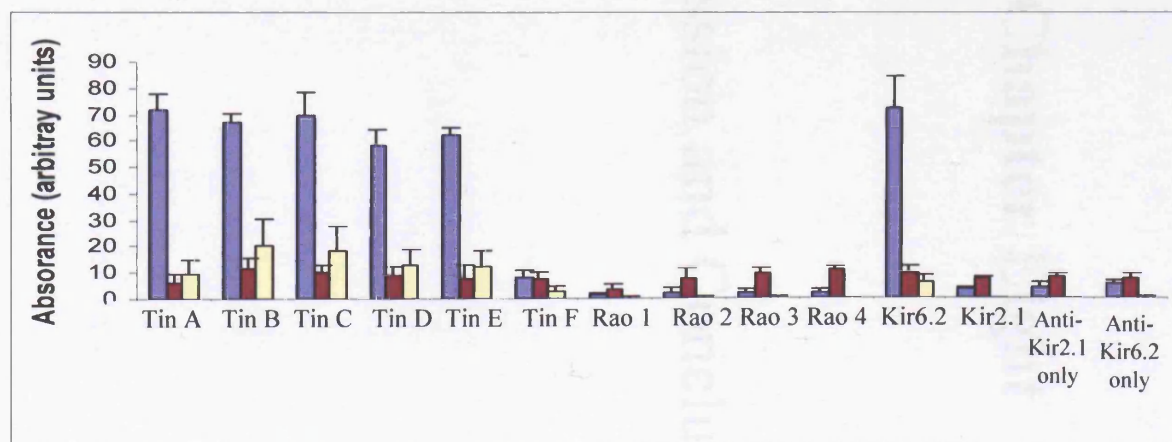
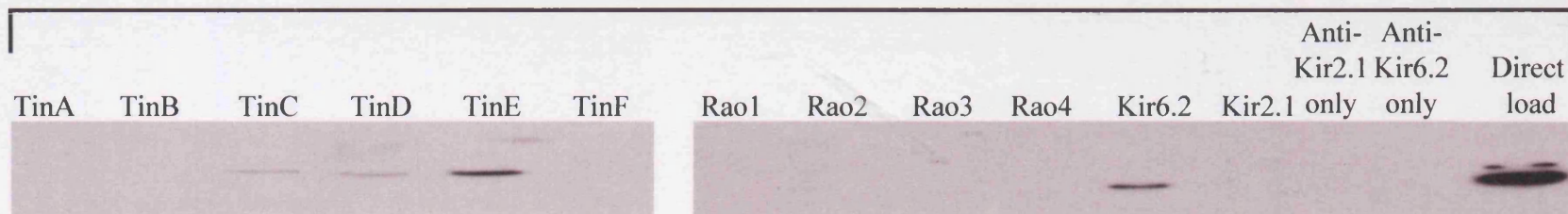


**Figure 7-6 Co-immunoprecipitation of MBP-MRP1-CT-C fragment with WT-Kir subunits and Kir6.2/Kir2.1 chimaeras.** A, ECL-film exposure of a Western blot stained with mouse anti-MBP IgG as primary antibody and anti-mouse IgG-HRP as secondary antibody, which shows the absence of co-immunoprecipitation of MBP-MRP-CT-C with any of the Kir6.2/Kir2.1 chimaeras or the full length Kir6.2 or Kir2.1 subunits, compared with the direct load of the fragment in 7.5% SDS-PAGE. B, Histogram representing mean  $\pm$  SEM of the amount of co-immunoprecipitation estimated by densitometry of anti-MBP stained band (N=3) of MBP-rSUR2A-CT-C (blue), MBP-MRP1-CT-C (purple) and MBP-rSUR2A-CT-D (yellow).

# **Chapter Eight**

## **Discussion and Conclusion**

### 8.1.1- Identification of a Kir6.2 binding site in the C-terminal of SUR2A by biochemical assay

The  $K_{ATP}$  channel in the cell surface of cardiomyocytes comprises four Kir6.2 subunits and four SUR2A subunits (Clement et al., 1997; Inagaki et al., 1997; Shyng and Nichols, 1997). Kir6.2 subunits contain two transmembrane segments M1 and M2, with a P-loop between them that forms the outer mouth of the pore (Aguilar-Bryan and Bryan, 1999). The N- and C-termini of the Kir6.2 subunit are located on the cytoplasmic side of the sarcolemma, as is the C-terminal domain of the SUR2A subunit (Bryan and Aguilar-Bryan, 1999). Assembly of the Kir6.2 and SUR2A subunits is necessary to form a functional channel (Clement et al., 1997; Inagaki et al., 1997; Shyng and Nichols, 1997). Although the masking of the RKR sequence in the C-terminal of Kir6.2 and in the NBF1 of SUR2A is necessary for  $K_{ATP}$  channel expression in the cell membrane (Zerangue et al., 1999), it is not the only requirement for  $K_{ATP}$  channel assembly. The transmembrane domains (TMDs) of the SUR2A subunit play an important role in channel expression in the cell membrane; the exchange of the TMDs of SUR2A with the equivalent TMDs from MRP1 can disrupt the channel assembly (Zerangue et al., 1999).

It was hypothesised that, in addition to domains located within the membrane bilayer which are important for assembly (Zerangue et al., 1999; Schwappach et al., 2000), cytoplasmic domains of the sulphonylurea receptor containing the nucleotide-binding folds make direct contact(s) with cytoplasmic N- and/or C-terminal domains in the pore-forming Kir6.0 subunits of  $K_{ATP}$  channels. Such contacts may allow the transfer of regulatory allosteric information between SUR and Kir6.0 subunits.

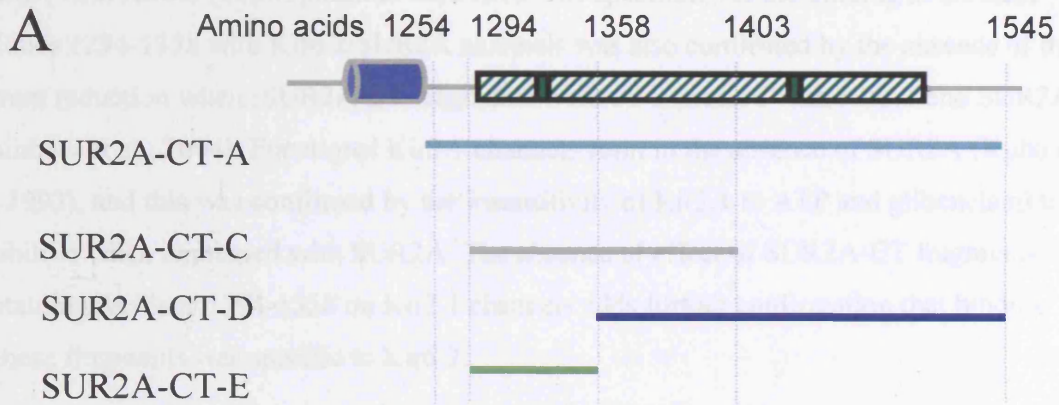
This study identified a novel cytoplasmic region in the proximal C-terminal domain of the SUR2A subunit, located between residues 1294 and 1358, which forms a direct interaction with the full-length Kir6.2 subunit. The region of interaction was determined using protein fragments of SUR2A fused to maltose binding proteins and then tested for their co-immunoprecipitation with full-length *in vitro* expressed Kir6.2 subunit. Three of the MBP-SUR2A fragments containing residues 1294-1358 (MBP-rSUR2A-CT-A, MBP-rSUR2A-

CT-B and MBP-rSUR2A-CT-C) showed binding with the full length of Kir6.2. At the same time, the fourth fragment (MBP-rSUR2A-CT-D), corresponding to the distal C-terminal domain of SUR2A, did not show binding. Kir2.1 expresses fully functional channels in the absence of associated accessory sulphonylurea receptor subunits. Therefore as a negative control, the binding of the interacting fragments and other fragments was investigated in the presence of Kir2.1 in place of Kir6.2 using anti-Kir2.1 antiserum for immunoprecipitation. None of the SUR2A-CT fragments showed binding with Kir2.1. This result confirmed the specificity of the interaction of the binding region 1294-1358 to the Kir6.2 subunit.

To further confirm the specificity of interaction of the SUR2A 1294-1358 binding region, the binding of an equivalent region (MRP1-CT-E) from the non-interacting multidrug resistance-associated protein 1 (MRP1) was tested with the Kir6.2 subunit. In co-immunoprecipitation experiments, the MRP1-CT-E fragment showed no binding with Kir6.2, which confirmed the specificity of the binding of the SUR2A fragments containing the binding region 1294-1358. The identified 65-amino-acid sequence between residues 1294 and 1358 in SUR2A is located over the proximal part of NBF2 within the C-terminal domain and contains the Walker A motif (Inagaki et al., 1996).

#### 8.1.2- Effect of the binding fragment on Kir6.2/SUR2A channel function

In studies carried out in parallel to those conducted in this thesis (Rainbow et al., 2004), the interaction of the binding fragments from SUR2A with Kir6.2/SUR2A channels were shown to have an important effect on the function of Kir6.2/SUR2A. When fragments containing residues 1294-1358 were co-transfected into HEK-293 cells stably expressing Kir6.2/SUR2A hetero-oligomers, a dramatic reduction in ATP- and glibenclamide-sensitive  $K_{ATP}$  channel current was observed (Rainbow et al., 2004) (Figure 8-1). The equivalent amino acid sequence from the non-interacting MRP1 (MRP1-CT-E) corresponding to the binding site in SUR2A (rSUR2A-CT-E aa 1294-1358) showed no reduction in the currents conducted by the Kir6.2/SUR2A channels. The MRP1-CT-E fragment corresponded to the minimal interacting sequence of rSUR2A-CT-E found in the



**B**

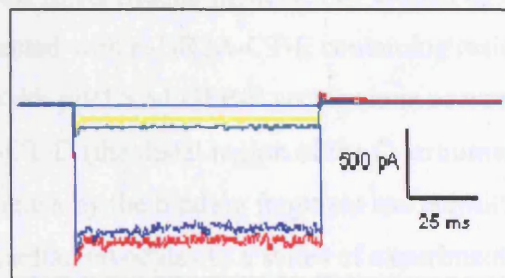


**Figure 8-1 Current recording of  $K_{ATP}$  channels in the presence of SUR2A-CT fragments.** A, shows the C-terminal fragments used in cell physiology experiments. B, Raw current traces (overlaid) from inside-out patches from HEK-293-transfected cells elicited by a square-wave pulse from 0 mV (approx.  $E_K$ ) to  $-80$  mV for 100 ms at 1 Hz, (■)SUR2A-CT-A, (□) SUR2A-CT-C, (■) SUR2A-CT-E, (■)SUR2A-CT-D and (■) pIRES-FGFP-F (taken from Rainbow et al., 2004).

ABC transporter (ATP-binding-cassette transporter-protein) MRP1, which is known not to interact with Kir6.2 (Schwappach et al., 2000). The specificity of the binding of SUR2A residues 1294-1358 with Kir6.2/SUR2A channels was also confirmed by the absence of the current reduction when rSUR2A-CT fragments were co-expressed with Kir2.1 and SUR2A (Rainbow et al., 2004). Functional Kir2.1 channels form in the absence of SUR2A (Kubo et al., 1993), and this was confirmed by the insensitivity of Kir2.1 to ATP and glibenclamide inhibition when expressed with SUR2A. The absence of effect of SUR2A-CT fragments containing residues 1294-1358 on Kir2.1 channels adds further confirmation that binding of these fragments was specific to Kir6.2.

In a subsequent study, Rainbow et al (2004,b) showed a reduction in the surface expression of functional sarcK<sub>ATP</sub> channels in ventricular myocytes by around 85%, measured 2 days after transfection, when transfected with rSUR2A-CT-E containing residues 1294-1358 compared to cells transfected with pIRES2-EGFP-F vector alone or with the non-interacting fragment rSUR2A-CT-D (the distal region of the C-terminus residue 1358-1545). Disruption of K<sub>ATP</sub> channels by the binding fragment has permitted targeted K<sub>ATP</sub> channel knockout in isolated cardiac myocytes in a series of experiments to investigate the contribution of sarcolemmal K<sub>ATP</sub> (sarcK<sub>ATP</sub>) channels to protective responses to metabolic poisoning. In control cells subjected to metabolic inhibition, ATP levels fall resulting in activation of K<sub>ATP</sub> channels. This leads to action potential shortening associated with membrane hyperpolarisation. Transfection of the binding fragment rSUR2A-CT-E reduced sarcK<sub>ATP</sub> channel activity and delayed action potential shortening (Rainbow et al., 2004). This knockout of functional sarcK<sub>ATP</sub> channels resulted further in delayed contractile failure but accelerated passage into rigor due to increased cytoplasmic free Ca<sup>2+</sup> concentration. Expression of the active fragment also reduced the number of cells able to recover from metabolic poisoning and abolished the protective effect of pre-treatment with 2,4-dinitrophenol, suggesting an important role for the sarcK<sub>ATP</sub> channels in cardioprotection (Rainbow et al., 2004b).

These results are also in agreement with the findings of Suzuki et al. (2002) in Kir6.2 knockout mice, where the damaging effects of ischaemia and reperfusion were exacerbated

and protection by ischaemic preconditioning was abolished.

#### 8.1.3- Effect of the binding fragment SUR2A-CT-E on the subcellular localization of Kir6.2/SUR2A channels using confocal microscopy

Immunocytochemistry was employed to investigate whether the reduction of the Kir6.2/SUR2A current in the presence of the interacting rSUR2A-CT fragments containing residues 1294-1358 was caused by disruption of channels on the cell surface or by a lowering of the surface expression of the channels. This was investigated in HEK293 cells stably expressing Kir6.2 and SUR2A subunits and transiently transfected with the rSUR2A-CT fragments. It was found that cells transfected with rSUR2A-CT fragments containing the amino acid residues 1294-1359 showed a significant decrease of Kir6.2 and SUR2A subunit-associated immunofluorescence at the plasma membrane and increased intracellular fluorescence compared with cells transiently transfected with an empty pIRES2-EGFP-F vector or the non-interacting fragment rSUR2A-CT-D. The reduction of cell-surface labelling in the presence of an interacting fragment indicated that the decreased current density was caused by decreasing numbers of channel oligomers and not by the disruption of channel hetero-oligomers within the plasma membrane.

#### 8.1.4- Truncation of the Kir6.2 binding site in NBF2 of SUR2A (rSUR2A-CT-C)

The truncation of the binding fragment (rSUR2A-CT-C) to further localize the binding site within a smaller region using biochemical assay was unsuccessful. It was not possible to produce sufficient tagged polypeptide from the MBP-rSUR2A-CT-E construct to perform the biochemical assay; as was the case for MBP-SUR2A-CT-F, eleven amino acids shorter than MBP-SUR2A-CT-E at the C-terminal. The eleven amino acids at the end of the rSUR2A-CT-E are thought to play a role in the binding with full-length Kir6.2. These assumptions are built on the finding that MBP-rSUR2A-CT-E, MBP-SUR2A-CT-F and MBP-SUR2A-CT-G all failed to show binding with Kir6.2. A potentially co-immunoprecipitation in these experiments was made more difficult by the low amounts of

the tagged polypeptides available, although it was possible to add MBP-rSUR2A-CT-G within the normal working concentration.

To confirm the absence of interaction of the truncated fragments rSUR2A-CT-G and rSUR2A-CT-F with Kir6.2 it was considered important to investigate possible disruption of channel assembly in the immunofluorescence cell surface expression assay in HEK cells expressing Kir6.2/SUR2A channels. Both rSUR2A-CT-F and rSUR2A-CT-G failed to show any effect on the Kir6.2/SUR2A channel assembly. The tentative conclusion drawn from this experiment was that the last eleven amino acids in rSUR2A-CT-E play an important role in the binding of SUR2A-CT with the Kir6.2 subunit or somehow contributes to the binding site. It is possible that rather than removing part of a binding motif, removal of the C-terminal 11 amino acids from rSUR2A-CT-E, disrupted the structure of the resulting fragment thereby preventing interaction. Therefore, in order to investigate whether overall structure of the fragment was important, the eleven amino acids from the C-terminal of rSUR2A-CT-E were removed and added to MRP1-CT-F to make MRP1-CT-F/rSUR2A-CT-E (aa 1349-1359). The new construct (MRP1-CT-F/rSUR2A-CT-E) showed no binding with full-length Kir6.2 with the biochemical assay experiment. This suggests that the C-terminal of rSUR2A-CT-E does not contain the binding site of Kir6.2. The eleven amino acids may help to form the three-dimensional structure for the binding site or be necessary for the stability of the fragment.

The bioinformatics tools available at the NCBI Structure web site (<http://www.ncbi.nlm.nih.gov/Structure/CN3D/cn3d.shtml>) were used to examine the three-dimensional modelling of rSUR2A-CT-E against the template of a bacterial nucleotide-binding protein MalK (Bohm et al., 2002) with homologous structure to the nucleotide-binding folds in SUR subunits. The structure of regions of sequence in MalK that were equivalent to those of the interacting rSUR2A-CT-E fragment were highlighted to model the potential structure of rSUR2A-CT-E. The structure showed that the SUR2A-CT-E fragment models as  $\beta$ -pleated sheet located on the surface of NBF2, with the last eleven amino acids forming an alpha helix which is embedded in the structure and thus inaccessible to form interaction with Kir6.2 (Figure8-2).

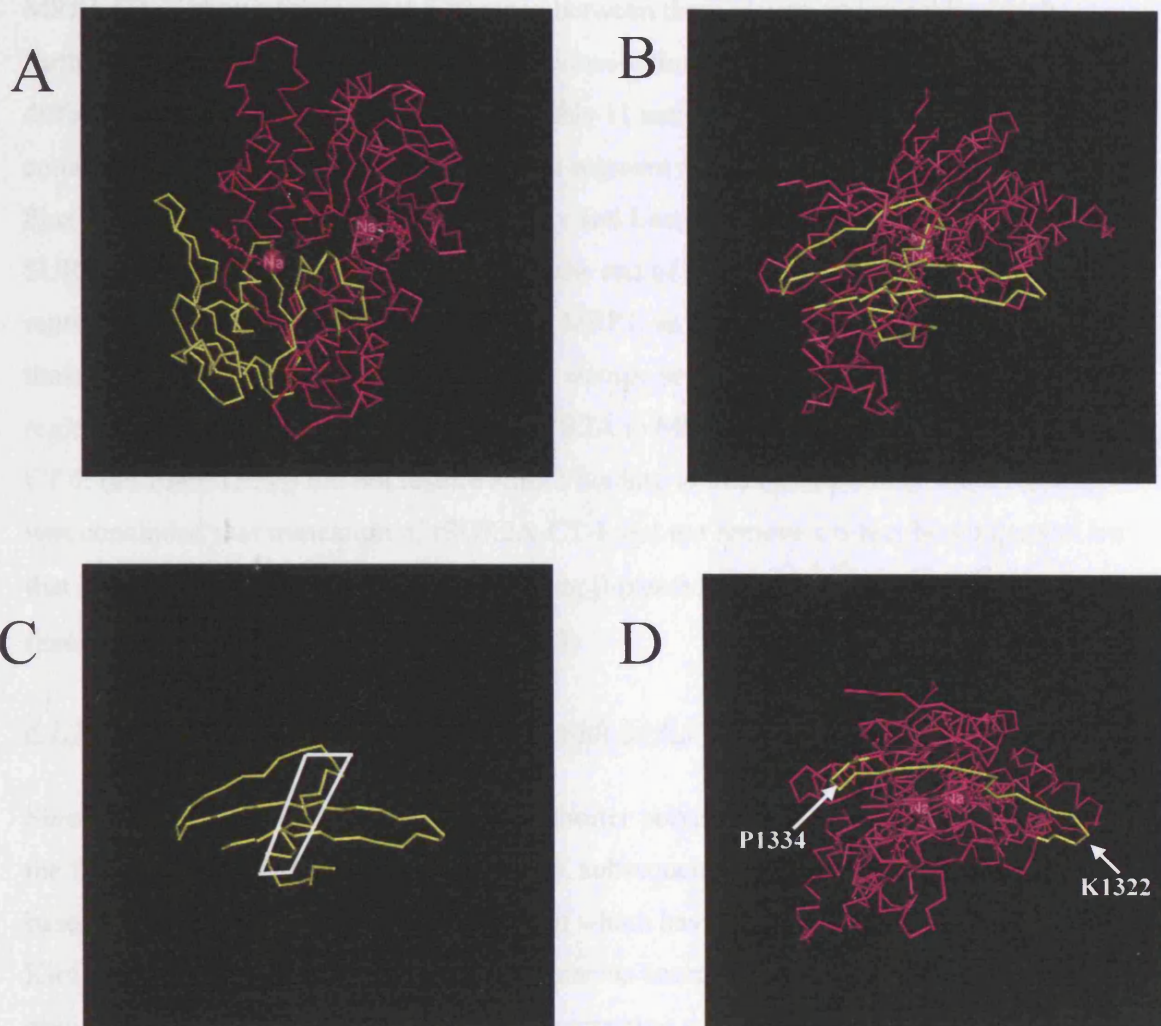


**Figure 8-2** Three dimensional modelling of the Kir6.2 binding motif in the proximal C-terminal domain of rSUR2A using the crystal structure of MalK as template. The region equivalent to rSUR2A-CT-E sequence in the published MalK (MJ0796) structure was highlighted (highlighted in yellow). A, shows the surface orientation of the sequence equivalent to the large interacting fragment rSUR2A-CT-C on the MalK NBF dimer structure. B. shows the position of the minimal rSUR2A-CT-E fragment (highlighted in yellow) within the MalK NBF monomer structure. C, Isolated SUR2A-CT-E structure prediction highlighting  $\alpha$ -helix structure of the last eleven amino acids in the SUR2A-CT-E, which when removed resulted in a loss of Kir6.2 binding activity (box). D. shows the 20 amino acid Kir6.2 binding motif identified in the SUR2A/MRP1 chimaera experiments that maps to the surface of the NBF structure. Amino acids of potential importance in defining the binding motif P1334 and K1322 are indicated by arrows.

In addition, the amino acid alignment of SUR2A-CT-C and the equivalent sequence from MRP1-CT-C showed a minimal difference between these eleven amino acids, which further suggested a low possibility of their contribution to the binding motif. All the differences between SUR2A and MRP1 in this 11 amino acid sequences were relatively conservative of the overall properties of this segment of sequence. Ala(1354) and Phe(1355) in SUR2A are represented by Gly and Leu, respectively, in MRP1. In addition, SUR2A Met(1358) and Val(1359) towards the end of the eleven amino acid segment are represented by Ile and Asn, respectively, in MRP1, as underlined in the figure 8-3. None of these differences would result in significant change in overall charge properties in this region. Adding the 11 amino acids from SUR2A to MRP1-CT-F (MRP1-CT-F/rSUR2A-CT-E (aa 1349-1359)) did not restore Kir6.2 binding to this construct. For these reasons, it was concluded that truncation of rSUR2A-CT-E did not remove a direct binding motif but that it disturbed the structure of the remaining  $\beta$ -pleated sheet in the interaction domain by removing the underlying  $\alpha$ -helix (Figure 8-3).

#### 8.1.5- Binding of SUR2A/MRP1 chimaeras with Kir6.2

Since the truncation of SUR2A-CT-C to a shorter polypeptide weakened the interaction of the fragment with Kir6.2 *in vitro* expression, subsequent experiments were carried out based in the longer rSUR2A-CT-C fragment which has a higher apparent affinity for Kir6.2. Construction of SUR2A/MRP1 chimaeras based on rSUR2A-CT-C were an obvious way to further test the location of interacting structures, while at the same time producing three dimensional supports to the fragment constructs. Based in this idea, four SUR2A/MRP1 chimaeras constructs were made, also the full-length of rSUR2A-CT-C and the full-length of MRP1-CT-C were used as a positive and negative controls, respectively. Two of the SUR2A/MRP1 chimaeras containing residues 1318-1337 from SUR2A (MBP-MRP1(25) SUR2A and MBP-SUR2A(45)MRP1) and the full length of SUR2A-CT-C showed binding with the full length of Kir6.2 in co-immunoprecipitation experiments. At the same time, two of the SUR2A/MRP1 chimaeras containing the equivalent residues from MRP1 (MBP-MRP1(45)/SUR2A and MBP-SUR2A(25)MRP1) and the full length of MRP1-CT-C did not show binding. In conclusion, the direct interacting site localized between residues (1318-1337) in rSUR2A.



In this experiment, the non-specific binding of the chimaeras in the absence of the full length of Kir6.2 (in the control track) was higher than that observed in earlier studies. Although the expression levels of the chimaeras was high enough to allow the co-immunoprecipitation experiment to be performed, it may be that the folding of the chimaeras did not reflect the nature of the wild type SUR2A subunit in all cases. The binding of SUR2A-CT-C and MRP1(25)SUR2A to Kir6.2 was higher than the non-binding polypeptide MRP1-CT-C ( $P < 0.05$  and  $P < 0.1$ , respectively), suggesting that the binding motif was located beyond the first 25 amino acids in SUR2A-CT-C. The absence of binding of MRP1-CT-C, MRP1(45)SUR2A, SUR2A(25)MRP1 all suggested that sequence beyond residue 45 was also not involved in the binding motif, consistent with localisation of the binding motif in the region between residues 26 and 45. In this case, SUR2A(45)MRP1 would have been predicted to interact with Kir6.2. Although total binding of SUR2A(45)MRP1 was slightly higher than the background binding of other non-interacting constructs (MRP1-CT-C, MRP1(45)SUR2A, SUR2A(25)MRP1) the difference was not statistically significant and prevented unequivocal demonstration of the importance of this domain in this experimental system.

To confirm the above observation, a HEK 293 cell line stably expressing Kir6.2 and SUR2A was used to investigate the effects of the SUR2A/MRP1-CT-C chimaera fragments on the surface targeting of functional Kir6.2/SUR2A channels. In electrophysiology experiments conducted by Dr. R. Rainbow (Cell Physiology and Pharmacology, Leicester) transient expression of SUR2A/MRP1-CT-C chimaeras containing SUR2A residues 1318-1337 resulted in a significant reduction in channel current density at the cell surface as seen with the rSUR2A-CT-C fragment, while constructs with MRP1 sequence in this position were without significant effect. This result further localized the Kir6.2 binding motif in SUR2A to residues 26-45 in rSUR2A-CT-C (1318-1337 in SUR2A).

The pharmacology of cells expressing Kir6.2/SUR2A channel alone or with transiently expressing of SUR2A/MRP1-CT-C chimaeras was studied to determine the effect of these chimaeras on the channel properties. In cells expressing Kir6.2/SUR2A alone or with

MRP1-CT-C, perfusion with 100  $\mu$ M pinacidil showed a significant increase in outward current in the whole cell patch, which was blocked by 10  $\mu$ M glibenclamide, indicating a normal  $K_{ATP}$  channel response (Rainbow et al., 2004). Similarly, cells stably expressing Kir6.2/SUR2A and transiently transfected with SUR2A(25)MRP1 or MRP(45)SUR2A, also showed pinacidil stimulation and glibenclamide blocking, indicating that co-expressed fragments were having no effect on channel function in these experiments. On the other hand, cells transfected with SUR2A-CT-C (see Rainbow et al., 2004) or with either SUR2A(45)MRP1 or MRP1(25)SUR2A showed significantly reduced current. However, the residual current was still activated by pinacidil and blocked by glibenclamide, indicating that the current reduction was due to a reduction in active channels, rather than a gross change in pharmacological properties.

From the biochemical and cell physiological studies we may conclude that SUR2A residues 1318-1337 present a weak binding with the full length of *in vitro* expressed Kir6.2 and a significant reduction in the channel current of Kir6.2/SUR2A, while those with the equivalent sequence from MRP1 did not, which further localises the Kir6.2 interaction site to this domain.

Using the SWISS-MODEL protein modelling software, the rSUR2A-CT-C sequence was modelled onto both the crystallographic co-ordinates of the nucleotide binding folds of bacterial MalK (MJ0796) (Bohm et al., 2002) and the cystic fibrosis conductance regulator (CFTR) (Bianchet et al., 1997) to help with understanding of the three dimensional structure for this region in SUR2A NBF2. As identified by the NCBI Structure web site (Figure 8-2,D), the modelling confirmed that the identified 20 amino acid binding motif in the rSUR2A-CT-C fragment (1318-1337) models on the surface of the NBF protein structure, forming a beta-pleated sheet which could be accessible for the Kir6.2 subunit to make an interaction (Campbell et al., 2004). On the basis that the Kir6/SUR interaction is likely to be common for different hetero-oligomer combinations (Rainbow et al., 2004b), it is predicted that residues involved in the interaction should be conserved in SUR1 and SUR2A but be dissimilar in MRP1. Sequences of rSUR2A-CT-C, MRP1-CT-C and the equivalent sequence from rSUR1 were aligned to identify residue similarities between

SUR1 and SUR2A and residues that differ between SUR2A and MRP1 (Figure 8.4). In addition, greater emphasis was given to charged residues, which could alter the surface charge characteristics of these two fragments. These alignments highlighted several amino acids that satisfied the above criteria as underlined in figure 8-3. Taking all the above factors into account the amino acid comparisons suggested E1318, K1322, P1334 and Q1335 as potential amino acids involved in the binding with Kir6.2. Of these, K1322 and P1334 map to the surface of predicted NBF structures.

#### 8.1.6- Binding of NBF1 fragment with Kir6.2

In addition to interaction of SUR2A NBF2, a possible interaction between the NBF1 of SUR2A and Kir6.2 was also investigated. As was the case in SUR2A NBF2, NBF1 also showed binding with the full length Kir6.2 subunit in co-immunoprecipitation experiments. Two of the fragments corresponding to the nucleotide binding fold 1, containing most of NBF1, including the Walker A and Walker B motifs (rSUR2A-NBF1-1, amino acid 683-873), and the C-terminal half of nucleotide binding fold 1 starting from the Walker B motif (rSUR2A-NBF1-2, amino acids 832-975) showed binding with the full length of Kir6.2, while the control reaction, rSUR2A-NBF1 fragment without Kir6.2 subunit, showed no binding. In these experiments, the amount of the tagged fragment was increased three times higher than in experiments with rSUR2A-CT fragments. This suggested that NBF1 shows binding to Kir6.2 but with less affinity than was observed in the case of the SUR2A-CT fragments. The binding site could be in the area shared by the fragments between amino acid residues 832 and 873. The present nature of the Kir6.2 interaction site in SUR2A remains to be localized, as does its cognate binding site in Kir6.2.

#### 8.2- Investigation of the cognate binding site for the proximal C-terminal domain of SUR2A on the Kir6.2 subunit using Kir6.2/Kir2.1 subunit chimaeras

Possible site(s) of interaction in the Kir6.0 subunit with SUR subunits have been investigated. Co-immunoprecipitation assays using Kir6.2 deletion mutants (Lorenz and

SUR2A	1297	MDPSQV	FEHWPQE	GEIKIHDL	CVRYENN	LKPV	LKHVKAY	IKPGQ	KVGI	CGRTGS	SGKSSL	SLAFFRMV	1363
SUR1	1330	LAPSLI	FKNWEDQ	GKIQIQNLS	VRYDSSL	LKPV	LKHVNALIS	PGQKIGI	CGRTGS	SGKSSF	SLAFFRMV	1396	
MRP1	1279	IQETAP	PSTWPHS	CRVEFRD	YCLRYRED	LDLVL	KHINVT	IEGGE	KVGI	VGRTGAG	GKSSLT	TLGLFRIN	1345

**Figure 8.4 Alignment of the rSUR2A-CT-E binding motif with SUR1 and MRP1 equivalents.** Sequences of rSUR2A-CT-C, MRP1-CT-C and the equivalent sequence from rSUR1 were aligned to identify residue similarities between SUR1 and SUR2A and residues that differ between SUR2A and MRP1 (blue) represent the similarity in all of them, (yellow) represent the similarity between the SUR1 and SUR2A, (green) represent similarity between any two sequence .

Terzic, 1999) or Kir6.2/Kir2.1 chimaeras (Giblin et al., 1999) and targeting assays with Kir6.2/Kir2.1 chimaeras (Hough et al., 2000) have suggested an important SUR interaction domain in the proximal C-terminus of Kir6.2 (see section 1.14). Deletion of the transmembrane domain TM2 and the proximal C-terminal domain of Kir6.2 prevented the association of SUR2A (Lorenz and Terzic, 1999). Similarly, the targeting of hetero-multimers of Kir6.2/SUR1 to the plasma membrane was prevented when a chimaeric Kir6.2/Kir2.1 construct containing the M2/proximal C-terminal domain of Kir2.1 in a background of Kir6.2 was expressed (Hough et al., 2000). Co-immunoprecipitation of various chimaeras of Kir6.2 and Kir2.1 with full-length SUR1 further localized a region of interaction in the proximal C-terminal domain of Kir6.2 between residues 208 and 279 (Giblin et al., 1999). Mutagenesis of K176 and K177 upstream in the proximal C-terminal domain of Kir6.2 prevented MgADP-dependent channel stimulation and sulphonylurea-induced inhibition of Kir6.2/SUR1 channels (John et al., 2001). This loss of allosteric regulation further implicated the proximal C-terminal of Kir6.0 subunits in SUR contacts.

The proximal C-terminal region, together with the M2 transmembrane segment, is also important in determining homotypic and heterotypic interactions between other Kir subunits (Tinker et al., 1996; Woodward et al., 1997; Koster et al., 1998; Minor et al., 1999) and represents an important region of biochemical contacts that could be associated with the SUR2A interaction identified in the present study. An alternative or complementary interaction of the Kir6.0 binding domain in SUR2A NBF2 with the cytoplasmic N-terminal domain of Kir6.2 could not be ruled out, as evidence for a cytoplasmic interaction between the N-terminus of Kir6.2 and other parts of SUR1, namely the sulphonylurea-binding L0 loop, had been reported (Reimann, 1999; Babenko, 2002; Babenko, 1999; Chan, 2003; Aguilar-Bryan, 1995; Mikhailov et al., 2000).

To investigate the binding site in the Kir6.2 with the C-terminal of SUR2A, chimaeras between Kir6.2 and Kir2.1 which had been established in other laboratories were used in this study. In this study two sets of Kir6.2/Kir2.1 chimaeras made by Dr. Tinker's and Dr Sivaprasadarao's laboratories (Giblin et al., 1999; Hough et al., 2000) were modified and expressed. The chimaeras were all immunoprecipitated by antibodies corresponding to the

appropriate C-terminal in each case: ones ending with the C-terminal of Kir6.2 immunoprecipitated with anti-Kir6.2 and ones ending with the C-terminal of Kir2.1 immunoprecipitated with anti-Kir2.1.

The co-immunoprecipitation of the binding fragment in the C-terminal of SUR2A, rSUR2A-CT-C, with five of the Kir6.2/Kir2.1 chimaeras containing the C-terminal of Kir6.2 aa 276-390 suggested that the binding site for SUR2A-CT-C is in the C-terminal of Kir6.2. The other chimaeras containing the equivalent of Kir2.1 in this region showed no binding, indicating that the binding of the SUR2A-CT-C was specific to structures within the kir6.2 subunit. Moreover the non-binding fragments from SUR2A, rSUR2A-CT-D, and the equivalent of the binding region to rSUR2A-CT-C from the MRP1 (MRP1-CT-C) did not show a significant binding with any of the Kir6.2/Kir2.1 chimaeras indicating specificity in the interaction seen between rSUR2A-CT-C and the Kir6.2/Kir2.1 chimaeras containing the C-terminal of Kir6.2. Furthermore, the inability of the Tin F chimaera, which contains the N-terminal of Kir6.2 up to residue 315, to co-immunoprecipitate the rSUR2A-CT-C fragment localised the interacting site of SUR2A-CT-C to the C-terminal Kir6.2 domain beyond 315 (316-390 Kir6.2 amino acids). Alignment of the primary sequence of Kir6.2 with Kir2.1 showed a highly conserved region between residues 277-315 in Kir6.2. Since this conserved sequence was present in both Tin E and Tin F chimaeras, only one of which (TinE) bound rSUR2A-CT-C, this suggests that these conserved residues play no role in the binding of SUR2A-CT-C (Figure 8-5).

The amino acids sequence of Kir6.2 from 315 to 390 was examined to make predictions of potential residues involved in the binding with SUR2A NBF motif. It is reasonable to propose that the interacting residues/amino acid sequences in the NBF2 binding domain should be similar in Kir6.1 and Kir6.2 but different in the non-interacting Kir2.1 subunit. On these assumptions, the following can be hypothesised:

- Residues 383-406 in Kir6.1 which aligns with sequence 386-409 in Kir2.1 but which has no corresponding sequence alignment in Kir6.2 is not involved, since an NBF2 interaction domain must be present in both Kir6.1 and Kir6.2.

```

Kir6.2      ---MLSRKGIPEEY---VLTRLAED---PTEPRYRTRER-RARFVSKKGNCNVAHKN 48
Kir6.1      ---MLARKSIIPEEY---VLARIAAEN---LRKPRIRDRLP-KARFIKSGACNLAHKN 49
Kir2.1      MGSVRTRNYSIVSSEEDGMKLMATAVANGFNGKSKVHTRQQCRSRFVKKDGHCNVQFIN 60
          * . * . . *      * : *      : : *      : * * : * . * * : . *

Kir6.2      IREQG-RFLQDVFTTLVLDLKWPHLLIFTMSFLCSWLLFAMVWVLIAPAHGDLAPGEGTN 107
Kir6.1      IREQG-RFLQDIFTTLVLDLKWRTLVIPTMSFLCSWLLFAMVWLVAFAHGDIYAYMEKG 108
Kir2.1      VGEKGRYLDIPTTCVDIRWRNMLVIPCLAFVLSWLFPGCVFNLIALHGLDASKES- 119
          : * * * * * : * * * * * : * * * * * : * * * * * : * * * * * :

Kir6.2      VP-----CVTSIHSFSSAPLFSIEVQVTIGFGRMVTEECPLAILLIVQNIIVGLM 158
Kir6.1      ITEKSGLESAVCVTNVRSPTSAFLFSIEVQVTIGFGRMMTEECPLAITVLILQNIIVGLI 168
Kir2.1      -----KACVSEVNSFTAALFSIETQTTIGYGFRCVTDECPVAVFMVVFQSIIVGCI 170
          * * : : * * : * * * * * * * * * * * * * * * * * : : . * * * * :

Kir6.2      INAIMLGCIFMKTQAHRRAETLIFSRAVITLRHGRLCFMLRVGDLRKSMMIISATIHMQ 218
Kir6.1      INAVMLGCIFMKTQAHRRAETLIFSRAVIAVRNGKLCFMRVGDRLRKSMMIISASVRIQ 228
Kir2.1      IDAFIIGAVMAKMAKPKRRNETLVFSHNAVIAMRDGKLCMLWRVGNLRKSHLVEAHVRAQ 230
          * : * * * * * : * * * * * : * * * * * : * * * * * : * * * * * :

Kir6.2      VVKRTTSPERGEVVPVPLHQVDIPMENGVGNSIFLVAPLIIVHVIDSNSPLYDLAPSDLHHH 278
Kir6.1      VVKRTTPEGEVVPVPHQVDIPVDNPIESNNIFLVAPLIICHVIDKRSPLYDISATDLVN- 287
Kir2.1      LLKSRTTSEGEYIPLDQIDINVGFDSGIDRIFLVSPITIVHEIDEDSPLYDLKQDIDN- 289
          : : . : * * * : * : * * * :      : * * * * * : * * * * * : * * :

Kir6.2      QDLEIIVILEGVVETTGITQARTSYLADEILWGQRFVPIVAEEDGRYSVDYSKFGNTVK 338
Kir6.1      QDLEIVIVILEGVVETTGITQARTSYIAEEIQWGHRFVSIIVTEEEGVYSVDYSKFGNTR 347
Kir2.1      ADFEIIVILEGMVEATAMTTQCRSSYLANEILWGHRYEPVLPFEKHCYKVDYSRPHKTYE 349
          * : * * * * * * * * * * * * * * * * * * * * * * * * * * * * * *

Kir6.2      VP-TPLCTARQLDEDRSLLDALTLAS---SRGFLRKR-----SVA 374
Kir6.1      VA-APRCSARELDEKPSILIQTLQKSELHQNSLRKRNSMRRNNSMRRNSIIRNNSLM 406
Kir2.1      VPNTPLCSARDLAEKKYILSNANSFCYENEVALTSKEEEDSENGVPESTSDSPPGIDLH 409
          * . * * * * * * . *      *      *

Kir6.2      VAKAKPKFSISPDLS-- 390
Kir6.1      VPKVQFMTPEGNQCPSES 424
Kir2.1      NQASVPLEPRPLRRESEI 427

```

eqA Name	Len(aa)	SeqB Name	Len(aa)	Score
1 Kir6.2	390	2 Kir2.1	427	42
1 Kir6.2	390	3 Kir6.1	424	67
2 Kir2.1	427	3 Kir6.1	424	39

**Figure 8-5 Alignment of the full length Kir6.0 and Kir2.1 subunits.** Alignment of Kir6.1, Kir6.2 and Kir2.1, showing the similarity score between each other, where (\*) mean conserved amino acid in all of them, (:) highly similarity between them and (.) low similarity. The green, red, pink and blue letters represent the polar, hydrophobic, positive and negative amino acid groups, respectively. The underlined sequence highlights the binding site in Kir6.2 for the C-terminal fragment of SUR2A (rSUR2A-CT-C) (using <http://www.ebi.ac.uk/clustalw>).

- Segments between residues 328-335, 341-352, 355-357 and possibly 321-322 are not involved, since the sequence is highly conserved or identical to Kir2.1 in these areas.
- Sequence between 352-368 is dissimilar between Kir6.1 and Kir6.2 and, therefore, unlikely to contribute to a common site.
- Residues 409-424 and 378-390 at the C-terminals of Kir6.1 and Kir6.2, respectively, are not involved as these are unique sequences distinguished in structure as epitopes for subunit specific anti-Kir6.0 antisera (Singh et al., 2003).

After the elimination of the above regions this leaves the sequence between residues 315 and 327 (with the exception of a pair of glutamates shared between all three Kir subunits), 334-338, the RKR endoplasmic reticulum retention sequence at 368-371 and a triplet at 375-378 as highly important candidates for the binding with the C-terminal of SUR2A as potentially important in the interaction with the SUR2A NBF2 domain.

### 8.3- Conclusion

In this study, a binding site in the C-terminal of SUR2A that interacts with the Kir6.2 subunit was characterised. The study also highlighted the potential importance of this domain in the channel assembly of Kir6.2/SUR2A and illustrated the reason for current reduction in the presence of the binding fragment by lowering the channel number in the cell membrane. This study has localized the binding site on the SUR2A-CT amino acid sequence between 1294-1358; fragments containing this region showed binding with the full length of Kir6.2. It also demonstrated that the equivalent rSUR2A-CT 1294-1358 region from MRP1 did not interact with Kir6.2 or disrupt cell surface channel expression (Rainbow et al., 2004). Based on this observation, a series of rSUR2A-CT (1294-1358)/MRP1 chimaeric fragments were produced with junctions at positions 25 and 45 within the 65 amino acid rSUR2A-CT (1294-1358) fragment. MRP1(25)SUR2A and SUR2A(45)MRP1 retained the ability to disrupt surface channel expression measured electrophysiologically, while MRP1(45)SUR2A and SUR(25)MRP1 did not exhibit this

effect. Furthermore, MRP1(25)SUR2A but not MRP1(45)SUR2A, SUR2A(25)MRP1 or SUR2A(45)MRP1 was co-immunoprecipitated with full-length Kir6.2. Together, these results further localised the Kir6 interaction domain to residues 1318-1337 in SUR2A. On the basis that the Kir6/SUR interaction is likely to be common for different heterooligomer combinations (Rainbow et al., 2004), it is predicted that residues involved in the interaction should be conserved in SUR but dissimilar in MRP1. This reveals four residues at positions 1319, 1323, 1335 and 1337. Of these, K1323 and P1335 map to the surface of predicted NBF structures. However, the precise residues involved in binding remain to be resolved. Moreover, the study draws attention to a possible binding site in the NBF1 with the full length of Kir6.2, but this was not fully investigated in this study.

This study also identified a novel cytoplasmic interaction between the C-terminal domain of Kir6.2 (residues 315-390) and the nucleotide-binding fold-2 of the SUR2A subunits (residues 1294-1403). Both of these domains are important in the regulation of channel activity. The binding site on Kir6.2 for the SUR2A-CT-fragment (rSUR2A-CT-C) was defined using chimaeras between Kir6.2/Kir2.1 to the C-terminal of Kir6.2. Chimaeras containing the C-terminal of Kir6.2 showed binding with rSUR2A-CT-C, whereas the equivalent fragment from MRP1-CT-C failed to show any binding. Two series of Kir6.2/Kir2.1 chimaeras (Hough et al., 2000; Giblin et al., 1999) were used to screen for interaction with the rSUR2A-CT (1294-1403) interacting fragment in co-immunoprecipitation experiments. Co-immunoprecipitation was lost only when the sequence of the last 75 amino acids in the C-terminal of Kir6.2 was replaced by the Kir2.1 sequence, thereby localising the NBD2 interaction to the C-terminal domain of Kir6.2. High affinity interaction within the cytoplasm between the C-terminal domain of Kir6.2 (residues 315-390) and the nucleotide-binding fold-2 of the SUR2A subunits (residues 1294-1403) is important in determining the stability of channel expression at the cell surface and is likely to be involved in allosteric information transfer between heterologous subunits in  $K_{ATP}$  channels.

#### **8.4- Future work**

The following step in this project will be to determine the amino acid residues in the SUR2A-CT-C region responsible for the binding with Kir6.2. A single point mutation of most likely amino acids, in the 20 amino acids in the middle of SUR2A-CT-C would be carried out, with particular attention to residues K1323 and P1325, which are predicted to be located on the surface of NBF2 (see Figure 8-2 above). Scanning alanine mutagenesis should be used to further refine the definition of the Kir6 binding site within the 20 amino acid, Kir6.2-binding sequence in rSUR2A (residues 1319-1338). In addition, single amino acid replacements of SUR2A for MRP1 residues should be investigated in the same assay for residues E1319R, P1323L, P1335G and Q1337E. For positions that result in loss of co-immunoprecipitation of the rSUR2A-CT-C fragment with Kir6.2, the rSUR2A residue should be mutated into the equivalent non-interacting MBP-MRP1-CT-C fragment, either singly or in combination, and assayed for restoration of co-immunoprecipitation with Kir6.2. While chances of restoration of binding activity may be low, a positive result in this assay would confirm the importance of SUR2A residues in the interaction of this shared structural motif.

The same series of mutations should be analysed in the surface expression assay by confocal microscopy and/or electrophysiological recording, as previously described (Rainbow et al., 2004). Such assays would be conducted to ensure channel assembly and changes in channel properties, such as sensitivity to MgADP and  $K_{ATP}$  channel openers and antagonists for the mutants and the wild-type. These experiments would identify residues involved in inter-subunit interaction and allosteric information transfer between rSUR2A residues 1318-1337 and Kir6.2, and would provide necessary data to validate three-dimensional models of  $K_{ATP}$  channel structure as these become available.

Fragments and chimaeras from the SUR2A-NBF1 should also be made to determine the binding site in this region. Although this region needed a higher tagged polypeptide concentration than other fragments from the SUR2A-CT to show binding, it is nevertheless worth investigating it with a different tagging system, or perhaps with a different approach.

To identify the binding site of the SUR2A-CT on the Kir6.2 subunit, a series of experiments needs to be made. As has been shown, the co-immunoprecipitation of the rSUR2A-CT-C fragment with a series of Kir6.2/Kir2.1 chimaeras has localised the binding site for the rSUR2A NBF2 1318-1337 binding site to the C-terminal 75 amino acids of Kir6.2, within which four short regions of sequence are predicted to be involved (see above). To further map the NBF2 1318-1337 binding site in Kir6.2, the following chimaeric constructs are suggested for use in co-immunoprecipitation experiments with MBP-rSUR2A-CT-C: (a) Kir6.2(1-356)/Kir2.1(368-427) (i.e. C-terminal half of Tin F domain as Kir2.1), (b) Kir6.2(1-314)/Kir2.1(326-368)/Kir6.2(357-390) (i.e. N-terminal half of Tin F domain as Kir2.1), (c) Kir6.2 with the RKR retention signal mutated to AAA and (d) Kir2.1 with SKE(384-386) mutated to RKR. From current data and on the assumption that charged residues are most likely to contribute to interactions within these target sequences, three charged residues in the C-terminal 75 amino acids of Kir6.2 have been identified as of interest (D323, K338 and K378). Close attention should be given to the mutagenesis of these residues to those in Kir2.1 (i.e. D323K, K338E, K378A), but experiments should be widened to include a more systematic scanning mutagenesis in the C-terminal of Kir6.2. Co-immunoprecipitation experiments should be complemented by electrophysiological analysis of the nucleotide and  $K_{ATP}$  channel drug sensitivity of mutant Kir6.2 subunits expressed with wild-type SUR2A in CHO cells. An ultimate goal is to be able to describe the structure and function of the  $K_{ATP}$  channel hetero-oligomer in three dimensions.

The identification of the amino acid residues involved in inter-subunit interaction between rSUR2A residues 1318-1337 and Kir6.2 and will provide necessary data to validate three-dimensional models of  $K_{ATP}$  channel structure and will help to form three-dimensional to SUR2A-CT and the C-terminal domain of Kir6.2. This may lead to a clearer understanding of the allosteric function formed between the two subunits.

Conditions for crystal preparation from individual polypeptide preparations or mixtures of interacting domains could be explored by X-ray diffraction analysis. While structural

studies on membrane proteins remains challenging, the construction of cytoplasmic N- and C-terminal domains of Kir2.1 and Kir3.1 using variable linkers has permitted crystal growth for X-ray diffraction analysis (Kuo et al., 2003; Nishida and Mackinnon, 2002). Conditions for the production of crystals from intracellular N- and C-terminal domains of Kir6.2 linked by a variable linker could be explored, although it is acknowledged that this method has not proven successful for all Kir species e.g. Kir3.4 (Pegan et al., 2005). Crystallization of SUR2A NBF1 and NBF2 and the full C-terminal domain (1254-1545) of SUR2A could also be attempted. The crystallization of the binding motif in SUR2A (SUR2A-CT-C) and the cognate binding region corresponding to the Kir6.2 C-terminal will help to understand the subunit interaction.

## References

- Aguilar-Bryan, L. and J. Bryan (1999). "Molecular biology of adenosine triphosphate-sensitive potassium channels." Endocr Rev 20(2): 101-35.
- Aguilar-Bryan, L., J. P. t. Clement, G. Gonzalez, K. Kunjilwar, A. Babenko and J. Bryan (1998). "Toward understanding the assembly and structure of KATP channels." Physiol Rev 78(1): 227-45.
- Aguilar-Bryan, L., C. G. Nichols, S. W. Wechsler, J. P. t. Clement, A. E. Boyd, 3rd, G. Gonzalez, H. Herrera-Sosa, K. Nguy, J. Bryan and D. A. Nelson (1995). "Cloning of the beta cell high-affinity sulfonylurea receptor: a regulator of insulin secretion." Science 268(5209): 423-6.
- Aguilar-Bryan L., Clement J. P. and Nelson D. A. (1998). "Sulfonylurea receptors and ATP-sensitive potassium ion channels." Meth. Enzymol. 292: 732-744.
- Aidley, D. and P. R. Stanfield (1996). Ion Channels, The press syndicate of the university of cambridge.
- Allen, D. G. and C. H. Orchard (1987). "Myocardial contractile function during ischemia and hypoxia." Circ Res 60(2): 153-68.
- Ames, G. F. and H. Lecar (1992). "ATP-dependent bacterial transporters and cystic fibrosis: analogy between channels and transporters." Faseb J 6(9): 2660-6.
- Ardehali, H. (2004). "Role of the mitochondrial ATP-sensitive K<sup>+</sup> channels in cardioprotection." Acta Biochim Pol 51(2): 379-90.
- Ashcroft F. M. and G. F. M. (1998). "Correlating structure and function in ATP-sensitive K<sup>+</sup> channels." Trends Neurosci. 21: 288-294.

Ashcroft, F. M. (1996). "Mechanisms of the glycaemic effects of sulfonylureas." Horm Metab Res 28(9): 456-63.

Ashcroft, F. M. and F. M. Gribble (2000). "New windows on the mechanism of action of K(ATP) channel openers." Trends Pharmacol Sci 21(11): 439-45.

Ashcroft, F. M. and P. Rorsman (1989). "Electrophysiology of the pancreatic beta-cell." Prog Biophys Mol Biol 54(2): 87-143.

Ashcroft, S. J. and F. M. Ashcroft (1990). "Properties and functions of ATP-sensitive K-channels." Cell Signal 2(3): 197-214.

Ashfield, R., F. M. Gribble, S. J. Ashcroft and F. M. Ashcroft (1999). "Identification of the high-affinity tolbutamide site on the SUR1 subunit of the K(ATP) channel." Diabetes 48(6): 1341-7.

Aynsley-Green, A., N. D. Barnes, T. E. Adrian, J. Kingston, S. Boyes and S. R. Bloom (1981). "Effect of somatostatin infusion on intermediary metabolism and entero-insular hormone release in infants with hyperinsulinaemic hypoglycaemia." Acta Paediatr Scand 70(6): 889-95.

Azzaria, M., E. Schurr and P. Gros (1989). "Discrete mutations introduced in the predicted nucleotide-binding sites of the *mdr1* gene abolish its ability to confer multidrug resistance." Mol Cell Biol 9(12): 5289-97.

Babenko A. P., Gonzalez G., Aguilar-Bryan L. and B. J. (1998). "Reconstituted human cardiac KATP channels. Functional identity with the native channels from the sarcolemma of human ventricular cells." Circ. Res. 83: 1132-1143.

- Babenko, A. P., G. Gonzalez and J. Bryan (1999). "The N-terminus of KIR6.2 limits spontaneous bursting and modulates the ATP-inhibition of KATP channels." Biochem Biophys Res Commun **255**(2): 231-8.
- Bader, C. R., L. Bernheim and D. Bertrand (1985). "Sodium-activated potassium current in cultured avian neurones." Nature **317**(6037): 540-2.
- Baukrowitz, T., U. Schulte, D. Oliver, S. Herlitz, T. Krauter, S. J. Tucker, J. P. Ruppersberg and B. Fakler (1998). "PIP2 and PIP as determinants for ATP inhibition of KATP channels." Science **282**(5391): 1141-4.
- Baukrowitz, T., S. J. Tucker, U. Schulte, K. Benndorf, J. P. Ruppersberg and B. Fakler (1999). "Inward rectification in KATP channels: a pH switch in the pore." Embo J **18**(4): 847-53.
- Begenisich, T., T. Nakamoto, C. E. Ovitt, K. Nehrke, C. Brugnara, S. L. Alper and J. E. Melvin (2004). "Physiological roles of the intermediate conductance, Ca<sup>2+</sup>-activated potassium channel Kcnn4." J Biol Chem **279**(46): 47681-7.
- Bernardi, H., J. R. De Welle, J. Epelbaum, C. Mourre, S. Amoroso, A. Slama, M. Fosset and M. Lazdunski (1993). "ATP-modulated K<sup>+</sup> channels sensitive to antidiabetic sulfonylureas are present in adenohipophysis and are involved in growth hormone release." Proc Natl Acad Sci U S A **90**(4): 1340-4.
- Bianchet, M. A., Y. H. Ko, L. M. Amzel and P. L. Pedersen (1997). "Modeling of nucleotide binding domains of ABC transporter proteins based on a F1-ATPase/recA topology: structural model of the nucleotide binding domains of the cystic fibrosis transmembrane conductance regulator (CFTR)." J Bioenerg Biomembr **29**(5): 503-24.
- Bischoff, U., W. Vogel and B. V. Safronov (1998). "Na<sup>+</sup>-activated K<sup>+</sup> channels in small dorsal root ganglion neurones of rat." J Physiol **510** ( Pt 3): 743-54.

Bissonnette, J. M. (2002). "The role of calcium-activated potassium channels in respiratory control." Respir Physiol Neurobiol **131**(1-2): 145-53.

Blatz, A. L. and K. L. Magleby (1986). "Single apamin-blocked Ca-activated K<sup>+</sup> channels of small conductance in cultured rat skeletal muscle." Nature **323**(6090): 718-20.

Bohm, A., J. Diez, K. Diederichs, W. Welte and W. Boos (2002). "Structural model of MalK, the ABC subunit of the maltose transporter of Escherichia coli: implications for mal gene regulation, inducer exclusion, and subunit assembly." J Biol Chem **277**(5): 3708-17.

Boim, M. A., K. Ho, M. E. Shuck, M. J. Bienkowski, J. H. Block, J. L. Slightom, Y. Yang, B. M. Brenner and S. C. Hebert (1995). "ROMK inwardly rectifying ATP-sensitive K<sup>+</sup> channel. II. Cloning and distribution of alternative forms." Am J Physiol **268**(6 Pt 2): F1132-40.

Bond, C. T., M. Pessia, X. M. Xia, A. Lagrutta, M. P. Kavanaugh and J. P. Adelman (1994). "Cloning and expression of a family of inward rectifier potassium channels." Receptors Channels **2**(3): 183-91.

Bradford, M. M. (1976). "A rapid and sensitive method for the quantitation of microgram quantities of protein utilizing the principle of protein-dye binding." Anal Biochem **72**: 248-54.

Bradley, J., J. Li, N. Davidson, H. A. Lester and K. Zinn (1994). "Heteromeric olfactory cyclic nucleotide-gated channels: a subunit that confers increased sensitivity to cAMP." Proc Natl Acad Sci U S A **91**(19): 8890-4.

Brayden, J. E. (2002). "Functional roles of KATP channels in vascular smooth muscle." Clin Exp Pharmacol Physiol **29**(4): 312-6.

Brickley, S. G., V. Revilla, S. G. Cull-Candy, W. Wisden and M. Farrant (2001). "Adaptive regulation of neuronal excitability by a voltage-independent potassium conductance."

Nature 409(6816): 88-92.

Campbell, J. D., P. Proks, J. D. Lippiat, M. S. Sansom and F. M. Ashcroft (2004).

"Identification of a functionally important negatively charged residue within the second catalytic site of the SUR1 nucleotide-binding domains." Diabetes 53 Suppl 3: S123-7.

Carson, M. R., S. M. Travis and M. J. Welsh (1995). "The two nucleotide-binding domains of cystic fibrosis transmembrane conductance regulator (CFTR) have distinct functions in controlling channel activity." J Biol Chem 270(4): 1711-7.

Cartier, E. A., L. R. Conti, C. A. Vandenberg and S. L. Shyng (2001). "Defective trafficking and function of KATP channels caused by a sulfonylurea receptor 1 mutation associated with persistent hyperinsulinemic hypoglycemia of infancy." Proc Natl Acad Sci U S A 98(5): 2882-7.

Catterall, W. A., R. P. Hartshorne and D. A. Beneski (1982). "Molecular Properties of neurotoxin receptors sites associated with sodium channels from mammalian brain."

Toxicon 20(1): 27-40.

Choe, S. (2002). "Potassium channel structures." Nat Rev Neurosci 3(2): 115-21.

Chutkow, W. A., M. C. Simon, M. M. Le Beau and C. F. Burant (1996). "Cloning, tissue expression, and chromosomal localization of SUR2, the putative drug-binding subunit of cardiac, skeletal muscle, and vascular KATP channels." Diabetes 45(10): 1439-45.

Clement, J. P. t., K. Kunjilwar, G. Gonzalez, M. Schwanstecher, U. Panten, L. Aguilar-Bryan and J. Bryan (1997). "Association and stoichiometry of K(ATP) channel subunits."

Neuron 18(5): 827-38.

Cole, K. (1949). "Dynamic electrical characteristics of the squid axon membrane." Arch. Sci. Physiol. 3: 253-258.

Cole, K. and H. Curtis (1939). "Electrical impedance of the squid giant axon during activity." J. Gen. Physiol. 22: 649-670.

Cole, W. C., C. D. McPherson and D. Sontag (1991). "ATP-regulated K<sup>+</sup> channels protect the myocardium against ischemia/reperfusion damage." Circ Res 69(3): 571-81.

Conti, L. R., C. M. Radeke, S. L. Shyng and C. A. Vandenberg (2001). "Transmembrane topology of the sulfonylurea receptor SUR1." J Biol Chem 276(44): 41270-8.

Curtis, H. and K. Cole (1940). "Membrane action potential from the squid giant axon." J. Cell. Comp. Physiol. 15: 147-157.

Cook, D. and G. Taborsky (1990). B-cell function and insulin secretion. In Diabetes Mellitus: Theory and Practice. Amsterdam, H. Rifkin and D. Prentki.

Cook, D. L., L. S. Satin, M. L. Ashford and C. N. Hales (1988). "ATP-sensitive K<sup>+</sup> channels in pancreatic beta-cells. Spare-channel hypothesis." Diabetes 37(5): 495-8.

Cook, N. (1990). Potassium channels (structure, classification, function and therapeutic potential). Chichester, Ellis Horwood limited.

Cui, Y., J. P. Giblin, L. H. Clapp and A. Tinker (2001). "A mechanism for ATP-sensitive potassium channel diversity: Functional coassembly of two pore-forming subunits." Proc Natl Acad Sci U S A 98(2): 729-34.

Dabrowski, M., F. M. Ashcroft, R. Ashfield, P. Lebrun, B. Pirotte, J. Egebjerg, J. Bondo Hansen and P. Wahl (2002). "The novel diazoxide analog 3-isopropylamino-7-methoxy-

4H-1,2,4-benzothiadiazine 1,1-dioxide is a selective Kir6.2/SUR1 channel opener." Diabetes **51(6)**: 1896-906.

Dascal, N., N. F. Lim, W. Schreibmayer, W. Wang, N. Davidson and H. A. Lester (1993). "Expression of an atrial G-protein-activated potassium channel in *Xenopus* oocytes." Proc Natl Acad Sci U S A **90(14)**: 6596-600.

Dascal, N., W. Schreibmayer, N. F. Lim, W. Wang, C. Chavkin, L. DiMugno, C. Labarca, B. L. Kieffer, C. Gaveriaux-Ruff, D. Trollinger and et al. (1993). "Atrial G protein-activated K<sup>+</sup> channel: expression cloning and molecular properties." Proc Natl Acad Sci U S A **90(21)**: 10235-9.

Davies, N. W., N. B. Standen and P. R. Stanfield (1992). "The effect of intracellular pH on ATP-dependent potassium channels of frog skeletal muscle." J Physiol **445**: 549-68.

Deutsch, N., T. S. Klitzner, S. T. Lamp and J. N. Weiss (1991). "Activation of cardiac ATP-sensitive K<sup>+</sup> current during hypoxia: correlation with tissue ATP levels." Am J Physiol **261(3 Pt 2)**: H671-6.

D'Hahan, N., C. Moreau, A. L. Prost, H. Jacquet, A. E. Alekseev, A. Terzic and M. Vivaudou (1999). "Pharmacological plasticity of cardiac ATP-sensitive potassium channels toward diazoxide revealed by ADP." Proc Natl Acad Sci U S A **96(21)**: 12162-7.

D'Hahan N., Jacquet H., Moreau C., Catty P. and V. M. (1999). "A transmembrane domain of the sulfonylurea receptor mediates activation of ATP-sensitive K<sup>+</sup> channels by K<sup>+</sup> channel openers." Mol. Pharmacol. **56**: 308-315.

Douppnik, C. A., N. Davidson and H. A. Lester (1995). "The inward rectifier potassium channel family." Curr Opin Neurobiol **5(3)**: 268-77.

Drain, P., L. Li and J. Wang (1998). "KATP channel inhibition by ATP requires distinct functional domains of the cytoplasmic C terminus of the pore-forming subunit." Proc Natl Acad Sci U S A **95**(23): 13953-8.

Dryer, S. E. (1994). "Na(+)-activated K<sup>+</sup> channels: a new family of large-conductance ion channels." Trends Neurosci **17**(4): 155-60.

Dryer, S. E., J. T. Fujii and A. R. Martin (1989). "A Na<sup>+</sup>-activated K<sup>+</sup> current in cultured brain stem neurones from chicks." J Physiol **410**: 283-96.

Duflot, S., B. Riera, S. Fernandez-Veledo, V. Casado, R. I. Norman, F. J. Casado, C. Lluís, R. Franco and M. Pastor-Anglada (2004). "ATP-sensitive K(+) channels regulate the concentrative adenosine transporter CNT2 following activation by A(1) adenosine receptors." Mol Cell Biol **24**(7): 2710-9.

Edwards, G. and A. H. Weston (1993). "The pharmacology of ATP-sensitive potassium channels." Annu Rev Pharmacol Toxicol **33**: 597-637.

Fakler, B., J. H. Schultz, J. Yang, U. Schulte, U. Brandle, H. P. Zenner, L. Y. Jan and J. P. Ruppersberg (1996). "Identification of a titratable lysine residue that determines sensitivity of kidney potassium channels (ROMK) to intracellular pH." Embo J **15**(16): 4093-9.

Fan, Z. and J. C. Makielski (1999). "Phosphoinositides decrease ATP sensitivity of the cardiac ATP-sensitive K(+) channel. A molecular probe for the mechanism of ATP-sensitive inhibition." J Gen Physiol **114**(2): 251-69.

Fan, Z., Y. Tokuyama and J. C. Makielski (1994). "Modulation of ATP-sensitive K<sup>+</sup> channels by internal acidification in insulin-secreting cells." Am J Physiol **267**(4 Pt 1): C1036-44.

Furukawa, T., T. Yamane, T. Terai, Y. Katayama and M. Hiraoka (1996). "Functional linkage of the cardiac ATP-sensitive K<sup>+</sup> channel to the actin cytoskeleton." Pflugers Arch **431**(4): 504-12.

Galvez, A., G. Gimenez-Gallego, J. P. Reuben, L. Roy-Contancin, P. Feigenbaum, G. J. Kaczorowski and M. L. Garcia (1990). "Purification and characterization of a unique, potent, peptidyl probe for the high conductance calcium-activated potassium channel from venom of the scorpion *Buthus tamulus*." J Biol Chem **265**(19): 11083-90.

Garlid, K. D., P. Paucek, V. Yarov-Yarovoy, H. N. Murray, R. B. Darbenzio, A. J. D'Alonzo, N. J. Lodge, M. A. Smith and G. J. Grover (1997). "Cardioprotective effect of diazoxide and its interaction with mitochondrial ATP-sensitive K<sup>+</sup> channels. Possible mechanism of cardioprotection." Circ Res **81**(6): 1072-82.

Gembal, M., P. Detimary, P. Gilon, Z. Y. Gao and J. C. Henquin (1993). "Mechanisms by which glucose can control insulin release independently from its action on adenosine triphosphate-sensitive K<sup>+</sup> channels in mouse B cells." J Clin Invest **91**(3): 871-80.

Giblin, J. P., J. L. Leaney and A. Tinker (1999). "The molecular assembly of ATP-sensitive potassium channels. Determinants on the pore forming subunit." J Biol Chem **274**(32): 22652-9.

Girard, C., F. Duprat, C. Terrenoire, N. Tinel, M. Fosset, G. Romey, M. Lazdunski and F. Lesage (2001). "Genomic and functional characteristics of novel human pancreatic 2P domain K(+) channels." Biochem Biophys Res Commun **282**(1): 249-56.

Glaser, B., P. Thornton, T. Otonkoski and C. Junien (2000). "Genetics of neonatal hyperinsulinism." Arch Dis Child Fetal Neonatal Ed **82**(2): F79-86.

Goldstein, S. A., D. Bockenhauer, I. O'Kelly and N. Zilberberg (2001). "Potassium leak channels and the KCNK family of two-P-domain subunits." Nat Rev Neurosci 2(3): 175-84.

Gribble, F. M., S. J. Tucker and F. M. Ashcroft (1997). "The essential role of the Walker A motifs of SUR1 in K-ATP channel activation by Mg-ADP and diazoxide." Embo J 16(6): 1145-52.

Gribble, F. M., S. J. Tucker, S. Seino and F. M. Ashcroft (1998). "Tissue specificity of sulfonylureas: studies on cloned cardiac and beta-cell K(ATP) channels." Diabetes 47(9): 1412-8.

Gross, G. J. and J. N. Peart (2003). "KATP channels and myocardial preconditioning: an update." Am J Physiol Heart Circ Physiol 285(3): H921-30.

Grover, G. J. and K. D. Garlid (2000). "ATP-Sensitive potassium channels: a review of their cardioprotective pharmacology." J Mol Cell Cardiol 32(4): 677-95.

Haimann, C., J. Magistretti and B. Pozzi (1992). "Sodium-activated potassium current in sensory neurons: a comparison of cell-attached and cell-free single-channel activities." Pflugers Arch 422(3): 287-94.

Halestrap, A. P. (1989). "The regulation of the matrix volume of mammalian mitochondria in vivo and in vitro and its role in the control of mitochondrial metabolism." Biochim Biophys Acta 973(3): 355-82.

Hall, J. and D. Baker (1977). Cell membranes and ion transport. London, Longman group limited.

Hamill, O., A. Marty, B. Neher, B. Sakmann and F. Sigworth (1981). "Improved patch-clamp techniques for high-resolution current recording from cells and cell-free membrane patches." Pflugers Arch 391: 85-100.

Hancox, J. C., A. J. Levi and H. J. Witchel (1998). "Time course and voltage dependence of expressed HERG current compared with native "rapid" delayed rectifier K current during the cardiac ventricular action potential." Pflugers Arch 436(6): 843-53.

Haruna, T., M. Horie, M. Takano, Y. Kono, H. Yoshida, H. Otani, T. Kubota, T. Ninomiya, M. Akao and S. Sasayama (2000). "Alteration of the membrane lipid environment by L-palmitoylcarnitine modulates K(ATP) channels in guinea-pig ventricular myocytes." Pflugers Arch 441(2-3): 200-7.

Hegde, P., G. G. Gu, D. Chen, S. J. Free and S. Singh (1999). "Mutational analysis of the Shab-encoded delayed rectifier K(+) channels in Drosophila." J Biol Chem 274(31): 22109-13.

Henquin, J. C. and H. P. Meissner (1984). "Significance of ionic fluxes and changes in membrane potential for stimulus-secretion coupling in pancreatic B-cells." Experientia 40(10): 1043-52.

Heron, L., A. Virsolvy, K. Peyrollier, F. M. Gribble, A. Le Cam, F. M. Ashcroft and D. Bataille (1998). "Human alpha-endosulfine, a possible regulator of sulfonylurea-sensitive KATP channel: molecular cloning, expression and biological properties." Proc Natl Acad Sci U S A 95(14): 8387-91.

Hodgkin, A. (1937). "Evidence for electrical transmission in nerve." J. Physiol (Lond.) 90(1): 183-210.

Hodgkin, A. and A. Huxley (1939). "Action potentials recorded from inside a nerve fibre." Nature (Lond.) 144: 710-711.

Hilgemann, D. W. and R. Ball (1996). "Regulation of cardiac Na<sup>+</sup>,Ca<sup>2+</sup> exchange and KATP potassium channels by PIP<sub>2</sub>." Science 273(5277): 956-9.

Hille, b. (2001). Ion Channels of Excitable Membranes. Sunderland, MA, USA, Sinauer Associates Inc.

Hirata, Y. and K. Aisaka (1997). "Effect of JTV-506, a novel vasodilator, on coronary blood flow in conscious dogs." J Cardiovasc Pharmacol 29(3): 397-405.

Ho, K., C. G. Nichols, W. J. Lederer, J. Lytton, P. M. Vassilev, M. V. Kanazirska and S. C. Hebert (1993). "Cloning and expression of an inwardly rectifying ATP-regulated potassium channel." Nature 362(6415): 31-8.

Hough, E., D. J. Beech and A. Sivaprasadarao (2000). "Identification of molecular regions responsible for the membrane trafficking of Kir6.2." Pflugers Arch 440(3): 481-7.

Hough, E., L. Mair, W. Mackenzie and A. Sivaprasadarao (2002). "Expression, purification, and evidence for the interaction of the two nucleotide-binding folds of the sulphonylurea receptor." Biochem Biophys Res Commun 294(1): 191-7.

Huang, C. L., S. Feng and D. W. Hilgemann (1998). "Direct activation of inward rectifier potassium channels by PIP<sub>2</sub> and its stabilization by Gbetagamma." Nature 391(6669): 803-6.

Inagaki, N., T. Gono, J. P. Clement, C. Z. Wang, L. Aguilar-Bryan, J. Bryan and S. Seino (1996). "A family of sulphonylurea receptors determines the pharmacological properties of ATP-sensitive K<sup>+</sup> channels." Neuron 16(5): 1011-7.

Inagaki, N., T. Gono, J. P. t. Clement, N. Namba, J. Inazawa, G. Gonzalez, L. Aguilar-Bryan, S. Seino and J. Bryan (1995). "Reconstitution of IKATP: an inward rectifier subunit plus the sulfonylurea receptor." Science 270(5239): 1166-70.

Inagaki, N., T. Gono and S. Seino (1997). "Subunit stoichiometry of the pancreatic beta-cell ATP-sensitive K<sup>+</sup> channel." FEBS Lett 409(2): 232-6.

Inagaki, N., J. Inazawa and S. Seino (1995). "cDNA sequence, gene structure, and chromosomal localization of the human ATP-sensitive potassium channel, uKATP-1, gene (KCNJ8)." Genomics 30(1): 102-4.

Inagaki, N., Y. Tsuura, N. Namba, K. Masuda, T. Gono, M. Horie, Y. Seino, M. Mizuta and S. Seino (1995). "Cloning and functional characterization of a novel ATP-sensitive potassium channel ubiquitously expressed in rat tissues, including pancreatic islets, pituitary, skeletal muscle, and heart." J Biol Chem 270(11): 5691-4.

Ishii, T. M., J. Maylie and J. P. Adelman (1997). "Determinants of apamin and d-tubocurarine block in SK potassium channels." J Biol Chem 272(37): 23195-200.

Ishii, T. M., C. Silvia, B. Hirschberg, C. T. Bond, J. P. Adelman and J. Maylie (1997). "A human intermediate conductance calcium-activated potassium channel." Proc Natl Acad Sci U S A 94(21): 11651-6.

Isomoto, S., C. Kondo, M. Yamada, S. Matsumoto, O. Higashiguchi, Y. Horio, Y. Matsuzawa and Y. Kurachi (1996). "A novel sulfonylurea receptor forms with BIR (Kir6.2) a smooth muscle type ATP-sensitive K<sup>+</sup> channel." J Biol Chem 271(40): 24321-4.

Janigro, D., G. A. West, E. L. Gordon and H. R. Winn (1993). "ATP-sensitive K<sup>+</sup> channels in rat aorta and brain microvascular endothelial cells." Am J Physiol 265(3 Pt 1): C812-21.

Joiner, W. J., L. Y. Wang, M. D. Tang and L. K. Kaczmarek (1997). "hSK4, a member of a novel subfamily of calcium-activated potassium channels." Proc Natl Acad Sci U S A **94**(20): 11013-8.

Kameyama, M., M. Kakei, R. Sato, T. Shibasaki, H. Matsuda and H. Irisawa (1984). "Intracellular Na<sup>+</sup> activates a K<sup>+</sup> channel in mammalian cardiac cells." Nature **309**(5966): 354-6.

Kane, C., R. M. Shepherd, P. E. Squires, P. R. Johnson, R. F. James, P. J. Milla, A. Aynsley-Green, K. J. Lindley and M. J. Dunne (1996). "Loss of functional KATP channels in pancreatic beta-cells causes persistent hyperinsulinemic hypoglycemia of infancy." Nat Med **2**(12): 1344-7.

Katnik, C. and D. J. Adams (1995). "An ATP-sensitive potassium conductance in rabbit arterial endothelial cells." J Physiol **485** ( Pt 3): 595-606.

Katnik, C. and D. J. Adams (1997). "Characterization of ATP-sensitive potassium channels in freshly dissociated rabbit aortic endothelial cells." Am J Physiol **272**(5 Pt 2): H2507-11.

Ketchum, K. A., W. J. Joiner, A. J. Sellers, L. K. Kaczmarek and S. A. Goldstein (1995). "A new family of outwardly rectifying potassium channel proteins with two pore domains in tandem." Nature **376**(6542): 690-5.

Kim, D. and C. Gnatenco (2001). "TASK-5, a new member of the tandem-pore K(+) channel family." Biochem Biophys Res Commun **284**(4): 923-30.

Ko, Y. H. and P. L. Pedersen (1995). "The first nucleotide binding fold of the cystic fibrosis transmembrane conductance regulator can function as an active ATPase." J Biol Chem **270**(38): 22093-6.

Kono, Y., M. Horie, M. Takano, H. Otani, L. H. Xie, M. Akao, K. Tsuji and S. Sasayama (2000). "The properties of the Kir6.1-6.2 tandem channel co-expressed with SUR2A."

Pflugers Arch **440(5)**: 692-8.

Koyano, T., M. Kakei, H. Nakashima, M. Yoshinaga, T. Matsuoka and H. Tanaka (1993).

"ATP-regulated K<sup>+</sup> channels are modulated by intracellular H<sup>+</sup> in guinea-pig ventricular cells." J Physiol **463**: 747-66.

Krapivinsky, G., I. Medina, L. Eng, L. Krapivinsky, Y. Yang and D. E. Clapham (1998).

"A novel inward rectifier K<sup>+</sup> channel with unique pore properties." Neuron **20(5)**: 995-1005.

Kuo, A., J. M. Gulbis, J. F. Antcliff, T. Rahman, E. D. Lowe, J. Zimmer, J. Cuthbertson, F.

M. Ashcroft, T. Ezaki and D. A. Doyle (2003). "Crystal structure of the potassium channel KirBac1.1 in the closed state." Science **300(5627)**: 1922-6.

Kuo, L. and J. D. Chancellor (1995). "Adenosine potentiates flow-induced dilation of

coronary arterioles by activating KATP channels in endothelium." Am J Physiol **269(2 Pt 2)**: H541-9.

LaRochelle, W. J., B. E. Wray, R. Sealock and S. C. Froehner (1985). "Immunochemical

demonstration that amino acids 360-377 of the acetylcholine receptor gamma-subunit are cytoplasmic." J Cell Biol **100(3)**: 684-91.

Lawson, K. (1996). "Is there a therapeutic future for "potassium channel openers'?" Clin

Sci (Lond) **91(6)**: 651-63.

Lederer, W. J., C. G. Nichols and G. L. Smith (1989). "The mechanism of early contractile

failure of isolated rat ventricular myocytes subjected to complete metabolic inhibition." J Physiol **413**: 329-49.

Lesage, F., F. Duprat, M. Fink, E. Guillemare, T. Coppola, M. Lazdunski and J. P. Hugnot (1994). "Cloning provides evidence for a family of inward rectifier and G-protein coupled K<sup>+</sup> channels in the brain." FEBS Lett **353**(1): 37-42.

Lesage, F., J. P. Hugnot, E. Z. Amri, P. Grimaldi, J. Barhanin and M. Lazdunski (1994). "Expression cloning in K<sup>+</sup> transport defective yeast and distribution of HBP1, a new putative HMG transcriptional regulator." Nucleic Acids Res **22**(18): 3685-8.

Liou, H. H., S. S. Zhou and C. L. Huang (1999). "Regulation of ROMK1 channel by protein kinase A via a phosphatidylinositol 4,5-bisphosphate-dependent mechanism." Proc Natl Acad Sci U S A **96**(10): 5820-5.

Liu, G. X., C. Derst, G. Schlichthorl, S. Heinen, G. Seebohm, A. Bruggemann, W. Kummer, R. W. Veh, J. Daut and R. Preisig-Muller (2001). "Comparison of cloned Kir2 channels with native inward rectifier K<sup>+</sup> channels from guinea-pig cardiomyocytes." J Physiol **532**(Pt 1): 115-26.

Lopez, J. R., R. Jahangir, A. Jahangir, W. K. Shen and A. Terzic (1996). "Potassium channel openers prevent potassium-induced calcium loading of cardiac cells: possible implications in cardioplegia." J Thorac Cardiovasc Surg **112**(3): 820-31.

Loussouarn, G., L. J. Pike, F. M. Ashcroft, E. N. Makhina and C. G. Nichols (2001). "Dynamic sensitivity of ATP-sensitive K(+) channels to ATP." J Biol Chem **276**(31): 29098-103.

Lupu, V. D., E. Kaznacheyeva, U. M. Krishna, J. R. Falck and I. Bezprozvanny (1998). "Functional coupling of phosphatidylinositol 4,5-bisphosphate to inositol 1,4,5-trisphosphate receptor." J Biol Chem **273**(23): 14067-70.

Malhi, H., A. N. Irani, P. Rajvanshi, S. O. Suadicani, D. C. Spray, T. V. McDonald and S. Gupta (2000). "KATP channels regulate mitogenically induced proliferation in primary rat

hepatocytes and human liver cell lines. Implications for liver growth control and potential therapeutic targeting." J Biol Chem 275(34): 26050-7.

Mangel, A. W., V. Prpic, N. D. Snow, S. Basavappa, L. J. Hurst, A. I. Sharara and R. A. Liddle (1994). "Regulation of cholecystokinin secretion by ATP-sensitive potassium channels." Am J Physiol 267(4 Pt 1): G595-600.

Manning, A. S. and D. J. Hearse (1984). "Reperfusion-induced arrhythmias: mechanisms and prevention." J Mol Cell Cardiol 16(6): 497-518.

Manning Fox, J. E., H. D. Kanji, R. J. French and P. E. Light (2002). "Cardioselectivity of the sulphonylurea HMR 1098: studies on native and recombinant cardiac and pancreatic K(ATP) channels." Br J Pharmacol 135(2): 480-8.

Matsuo, N., Y. Nagata, J. Nakamura and T. Yamamoto (2002). "Coupling of calcium transport with ATP hydrolysis in scallop sarcoplasmic reticulum." J Biochem (Tokyo) 131(3): 375-81.

Meera, P., M. Wallner, M. Song and L. Toro (1997). "Large conductance voltage- and calcium-dependent K<sup>+</sup> channel, a distinct member of voltage-dependent ion channels with seven N-terminal transmembrane segments (S0-S6), an extracellular N terminus, and an intracellular (S9-S10) C terminus." Proc Natl Acad Sci U S A 94(25): 14066-71.

Michailova, A., J. Saucerman, M. E. Belik and A. D. McCulloch (2005). "Modeling regulation of cardiac KATP and L-type Ca<sup>2+</sup> currents by ATP, ADP, and Mg<sup>2+</sup>." Biophys J 88(3): 2234-49.

Mikhailov, M. V. and S. J. Ashcroft (2000). "Interactions of the sulphonylurea receptor 1 subunit in the molecular assembly of beta-cell K(ATP) channels." J Biol Chem 275(5): 3360-4.

- Millar, J. A., L. Barratt, A. P. Southan, K. M. Page, R. E. Fyffe, B. Robertson and A. Mathie (2000). "A functional role for the two-pore domain potassium channel TASK-1 in cerebellar granule neurons." Proc Natl Acad Sci U S A **97**(7): 3614-8.
- Moczydlowski, E., K. Lucchesi and A. Ravindran (1988). "An emerging pharmacology of peptide toxins targeted against potassium channels." J Membr Biol **105**(2): 95-111.
- Morishige, K., N. Takahashi, A. Jahangir, M. Yamada, H. Koyama, J. S. Zanelli and Y. Kurachi (1994). "Molecular cloning and functional expression of a novel brain-specific inward rectifier potassium channel." FEBS Lett **346**(2-3): 251-6.
- Murata, M., M. Akao, B. O'Rourke and E. Marban (2001). "Mitochondrial ATP-sensitive potassium channels attenuate matrix Ca(2+) overload during simulated ischemia and reperfusion: possible mechanism of cardioprotection." Circ Res **89**(10): 891-8.
- Murry, C. E., R. B. Jennings and K. A. Reimer (1986). "Preconditioning with ischemia: a delay of lethal cell injury in ischemic myocardium." Circulation **74**(5): 1124-36.
- Nelson, M. T. and J. M. Quayle (1995). "Physiological roles and properties of potassium channels in arterial smooth muscle." Am J Physiol **268**(4 Pt 1): C799-822.
- Nichols, C. G. and W. J. Lederer (1991). "Adenosine triphosphate-sensitive potassium channels in the cardiovascular system." Am J Physiol **261**(6 Pt 2): H1675-86.
- Nichols, C. G. and A. N. Lopatin (1997). "Inward rectifier potassium channels." Annu Rev Physiol **59**: 171-91.
- Nichols, C. G., S. L. Shyng, A. Nestorowicz, B. Glaser, J. P. t. Clement, G. Gonzalez, L. Aguilar-Bryan, M. A. Permutt and J. Bryan (1996). "Adenosine diphosphate as an intracellular regulator of insulin secretion." Science **272**(5269): 1785-7.

Nishida, M. and R. MacKinnon (2002). "Structural basis of inward rectification: cytoplasmic pore of the G protein-gated inward rectifier GIRK1 at 1.8 Å resolution." Cell **111**(7): 957-65.

Noma, A. (1983). "ATP-regulated K<sup>+</sup> channels in cardiac muscle." Nature **305**(5930): 147-8.

Ozcan, C., M. Bienengraeber, P. P. Dzeja and A. Terzic (2002). "Potassium channel openers protect cardiac mitochondria by attenuating oxidant stress at reoxygenation." Am J Physiol Heart Circ Physiol **282**(2): H531-9.

Ozcan, C., E. L. Holmuhamedov, A. Jahangir and A. Terzic (2001). "Diazoxide protects mitochondria from anoxic injury: implications for myopreservation." J Thorac Cardiovasc Surg **121**(2): 298-306.

Park, Y. B. (1994). "Ion selectivity and gating of small conductance Ca<sup>2+</sup>-activated K<sup>+</sup> channels in cultured rat adrenal chromaffin cells." J Physiol **481** ( Pt 3): 555-70.

Partridge, C. J., D. J. Beech and A. Sivaprasadarao (2001). "Identification and pharmacological correction of a membrane trafficking defect associated with a mutation in the sulfonylurea receptor causing familial hyperinsulinism." J Biol Chem **276**(38): 35947-52.

Patel, A. J., E. Honore, F. Lesage, M. Fink, G. Romey and M. Lazdunski (1999). "Inhalational anesthetics activate two-pore-domain background K<sup>+</sup> channels." Nat Neurosci **2**(5): 422-6.

Pegan, S., C. Arrabit, W. Zhou, W. Kwiatkowski, A. Collins, P. A. Slesinger and S. Choe (2005). "Cytoplasmic domain structures of Kir2.1 and Kir3.1 show sites for modulating gating and rectification." Nat Neurosci **8**(3): 279-87.

Perier, F., C. M. Radeke and C. A. Vandenberg (1994). "Primary structure and characterization of a small-conductance inwardly rectifying potassium channel from human hippocampus." Proc Natl Acad Sci U S A **91**(13): 6240-4.

Permutt, M. A. and S. Ghosh (1996). "Rat model contributes new loci for NIDDM susceptibility in man." Nat Genet **12**(1): 4-6.

Piao, L., Y. Li, L. Li and W. X. Xu (2001). "Increment of calcium-activated and delayed rectifier potassium current by hyposmotic swelling in gastric antral circular myocytes of guinea pig." Acta Pharmacol Sin **22**(6): 566-72.

Piskorowski, R. and R. W. Aldrich (2002). "Calcium activation of BK(Ca) potassium channels lacking the calcium bowl and RCK domains." Nature **420**(6915): 499-502.

Pongs, O. (1992). "Molecular biology of voltage-dependent potassium channels." Physiol Rev **72**(4 Suppl): S69-88.

Pongs, O., N. Kecskemethy, R. Muller, I. Krah-Jentgens, A. Baumann, H. H. Kiltz, I. Canal, S. Llamazares and A. Ferrus (1988). "Shaker encodes a family of putative potassium channel proteins in the nervous system of *Drosophila*." Embo J **7**(4): 1087-96.

Pountney, D. J., Z. Q. Sun, L. M. Porter, M. N. Nitabach, T. Y. Nakamura, D. Holmes, E. Rosner, M. Kaneko, T. Manaris, T. C. Holmes and W. A. Coetzee (2001). "Is the molecular composition of K(ATP) channels more complex than originally thought?" J Mol Cell Cardiol **33**(8): 1541-6.

Prentki, M. and F. M. Matschinsky (1987). "Ca<sup>2+</sup>, cAMP, and phospholipid-derived messengers in coupling mechanisms of insulin secretion." Physiol Rev **67**(4): 1185-248.

Quast, U. (1996). "ATP-sensitive K<sup>+</sup> channels in the kidney." Naunyn Schmiedebergs Arch Pharmacol **354**(3): 213-25.

Quayle, J. M., M. T. Nelson and N. B. Standen (1997). "ATP-sensitive and inwardly rectifying potassium channels in smooth muscle." Physiol Rev 77(4): 1165-232.

Rainbow, R. D., M. James, D. Hudman, M. Al Johi, H. Singh, P. J. Watson, I. Ashmole, N. W. Davies, D. Lodwick and R. I. Norman (2004). "Proximal C-terminal domain of sulphonylurea receptor 2A interacts with pore-forming Kir6 subunits in KATP channels." Biochem J 379(Pt 1): 173-81.

Rainbow, R. D., D. Lodwick, D. Hudman, N. W. Davies, R. I. Norman and N. B. Standen (2004). "SUR2A C-terminal fragments reduce KATP currents and ischaemic tolerance of rat cardiac myocytes." J Physiol 557(Pt 3): 785-94.

Rasmussen, H., K. C. Zawalich, S. Ganesan, R. Calle and W. S. Zawalich (1990). "Physiology and pathophysiology of insulin secretion." Diabetes Care 13(6): 655-66.

Reuveny, E., P. A. Slesinger, J. Inglese, J. M. Morales, J. A. Iniguez-Lluhi, R. J.

Lefkowitz, H. R. Bourne, Y. N. Jan and L. Y. Jan (1994). "Activation of the cloned muscarinic potassium channel by G protein beta gamma subunits." Nature 370(6485): 143-6.

Reyes, R., F. Duprat, F. Lesage, M. Fink, M. Salinas, N. Farman and M. Lazdunski (1998). "Cloning and expression of a novel pH-sensitive two pore domain K<sup>+</sup> channel from human kidney." J Biol Chem 273(47): 30863-9.

Roman, R., A. P. Feranchak, M. Troetsch, J. C. Dunkelberg, G. Kilic, T. Schlenker, J. Schaack and J. G. Fitz (2002). "Molecular characterization of volume-sensitive SK(Ca) channels in human liver cell lines." Am J Physiol Gastrointest Liver Physiol 282(1): G116-22.

Sah, P. and E. S. Faber (2002). "Channels underlying neuronal calcium-activated potassium currents." Prog Neurobiol 66(5): 345-53.

Sanguinetti, M. C. and Q. P. Xu (1999). "Mutations of the S4-S5 linker alter activation properties of HERG potassium channels expressed in *Xenopus oocytes*." J Physiol **514** ( Pt 3): 667-75.

Saraste, M., P. R. Sibbald and A. Wittinghofer (1990). "The P-loop--a common motif in ATP- and GTP-binding proteins." Trends Biochem Sci **15**(11): 430-4.

Sasaki, N., T. Sato, A. Ohler, B. O'Rourke and E. Marban (2000). "Activation of mitochondrial ATP-dependent potassium channels by nitric oxide." Circulation **101**(4): 439-45.

Sato, T., B. O'Rourke and E. Marban (1998). "Modulation of mitochondrial ATP-dependent K<sup>+</sup> channels by protein kinase C." Circ Res **83**(1): 110-4.

Schulte, U., H. Hahn, H. Wiesinger, J. P. Ruppersberg and B. Fakler (1998). "pH-dependent gating of ROMK (Kir1.1) channels involves conformational changes in both N and C termini." J Biol Chem **273**(51): 34575-9.

Schwanstecher, M., C. Sieverding, H. Dorschner, I. Gross, L. Aguilar-Bryan, C. Schwanstecher and J. Bryan (1998). "Potassium channel openers require ATP to bind to and act through sulfonylurea receptors." Embo J **17**(19): 5529-35.

Schwappach, B., N. Zerangue, Y. N. Jan and L. Y. Jan (2000). "Molecular basis for K(ATP) assembly: transmembrane interactions mediate association of a K<sup>+</sup> channel with an ABC transporter." Neuron **26**(1): 155-67.

Seharaseyon, J., N. Sasaki, A. Ohler, T. Sato, H. Fraser, D. C. Johns, B. O'Rourke and E. Marban (2000). "Evidence against functional heteromultimerization of the KATP channel subunits Kir6.1 and Kir6.2." J Biol Chem **275**(23): 17561-5.

Sharma, N., A. Crane, G. Gonzalez, J. Bryan and L. Aguilar-Bryan (2000). "Familial hyperinsulinism and pancreatic beta-cell ATP-sensitive potassium channels." Kidney Int 57(3): 803-8.

Shuck, M. E., J. H. Bock, C. W. Benjamin, T. D. Tsai, K. S. Lee, J. L. Slightom and M. J. Bienkowski (1994). "Cloning and characterization of multiple forms of the human kidney ROM-K potassium channel." J Biol Chem 269(39): 24261-70.

Shyng, S. and C. G. Nichols (1997). "Octameric stoichiometry of the KATP channel complex." J Gen Physiol 110(6): 655-64.

Shyng, S. L., C. A. Cukras, J. Harwood and C. G. Nichols (2000). "Structural determinants of PIP(2) regulation of inward rectifier K(ATP) channels." J Gen Physiol 116(5): 599-608.

Shyng, S. L., T. Ferrigni, J. B. Shepard, A. Nestorowicz, B. Glaser, M. A. Permutt and C. G. Nichols (1998). "Functional analyses of novel mutations in the sulfonylurea receptor 1 associated with persistent hyperinsulinemic hypoglycemia of infancy." Diabetes 47(7): 1145-51.

Shyng, S. L. and C. G. Nichols (1998). "Membrane phospholipid control of nucleotide sensitivity of KATP channels." Science 282(5391): 1138-41.

Singh, H., D. Hudman, C. L. Lawrence, R. D. Rainbow, D. Lodwick and R. I. Norman (2003). "Distribution of Kir6.0 and SUR2 ATP-sensitive potassium channel subunits in isolated ventricular myocytes." J Mol Cell Cardiol 35(5): 445-59.

Spauschus, A., K. U. Lentz, E. Wischmeyer, E. Dissmann, C. Karschin and A. Karschin (1996). "A G-protein-activated inwardly rectifying K<sup>+</sup> channel (GIRK4) from human hippocampus associates with other GIRK channels." J Neurosci 16(3): 930-8.

Stonehouse, A. H., J. H. Pringle, R. I. Norman, P. R. Stanfield, E. C. Conley and W. J. Brammar (1999). "Characterisation of Kir2.0 proteins in the rat cerebellum and hippocampus by polyclonal antibodies." Histochem Cell Biol **112**(6): 457-65.

Strong, P. N. (1990). "Potassium channel toxins." Pharmacol Ther **46**(1): 137-62.

Subbiah, R. N., C. E. Clarke, D. J. Smith, J. Zhao, T. J. Campbell and J. I. Vandenberg (2004). "Molecular basis of slow activation of the human ether-a-go-go related gene potassium channel." J Physiol **558**(Pt 2): 417-31.

Sui, J. L., J. Petit-Jacques and D. E. Logothetis (1998). "Activation of the atrial KACH channel by the  $\beta$ gamma subunits of G proteins or intracellular  $\text{Na}^+$  ions depends on the presence of phosphatidylinositol phosphates." Proc Natl Acad Sci U S A **95**(3): 1307-12.

Tagliatela, M., E. Ficker, B. A. Wible and A. M. Brown (1995). "C-terminus determinants for  $\text{Mg}^{2+}$  and polyamine block of the inward rectifier  $\text{K}^+$  channel IRK1." Embo J **14**(22): 5532-41.

Takahashi, N., K. Morishige, A. Jahangir, M. Yamada, I. Findlay, H. Koyama and Y. Kurachi (1994). "Molecular cloning and functional expression of cDNA encoding a second class of inward rectifier potassium channels in the mouse brain." J Biol Chem **269**(37): 23274-9.

Takumi, T., T. Ishii, Y. Horio, K. Morishige, N. Takahashi, M. Yamada, T. Yamashita, H. Kiyama, K. Sohmiya, S. Nakanishi and et al. (1995). "A novel ATP-dependent inward rectifier potassium channel expressed predominantly in glial cells." J Biol Chem **270**(27): 16339-46.

Talley, E. M., Q. Lei, J. E. Sirois and D. A. Bayliss (2000). "TASK-1, a two-pore domain  $\text{K}^+$  channel, is modulated by multiple neurotransmitters in motoneurons." Neuron **25**(2): 399-410.

Taschenberger, G., A. Mougey, S. Shen, L. B. Lester, S. LaFranchi and S. L. Shyng (2002). "Identification of a familial hyperinsulinism-causing mutation in the sulfonylurea receptor 1 that prevents normal trafficking and function of KATP channels." J Biol Chem **277**(19): 17139-46.

Terzic, A., A. Jahangir and Y. Kurachi (1995). "Cardiac ATP-sensitive K<sup>+</sup> channels: regulation by intracellular nucleotides and K<sup>+</sup> channel-opening drugs." Am J Physiol **269**(3 Pt 1): C525-45.

Tian, G. C., H. G. Yan, R. T. Jiang, F. Kishi, A. Nakazawa and M. D. Tsai (1990). "Mechanism of adenylate kinase. Are the essential lysines essential?" Biochemistry **29**(18): 4296-304.

Topert, C., F. Doring, E. Wischmeyer, C. Karschin, J. Brockhaus, K. Ballanyi, C. Derst and A. Karschin (1998). "Kir2.4: a novel K<sup>+</sup> inward rectifier channel associated with motoneurons of cranial nerve nuclei." J Neurosci **18**(11): 4096-105.

Trapp, S., S. J. Tucker and F. M. Ashcroft (1997). "Activation and inhibition of K-ATP currents by guanine nucleotides is mediated by different channel subunits." Proc Natl Acad Sci U S A **94**(16): 8872-7.

Tucker S. J., Gribble F. M., Zhao C., Trapp S. and A. F. M. (1997). "Truncation of Kir6.2 produces ATP-sensitive K<sup>+</sup> channels in the absence of the sulphonylurea receptor." Nature **387**: 179-183.

Tucker S. J. and A. F. M. (1999). "Mapping of the physical interaction between the intracellular domains of an inwardly rectifying potassium channel, Kir6.2." J. Biol. Chem. **274**: 33393-33397.

Tucker, S. J., F. M. Gribble, P. Proks, S. Trapp, T. J. Ryder, T. Haug, F. Reimann and F. M. Ashcroft (1998). "Molecular determinants of KATP channel inhibition by ATP." Embo J **17**(12): 3290-6.

Tusnady, G. E., E. Bakos, A. Varadi and B. Sarkadi (1997). "Membrane topology distinguishes a subfamily of the ATP-binding cassette (ABC) transporters." FEBS Lett **402**(1): 1-3.

Ueda, K., N. Inagaki and S. Seino (1997). "MgADP antagonism to Mg<sup>2+</sup>-independent ATP binding of the sulfonylurea receptor SUR1." J Biol Chem **272**(37): 22983-6.

Ueda, K., J. Komine, M. Matsuo, S. Seino and T. Amachi (1999). "Cooperative binding of ATP and MgADP in the sulfonylurea receptor is modulated by glibenclamide." Proc Natl Acad Sci U S A **96**(4): 1268-72.

Uhde, I., A. Toman, I. Gross, C. Schwanstecher and M. Schwanstecher (1999). "Identification of the potassium channel opener site on sulfonylurea receptors." J Biol Chem **274**(40): 28079-82.

Van Bever, L., S. Poitry, C. Faure, R. I. Norman, A. Roatti and A. J. Baertschi (2004). "Pore loop-mutated rat KIR6.1 and KIR6.2 suppress KATP current in rat cardiomyocytes." Am J Physiol Heart Circ Physiol **287**(2): H850-9.

Vanden Hoek, T., L. B. Becker, Z. H. Shao, C. Q. Li and P. T. Schumacker (2000). "Preconditioning in cardiomyocytes protects by attenuating oxidant stress at reperfusion." Circ Res **86**(5): 541-8.

Vanden Hoek, T. L., L. B. Becker, Z. Shao, C. Li and P. T. Schumacker (1998). "Reactive oxygen species released from mitochondria during brief hypoxia induce preconditioning in cardiomyocytes." J Biol Chem **273**(29): 18092-8.

- Vergara, C., R. Latorre, N. V. Marrion and J. P. Adelman (1998). "Calcium-activated potassium channels." Curr Opin Neurobiol **8**(3): 321-9.
- Virsolvy-Vergine, A., G. Salazar, R. Sillard, L. Denoroy, V. Mutt and D. Bataille (1996). "Endosulfine, endogenous ligand for the sulphonylurea receptor: isolation from porcine brain and partial structural determination of the alpha form." Diabetologia **39**(2): 135-41.
- Walker, J. E., M. Saraste, M. J. Runswick and N. J. Gay (1982). "Distantly related sequences in the alpha- and beta-subunits of ATP synthase, myosin, kinases and other ATP-requiring enzymes and a common nucleotide binding fold." Embo J **1**(8): 945-51.
- Walter, C., S. Wilken and E. Schneider (1992). "Characterization of site-directed mutations in conserved domains of MalK, a bacterial member of the ATP-binding cassette (ABC) family [corrected]." FEBS Lett **303**(1): 41-4.
- Wang, W. H., A. Schwab and G. Giebisch (1990). "Regulation of small-conductance K<sup>+</sup> channel in apical membrane of rat cortical collecting tubule." Am J Physiol **259**(3 Pt 2): F494-502.
- Warmke, J. W. and B. Ganetzky (1994). "A family of potassium channel genes related to eag in Drosophila and mammals." Proc Natl Acad Sci U S A **91**(8): 3438-42.
- Wei, A., C. Solaro, C. Lingle and L. Salkoff (1994). "Calcium sensitivity of BK-type K<sub>Ca</sub> channels determined by a separable domain." Neuron **13**(3): 671-81.
- Wible, B. A., M. De Biasi, K. Majumder, M. Tagliatela and A. M. Brown (1995). "Cloning and functional expression of an inwardly rectifying K<sup>+</sup> channel from human atrium." Circ Res **76**(3): 343-50.

Wolf, B. A., J. R. Colca, J. Turk, J. Florholmen and M. L. McDaniel (1988). "Regulation of Ca<sup>2+</sup> homeostasis by islet endoplasmic reticulum and its role in insulin secretion." Am J Physiol **254**(2 Pt 1): E121-36.

Wollheim, C. B. and T. J. Biden (1986). "Signal transduction in insulin secretion: comparison between fuel stimuli and receptor agonists." Ann N Y Acad Sci **488**: 317-33.

Womack, K. B., S. E. Gordon, F. He, T. G. Wensel, C. C. Lu and D. W. Hilgemann (2000). "Do phosphatidylinositides modulate vertebrate phototransduction?" J Neurosci **20**(8): 2792-9.

Wu, J., N. Cui, H. Piao, Y. Wang, H. Xu, J. Mao and C. Jiang (2002). "Allosteric modulation of the mouse Kir6.2 channel by intracellular H<sup>+</sup> and ATP." J Physiol **543**(Pt 2): 495-504.

Xie, L. H., M. Horie and M. Takano (1999). "Phospholipase C-linked receptors regulate the ATP-sensitive potassium channel by means of phosphatidylinositol 4,5-bisphosphate metabolism." Proc Natl Acad Sci U S A **96**(26): 15292-7.

Xie, L. H., M. Takano, M. Kakei, M. Okamura and A. Noma (1999). "Wortmannin, an inhibitor of phosphatidylinositol kinases, blocks the MgATP-dependent recovery of Kir6.2/SUR2A channels." J Physiol **514** ( Pt 3): 655-65.

Xu, H., J. Wu, N. Cui, L. Abdulkadir, R. Wang, J. Mao, L. R. Giwa, S. Chanchevalap and C. Jiang (2001). "Distinct histidine residues control the acid-induced activation and inhibition of the cloned K(ATP) channel." J Biol Chem **276**(42): 38690-6.

Xu, H., Z. Yang, N. Cui, S. Chanchevalap, W. W. Valesky and C. Jiang (2000). "A single residue contributes to the difference between Kir4.1 and Kir1.1 channels in pH sensitivity, rectification and single channel conductance." J Physiol **528** Pt 2: 267-77.

Yang, Z. and C. Jiang (1999). "Opposite effects of pH on open-state probability and single channel conductance of kir4.1 channels." J Physiol **520 Pt 3**: 921-7.

Yokoshiki, H., M. Sunagawa, T. Seki and N. Sperelakis (1998). "ATP-sensitive K<sup>+</sup> channels in pancreatic, cardiac, and vascular smooth muscle cells." Am J Physiol **274(1 Pt 1)**: C25-37.

Zerangue, N., B. Schwappach, Y. N. Jan and L. Y. Jan (1999). "A new ER trafficking signal regulates the subunit stoichiometry of plasma membrane K(ATP) channels." Neuron **22(3)**: 537-48.

Zhang, D. X., Y. F. Chen, W. B. Campbell, A. P. Zou, G. J. Gross and P. L. Li (2001). "Characteristics and superoxide-induced activation of reconstituted myocardial mitochondrial ATP-sensitive potassium channels." Circ Res **89(12)**: 1177-83.

Zhou, H., S. S. Tate and L. G. Palmer (1994). "Primary structure and functional properties of an epithelial K channel." Am J Physiol **266(3 Pt 1)**: C809-24.

Zhou, Z., Q. Gong, B. Ye, Z. Fan, J. C. Makielski, G. A. Robertson and C. T. January (1998). "Properties of HERG channels stably expressed in HEK 293 cells studied at physiological temperature." Biophys J **74(1)**: 230-41.

Zhu, G., Z. Qu, N. Cui and C. Jiang (1999). "Suppression of Kir2.3 activity by protein kinase C phosphorylation of the channel protein at threonine 53." J Biol Chem **274(17)**: 11643-6.

Zunkler, B. J., S. Lins, T. Ohno-Shosaku, G. Trube and U. Panten (1988). "Cytosolic ADP enhances the sensitivity to tolbutamide of ATP-dependent K<sup>+</sup> channels from pancreatic B-cells." FEBS Lett **239(2)**: 241-4.

Zweier, J. L. and W. E. Jacobus (1987). "Substrate-induced alterations of high energy phosphate metabolism and contractile function in the perfused heart." J Biol Chem **262**(17): 8015-21.